SEMICONDUCTIVE AND SPECTROSCOPIC INVESTIGATIONS OF SOME NITROAROMATIC COMPOUNDS

THESIS
SUBMITTED FOR THE DEGREE OF
DOCTOR OF PHILOSOPHY (SCIENCE)
OF THE
UNIVERSITY OF NORTH BENGAL

By
KAPUR MAL JAIN, M. Sc.
DEPARTMENT OF OPTICS
INDIAN ASSOCIATION FOR THE CULTIVATION OF SCIENCE
CALCUTTA-700 032
1981

CONTENTS

List of Figures

.....

PREFACE

The present thesis entitled "Semiconductive and Spectroscopic Investigations of Some Nitroaromatic Compounds" is in fulfilment of the requirements for the degree of Doctor of Philosophy (Science) of the North Bengal University, Rajarammohunpur, Darjeeling (W.B.). It embodies results of investigation on the semiconductive and spectroscopic properties of some nitro-aromatic compounds. The most of the work was carried-out in the Physics department of North Bengal University, Darjeeling and in the Optics department of Indian Association for the Cultivation of Science, Jadavpur.

The thesis has two parts and an appendix. There are four chapters in each part. First chapter of each part contains a general introduction with a brief review on the relevent parts of the existing theories.

The first part deals with the semiconductive properties of some nitroaromatics e.g. dark conductivity, the effect of adsorption of vapours on the electrical conductivity and on semiconduction activation energy, adsorption and desorption processes and the Compensation effect. The experimental techniques used for the semiconductive investigations are presented in chapter 2 while the subsequent chapters contain the details of the experimental results together with the discussions.

Spectroscopic data are collected by UV - Visible spectrophoto -

and fluorimeters. The results and discussions of the electronic spectral investigations of some nitroaromatic compounds like 9-nitroanthracene, 2-nitrofluorene and 1,4-dinitronaphthalene are presented in the second, third and fourth chapters of part B.

Most of the results are published in the form of papers in various scientific journals. Some are awaiting publication too. A list of publications and available reprints are included in the Appendix.

The author wished to express his deep sense of gratitude to Dr. T. N. Misra, thesis supervisor, for his continuous guidance and untiring supervision throughout the course of the present investigation. The author feels much indebted to Prof. G. S. Kastha of I.A.C.S., Prof. S. N. Sen of N.B.U. and Prof. R. K. Mishra of AIIMS for providing with the laboratory facilities in their departments. Author is extremely thankful to Dr. B. Mallik, Sm. Alpana Ghosh and Dr. K. C. Mandal, with whom he has publications also, for their assistance, cooperation and many helpful suggestions. Thanks are due to the authorities of the Indian Association for the Cultivation of Science, Jadavpur and North Bengal University, Darjeeling for research facilities and also to the C.S.I.R. and U.G.C. for the research fellowships. Author expresses his greatfulness to the Government of Madhya Pradesh too for the sanction of study leave during the tenure of Teacher Fellowship. He sincerely records his thanks to all

those who helped and encouraged him, directly or indirectly, during the progress of the work and also to Mr. Asim Dey and Surendra Choudhuri for the help with the typing of papers in connection with the research work. For the competent technical assistance, author is thankful to Mr. S. K. Sarker also. Finally, it gives him a great pleasure in acknowledging the receipt of understanding encouragement from his patient family during the considerable length of time devoted for the research on the subject.

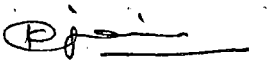

Jadavpur, Calcutta - 32. KAPUR MAL JAIN

January 1981.

ABSTRACT

Semiconductive and Spectroscopic Investigations of Some Nitroaromatic Compounds.

Adsorption and desorption of various chemical vapours at different vapour pressures on the crystallite surfaces of 9-nitroanthracene; 2-nitrofluorene; o-, m- and p-nitrobenzoic acids; 1,4-dinitronaphthalene and 1,3,5-trinitrobenzene have been investigated using electrical conductivity as a probe. An exponential dependence of the conductivity upon vapour pressure of the reagent chemical has been obtained. Adsorption and desorption kinetics follow the Roginsky-Zeldovich equation in a modified form. The activation energy for adsorption and desorption is found to depend upon the vapour pressure as well as upon the nature of the chemical vapours. Kinetic analysis data show that in these Vapour-Semiconductor systems, the adsorption is generally a two stage process. In some cases of vapour adsorption on 1,4-dinitronaphthalene and 1,3,5-trinitrobenzene crystal surfaces, a three stage adsorption process is also observed.

The validity of the Compensation effect in various nitroaromatic semiconductors has been examined. The nonbonding electrons of nitrogroup seem to play an important role in the compensation mechanism. A low value of compensation temperature is obtained. Existence of any relationship between the adsorption process and the compensation effect in dark conduction process has been investigated. It has been concluded that the compensation effect is generally observed in cases where the change in the semiconduction activation energy is caused by a two stage adsorption process.

In case where the activation energy is changed by a three stage adsorption process, compensation effect is not observed. All these results are presented in part A of the thesis.

In second part (B) of the thesis, electronic spectral investigations of 9-nitroanthracene, 2-nitrofluorene and 1,4-dinitronaphthalene have been presented.

The electronic spectra of 9-nitroanthracene have been investigated in solution. Two close-lying states have been observed in the low-energy region of the electronic absorption spectra of this molecule. $^1A \longrightarrow {}^1L_b$ band which is hidden under the intense $^1A \longrightarrow {}^1L_a$ band in anthracene shifts to an accessible spectral region and seperates out from ^1L_a band in this molecule. The molecule is observed to fluoresce very weakly. A good overlapping between the emission spectra and the $^1A \longrightarrow {}^1L_b$ absorption band has been observed. It has been suggested that the low energy excited singlet state is a π-π^* and not n-π^* state as is observed in some other nitroaromatic compounds. The solvent effect on the ^1L_a band has been explained interms of predominant dispersive interaction and weak dipolar interaction in nonpolar solvents and interms of Orientation-Induction effect and local interactions in polar solvents. The observed change in the oscillator strength of ^1L_a band is explained interms of intermolecular forces between the solute and the solvent molecules.

Results on the electronic spectral analysis of 2-nitrofluorene are presented in third chapter of part B. Only one intense $^1A \longrightarrow {}^1L_a$ band system has been observed in the solution electronic absorption spectra of this molecule. The nitro-group perturbation confirms that the ^1L_a band is long axis polarised. In solution, the ^1L_b band of fluorene is hidden under the intense band of 2-nitrofluorene. In a mixed-crystal spectra, three band systems have been observed which are assigned as $^1A \longrightarrow {}^1L_b$, $^1A \longrightarrow {}^1L_a$ and intramolecular CT bands. The solvent effect on $^1A \longrightarrow {}^1L_a$ transition energy has also been investigated in various polar and nonpolar solvents.

The electronic absorption and emission spectra of 1,4-dinitronaphthalene have been studied in various protic and nonprotic solvents in various concentrations and at different temperatures. Results are presented in the last chapter of second part B. The low-lying singlet and triplet states have been assigned from solvent effect on the absorption and the emission spectra and also from some luminescent features of this molecule. Phosphorescence polarisation is found to be negative with $^1\pi\text{-}\pi^*$ excitation. It has been suggested that the low-lying states in this molecule, in order of increasing energy, are :
$E(S_0) < E(^3\pi\text{-}\pi^*) < E(^3n\text{-}\pi^*) < E(^1n\text{-}\pi^*) < E(^1CT) < E(^1\pi\text{-}\pi^*)$.
The $^3\pi\text{-}\pi^* \longrightarrow S_0$ phosphorescence mean life time is significantly low. This has been attributed to strong "proximity effect" i.e. the

vibronic interaction between the close-lying $^3n\text{-}\pi^*$ and $^3\pi\text{-}\pi^*$ states. The luminescence behaviour in protic and nonprotic solvents at 77°K is different. The molecule is nonfluorescent and shows a weak phosphorescence in hydrocarbon media while a weak fluorescence from $^1n\text{-}\pi^*$ along with the intensification and red shift of the phosphorescence have been observed in protic solvents. The quenching of radiative $^1n\text{-}\pi^* \longrightarrow S_0$ transition in hydrocarbon confined media, however, has been attributed not to the proximity effect but to some other intermolecular energy transfer process where a different energy transfer route from $^1n\text{-}\pi^*$ to the excimer state (D^*) resulting in excimer fluorescence emission $D^* \longrightarrow S_0$ is observed. In protic solvents, the local solute-solvent interaction impedes excimer formation and $^1n\text{-}\pi^* \rightsquigarrow D^*$ route is absent. Also the intersystem crossings from ^1CT to $^3n\text{-}\pi^*$ and $^3\pi\text{-}\pi^*$ are enhanced to some extent there.

.....

PART - A

SEMICONDUCTIVE INVESTIGATIONS

CHAPTER - 1

GENERAL INTRODUCTION

There have been a considerable interests[1-15] in the electrical conductivity of organic semiconductors in recent years to unfold their various properties both theoretically and experimentally. Due to its wide range of applicability in a number of fields, organic semiconductor research has opened a new frontier in solid state physics[2,16-30]. The formation of charge carriers and the mode of transportation even in highly disordered solids pose continuing challenges to the very fundamental concepts of charge transport mechanism. The most important feature of the organic solid state is the persistence of molecular identity which distinguishes it from the inorganic solid state. The molecular identity derives from the weakness of the interaction between the molecules. The traditional energy band model, though applied in some cases, is only partially successful in the case of organic molecular crystals.

Gas or vapour adsorption effect on the biologically important semiconductors was used to explain the olfactory transduction by Rosenberg, Misra and Switzer[36]. Gas or vapour adsorption is known to enhance the conductivity with concomitant change in the semiconduction activation energy and the pre-exponential factor in the

conductivity equation. At present, however, there does not seem to be any convincing evidence in favour of any particular assumption as to the type of interaction of the gas with the substrate. Though, a weak charge transfer complex formation has often been suggested[36-38].

Compensation behaviour[40-50] in dark conduction processes of the organic semiconductors is among the central problems in the field. Recent interest yielded many new observations along with some theoretical developments.

The present investigation is concerned with the semiconductive properties, in particular the gas or vapour adsorption effect and the compensation effect, of some nitroaromatic semiconductors.

In the subsequent sections of this chapter we will briefly review the theoretical back-ground.

1.1 Band Theory and Molecular Crystals

The band theory, originally developed for metals, ionic and valence crystals has been applied with some success to molecular crystals as well[51-54].

In one electron approximation, the wave function for a single electron can be written as

$$\Psi_k(\bar{r}) = \Phi_k(\bar{r}) \exp(i\bar{k}\cdot\bar{r}) \qquad (1.11)$$

where the wavenumber vector $\bar{k} = \frac{2\pi}{\lambda}$, λ is the associated wave length; Φ_k is the function which has the translational periodicity of the crystal lattice. If $\Phi_k(\bar{r})$ is constant throughout the crystal, then Ψ_k is applicable to the metals. But if $\Phi_k(\bar{r})$ varies greatly within a unit cell and falls to zero between adjecent cells, then the motion of the electron is restricted and we get a "tight bonding condition".[56-59] This tight bonding is a characteristic of molecular crystals. Unier this approximation, the one electron crystal wavefunctions Ψ_k are constructed from linear combinations of one electron molecular functions χ_n:

$$\Psi_k(\bar{r}) = N^{-\frac{1}{2}} \sum_{n=1}^{N} \exp(i\bar{k}\cdot\bar{r}_n)\chi_n(\bar{r}-\bar{r}_n) \qquad (1.12)$$

Here, $\bar{r}_n$ locates the geometrical centre of n th molecule and N is the total number of molecules in the crystal. It is assumed that $\langle \chi_m | \chi_n \rangle = 0$ if $m \neq n$.

The crystal field is approximated by :

$$V(\bar{r}) = \sum_n V_n(\bar{r}-\bar{r}_n) \qquad (1.13)$$

where V_n is the Hartee Fock type of potential of an isolated

neutral molecule. [This consists of three components - V′: field acting on the electron that arises from all the nuclei, V″: the coulomb potential of the electronic charge distribution and V‴: the exchange term.]

The eigen value of ψ_k is written as :

$$\mathcal{E}(\bar{K}) = \mathcal{E}_0 + \mathcal{E}_1 + 2\sum_s{}' \mathcal{E}_s \cos(\bar{K}\cdot\bar{r}_s) \qquad (1.14)$$

where

$$\mathcal{E}_0 = \int \chi_n \left[-(\hbar^2\Delta/2m) - eV_n\right] \chi_n \, d\tau$$

$$\mathcal{E}_1 = \sum_s{}' \int |\chi_n|^2 V_{n+s} \, d\tau \qquad s \neq 0$$

$$\mathcal{E}_s = \int \chi_{n+s} V_{n+s} \chi_n \, d\tau$$

and the lattice vectors ($\bar{r}_s$) and ($-\bar{r}_s$) are counted as one in the equation (1.14). The prime on $\sum$ indicates that the term with $\bar{r}_s = 0$ is omitted from the summation.

The intermolecular resonance integrals $\mathcal{E}_s$ determine the structure of the band[60]. The resonance integrals fall off rapidly with intermolecular distance and only nearest neighbour interactions are found to be important. Functional forms of V_n and the appropriate χ_n are required to evaluate $\mathcal{E}_s$. The band structure depends on the crystal lattice structure.

1.2 Operational Definition of Semiconductor

If the interaction between different carrier species is neglected, then for semiconductor, where the charge carriers are electrons (e) and holes (h), the conduction equation is :

$$\sigma = n_e e \mu_e + n_h e \mu_h \qquad (1.21)$$

where n is the density of the charge carriers in their respective bands, e is the electronic charge and μ is the mobility of the carriers.

The densities of the electrons in the conduction band and that of holes in the valence band are given by[56,58] ,

$$n_e = 2(2\pi m_e^* kT/h^2)^{3/2} \exp[(E_f - E_c)/kT] \qquad (1.22)$$

and $$n_h = 2(2\pi m_h^* kT/h^2)^{3/2} \exp[(E_v - E_f)/kT] \qquad (1.23)$$

respectively. Here m^* represents the effective mass near the conduction band E_c for electrons and near the top of the valence band E_v for holes. E_f is the Fermi - energy. From (1.22) and (1.23) and taking $n_e = n_h$ one gets :

$$E_f = [(E_c + E_v)/2] + \frac{3}{4} kT \log(m_h^*/m_e^*) \qquad (1.24)$$

Substitution of the value of E_f from (1.24) into (1.22) or (1.23) yields :

$$n_e = n_h = 2(2\pi RT/h^2)^{3/2}(m_e^* m_h^*)^{3/4} e^{-E/2RT} \quad (1.25)$$

where E represents the energy gap between the valance and conduction bands.

Equation (1.25) is applicable to an intrinsic semiconductor in thermal equilibrium and hence the conduction equation (1.21) becomes :

$$\sigma = \sigma_0 \exp(-E/2RT) \quad (1.26)$$

where $\sigma_0 = 2e(2\pi RT/h^2)^{3/2}(m_e^* m_h^*)^{3/4}(\mu_e + \mu_h)$

1.3 Tunneling and Hopping Mechanisms in Dark Conduction

1.31 Tunneling Mechanism :

The tunneling, an out come of the quantum mechanical concepts, is a mechanism in which a particle without even acquiring enough energy can pass through a potential barrier. Riley and Willis[61] have originally proposed that the dark conduction is possible through this mechanism.

In dark conduction, the charge carriers penetrate an intermolecular potential barrier. The number of times an electron penetrates this barrier gives a measure of its drift velocity (v_{de}). If the net displacement of the electron upon going through the barrier is (a + l) then the drift velocity is given by :

$$v_{de} = \left(\frac{v_e}{2l}\right)(a+l)(P_f - P_r) \qquad (1.311)$$

where P_f and P_r are the barrier penetration ~~penetration~~ probabilities in the direction of the field and in the reverse direction respectively; l is the distance across the potential well of width a and v_e is the velocity of the electron in the $(\frac{N}{2} + 1)$th level moving between the potential wells and is equal to $\left[\left(\frac{N}{2}+1\right)\cdot\left(h/2l\,m_e^*\right)\right]$. The current density which is equal to ($n_e \cdot v_{de}$) thus becomes :

$$i = \left[2\left(2\pi m_e^* kT\right)^{3/2}/h^3\right]\left[\exp\left(-E/2kT\right)\right]\left(\frac{N}{2}+1\right)\cdot$$

$$eh(a+l)(P_f - P_r)/4l^2 m_e^* \qquad (1.312)$$

which is of the form of the conductivity equation :

$$i = \sigma_0 V \exp\left(-B/2kT\right) \qquad (1.313)$$

1.32 Hopping Mechanism :

Hopping is a process in which a charge carrier on a molecular site can move to the other by moving over the barrier between the sites via an activated state.

A simple hopping model for the dark conduction in organic solids has been applied by Pohl[62] and by Pohl and Opp[63]. In the hopping process, the motion of the carriers to the neighbouring sites is random except for the anisotropy caused by the applied field F. Hopping of the carriers depends upon the following factors :

1) The average angle of hopping with the field direction,
2) The intermolecular distance,
3) Number of the neighbouring sites,
4) Frequency of vibration in the two directions normal to the carrier motion's direction across the barrier, and
5) The barrier height.

The interaction of the carriers with vibration in the lattice may also give hopping of charge carriers without having these to cross the barrier[64]. For hopping, it is essential that the relaxation time in which the electrons hops from a site to the another must be much greater than the period of a vibration.

1.4 Polarons & Role in conduction Process in Molecular Crystals Through Tunneling and Hopping

A polaron is an entity of electron accompanied by a localised vibration which moves through the crystal under some circumstances when electron - phonon interaction leads to the electrons being trapped in a self-induced potential wells[64]. A major contribution to the polaron formation comes from the molecular vibrations. Slow intermolecular vibrations of the lattice weakly interact with the carriers and can be neglected. Siebrand[65] has considered a molecular crystal with one excess electron and calculated the binding energy of the polaron as :

$$E_b = \frac{1}{2} \sum_q M_q^2 \omega_q (\Delta x_q)^2 \qquad (1)$$

where M_q is the reduced mass of the q th oscillator; ω_q is the frequency and Δx_q is the difference between the equilibrium distances of the molecule and the ion.

By treating electron overlap as perturbation, the formation of Bloch-type bands from polarons are obtained. These bands are narrower than the corresponding electron bands by a vibrational overlap factor. Their width are approximately given by :

$$J_\upsilon(\upsilon^\circ+\upsilon) \simeq J_k (E_b/\hbar\omega)^{\upsilon^\circ+\upsilon} [\exp(-E_b/\hbar\omega)] \qquad (2)$$

where v° and v are vibrational quantum numbers of the neutral molecule and the ion respectively and J_k is the half width of one electron band in the tight-binding approximation. Thus, there exists a series of polaron bands below the electron band.

At a very low temperature, carriers will occupy the lowest - lying polaron band and will have very low mobility restricted by the lattice phonon scattering. In this case $\mu \propto T^{-3/2}$ to T^{-1}. Higher polaron bands will be populated with the rise in temperature (T) and the effective band - width will exponentially increase with T. As T approches E_b/k, the mobility is governed by the distribution between polaron bands and the electron band and the transport of carriers becomes an activated hoping process. $(d\mu / dT)$ gradually changes the sign. As T exceeds E_b/k, the distribution over the bands is approximately independent of T and the temperature dependence of μ becomes as that at low temperature.

For the strongly bound polarons, we have $E_b \quad J_k$ and $E_b >> \hbar\omega >> 2\pi J_\omega$. An electron should then remain on a lattice site for a much longer period than the period of vibration in order to get polaron formed. At temperature E_b/k the polaron will dissociate thermally. When the width of the polaron band is approximately equal to $\hbar\omega$, the electron will not remain on the lattice site longer than the period of vibration and so it

can be said to dissociate kinatically. Siebrand applied this notion to the case in which the carrier moves by activated hopping process from a polaron band to the electron band and showed that $\mu < 1\ cm^{-1}\ volt^{-1}\ sec^{-1}$.

When the carriers interact strongly with molecular vibrations, this interaction whould be included in zeroth order carrier wave functions and so the seperation into electronic and vibrational parts of the total wave function for the crystal is no longer possible. The electron vibration interaction results in a narrower band - widths. The coupling criteria has been discussed by Ho Hao and Siebrand[66] and are generatised by Siebrand[67] in three dimensions.

Now, we will discuss tunneling and hopping of polarons briefly. When an electron is surrounded by a cloud of phonons, transition from sites j to j'results in the destruction and creation of the cloud at j and j' respectively. The electron is scattered many times during the jump due to a large number of emissions and absorptions accompanying the transition. When electron on a site is trapped in a potential well, it is to pass a barrier of height equal to the polaron biming energy. The passage may be tunneling or hopping. Tunneling applies when the vibrational sites involve only a few quanta and are well seperated while hopping applies when a large number of excited vibrational states are crowded together and consists of randomly performed

jumps. If the phonon band-width exceeds that of the polaron band, the dispersion of the lattice frequencies introduces enough randomness to annihilate the polaron band structure. The crystal may, then, behave like a liquid drop in this circumstance with respect to the carrier transport (through hopping) and the mobility should not change much upon melting contrary to that generally observed[60]. Thus, the mechanism of carrier transport in molecular crystals is thought to be polaron tunneling. Tunneling is analogous to wave like motion and the translational symmetry of the lattice necessarily implies the same[68]. The thermal motion may however, destroy the translational symmetry.

1.5 Adsorption Process

When a gas is allowed to come to equilibrium with a solid or liquid surface, the concentration of the gas molecules is always found to be greater in the immediate vicinity of the surface than in the free gas phase, regardless of the nature of the gas or surface. The process by which this surface excess is found is termed "ADSORPTION"[69,70]. There are two types of adsorption ; Physical and Chemical, depending on the nature of the forces involved. Physical adsorption, also termed Vander waals adsorption (binding energy of the order of 10^{-2} ev[70-73]) is caused by molecular interaction forces whereas chemical adsorption (binding energy of the order of several ev[70-73]) involves transfer of

electrons i.e. a state of chemical binding between the solid and the gas. The shapes of the adsorption isotherms[69,70], which are the plots of free energy change as a function of the amount of vapour adsorbed, can also yield qualitative information about the adsorption process. Physisorption is of interest in its suggested role as a precursor stage of chemisorption and in the evaluation of the adsorption mechanism[71].

Various attempts have been made to understand the nature of the vander waals forces[74-95] resulting in several formulations of the interactions. The method presented by Pollard[83] uses classical dipole - dipole interaction[77] between the gas molecule and the solid substrate in the evaluation of the vander waals' interaction and Heitler-London coupling scheme in the estimation of the repulsive term. The calculation of Mavroyannis[80], on the other hand is based on the work of Lifshitz[82] and Dzyaloshinskii et al[79], where a uniform continuous model of the surface is employed and ignores the presence of the repulsive forces entirely. The neglect of repulsive contribution to the energy of physisorption, the assumption of an equilibrium position for the physisorbed atom, and the approximations introduced in the expression for the energy cause serious difficulties[85]. For atomic vapour adsorption on metal surface, the attractive and repulsive contributions to the physisorption interaction energy are derived from the assumption of weak coupling between an atom and a metal surface[86].

The effect of adsorption and desorption of oxygen on the oxides of copper, nickel, manganese and zinc of extremely high purity[130] shows that the rate of adsorption of oxygen is a function of the number of vacant sites present in the surface. They have considered the first order, second order and exponential relationships i.e. $\frac{dN_t}{dt} = KN_t$, $\frac{dN_t}{dt} = KN_t^2$ and $\frac{dN_t}{dt} = ae^{-\alpha N_t}$ respectively, where N_t is the number of atoms adsorbed at time t; K, a and α are constants. Derivation of these relationships were performed by many authors by measuring directly the amount of gases adsorbed[136,137(a),(b)]. Gray et al[130] have shown that the exponential plot is a better overall approximation for the complex order process than for one obeying the first order kinetics or a combination of the second and first order processes at the initial and final period of adsorption respectively. In working out the kinetics, the assumption made by Gray et al is that the measured conductivity is either proportional to $\sqrt{N_t}$ or to N_t. In some cases of vapour adsorption, adsorption time curves follow the Roginsky - Zeldovich equation in a slightly modified form.

Adsorption of water on some proteins followed the Brunauer - Emmett - Teller (B.E.T.) isotherm equation[133] i.e.

$$\left[X/V(1-X)\right] = \left[1/V_m c\right] + \left[(c-1)/V_m c\right] . X \quad (1.51)$$

where X is the relative pressure, V is the adsorbed vapour

expressed in gms per 100 gm of the adsorbate. By plotting the data according to this equation, V_m and C can be derived from slope and intercept. Here V_m is the quantity of adsorbed vapour corresponding to the monolayer and C is a constant related to the heat of adsorption. Heats of entropies of adsorption can be evaluated by thermodynamic methods. At low coverages, the strongly negative entropies of adsorption in many proteins indicated by localisation of water molecules on polar groups. Positive entropies of adsorption at low coverages were observed for crystalline albumin which is attributed to the configurational changes induced in the protein chains. The subject of adsorption thermodynamics has been developed by Hill[133(a),(b)].

1.6 Theory of the Compensation Effect

The compensation rule or Meyer-Neldel rule, a linear relationship between the logarithm of the pre-exponential factor (σ_0) and the activation energy (E), has been a subject of great interest[40-50, 96-99] and controversy[100-104] for many years. It was first noted by Many et al[96] that for a variety of polynuclear hydrocarbons and phthalocyanines, the value of varied over a range of 10^{23} and hence a rough correlation existed between the E's and σ_0's. Gutmann and Lyons[97] showed a linear relationship of the form:

$$\log \sigma_0 \simeq \alpha E + \beta \qquad (1.61)$$

for an entire class of substances where α and β are

constants. Cardew and Eley[98] have found a similar type of correlation to hold for a series of amino acids and proteins. Rosenberg et al[40] showed evidence that this formula is valid for a single organic substance when E is varied by hydration and complex formation.

Several mechanisms, namely, the charge carrier injection model[105], the tunneling of electrons from thermally activated energy levels through intermolecular potential barriers[43], thermally assisted tunneling (FAT) and pseudointrinsic conduction[106] were discussed by a number of authors[41-45, 105, 106] for the interpretation of the compensation effect. A simple quantum mechanical model Hamiltonian which described the physical picture of the 'Conferon' satisfying both the effects was proposed[42,44]. Kemeny and Mahanti[45] attempted to derive the compensation rule in the theory of rate processes within the quadratic polaron and Spin polaron models.

1.61 Charge-carrier Injection Model

A model for the generation of the charge carriers in organic substances was proposed by Green[107] which assumes injection of charge carriers at the surface of the crystal in a modification of a form of surface barrier proposed by Bardeen[108]. According to this model, the pre-exponential factor :

$$\sigma_0 \simeq n_0 (RT/h) K \qquad (1.612)$$

where n_o is the carrier density of the electrode, k is Boltzmann's constant, T is the absolute temperature, h is Planck's constant and K is the transmission co-efficient for tunneling through the barrier given by[107] :

$$\ln K \simeq -4\pi \left(\frac{2m}{h^2}\right)^{1/2} \left(\frac{2}{3Z}\right) \cdot \left[(x_1 - E_{act} + Za)^{3/2} - (x_1 - E_{act})^{3/2}\right] \qquad (1.613)$$

Here 'm' represents the electron mass, X_1 and X_2 are the work functions of the electrode and semiconductor respectively, E_{act} is the energy obtained from the slope of a $\ln\sigma$ vs. $1/T$ plot, 'a' is the barrier width and $Z = (X_2 - X_1)/a$. Assuming $E_{act} < X_1, X_2$, the right hand side of equation (1.613) can be approximated to

$$\ln K \simeq A + B E_{act} + C E_{act}^2 \qquad (1.614)$$

where,

$$A = -8\pi(3Z)^{-1}(2m/h^2)^{1/2}\left[(x_1+Za)^{3/2} - x_1^{3/2}\right] \qquad (1.615')$$

$$B = 4\pi(Z)^{-1}(2m/h^2)^{1/2}\left[(x_1+Za)^{1/2} - x_1^{1/2}\right] \qquad (1.615'')$$

$$C = -4\pi(3Z)^{-1}(2m/h^2)^{1/2}\left[(x_1+Za)^{-1/2} - x_1^{-1/2}\right] \qquad (1.616''')$$

For reasonable values of the parameters involved, the term in E_{act}^2 contributes approximately 10% - 20% of the linear term. If this quadratic term is neglected, equation (1.614) reduces to equation (1.61). For the validity of this model, X_2 must be greater than X_1 which is generally fulfilled in practice.

1.62 Electron Tunneling Model

The organic molecular solids consist of molecules with potential barriers surrounding them. For electrical conduction the electrons have to pass over or through these barriers. The first possibility requires high activation energies where as the latter requires a long time. If the effective wall height E_w is smaller than the total height E_p, the electrons can tunnel from activated levels of energy E through the potential barrier without requiring $E \simeq E_p$. Then the conductivity $\sigma(T)$ consists of three parts : (1) the temperature dependent exponential part (2) the exponential part of the barrier transmissivity and (3) a factor σ_x consisting of the non-exponential part of the barrier transmissivity and of the propagation characteristics of the electrons within the molecules. Employing the barrier transmissivity calculations of Mott and Gneddon[109]

$$\sigma(T) = \sigma_x \exp\left[-\left(\frac{2a}{\hbar}\right)(2m^* E_w)^{1/2}\right] e^{-E/2RT} \quad (1.621a)$$

for the square barrier and

$$\sigma(T) = \sigma_x \exp\left[-(4a/3\hbar)(2m^*)^{1/2}(E_W^{3/2}/E_T)\right] \cdot \exp(-E/2RT) \qquad (1.621\ b)$$

for the triangular barrier.

Here 'a' is the barrier width and m^* is the effective mass of the electron in the activated level involved in the tunneling. The barrier height E_T is equal to or less than the ionisation potential of the molecule for the square and the triangular barrier respectively. The tunneling electron will experience a potential which is the sum of the approximate coulomb potential attracting the electron to a positive ion and the potential of electron affinity of the originally neutral molecule, both varying smoothly being approximated better by the triangular than by the square barrier. For tunneling model to be satisfied, $E < E_T$ must be satisfied, otherwise there would be no tunneling and electrons would pass over the barrier. Therefore, substituting

$$E_W = E_T - E \qquad (1.622)$$

in equation (1.621) and expanding the fractional powers of E_W in a series stopping at the term linear in E gives

$$\sigma(T) = \sigma_x \exp\left[(-2a/\hbar)(2m^* E_T)^{1/2}\right] \cdot \exp\left[(a/\hbar)(2m^*/E_T)^{1/2} E\right] \exp(-E/2RT) \qquad (1.623\ a)$$

and

$$\sigma(T) = \sigma_x \exp\left[\left(-\frac{4a}{3\hbar}\right)(2m^* E_T)^{1/2}\right] \exp\left[\left(\frac{2a}{\hbar}\right)(2m^*/E_T)^{1/2} E\right] \exp\left(-\frac{E}{2RT}\right)$$

(1.623 b)

for the square and triangular barrier respectively. If $E < E_T$ but close to it, a better approximation is required.

For the materials obeying compensation rule leads to $E_T \simeq$ 2ev and 6 ev for the square and triangular barriers respectively. Only the last value i.e. 6 ev is reasonable so that the activation energies[40,99] are well below the top of the barrier in which case only the tunneling model is acceptable and is explained satisfactorily by the triangular barrier. If $m^* = 100\ m_0$, the intermolecular seperation $a \simeq 3 \times 10^{-8}$ cm which is quite justified. So the effective mass of the electron in the activated level is of the order of 100 electron masses.

1.63 Polaron Tunneling Model

An effective mass of 100 m_0, considered in the electron tunneling model, is much larger than those predicted[110,111]. In the narrow energy bands of organic semiconductors, tunneling of small polarons in thermally activated energy levels is possible. Holstein[112] deduced the mobility :

$$\mu = (e l^2 \tau / kT)(J_\omega / 2\hbar)^2 \qquad (1.631)$$

where l is the periodicity length, τ is the life-time of the polaron in a band state and $J_\sim$ is the small polaron band-width. Equation (1.631) is valid for $T < \theta/4$, where θ is the Debye temperature[112], and also satisfies the condition

$$J_\sim \ll kT \qquad (1.632)$$

so that all states in the polaron band are equally populated.

Two cases of small polaron theory may arise. The perturbation case for which $J < \hbar\omega_0$,

$$J_\sim = 2J \exp(-\gamma) \qquad (1.633\ a)$$

and the adiabatic case for which $J > \hbar\omega_0$

$$J_\sim = 2\hbar\omega_0 \exp(-\gamma) \qquad (1.633\ b)$$

and

$$\gamma = E_b/\hbar\omega_0 \qquad (1.633\ c)$$

E_b is the polaron binding energy, ω_0 is the optical vibration frequency and J is the hopping integral. The polarons which exist in a molecular lattice may have strong ionic properties upon complex formation. In an ionic system the coupling can be expressed using the effective dielectric constant as :

$$1/K_p = 1/K_\infty - 1/K \qquad (1.634)$$

where K and K_∞ are the static and high frequency dielectric constants

respectively. The coupling in a molecular lattice can also be expressed[113] in terms of K_p. Assimilating both effects into the effective dielectric constant, the binding energy of small polaron becomes :

$$E_b = \tfrac{1}{2} \left(e^2 / K_p r_p \right) \qquad (1.635)$$

where 'r_p' is the radious of the small polaron and may be less than half the periodicity length 'l'. The change in the polaron binding energy due to complex formation is then given by :

$$E_b - E_b^{(o)} = \tfrac{1}{2} \left(e^2 / r_p \right) \left[\left(1/K_p \right) - \left(1/K_p^{(o)} \right) \right] \qquad (1.636)$$

where the superscript (o) signifies the original semiconductor. K_∞ and $K_\infty^{(o)}$ are related to the refractive index, which is probably invarient, so that

$$E_b - E_b^{(o)} = \tfrac{1}{2} \left(e^2/r_p \right) \left(1/K^{(o)} \right) - \left(1/K \right) \qquad (1.637)$$

similarly

$$E - E^{(o)} = \left(- e^2/r_p \right) \left[\left(1/K^{(o)} \right) - \left(1/K \right) \right] \qquad (1.638)$$

where $E^{(o)}$ and E are the activation energy before and after complex formation. Substituting equation (1.638) in

equation (1.637), one gets :

$$E_b = E_b^{(o)} + \frac{1}{2}\left(E^{(o)} - E \right) \qquad (1.639)$$

or, $E + 2E_b = E^{(o)} + 2E_b^{(o)} \Rightarrow$ invariant (1.6310)

Now, the conductivity can be written as

$$\sigma = n e \mu = N \exp(-E/2kT)\, e\mu \qquad (1.6311)$$

where N is the number of electrons per unit volume available for activation. Making use of the equations (1.631) and (1.633) and (1.630), equation (1.6311) can be written as :

$$\sigma = \left(\frac{N e^2 l^2 \tau}{kT}\right)\left(\frac{J}{\hbar}\right)^2 \exp\left[\frac{2E_b^{(o)} + E^{(o)}}{\hbar\omega_o}\right] \exp\left\{E\left[(\hbar\omega_o)^{-1} - (2kT)^{-1}\right]\right\} \qquad (1.6312\,a)$$

for the perturbation case and

$$\sigma = \left(\frac{N e^2 l^2 \tau}{kT}\right)\omega_o^2 \exp\left[-\frac{(2E_b^{(o)} + E^{(o)}}{\hbar\omega_o}\right] \exp\left[E\left\{(\hbar\omega_o)^{-1} - (2kT)^{-1}\right\}\right] \qquad (1.6312\,b)$$

for the adiabatic case.

For the perturbation case, J and thus the rigid lattice

band-width depends[43] on the depth of the activated energy level below the top of the tunneling barrier and on the shape and width of the barrier. From equation (1.623), the formula for J is given by[43]

$$J^2 = J_o^2 \exp\left[(2a/\hbar)(2m^*/E_T)^{1/2} E\right] \qquad (1.6313)$$

where

$$J_o^2 = J_o'^2 \exp\left[(-4a/3\hbar)(3m^* E_T)^{1/2}\right] \qquad (1.6314)$$

J_o being the hopping integral for E = 0.

Substituting equation (1.6313) in equation (1.6312 a) we get :

$$\sigma = \frac{Ne^2 l^2 C}{RT} \left(\frac{J_o}{\hbar}\right)^2 \exp\left(-\frac{(2E_b^{(o)} + E^{(o)})}{\hbar\omega_o}\right) \cdot \exp\left[E\left\{(\hbar\omega_o)^{-1} + \left(\frac{2a}{\hbar}\right)\left(\frac{2m^*}{E_T}\right)^{1/2} - (2RT)^{-1}\right\}\right] \qquad (1.6315)$$

Therefore equations (1.6312 b) and (1.6315) are in the form of the compensation law.

1.64 Electronic states - Vibrational States Coupling Model

Kemeny and Goklany[42] noted that at experimental temperatures, small polaron tunneling is not possible, so that within

the assumption that conductivity is due to small polaron motion, hopping rather than tunneling must be the dominant conduction mechanism. But polaron hopping can not lead to the compensation effect via the mobility alone. Thus both the electron occupancy number 'n' and mobility ' μ ' are thought to be the sources for the compensation law. The mechanism postulated by Kemeny and Goldani is an interaction between the electrons and the vibrational motion which is able to explain both the enormous enhancement in the conductivity and the compensation effect. A change in electronic state gives rise to an activation entropy Δs because of a change in vibrational frequencies probably associated with the conformational changes[116] and this would contribute to the prefactor, giving its required enhancement.

Kaplan and Mohanti[44] considered only the contribution of 'n' to explain the conductivity enhancement and the compensation effect. Consider a solid made-up of N_M larger organic molecules. Each molecule has only two electronic states with energies $\varepsilon_1 < \varepsilon_2$ plus vibrational levels, and the total number of electrons is 1 per molecule. The vibrational frequencies are supposed to be different depending on the occupancy of these electronic states. Also, electron spin is neglected for simplicity. Then the physical picture of 'conformon' is clearly embodied in the Hamiltonian :

$$H = \sum_{i\nu} \varepsilon_\nu n_{i\nu} + \sum_{iK} \omega_K (n_{i1}, n_{i2}) (N_{iK} + \tfrac{1}{2}) \quad (1.641)$$

where $i = 1, 2, \cdots \cdots N$ labels the molecules; $\nu = 1, 2$ labels the one-electron states with energies $\varepsilon_1, \varepsilon_2$; $\omega_K(n_{i1}, n_{i2})$ is the vibrational frequency for mode K (with $\hbar = 1$); and, as the notation indicates, ω_K depends on the electron occupancy numbers $n_{i\nu}$ which have the possible values $n_{i\nu} = 0, 1$. N_{ik} labels the states of excitation of the k th vibrational mode on the i th molecule and takes on the values $0, 1, 2, \cdots \infty$. $E = (\varepsilon_2 - \varepsilon_1)$ is the electronic energy gap. If $E \simeq 1$ ev and the temperature is around room temperature and below, the number of electrons per molecule to the upper or conduction band is

$$\bar{n}_2 \simeq \exp\left[-\beta/2 (E + \Delta f_u)\right] \quad (1.642)$$

where Δf_u is the change in vibrational free energy in creating unbound electron-hole pair. In the low and high temperature region

$$n = n_0 \exp\left(-E_{eff}/2kT\right) \quad (1.643)$$

where E_{eff} is the modified activation energy. ω_K which contributes mainly to the free energy changes is ω_c. For $kT > \omega_c$,

$$\left.\begin{aligned} E_{eff} &\simeq E, \\ n_0 &\simeq \exp\left(\frac{S_a}{k}\right) \end{aligned}\right\} \quad (1.644)_c$$

and for $kT < \omega_c$,

$$E_{eff} \cong E + \tfrac{1}{2}\sum \left[\omega_k(1,1) + \omega_k(0,0) - 2\omega_k(1,0) \right]$$

$$n_0 \cong 1 \qquad (1.645)$$

Here, $$\frac{S_a}{k} = -\frac{1}{2}\sum_k \ln \frac{\omega_k(1,1)\,\omega_k(0,0)}{[\omega_k(1,0)]^2} \qquad (1.646)$$

Thus, an activated behaviour with an enhanced n_0 is obtained for high temperature range. Again $S_a > 0$, i.e. there is entropy enhancement if $\{\omega_k(1,1)\,\omega_k(0,0)/[\omega_k(1,0)]^2\} < 1$ which means that if there is an average softening of the vibrational modes upon the creation of the carriers. In the low temperature range, the entropic enhancement disappears, and the activation energy is modified by the zero-point energy.

In order to obtain compensation behaviour from this model, the vibrations in both the electronic energy gap E and the activation entropy S_a in going from one member to another within a given class is considered.

1.65 Quadratic Polaron Model

A theory for electronic charge transport as involved in kinetic processes has been derived by Kemeny and Mahanti[45] for quadratic generalisation of Holstein's one dimensional linear polaron theory[112]. To deduce the equation for the transition

rate per unit time they considered a system consisting of one electron and two possible sites (i = 1,2) in which the electron can reside. There are N oscillators corresponding to each site and J is the electronic transfer matrix element between two sites. Thus, in absence of the electron the potential energy of the system of N oscillators associated with the ith site, V_i, is given by

$$V_i = K \sum_{\mu=1}^{N} X_{i\mu}^2 \qquad (1.661)$$

where $X_{i\mu}$ is the displacement of the μ th oscillator from its equilibrium position and K is the force constant.

When the electron is present at the i th site it couples with the N oscillators associated with that site and there is an extra energy Φ_i which is given by :

$$\Phi_i = B \sum_{\mu=1}^{N} X_{i\mu}^2 - A \sum_{\mu=1}^{N} X_{i\mu} \qquad (1.662)$$

which is a generalisation of Holstein's linear polaron model in which B = 0 and N = 1. The probability that the electron initially at the site 1 goes to the site 2 is given by :

$$\left.\begin{aligned} i \frac{\partial a_1(t)}{\partial t} &= J a_2(t) + \Phi_1(t) a_1(t) \\ i \frac{\partial a_2(t)}{\partial t} &= J a_1(t) + \Phi_2(t) a_2(t) \end{aligned}\right\} \qquad (1.663)$$

where a_i (t) is the electronic amplitude associated with the i th site at time t and Φ_i (t) is a function of time through $X_{i\mu}$ (t). Equation (1.653) is valid only in the perturbation limit, i.e., for small J. In this limit, the electronic transition rate is obtained after carrying out the thermal average over all possible oscillator co-ordinates and velocities. At time $t = t_c$, where t_c is the coincidence point,

$$\Phi_1(t) = \Phi_2(t) \qquad (1.654)$$

and can be written as

$$\Phi(t_c) \equiv \Phi_1(\cdots x_{1\mu}(t_c)\cdots) - \Phi_2(\cdots x_{2\mu}(t_c)\cdots) = 0 \qquad (1.655)$$

which represents a (2N - 1) dimensional surface of stationary phase (SSP) in the space of oscillator coordinates ($\cdots x_{1\mu}\cdots$, $\cdots x_{2\mu}\cdots$). The linear term in equation (1.652) can be replaced by a simple transformation :

$$y_{i\mu} = x_{i\mu} - \frac{A}{2B} \quad , \quad i = 1, 2 \cdots \qquad (1.656)$$

Making use of equation (1.656), the equation for SSP may be denoted by

$$\Phi(t_c) = B\left[r^2(t_c) - s^2(t_c)\right] = 0 \qquad (1.657)$$

where

$$r^2 = \sum_{\mu=1}^{N} Y_{1\mu}^2 \quad \text{and} \quad S^2 = \sum_{\mu=1}^{N} Y_{2\mu}^2 \qquad (1.658)$$

The variations in r (t) and s (t) are linear in 't' in the neighbourhood of t_c and

$$\phi(t) = \phi(t_c) + \dot{\phi}(t_c)(t - t_c) \qquad (1.659)$$

The probability of a site jump per coincidence[112] W_c is given by

$$W_c = 2\pi J^2 / \dot{\phi}(t_c) \qquad (1.6510)$$

For large J, the perturbation approximation for W_c breaks down and the adiabatic approximation[112] is used.

W_c depends upon the positions and velocities of the 2N oscillators associated with the two sites. The transition rate per unit time is obtained from the probability that a coincidence occors in the interval t and t + dt for a specific position and velocity configuration of the 2N oscillators and then carry out a thermal averaging over all possible configurations which is valid in the perturbation limit.

For a particular configuration $X_{1\mu}(t)$, $X_{2\mu}(t)$, $v_{1\mu}(t)$, $v_{2\mu}(t)$, $\mu = 1, N$; the probability P_c that a

coincidence will occur during the time interval t and (t + dt) is given by the proportionality :

$$P_c \propto \delta(\Phi_1 - \Phi_2)(\dot{\Phi}_1 - \dot{\Phi}_2) \qquad (1.6511)$$

The transition rate per unit time, R, is given by

$$R = F/Z \qquad (1.6512)$$

and

$$F = \frac{2\pi J^2}{\hbar B}(\pi/2)^t \left[\frac{\pi}{\beta(K + B/2)}\right]^{N-1} \cdot \exp\frac{\beta N A^2}{2B}\left[\frac{K}{\beta}\left(\frac{K}{K + B/2}\right) - \left(\frac{K}{B} - \frac{1}{2}\right)\right] \qquad (1.6513)$$

where t = 1 if N is even and t = 0 if N is odd. Then

$$Z = \left(\frac{\pi}{K\beta}\right)^{N/2}\left(\frac{\pi}{\beta(K+B)}\right)^{N/2}\exp\left[\frac{\beta N A^2}{4(K+B)}\right] \qquad (1.6514)$$

In the theory of rate processes[116,116], the transition rate per unit time, R is given by

$$R = K\nu \exp\left[-\beta \Delta E^P + \frac{\Delta S^P}{R}\right] \qquad (1.6515)$$

where K is a transmission coefficient; ΔE^P and ΔS^P are the activation energy and entropy respectively, and the frequency ν is

given by $h\nu = RT$. Considering equations (1.6512), (1.6513) and (1.6514) and comparing with equation (1.6515) one gets :

$$\left.\begin{aligned} \frac{\Delta S^P}{R} &= N \log\left[\sqrt{K(K+B)}/(K+B/2)\right] \\ \Delta E^P &= \tfrac{1}{4} NA^2\left[\frac{1}{K+B} - \frac{1}{2K+B}\right] \end{aligned}\right\}$$

and

$$K\nu = 2\left(\frac{\pi}{2}\right)^{\frac{1}{2}} \frac{\beta J^2}{\hbar}\left(\frac{K}{B} + \frac{1}{2}\right) \qquad \left.\vphantom{\begin{aligned} a \\ b \end{aligned}}\right\} \text{(1.6516)}$$

From equation (1.6516) it is evident that if $B \neq 0$, it is important to have a nonzero value of A (linear coupling) to get an activation energy which is always positive whether B is positive or negative. For $B << K$, the activation energy is

$$E_a = \frac{NA^2}{8K}\left[1 - \frac{6B}{K}\right] \qquad \text{(1.6517)}$$

For positive B (hardening), E_a decreases, whereas for negative B (softening), E_a increases. The activation entropy is negative both for $B > 0$ and $B < 0$. The linear term does not contribute to the activation entropy. Thus, the quadratic polaron model hints out a transition rate which is always decreased by the entropy effect. Both ΔS^P and ΔE^P are proportional to N which provides the compensation rule and yields a negative compensation temperature $T_c = \frac{\Delta E^P}{\Delta S^P}$

1.66 Spin Polaron Model

Spin polaron or magnetic polaron model involves the coupling of electrons with a set of spins.

Let us consider two electronic sites each coupled to N spins μ_{ip} ($i = 1,2$ and $P = 1, \cdots N$) each of which can take two possible orientations, i.e., $\mu_{ip} = \pm 1$. In the absence of the electron the energy of the spins associated with the i th site, V_i, is given by

$$V_i = -B \sum_{p=1}^{N} \mu_{ip} \qquad (1.661)$$

where B is some sort of magnetic field which tends to order all the spins in one specific direction. If an electron is present at the i th site, then it couples to the N spins associated with that site and the additional interaction energy between the electron and the spins, Φ_i, is given by

$$\Phi_i = 2B \sum_{p=1}^{N} \mu_{ip} \qquad (1.662)$$

Therefore, the absence or presence of an electron leads to equally strong but oppositely oriented magnetic fields on the spins.

So the transition rate per unit time, R, is proportional to $\Gamma / _{B}$ and is given by

$$R = \frac{J^2}{2B\hbar} \left\{ \lfloor 2N / (\lfloor N)^2 \right\} \left(e^{-\beta B} + e^{\beta B} \right)^{-2N}$$

(1.663)

Equation (1.663) shows that, in spin polaron model, the transition rate R is activated only for temperatures $KT << B$, whereas for $KT \gg B$, there is no activation energy. It is due to the fact that at high temperature, both sites are essencially disordered and appear identical from an electron's point of view. At low T and large N,

$$R = K\nu \; e^{\Delta S^P / K} \; e^{-\Delta E^P / KT}$$

(1.664)

comparing equations (1.663) and (1.664) we have,

$$\left.\begin{aligned} K\nu &= \pi J^2 / hB, \\ \frac{\Delta S^P}{K} &= 2N \ln 2 \\ \text{and} \quad \Delta E^P &= 2NB \end{aligned}\right\} \qquad (1.665)$$

Here, both ΔS^P and ΔE^P are positive and proportional to 2N following a positive compensation temperature $T_c = \frac{B}{\ln 2}$. The activation energy 2 NB corresponds to flipping of half the total number of spins at both sites.

CHAPTER - 3

EXPERIMENTAL -- SET-UP -- PROCEDURE

In this chapter, we describe the general experimental techniques used in the present investigation on the electrical properties of organic semiconductors. Details of any particular experimental procedure will be described in conjunction with the discussions of the results thereby obtained in chapters 3 and 4.

1. Chemicals

The Eastman Organic Chemicals, nitro-aromatic semiconductors used in this investigation are 9-nitroanthracene, 2-nitrofluorene 1,4 dinitronaphthalene, 1,3,5-trinitrobenzene, o-, m- and p-nitrobenzoic acids which have been recrystallised several times from purified solvents before use. The organic liquids used were of spectrograde quality of B.D.H. and E. Merck. The teflon spacers and the conducting glass electrodes were obtained from Dielectric Corporation (U. S. A.) and Fisher Scientific Co. (U. S. A.) respectively.

2. Preparation of the Conductivity Cell

Applying the usual procedures[33,34,117,118], the conductivity sandwich cells were prepared in air by putting about 5 mgs of the

semiconducting materials on a clean stainless steel flat electrode surface in safe light illumination. Two teflon spacers, 2 mils (0.005 cm) thick, were positioned near the edges of the electrode, and the powdered crystals were flattened by gently rotating the conducting glass electrode with the conducting side in contact with the specimen. The teflon spacers maintained the seperation between the electrodes. Two spring clips were fixed at a moderate pressure to the ends of the electrodes in order to maintain the sandwich cell.

3. The Experimental Arrangement

The experimental set-up (Fig. 2.1) for the studies of semiconductivity is similar to that of Rosenberg et al[36,113]. The sandwich cells were placed in a conductivity chamber made of brass and fashioned entirely with teflon. (all the electrical surface leakage parts were also of teflon). The stainless steel electrode was placed on a thermal copper bar platform in good thermal contact through thermal paste and thus the temperature of the cell could be controlled from out side. A d.c. voltage of 22.5 volts from dry batteries was applied across the cells. There was a gas inlet and an out-let in the chamber for gas adsorption study and an arrangement for connecting the out-let with a suction pump. The chamber atmosphere could circulate freely through the opposite open sides of the sandwich cell.

FIGURE - 2.1

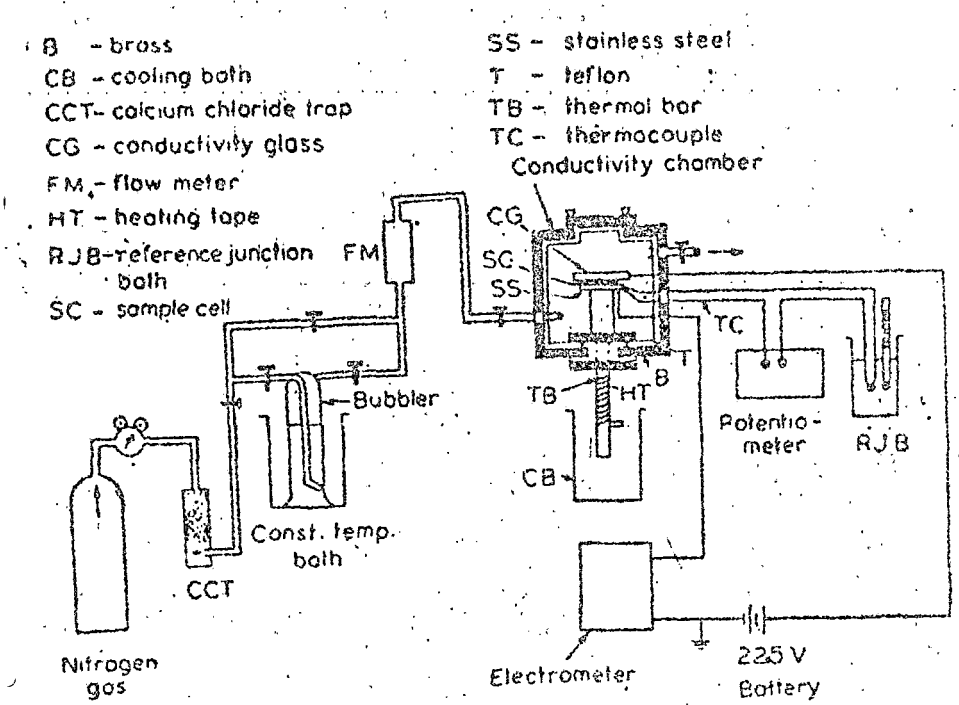

A schematic diagram of the apparatus used to study the effects of the adsorbed vapours on the conductivity of the nitroaromatic semiconductors.

Temperature measurements were made using a copper-constantan thermocouple attached at the top of the metal electrode and a millivolt potentiometer of Toshniwal Brothers Pvt. Ltd., India. The semiconduction currents were measured with an electrometer amplifier EA 813 of the Electronic Corporation of India Ltd. In order to eliminate the effects of oxygen, water vapour or any other vapours or gases adsorbed by the sample before experiment, the chamber was thoroughly flushed with dry nitrogen gas and the sample was then given repeated heating and cooling treatments in nitrogen atmosphere over the temperature range to be studied.

To pass various vapours inside the chamber, dry nitrogen gas was used as a carrier which was passed through a bubbler containing the organic liquid kept at a required temperature to maintain a fixed partial vapour pressure less than the saturation vapour pressure at sample cell temperatures. For desorption studies, dry nitrogen gas was allowed to pass directly through the chamber. The measurement of dark currents at a constant or different cell temperatures was carried out maintaining the cells in nitrogen, vacuum or different ambient atmospheres according to the experimental requirements.

CHAPTER - 3

ADSORPTION AND DESORPTION PROCESSES IN SOME NITROAROMATIC SEMICONDUCTOR-VAPOUR SYSTEMS : VAPOUR PRESSURE DEPENDENCE AND KINETIC ANALYSIS

1. Introduction

Adsorption of chemical vapours or gases produces a pronounced increase in the semiconduction currents of both organic[36,117,119-126] and inorganic[127-131] solids. It has been observed[36,117,119, 132] that the conductivity change is generally reversible i.e. the original vacuum or nitrogen atmosphere values are obtained by gently pumping the conductivity chamber or simply by flushing the chamber by dry nitrogen. This implies that the gas or vapour molecules are bound to the surface of semiconductor molecules by weak coupling forces[144]. In some cases, when the process is not efficiently reversible or the original value is not even regained, strong bound complexes are formed[133]. In polyenes,[134,135] adsorption and desorption kinetic analysis shows that the weakly bound complexes are formed and the adsorption and desorption is a 'two-stage process'.

Roginsky - Zeldovich (R - Z) equation[136,137] in a modified

form was applied to interprete the kinetic data in cases of hydration of proteins[133], adsorption of gases on β - carotene[117] and some linear long chain polyenes,[134,135] which may be written as :

$$dm/dt = A \exp\left[-\beta m / RT\right] \qquad (1.1)$$

where A and β are constants at a particular pressure. The derivation of E - S equation assumes that the rate of adsorption possesses an activation energy which increases linearly with the amount of the adsorbed gas or vapour. It has also been shown with a good degree of certainty that at a constant temperature and for lower percentage of gas adsorption, conductivity increases exponentially with the amount adsorbed.

It appears that the kinetic studies can throw much light on the nature of interaction and also on the process involved during adsorption and desorption of vapours on the semiconductor. We have examined the adsorption and desorption kinetics in a number of nitroaromatic semiconductor-vapour systems and found that along with a general two stage process in some cases of vapour adsorption a different three stage process is also operative.

In this chapter, we present our results followed by discussions on how the conductivity depends on the pressure of the

adsorbed vapour, the validity of R = Z equation and finally on the possible models for adsorption processes.

2. Experimental and Results

2.1 The effect of adsorption of vapours on the semiconduction current of the nitroaromatics :

The effects of adsorption of a series of vapours were studied in the usual manner as described in the previous chapter. The sandwich cell was temperature-cycled and dry nitrogen gas was allowed to pass through the chamber to desorb any vapour or gas adsorbed by the sample prior to the experiment. The cell was then kept at a constant temperature and the flow of the carrier gas, dry nitrogen, was maintained through the bubbler containing the reagent liquid at a constant temperature to attain a required vapour pressure. After a short pulse, when the powdered sample started adsorbing the vapour from the chamber atmosphere, the current increases and finally attains a saturation value after some time in most of the vapour - semiconductor systems. In some cases, the current enhancement was by several orders of magnitude. The result of such a measurement for vapour adsorption in 9-nitroanthracene, 1,4-dinitronaphthalene, 1,3,5-trinitrobenzene; 2-nitrofluorene; O-, m- and p- nitrobenzoic acids is shown in Fig. 3.1 - 3.7. When the chamber was flushed with dry nitrogen gas,

FIGURE - 3.1

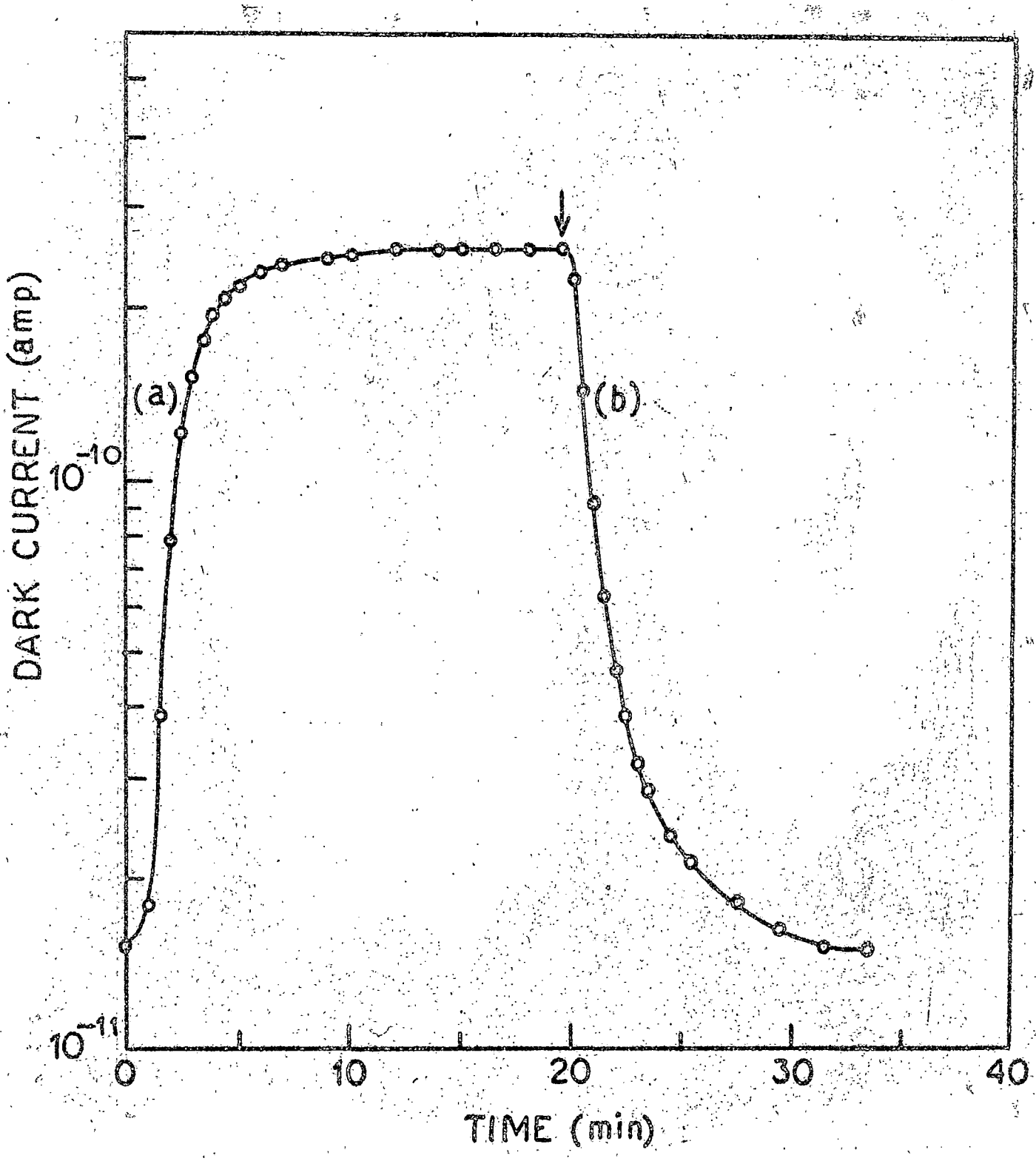

The change in dark current in a 9-nitroanthracene powder cell kept at 22°C with (a) adsorption and (b) desorption of carbontetrachloride vapour at 72.5 mm pressure.

FIGURE - 3.2

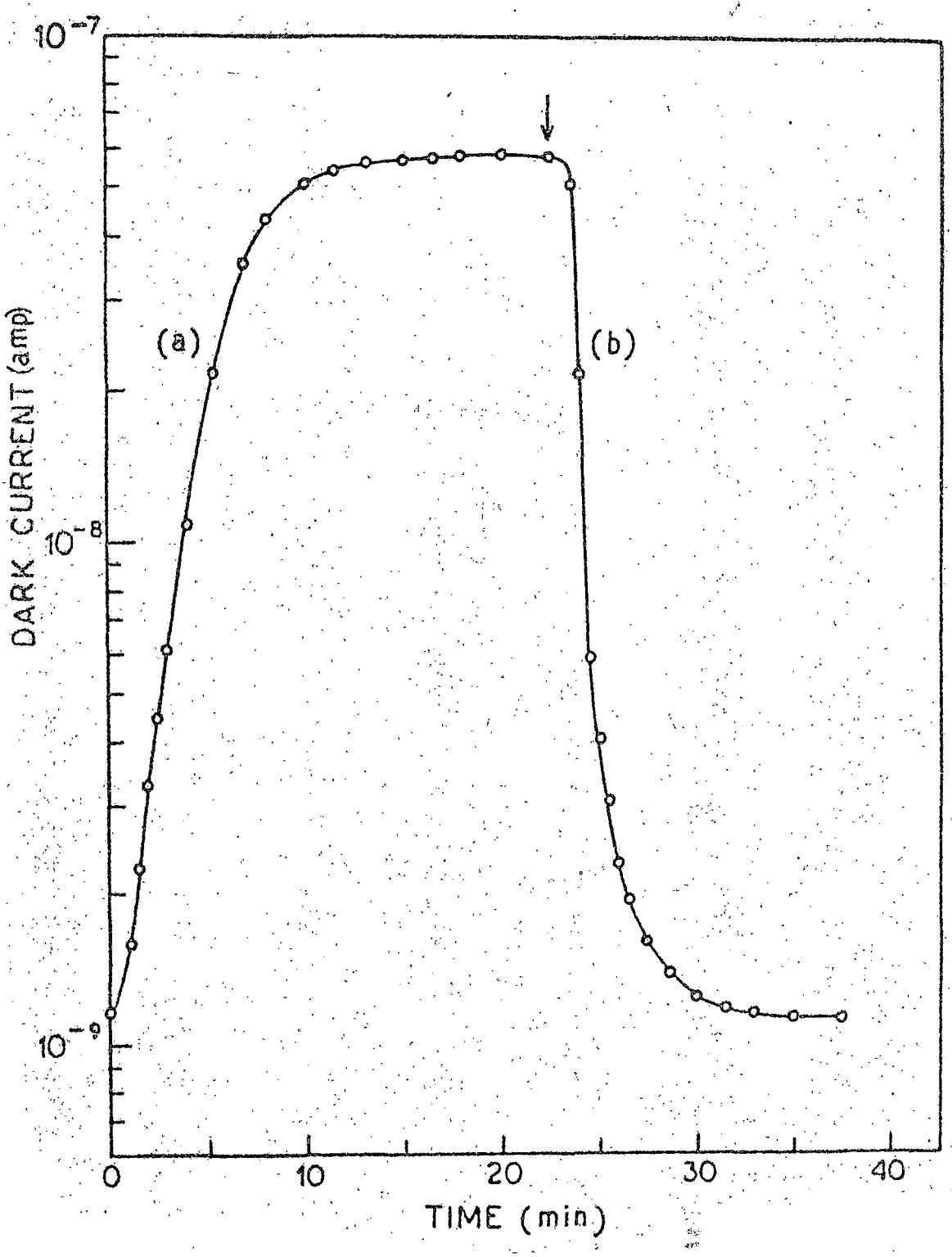

The change in dark current in a 1,4-dinitronaphthalene powder cell kept at 22°C with (a) adsorption and (b) desorption of methanol vapour at 71.3 mm pressure.

FIGURE - 3.3

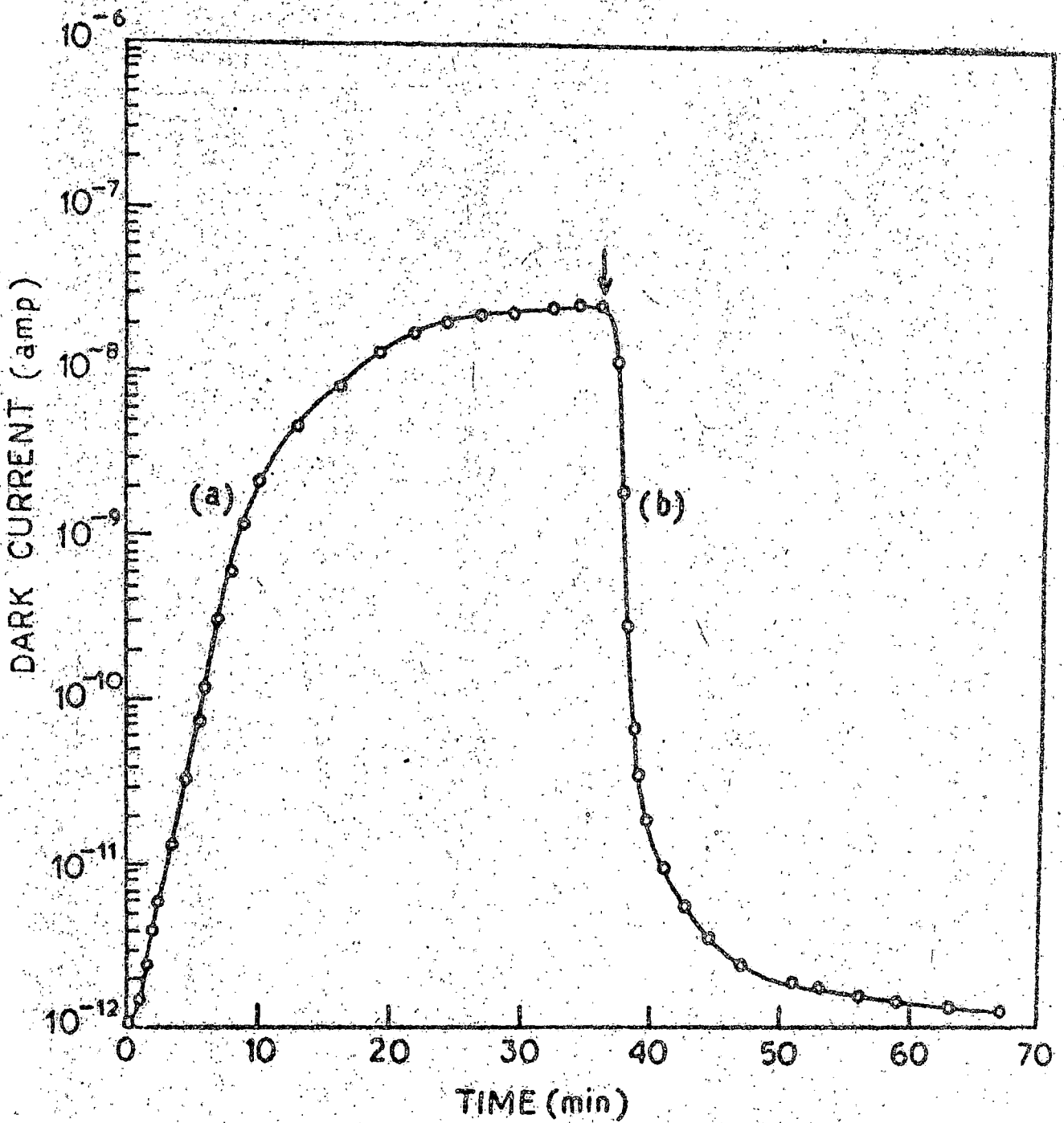

The change in dark current in a 1,3,5-trinitrobenzene powder cell kept at 22°C with (a) adsorption and (b) desorption of ethanol vapour at 38.8 mm pressure.

FIGURE - 3.4

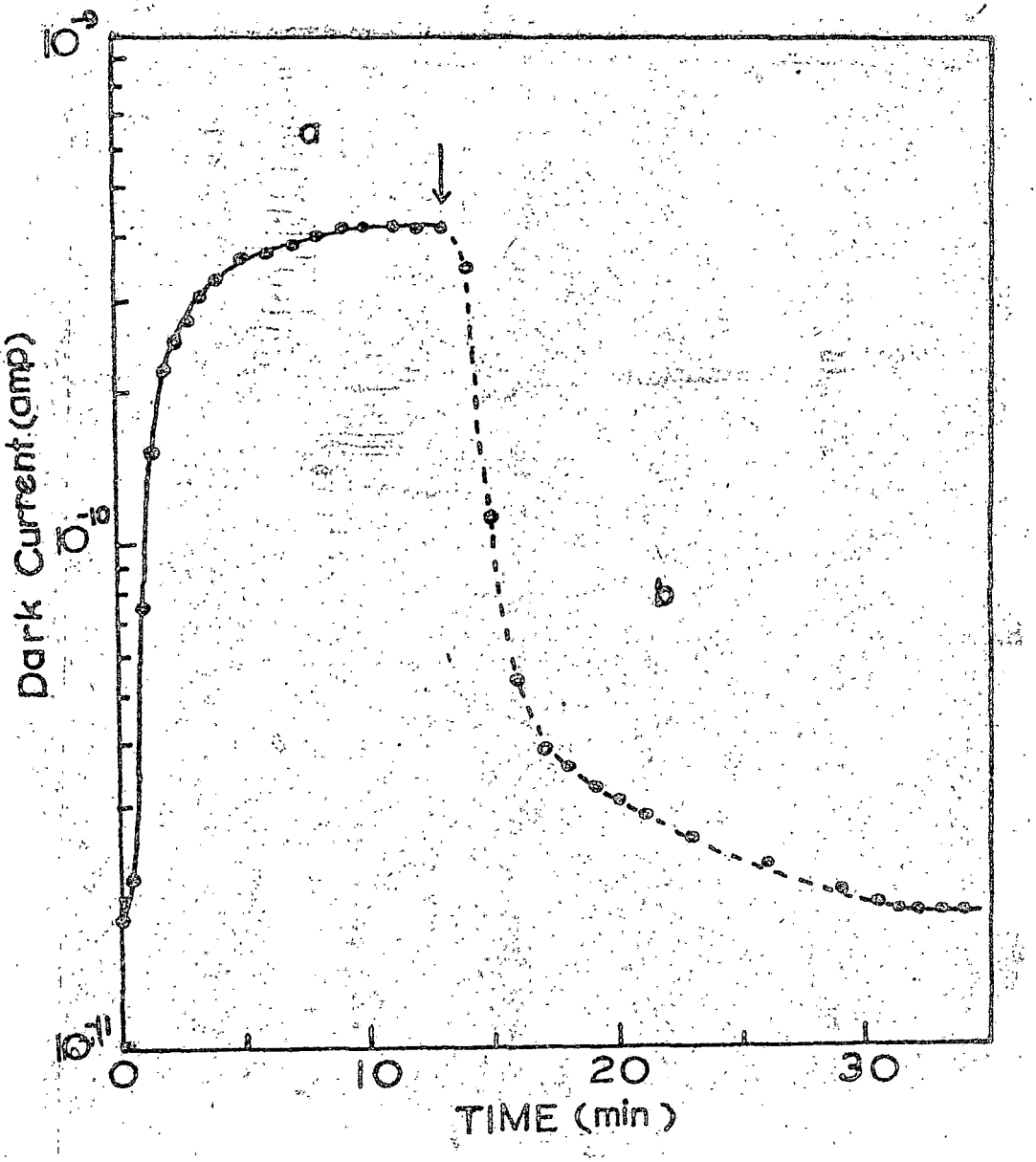

The change in dark current in a 2-nitrofluorene powder cell kept at 25°C with (a) adsorption and (b) desorption of ethylacetate vapour at 55 mm pressure.

FIGURE - 3.5

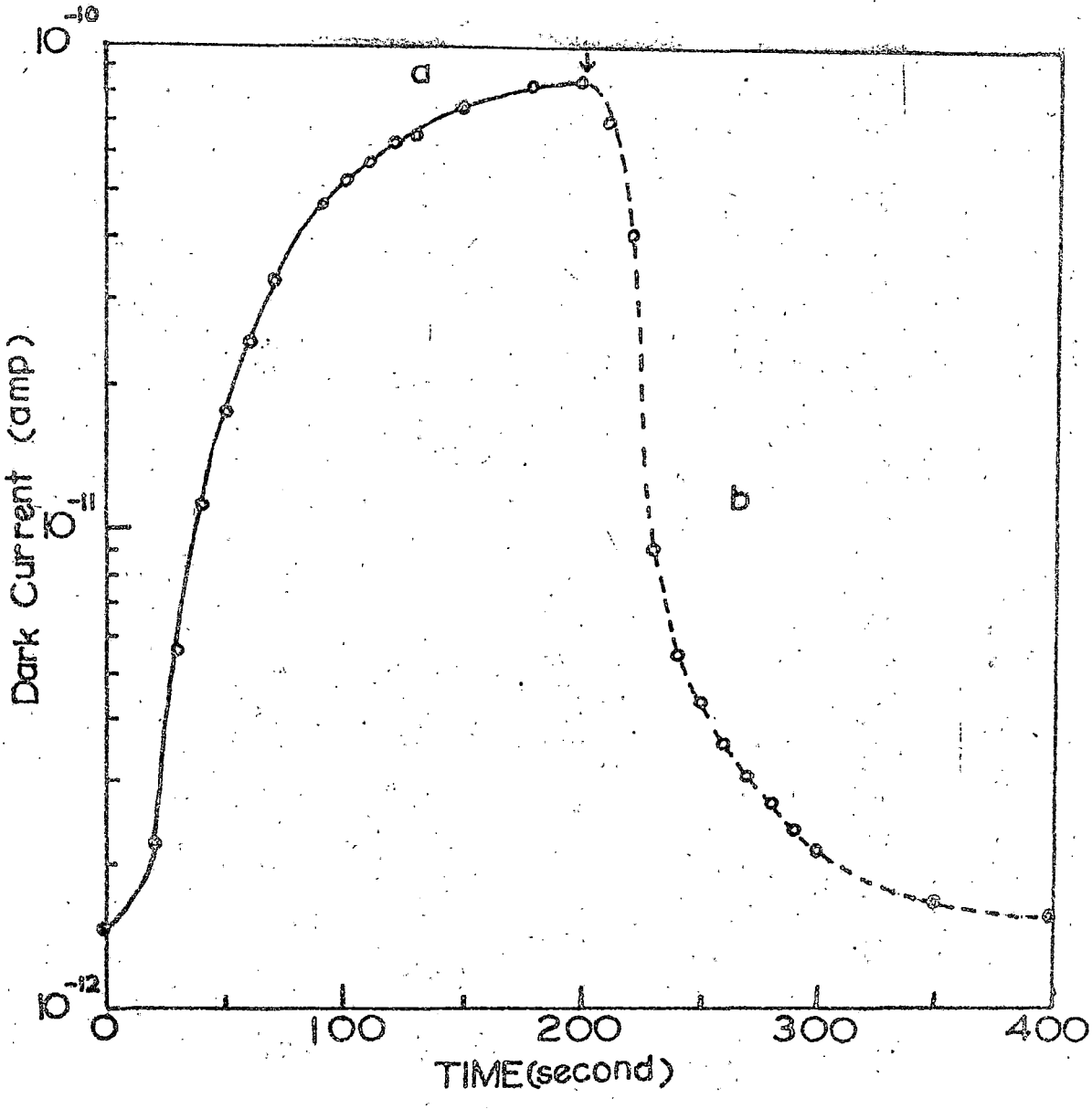

The change in dark current in a O-nitrobenzoic acid powder cell kept at 28°C with (a) adsorption and (b) desorption of ethyl-acetate vapour at 18.2 mm pressure.

FIGURE - 3.6

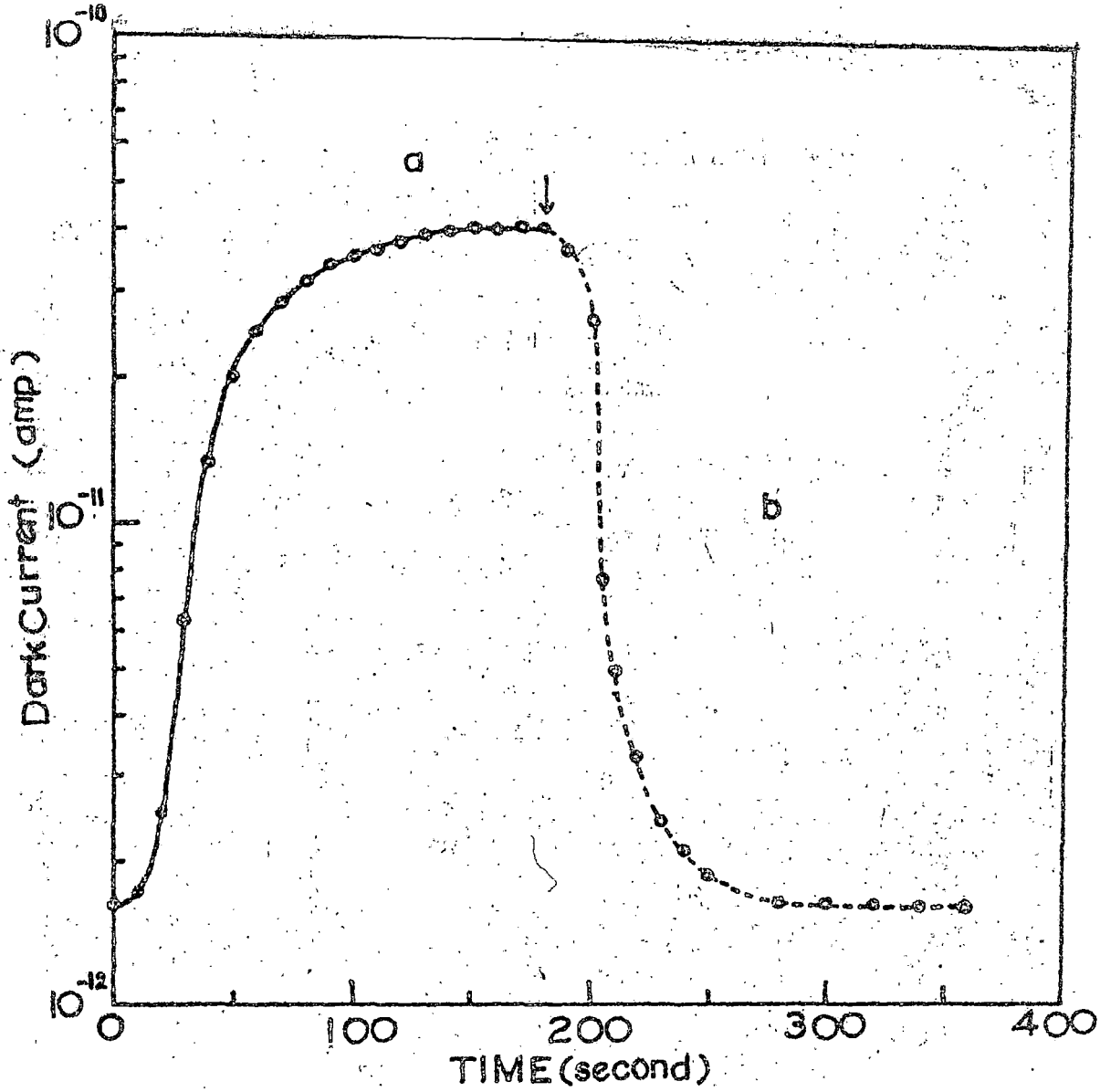

The change in dark current in a m-nitrobenzoic acid powder cell kept at 25°C with (a) adsorption and (b) desorption of ethylacetate vapour at 25.3 mm pressure.

FIGURE - 3.7

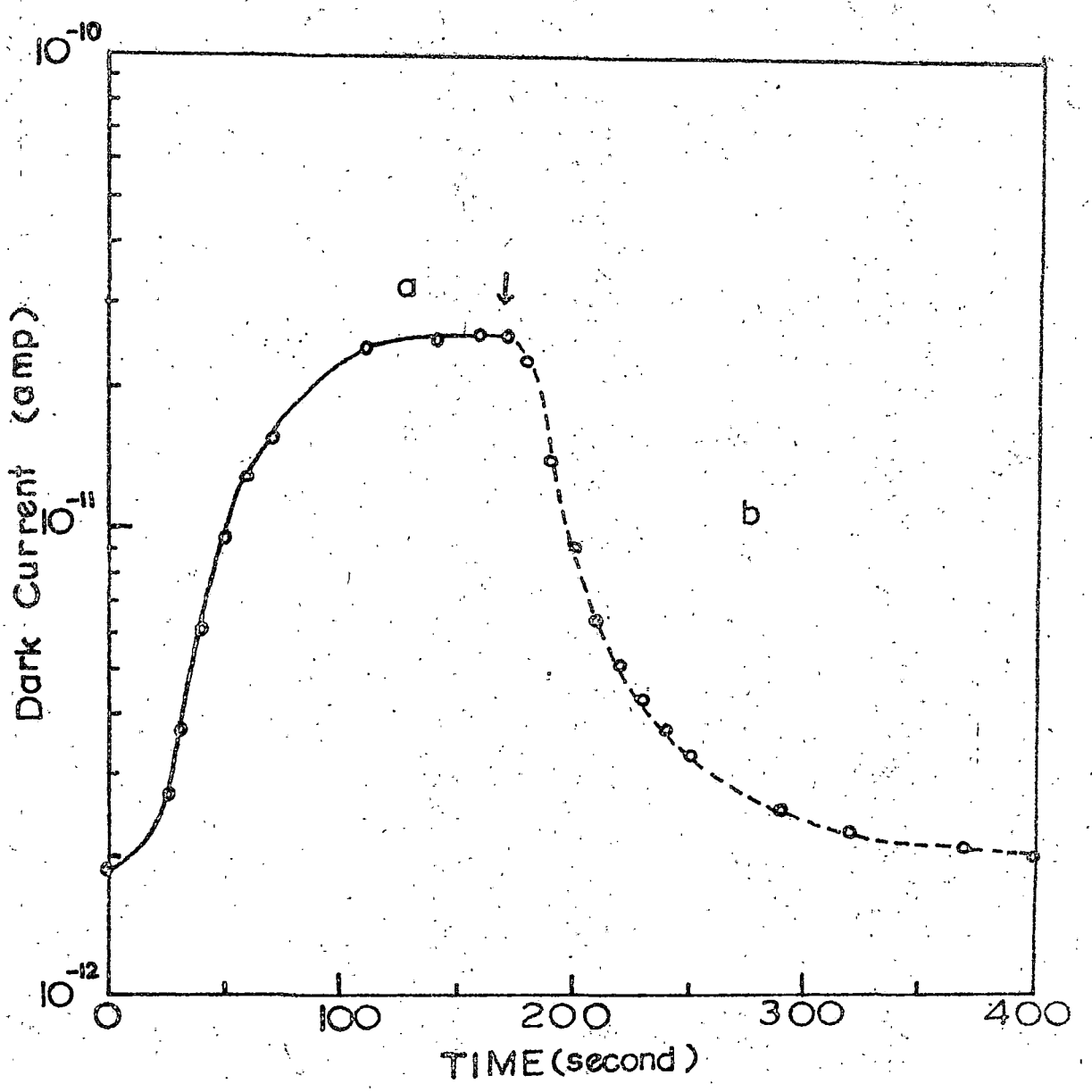

The change in dark current in a p-nitrobenzoic acid powder cell kept at 25°C with (a) adsorption and (b) desorption of ethylacetate vapour at 25.8 m pressure.

the vapour desorbs from the crystallite surfaces and the current comes back to the initial value. These are shown by the portion (b) of the curves. The arrow indicates the time when desorption starts. Such adsorption and desorption curves were obtained with other vapours also. Adsorption and desorption of vapours n-hexane, cyclohexane; carbontotrachlorides, methanol, benzene, ethyl acetate and ethanol on and from 9-nitroanthracene; 2-nitrofluorene; O-, m - and p - nitrobenzoic acids, vapours of ethanol, methanol and cyclohexane on and from 1,4 dinitronaphthalene and of ethanol, methanol, n - hexane and cyclohexane on and from 1,3,5-trinitrobenzene show similar behaviour as shown in Fig. 3.1 - 3.7.

But with certain vapour on 1,4 dinitronaphthalene and 1,3,5-trinitrobenzene such a saturation value was not reached and only a trend to reach a saturation value was observed in a long-time region as shown in Fig. 3.8 and 3.9. When the chamber was flushed with dry nitrogen the initial value was not attained even after 60 minutes. Adsorption and desorption curves similar to that shown in figure 3.8 and 3.9 are obtained for ethylacetate, benzene, carbontetrachloride and n-hexane adsorption on 1, 4 - dinitronaphthalene and for ethylacetate, benzene, carbontetrachloride, toluene, n-heptane and methyl-cyclohexane adsorption on 1,3,5-trinitrobenzene.

FIGURE - 3.8

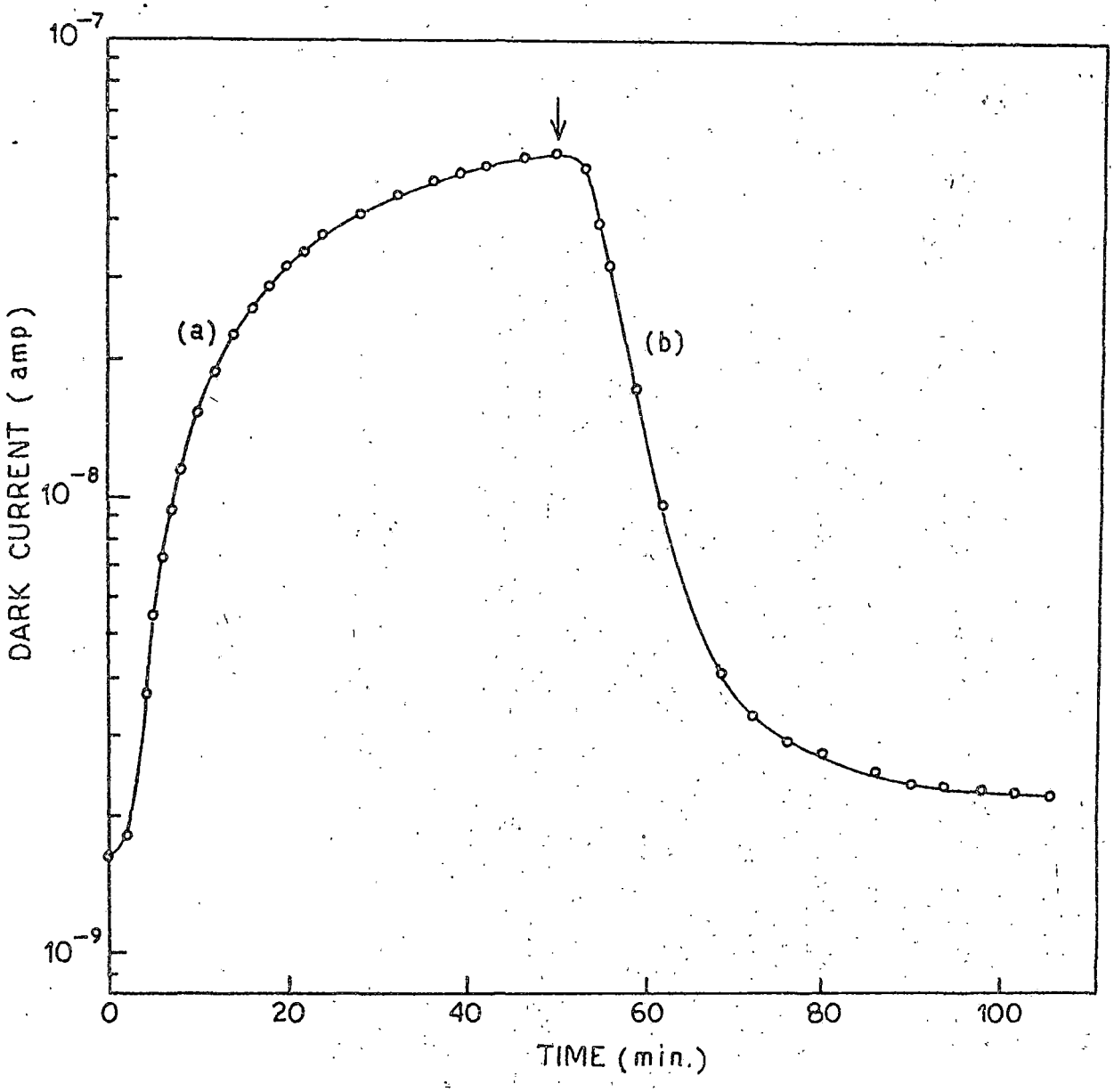

The change in dark current in a 1,4-dinitronaphthalene powder cell kept at 22°C with (a) adsorption and (b) desorption of ethylacetate vapour at 49.5 mm pressure (a trend to reach a saturation dark current value is seen at long time region).

FIGURE - 3.9

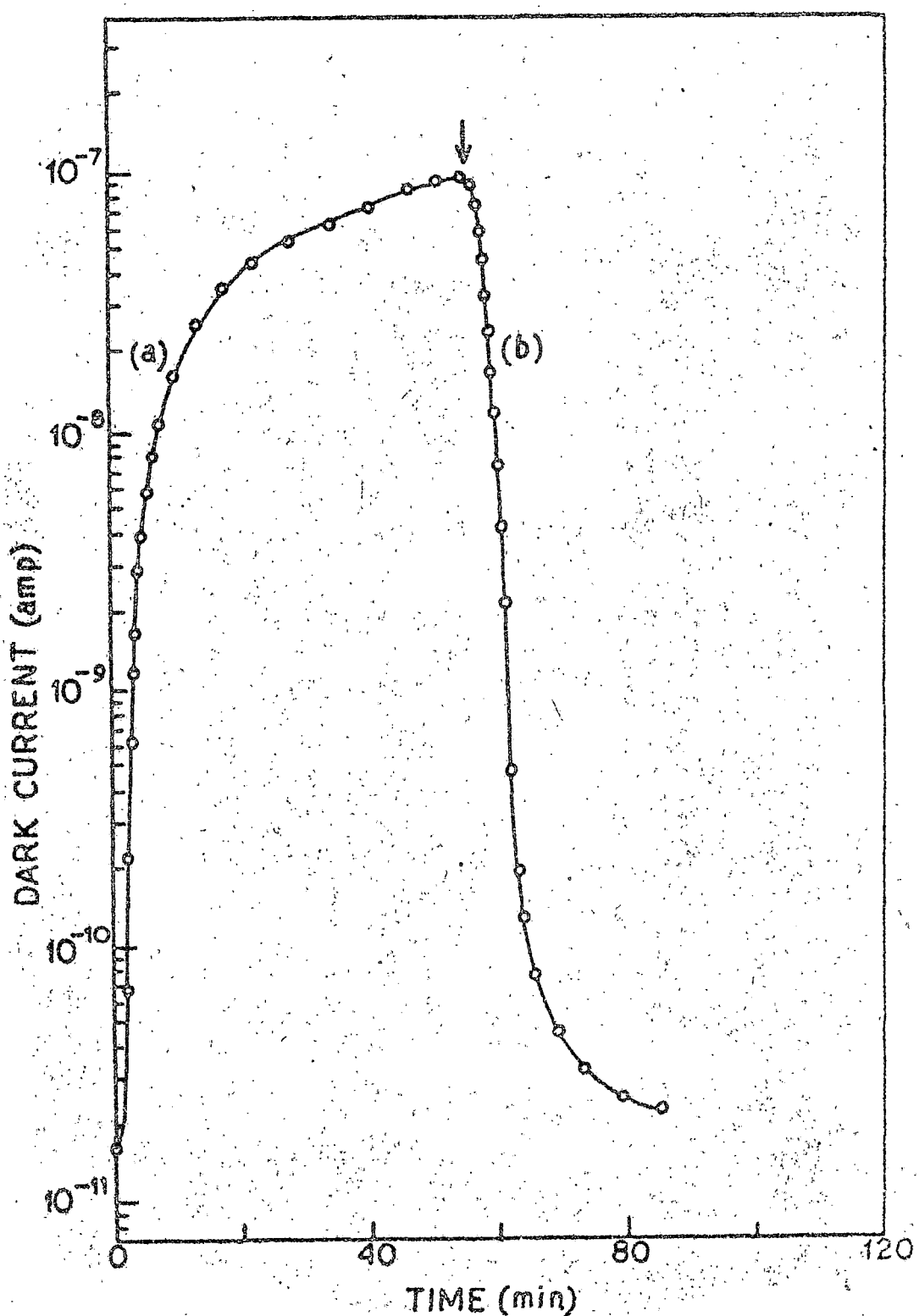

The change in dark current in a 1,3,5-trinitrobenzene powder cell kept at 32°C with (a) adsorption and (b) desorption of ethylacetate vapour at 61.4 mm pressure (a trend to reach a saturation dark current value is seen at long time region).

The saturation value of current in a vapour-semiconductor system under particular experimental condition depends on the vapour pressure of the reagent liquid and at the cell temperature, the time to attain this steady state value being dependent on the flow rate.

The sensitivity as measured by (σ_A/σ_V) values for adsorption of various vapours on the surfaces of different nitroaromatic semiconductors are summarised in tables 3.1 (a) and (b), where σ_A is the specific conductivity at saturation after vapour adsorption and σ_V is that before adsorption. The sensitivity depends on the chemical nature of the adsorbed molecules.

2.2 Vapour pressure dependence of conductivity

The magnitude of the current enhancement at a constant cell temperature was studied as a function of partial pressure of the vapours in the chamber. The partial pressure of the vapour in the chamber was varied by changing the temperature of the reagent chemical in the bubbler through which the dry nitrogen gas was passed and fed into the conductivity chamber. At a constant flow rate, the partial pressure of the reagent liquid vapour in the chamber atmosphere was proportional to the vapour pressure of the liquid at the temperature it was kept. The steady state

Table 3.1 (a)

Rise in the dark current in the powder cells of some nitroaromatic semiconductors at 22°C on adsorption of various vapours at the same pressure (p) for semiconductor-vapour pair where quick saturation is reached.

Vapour used	σ_A/σ_V		
	9-nitro-anthracene (p = 60 mm)	1,4-dinitro-naphthalene (p = 50 mm)	1,3,5-trinitro-benzene (p = 60 mm)
n-Hexane	-	-	8.5
Cyclo-hexane	-	3	10
Carbontetra-chloride	3	-	-
Methanol	6	8	2×10^1
Benzene	3×10^1	-	-
Ethyl-acetate	3×10^1	-	-
Ethanol	1.2×10^3	3×10^2	5×10^6

Table 3.1 (b)

Rise in the dark current in the powder cells of some nitroaromatic semiconductors at 25°C on adsorption of various vapours at the same pressure (50 mm) for semiconductor-vapour pair where quick saturation is reached.

Vapour used	σ_A/σ_V			
	nitro-fluorene	O-nitro-benzoic-acid	m-nitro-benzoic-acid	p-nitro-benzoic acid
n-Hexane	0.25 x 10	0.15 x 10	0.2 x 10	0.2 x 10
Cyclohexane	0.3 x 10	0.2 x 10	0.25x 10	0.27x 10
CCl_4	0.40 x 10	4.0	3.0	2.0
C_6H_6	0.1 x 10^2	4.30 x 10	6.0	2.5
Ethyl-acetate	0.14 x 10^2	1.00 x 10^4	1.3 x 10^3	9.0
Methanol	0.49 x 10^2	2.5 x 10^2	2.4 x 10^2	9.0
Ethanol	1.2 x 10^3	1.0 x 10^4	3.7 x 10^3	6.8 x 10^2

current (i.e. the saturation current) was noted for different vapour pressures. The kinetic data for the dark current enhancement for ethyl-acetate vapour adsorption at different vapour pressures were also recorded.

3. Discussions

3.1 Dependence of the conductivity on vapour pressure :

The rise in conductivity of the nitroaromatic semiconductors was studied as a function of the partial pressure of a vapour at a constant sample temperature.

At constant flow and constant vapour pressure, the conductivity after adsorption $\sigma_A(m)$ follows a relation

$$\sigma_A(m) = \sigma_V \exp (\alpha m) \qquad (3.11)$$

where ' α ' is a constant and 'm' is the amount of vapour adsorbed.

It is assumed that 'm' depends on the partial pressure (P) of the reagent chemical and in the initial period, also on the time of exposure. After some time, however, an equilibrium is established. Thus, we assume[119,133-135, 147] that in the initial

region

$$m(t) = Q(t) \cdot p \qquad (3.12)$$

where Q (t) is a function of time.

At equilibrium,

$$m_0 = Q_0 \cdot p \qquad (3.13)$$

where Q_0 now becomes independent of time. This is expected from Langmuir's adsorption isotherms[139], when a small fraction of the surface is covered by the gas or vapour molecules. Substituting equation (3.12) in equation (3.11), we get :

$$\sigma_A [m(t)] = \sigma_v \exp[\alpha \cdot Q(t) \cdot p] \qquad (3.14)$$

and at equilibrium,

$$\sigma_A (m_0) = \sigma_v \exp(\alpha \cdot Q_0 \cdot p) \qquad (3.15)$$

A plot of log σ_A (m_0) or logarithm of the saturation current vs. p at equilibrium is expected to be linear from equation (3.15).

In Figs. 3.10 and 3.11, we show such plots of the logarithm of the saturation dark current against the vapour pressure (p) at equilibrium if the adsorption kinetics are of the type shown

FIGURE - 3.10

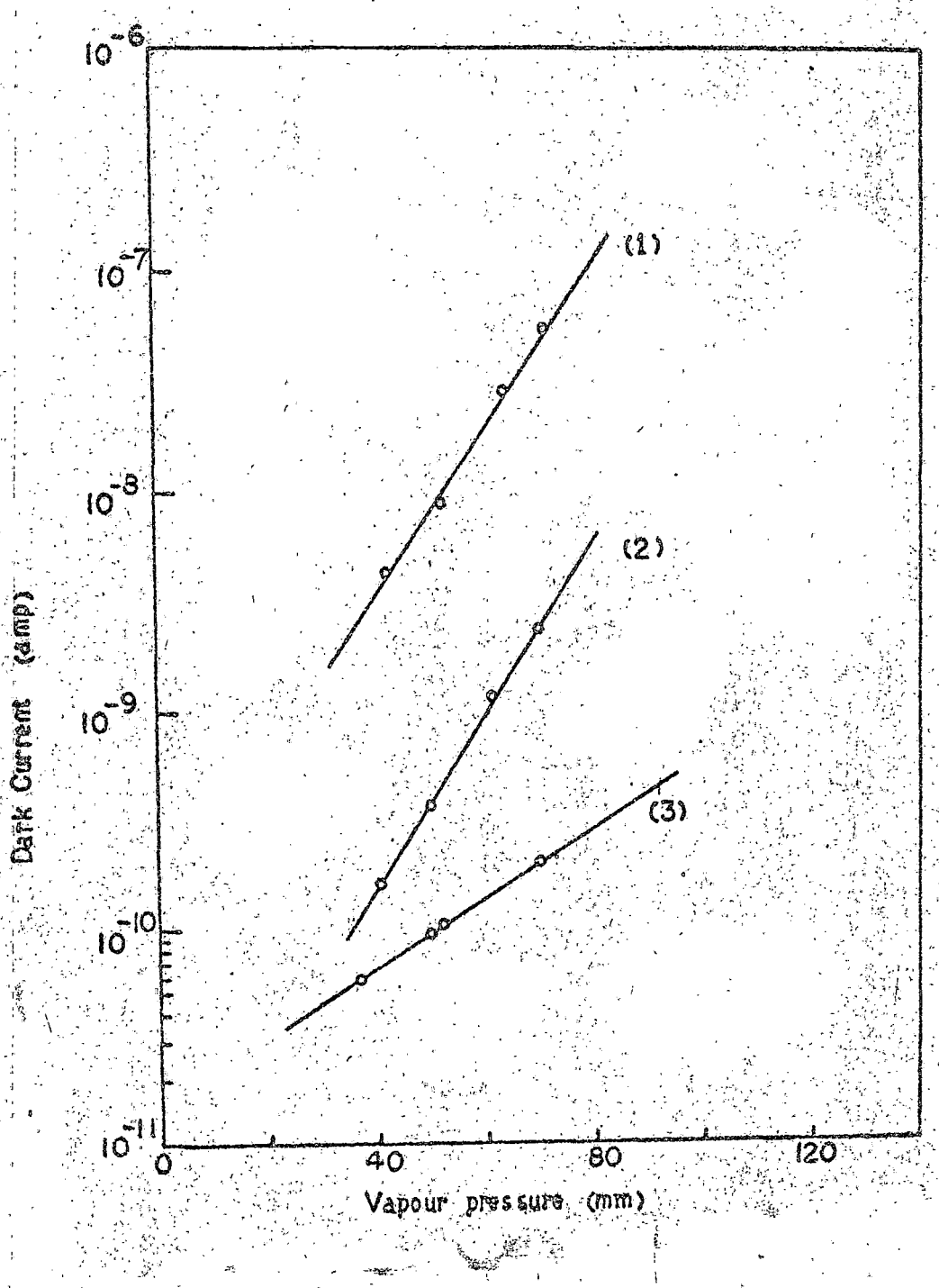

The change in dark current of (1) 1,4-dinitronaphthalene, (2) 1,3,6-trinitrobenzene and (3) 9-nitroanthracene powder cells at a constant cell temperature at 22°C as a function of the vapour pressure of methanol.

FIGURE - 2.11

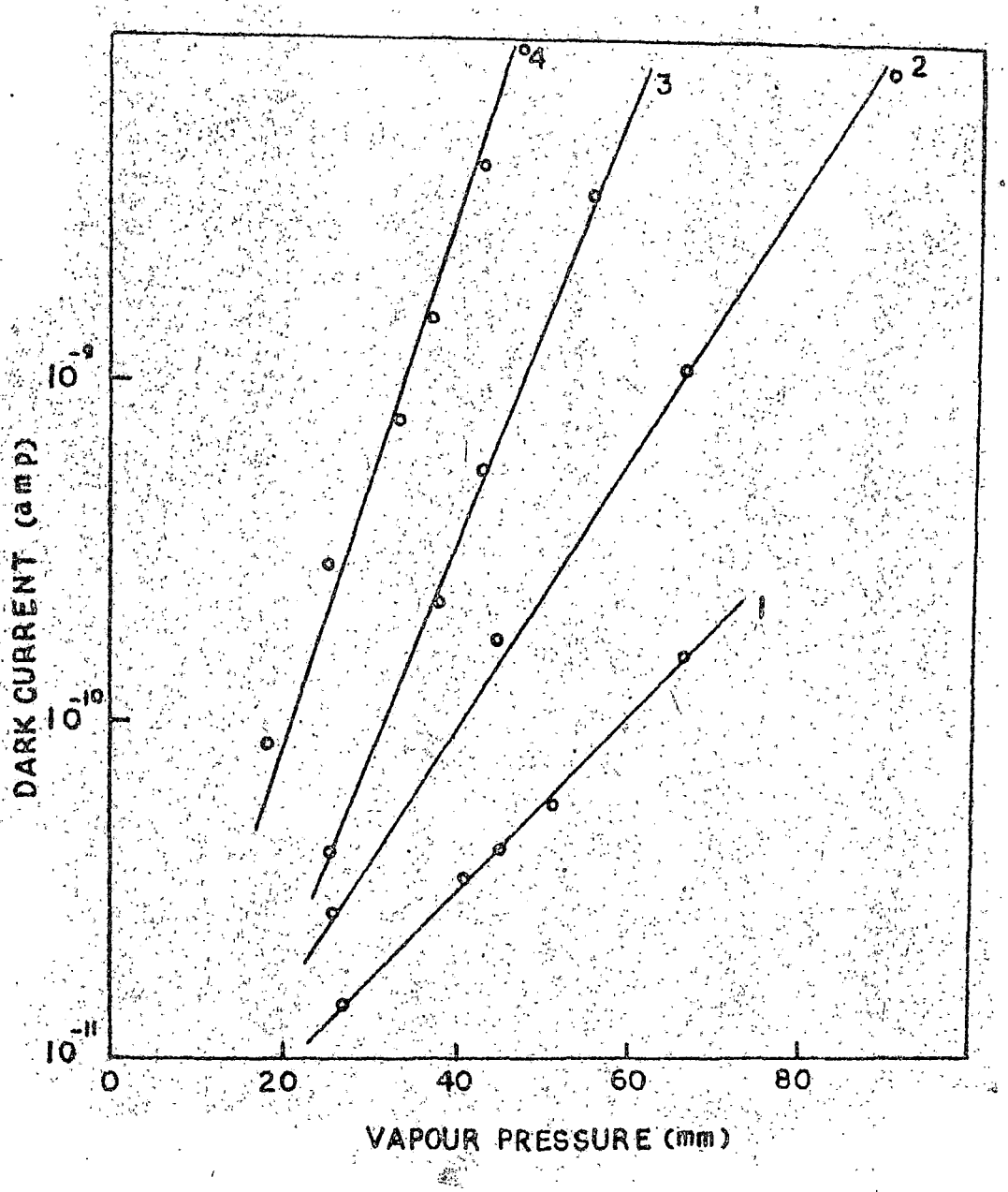

The change in saturation dark current of (1) 2-nitrofluorene, (2) p-nitrobenzoic acid, (3) m-nitrobenzoic acid and (4) o-nitrobenzoic acid powder cells at a constant cell temperature (25°C) as a function of the vapour pressure of ethyl acetate.

in Figs. 3.1 - 3.7. Fairly good straight lines are obtained. The slopes of these lines (αq_0) is the measure of the strength of interaction between the vapour molecules and the semiconductors. The values of αq_0 for different vapour - semiconductor pairs are presented in table 3.2 to gauge the relative strength of interaction. The linear plots (Figs. 3.10 and 3.11) suggest the applicability of the Langmuir's adsorption isotherm for small fraction of surface coverage in these cases of vapour adsorption.

3.2 Adsorption and desorption kinetics

In order to test whether the adsorption and desorption kinetics follow the Roginsky Zeldovich equation, let us integrate equation (1.1) giving :

$$n(t) = \frac{RT}{\beta} \log (t + t_0) + \text{const.} \quad (3.21)$$

From equations (3.11) and (3.21), we get :

$$\log \sigma_A = \frac{\alpha RT}{\beta} \log (t + t_0) + \text{const.} \quad (3.22)$$

Similarly, a suitable equation for desorption kinetics may be given by :

$$\log \sigma_A' = - \frac{\alpha RT}{\beta^*} \log (t + t'_0) + \text{const.} \quad (3.23)$$

Table 3.2

Values of ($\alpha \cdot Q_0$) for different vapour-semiconductor pairs

Semiconductor	Vapour	$\alpha \cdot Q_0$ (mm^{-1})
9-nitroanthracene	CCl_4	0.022
	Methanol	0.037
	Benzene	0.041
	Ethanol	0.125
1,4-dinitronaphthalene	Methanol	0.087
	Ethanol	0.176
1,3,5-trinitrobenzene	Methanol	0.094
	Ethanol	0.247
2-nitrofluorene	Ethyl acetate	0.0503
O-nitrobenzoic acid	Ethyl acetate	0.0179
m-nitrobenzoic acid	Ethyl acetate	0.0147
p-nitrobenzoic acid	Ethyl acetate	0.0943

Thus, for any empirically chosen t_o or t'_o, linear plots of log σ_A vs. log ($t + t_o$) for adsorption and log σ_A vs. log ($t + t'_o$) for desorption are suggested in the initial region of adsorption and desorption respectively.

Figures 3.12 - 3.20 show such R - z plots for adsorption whereas Figs 3.21 - 3.29 represent the same plots for desorption kinetic data. The time indicated in the abscissa is the time measured from the initiation of adsorption or desorption.

R - z plots of the kinetic data show that in the initial region of adsorption and desorption the slopes of the curves at different vapour pressures are different. This shows the pressure dependence of β and β^*. The higher the partial vapour pressure, the higher is the slope. The values of β/α ($= \beta'$) and β^*/α ($= \beta^{*\prime}$) have been estimated from the slopes. The variation of β' and $\beta^{*\prime}$ with vapour pressure are shown in table 3.3. Like β', $\beta^{*\prime}$ also decreases with increasing vapour pressure. For any particular pressure of ambient vapour, $\beta^{*\prime}$ is larger than β'.

Examination of Figs. 3.19, 3.20, 3.28 and 3.29 indicates that in the long time region the experimental points in R - z plots show excellent linearity with a different slope than the one in the short time region. This is different from that observed in Figs. 3.12 - 3.18 and 3.21 - 3.27 where in the long time region,

FIGURE - 3.12

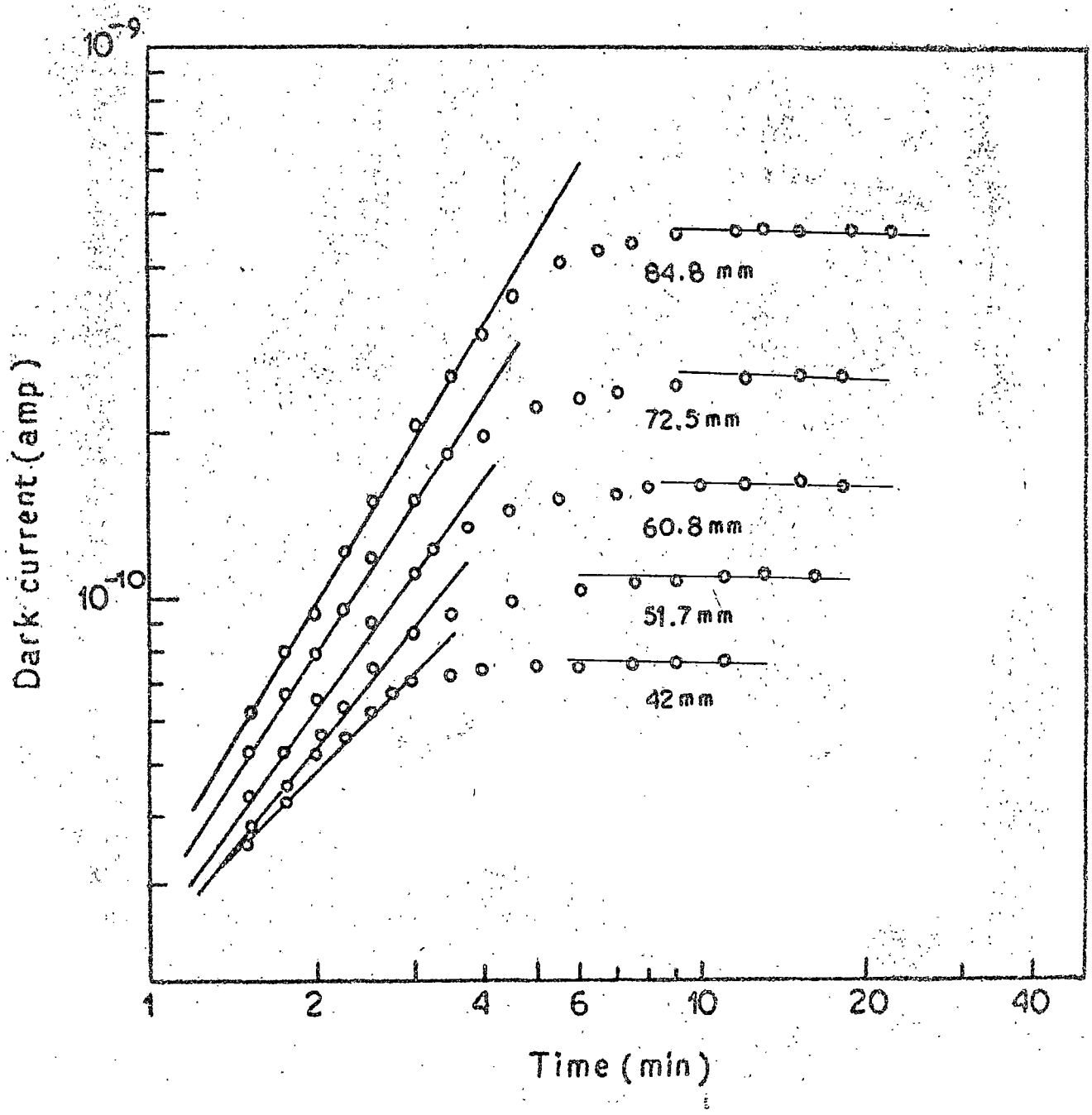

The R - S plot of the kinetic data at different vapour pressures for carbontetrachloride vapour adsorption on 9-nitro-anthracene.

FIGURE - 3.13

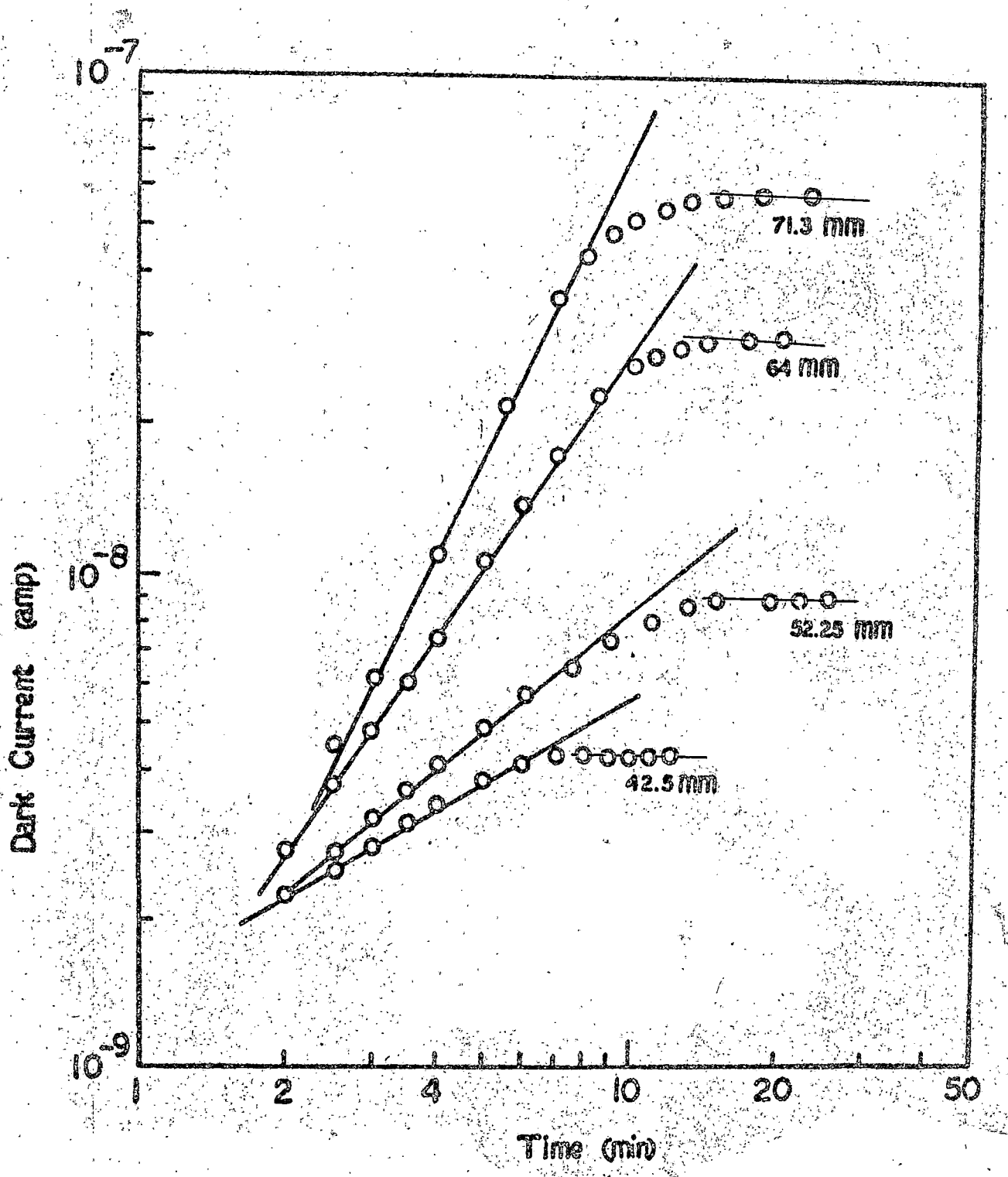

The H - Z plot of the kinetic data at different vapour pressures for methanol vapour adsorption on 1,4-dinitronaphthalene.

FIGURE - 3.14

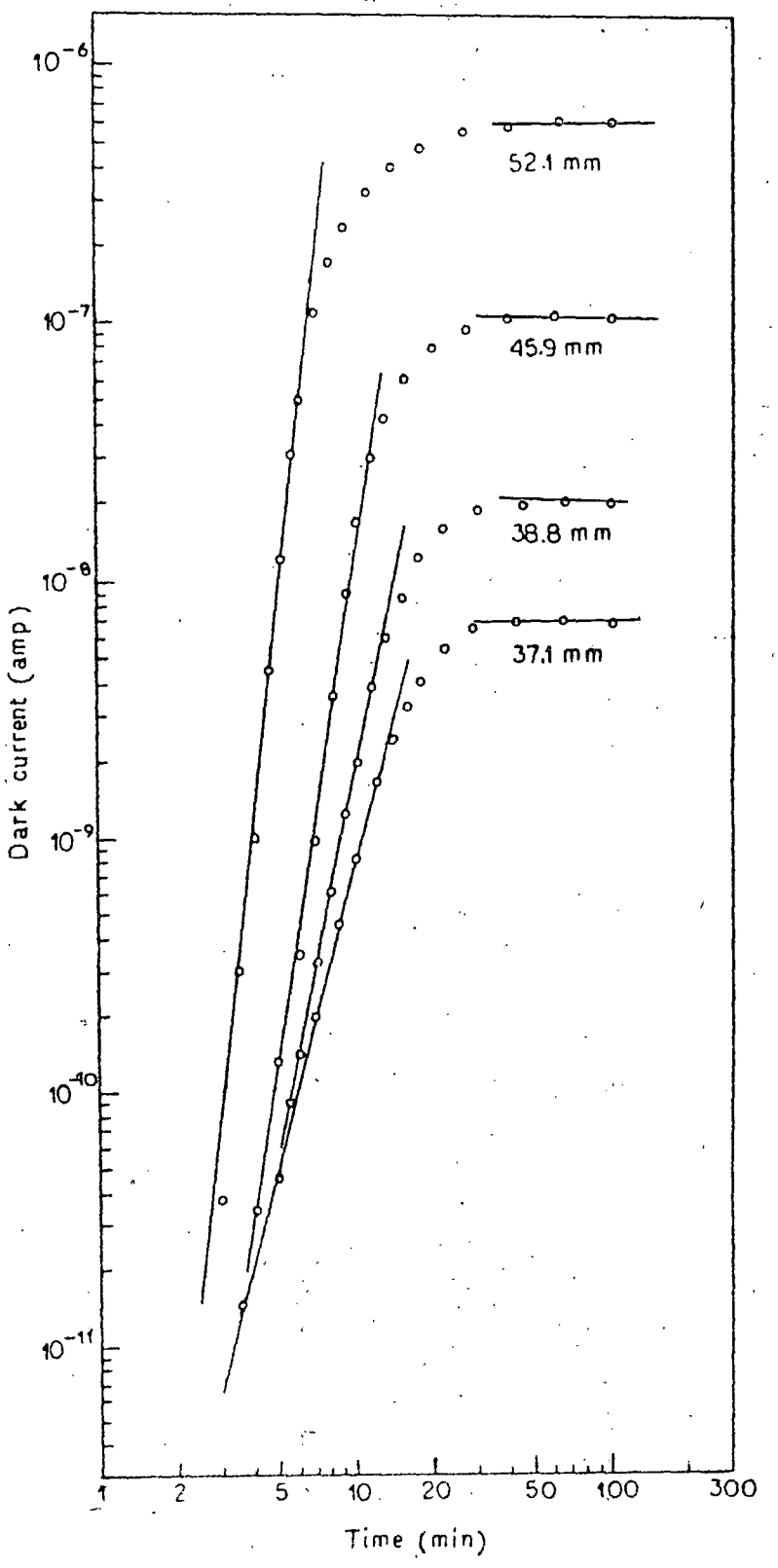

The n - t plot of the kinetic data at different vapour pressures for ethanol vapour adsorption on 1,3,5-trinitrobenzene.

FIGURE - 3.15

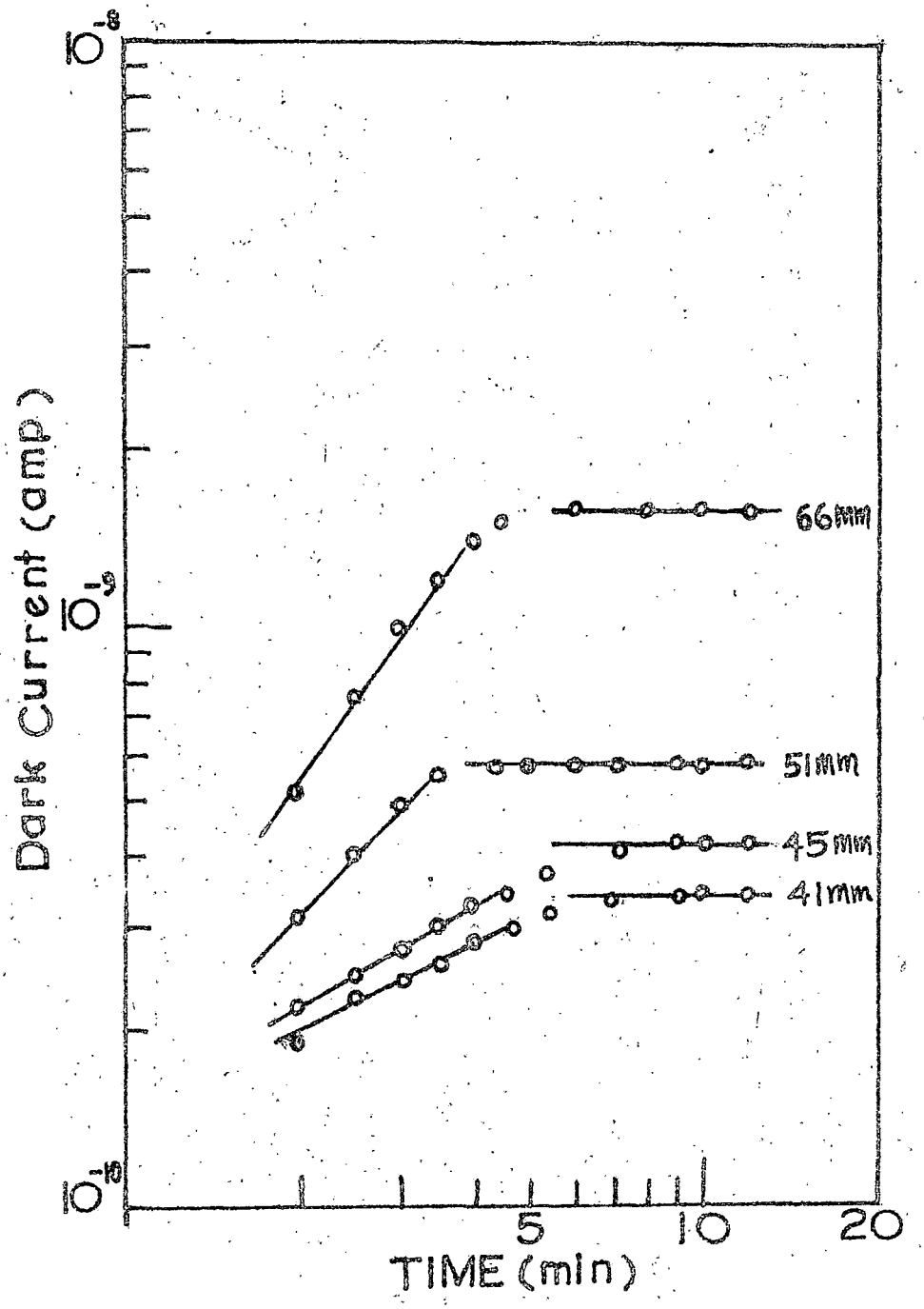

The R - t plot of adsorption kinetic data at different vapour pressures for ethyl acetate vapour adsorption on 2-nitrofluorene.

FIGURE - 3.16

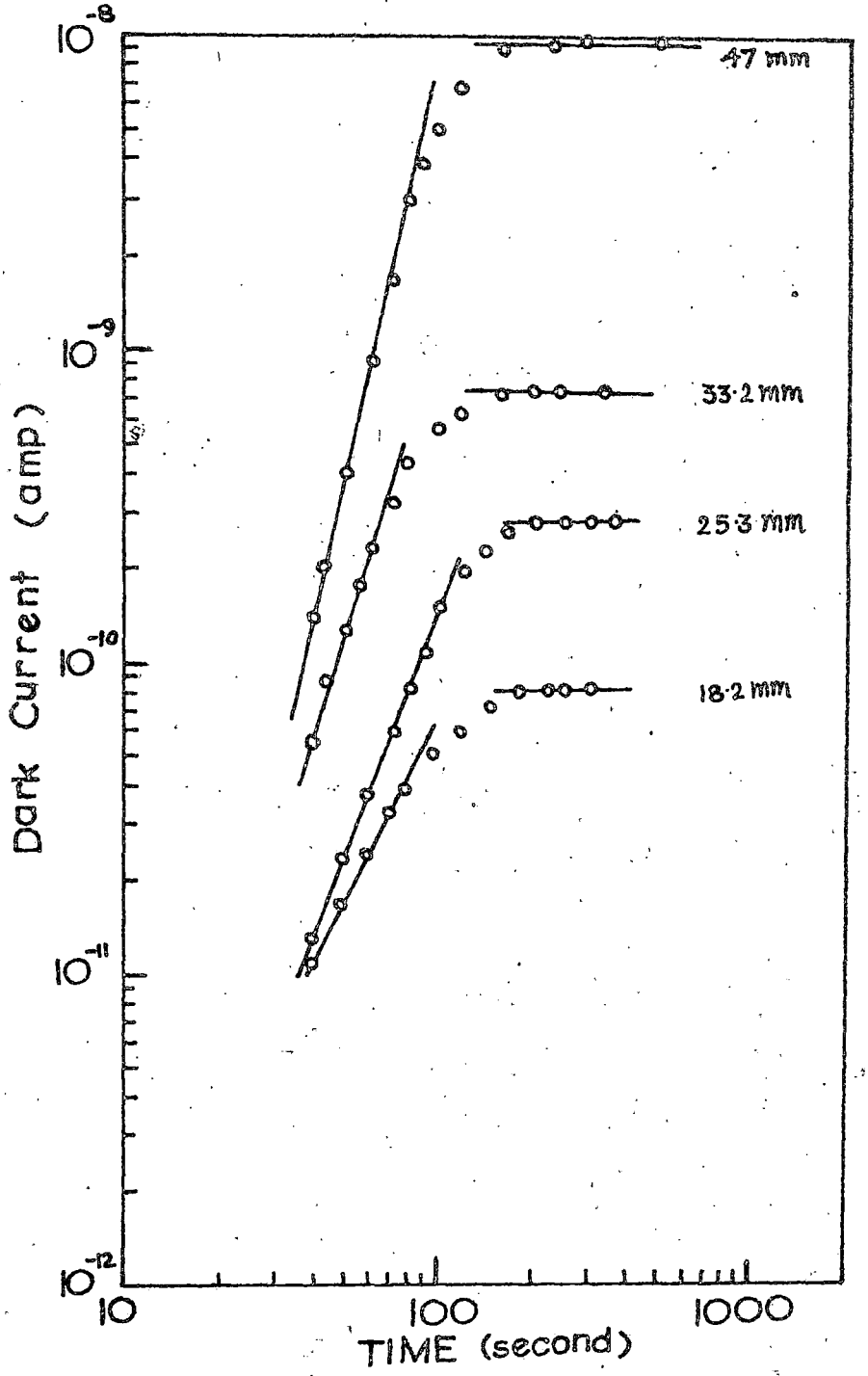

The R - 2 plot of adsorption kinetic data at different vapour pressures for ethyl acetate vapour adsorption on O-nitrobenzoic acid.

FIGURE - 3.17

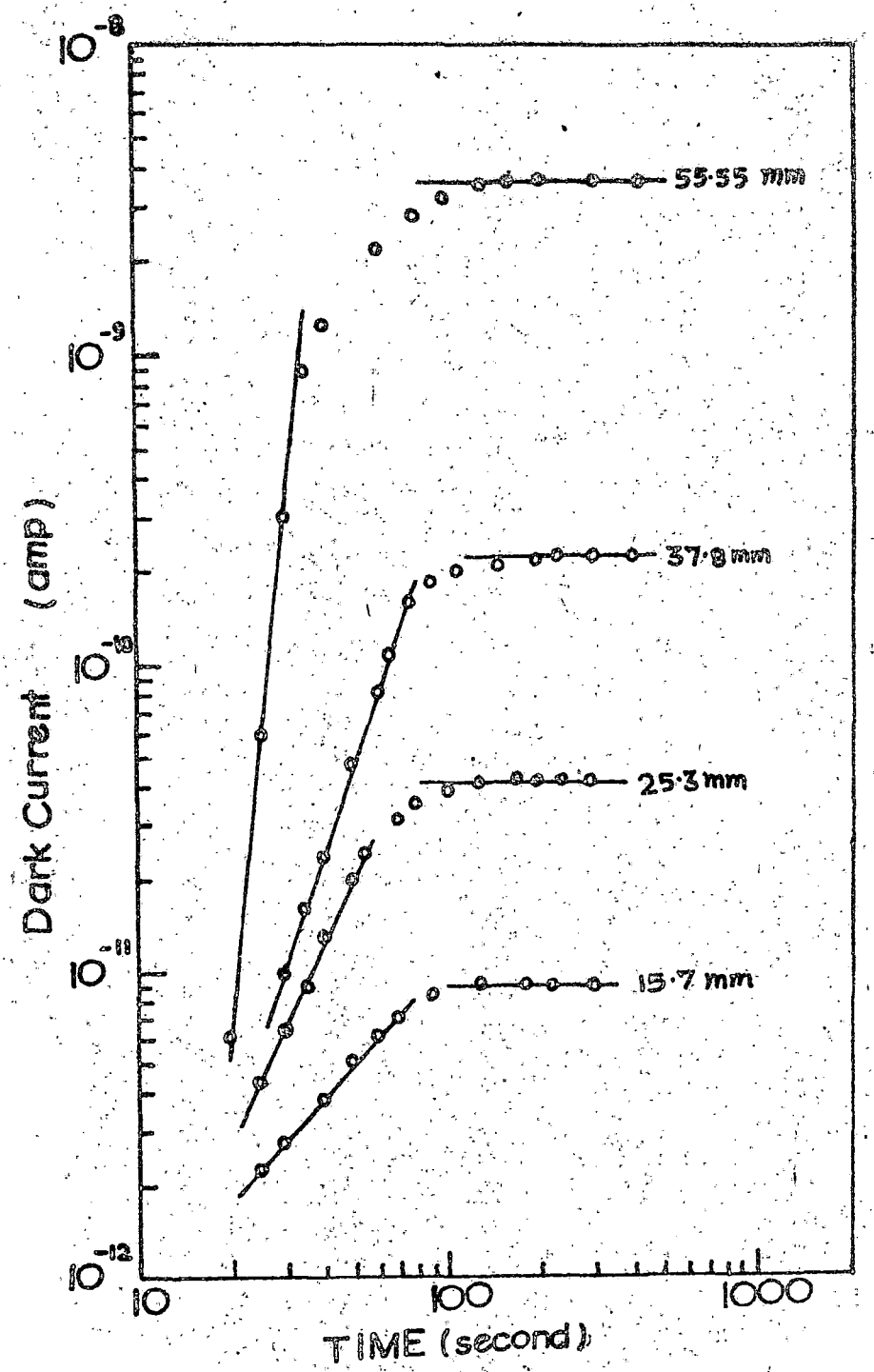

The B - t plot of adsorption kinetic data at different vapour pressures for ethyl acetate vapour adsorption on m-nitrobenzoic acid.

FIGURE - 3.18

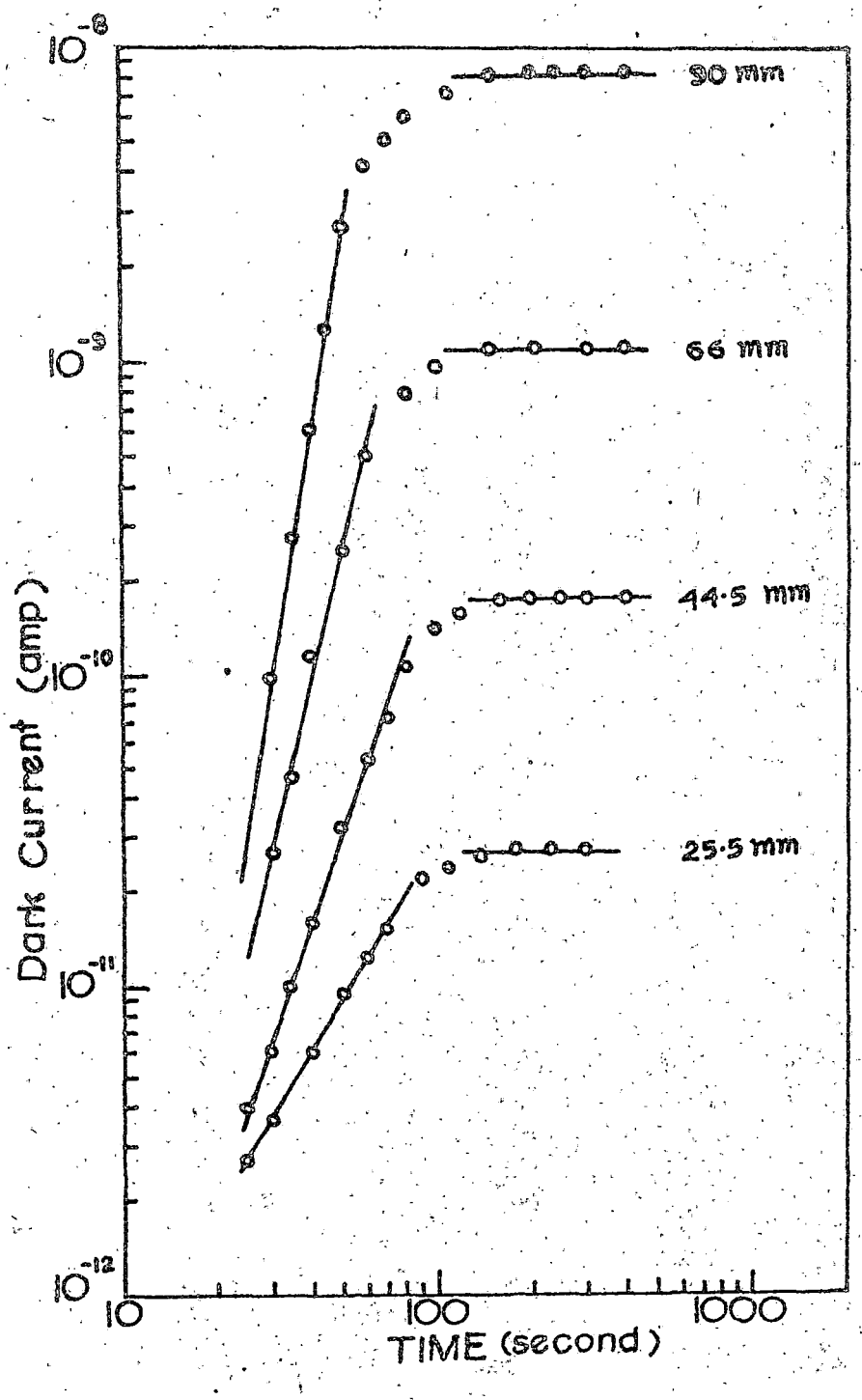

The R - S plot of adsorption kinetic data at different vapour pressures for ethyl acetate vapour adsorption on p-nitrobenzoic acid.

FIGURE - 3.10

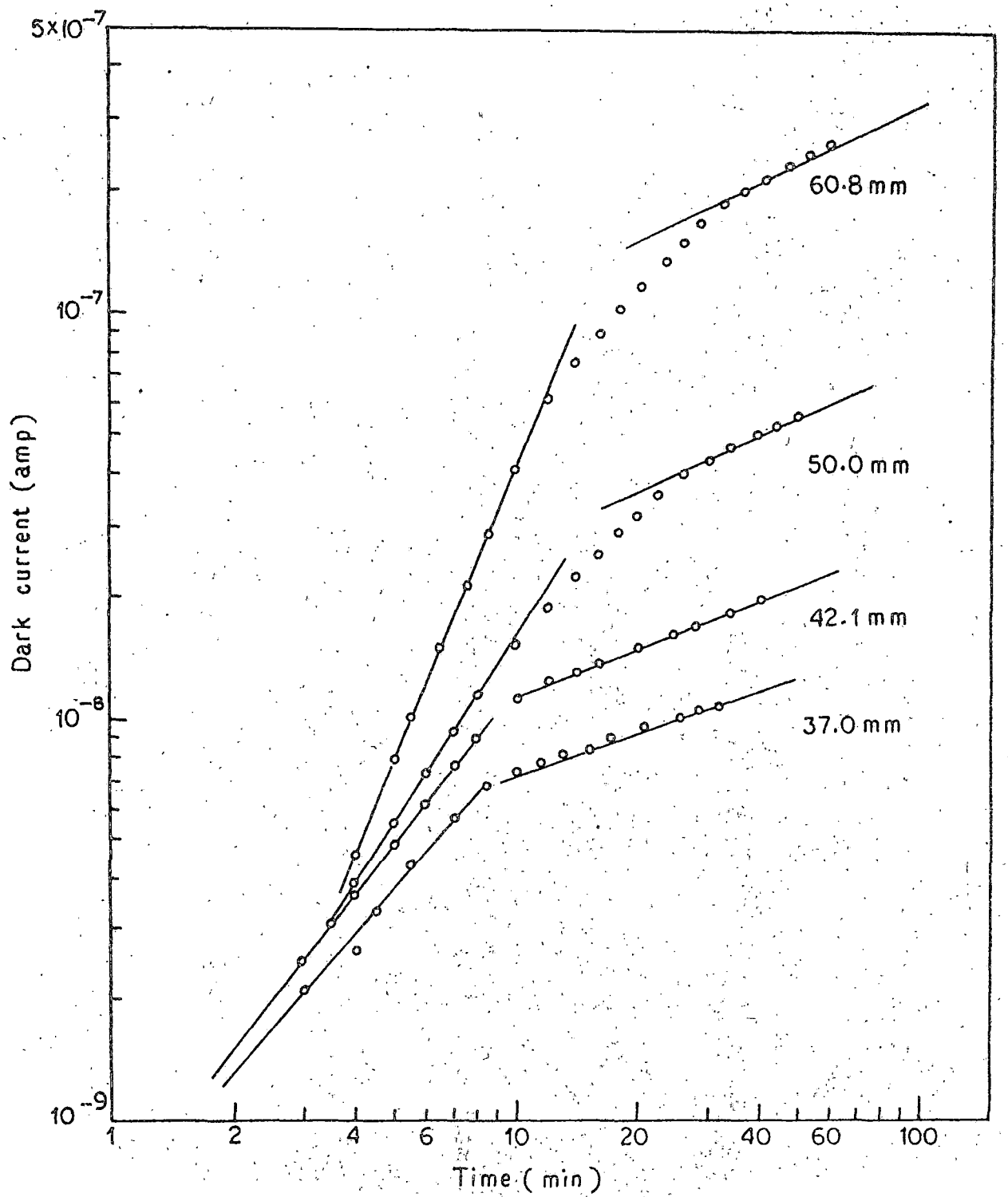

The n - t plot of adsorption kinetic data at different vapour pressures for ethyl acetate vapour adsorption on 1,4-dinitronaphthalene . (Showing two region linearity before reaching saturation)

FIGURE - 3.20

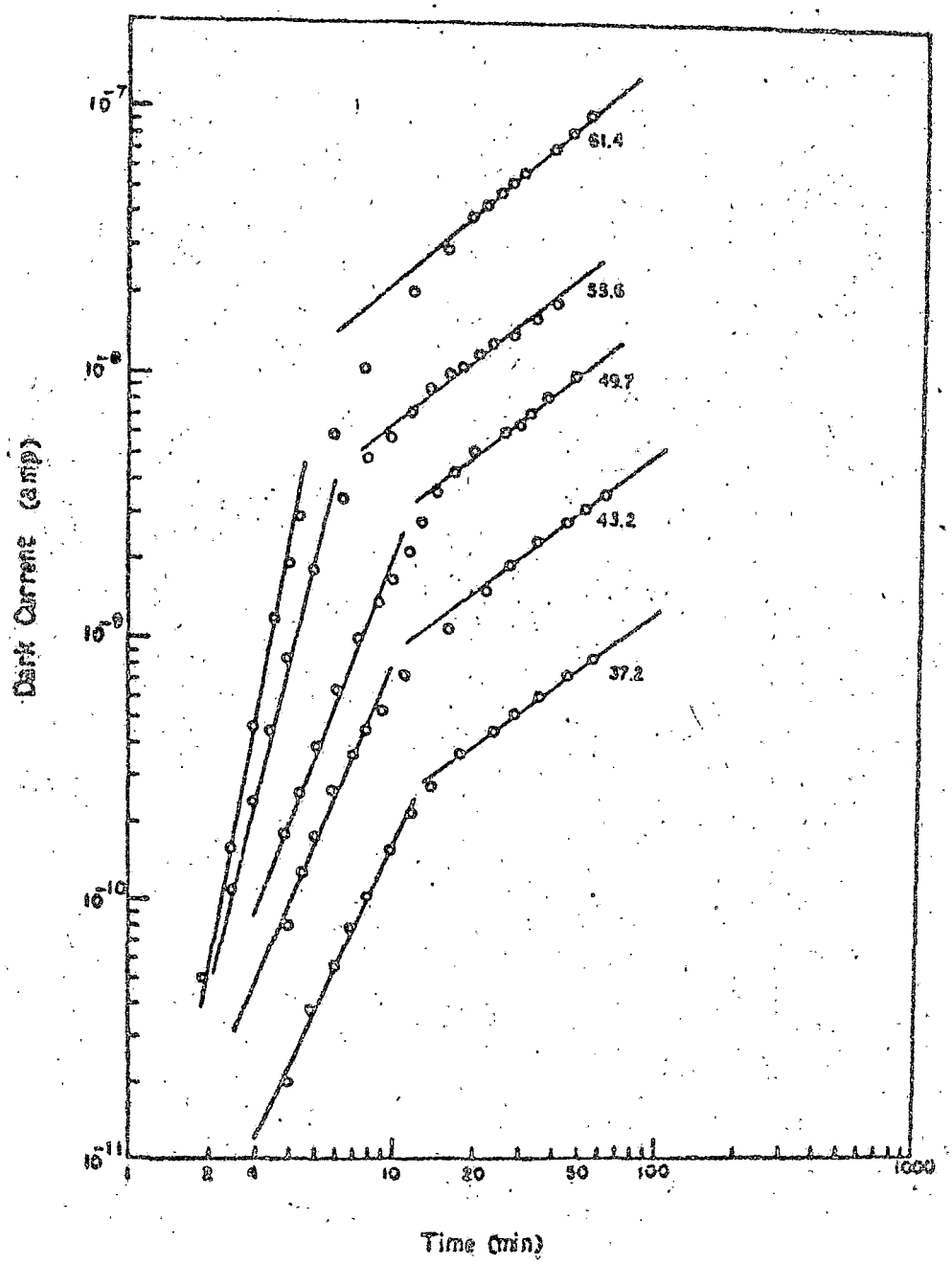

The R - t plot of adsorption kinetic data at different vapour pressures for ethyl acetate vapour adsorption on 1,3,5-trinitrobenzene. (Showing two region linearity before reaching saturation)

FIGURE - 3.21

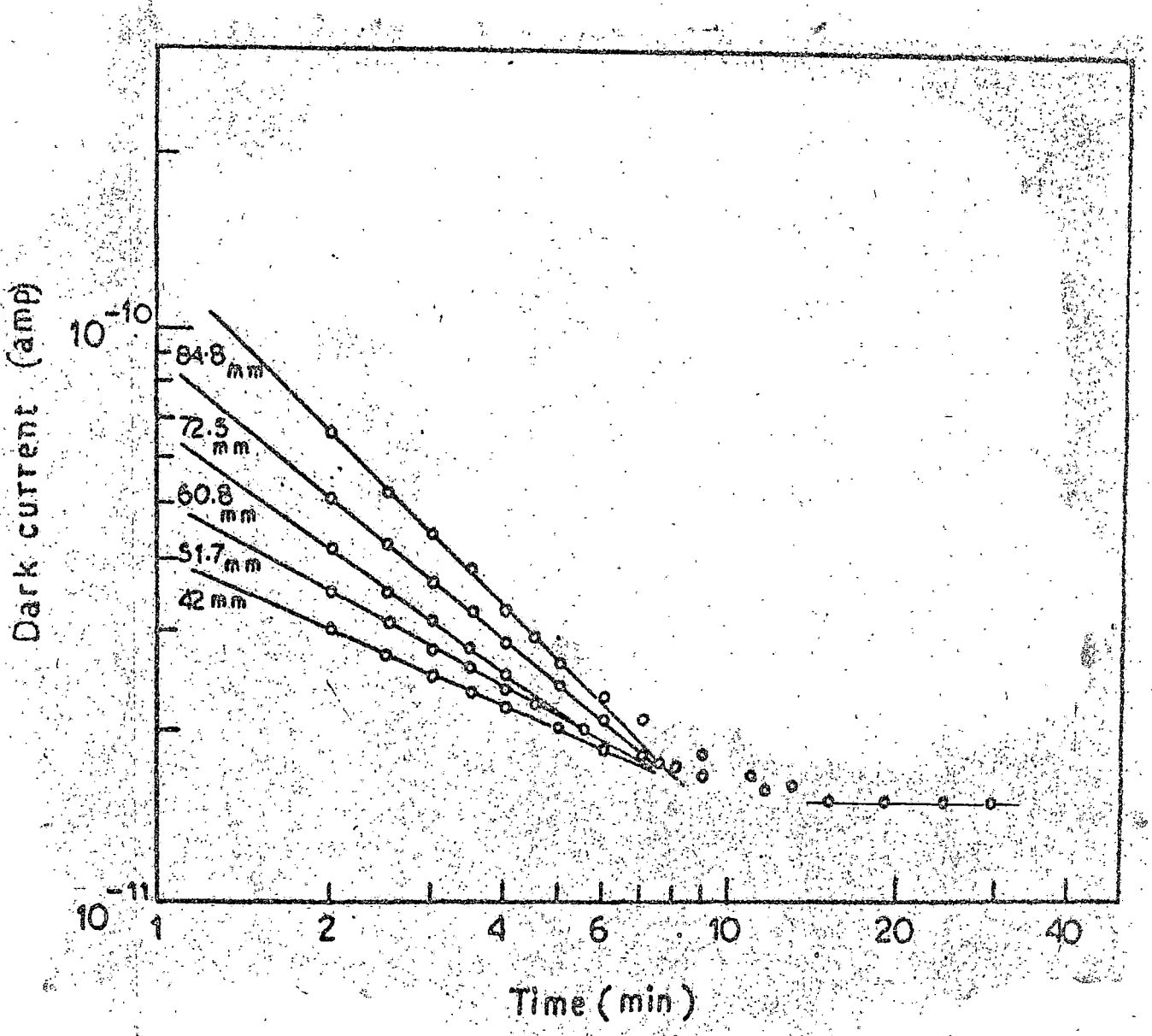

The R - t plot of desorption kinetic data at different vapour pressure for carbontotrachloride vapour desorption from 9-nitroanthracene.

FIGURE - 3.22

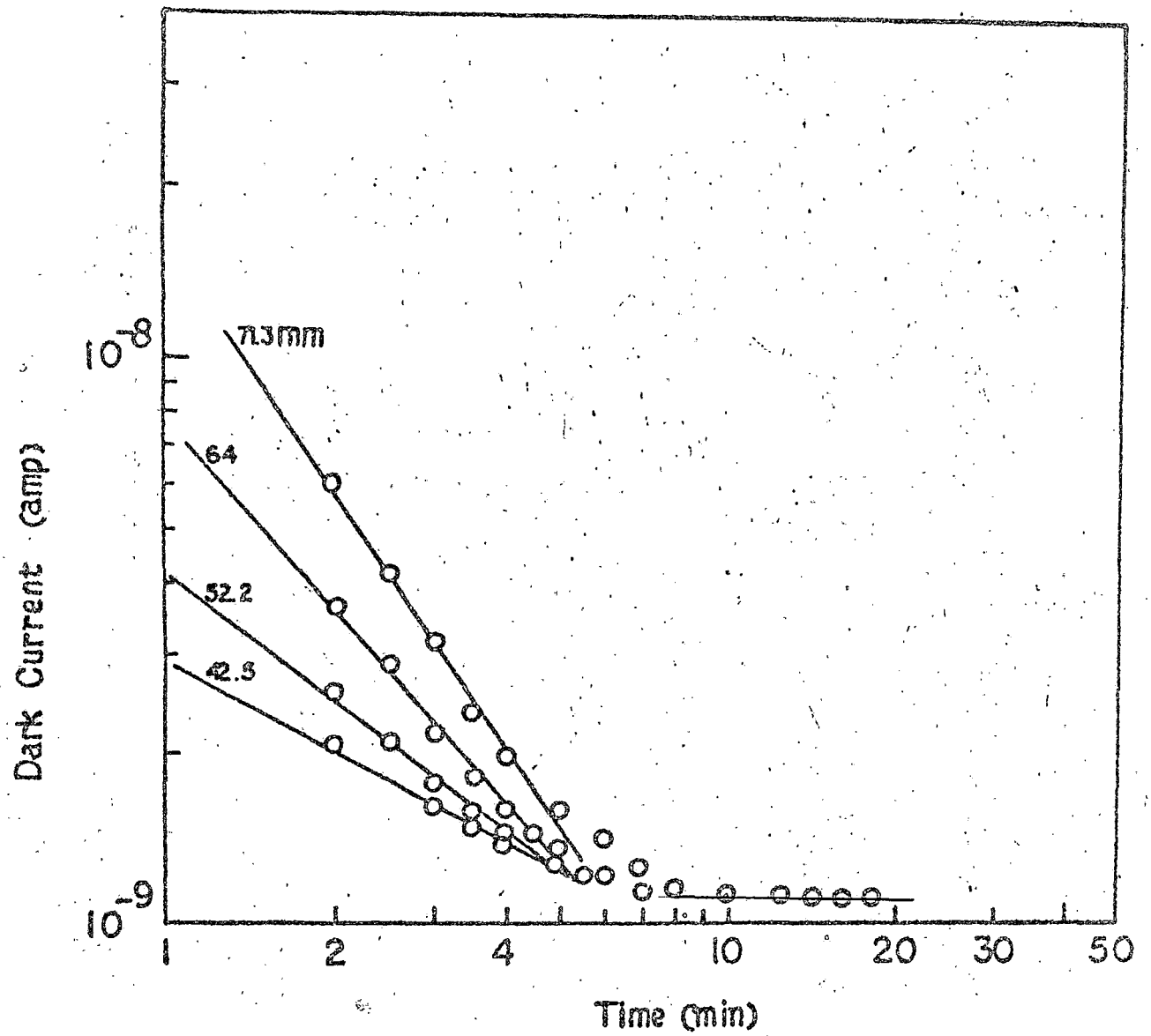

The R - S plot of desorption kinetic data at different vapour pressures for methanol vapour desorption from 1,4-dinitronaphthalene.

FIGURE - 3.23

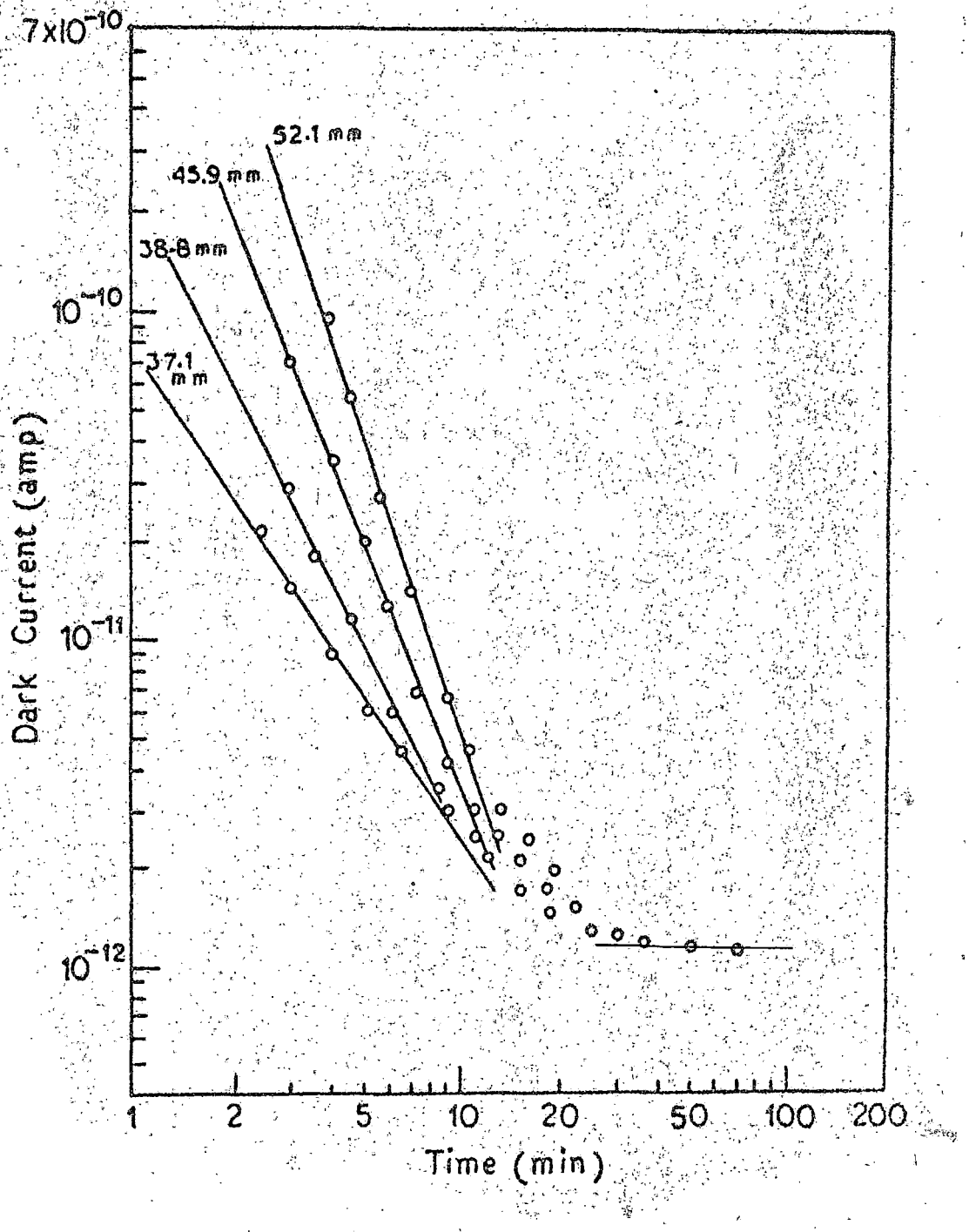

The n - t plot of desorption kinetic data at different vapour pressures for ethanol vapour desorption from 1, 3, 5-trinitrobenzene.

FIGURE - 3.24

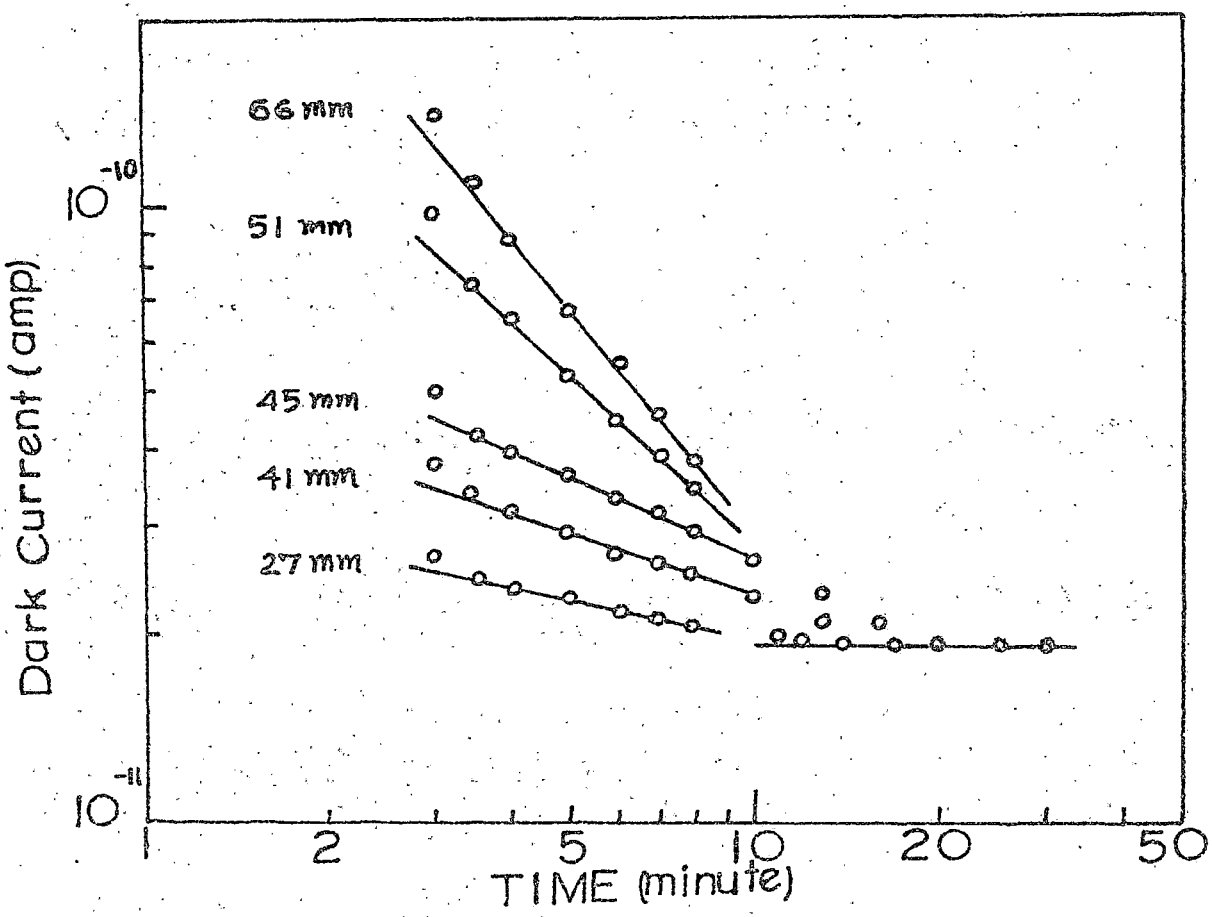

The R - t plot of desorption kinetic data at different vapour pressures for ethyl acetate vapour desorption from 2-nitrofluorene.

FIGURE - 3.25

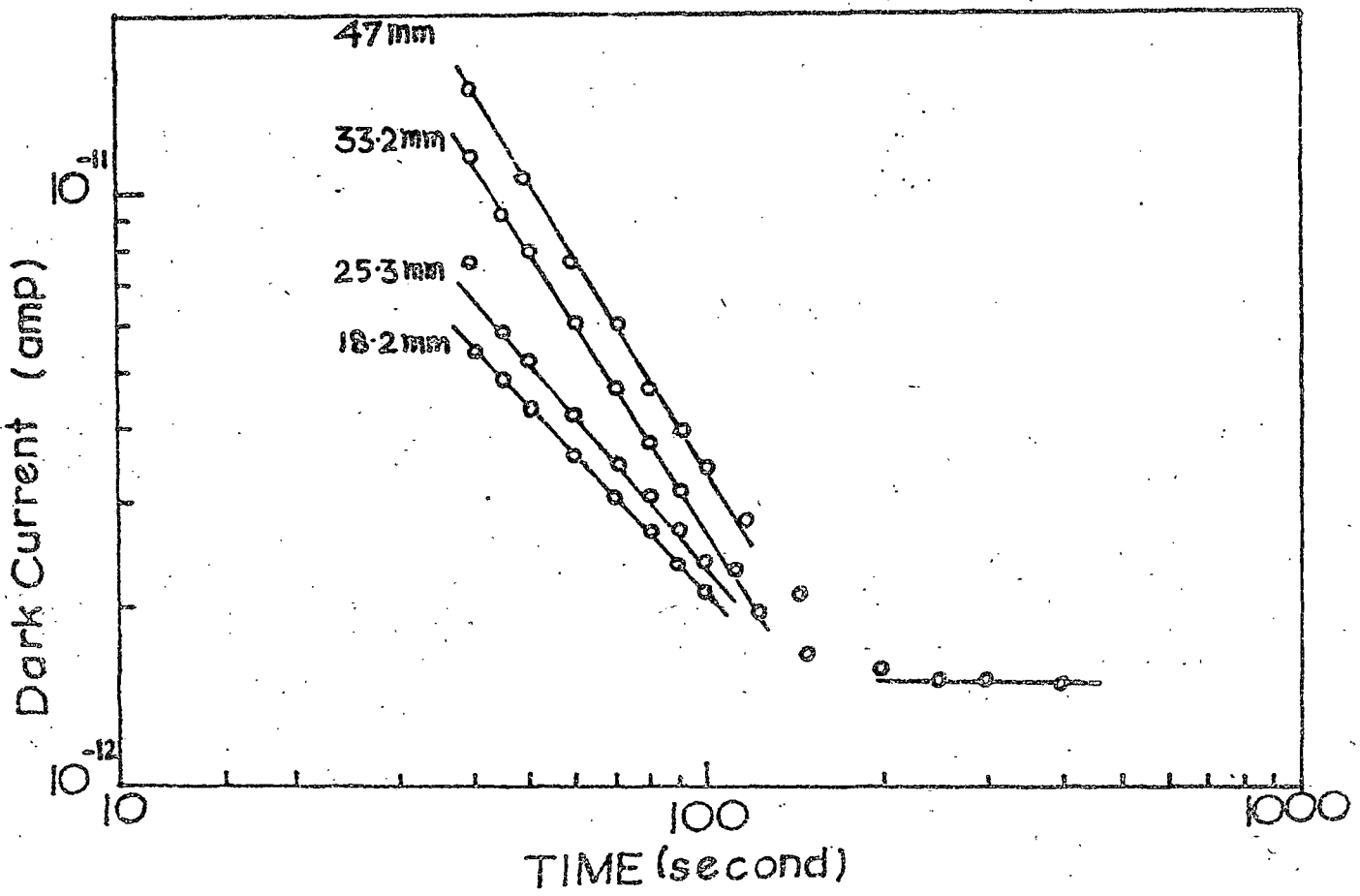

The R - t plot of desorption kinetic data at different vapour pressures for ethyl acetate vapour desorption from O-nitrobenzoic acid.

FIGURE - 3.26

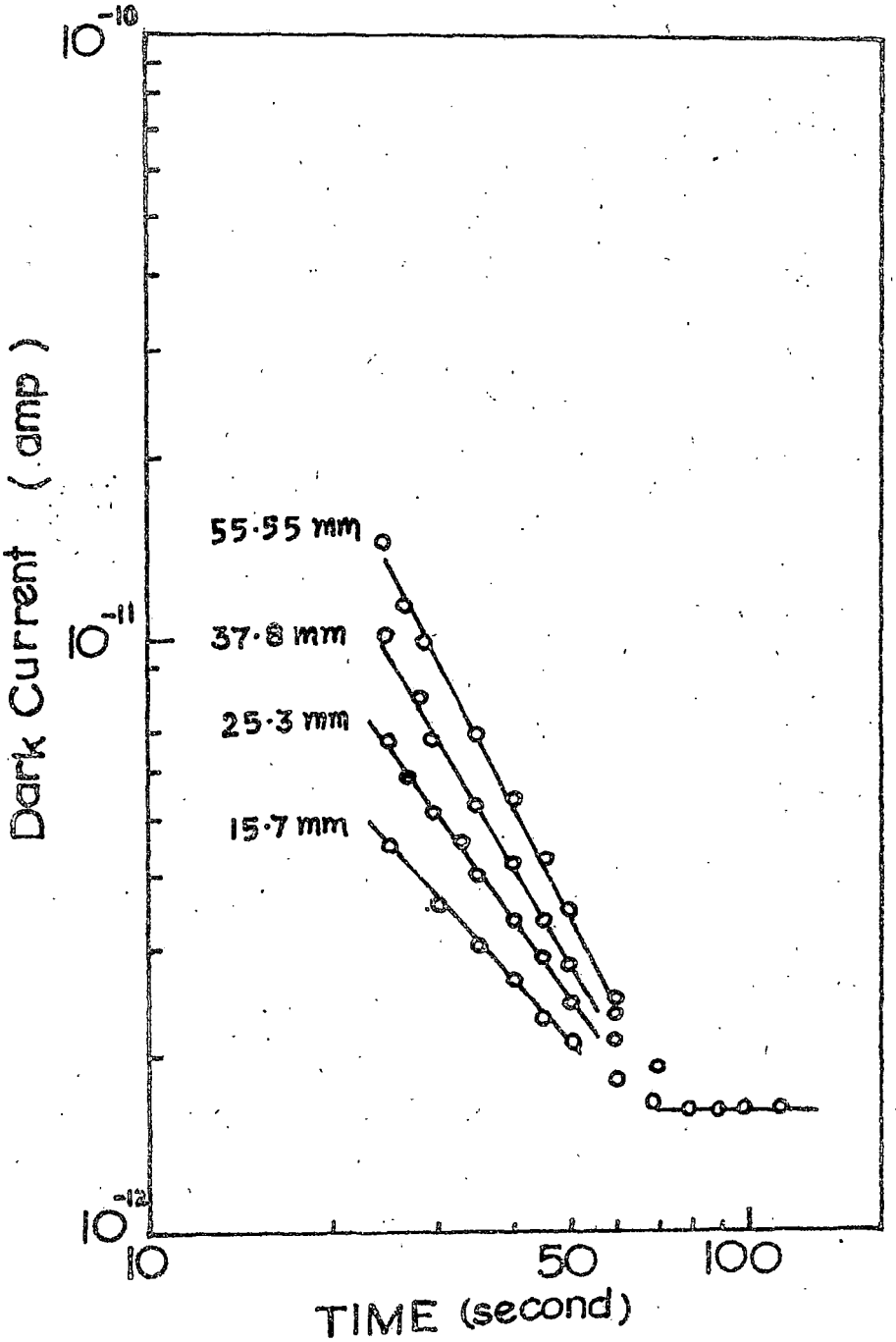

The R - t plot of desorption kinetic data at different vapour pressures for ethyl acetate vapour desorption from m-nitrobenzoic acid.

FIGURE - 3.27

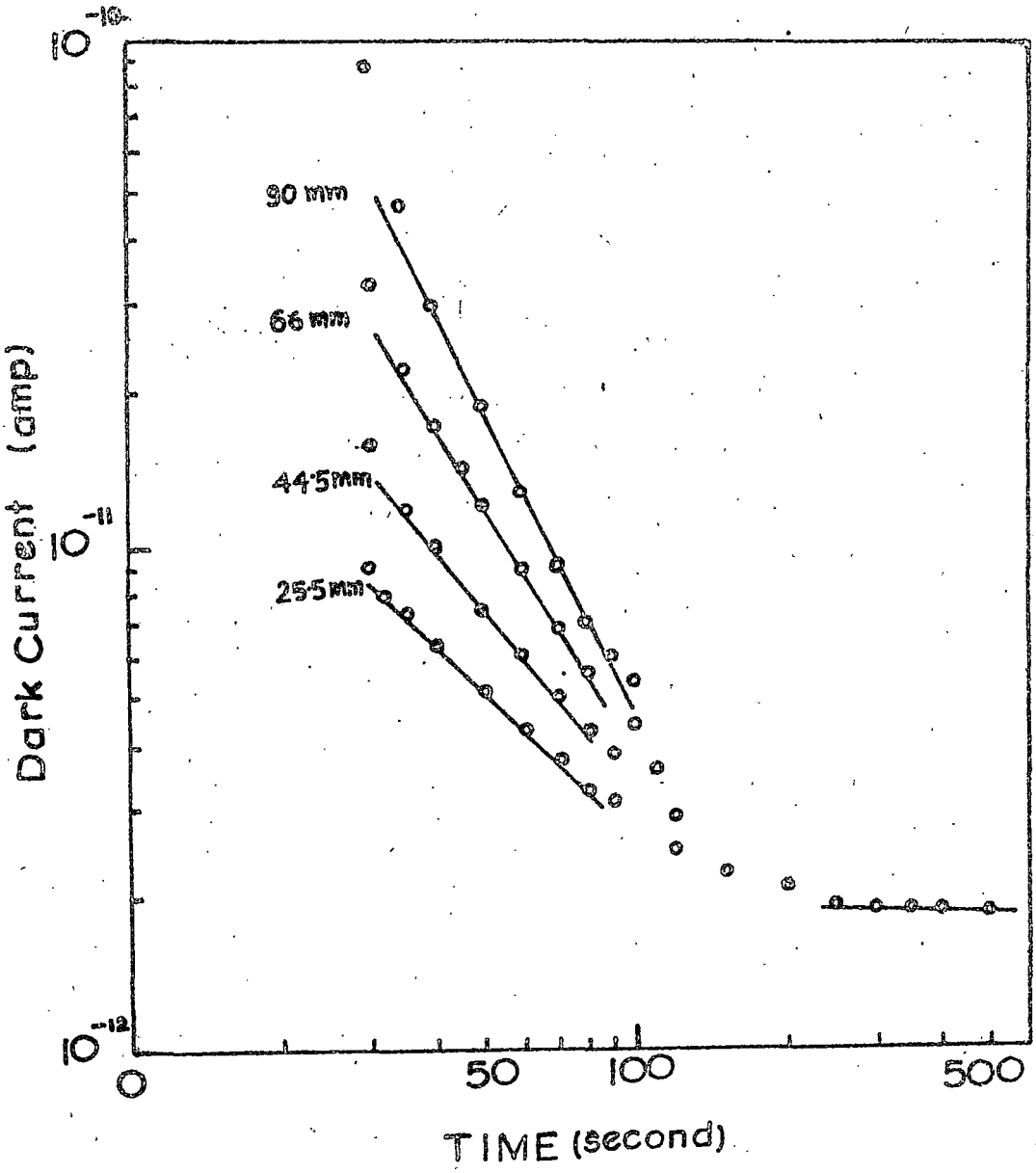

The R - t plot of desorption kinetic data at different vapour pressures for ethyl acetate vapour desorption from p-nitrobenzoic acid.

FIGURE - 3.23

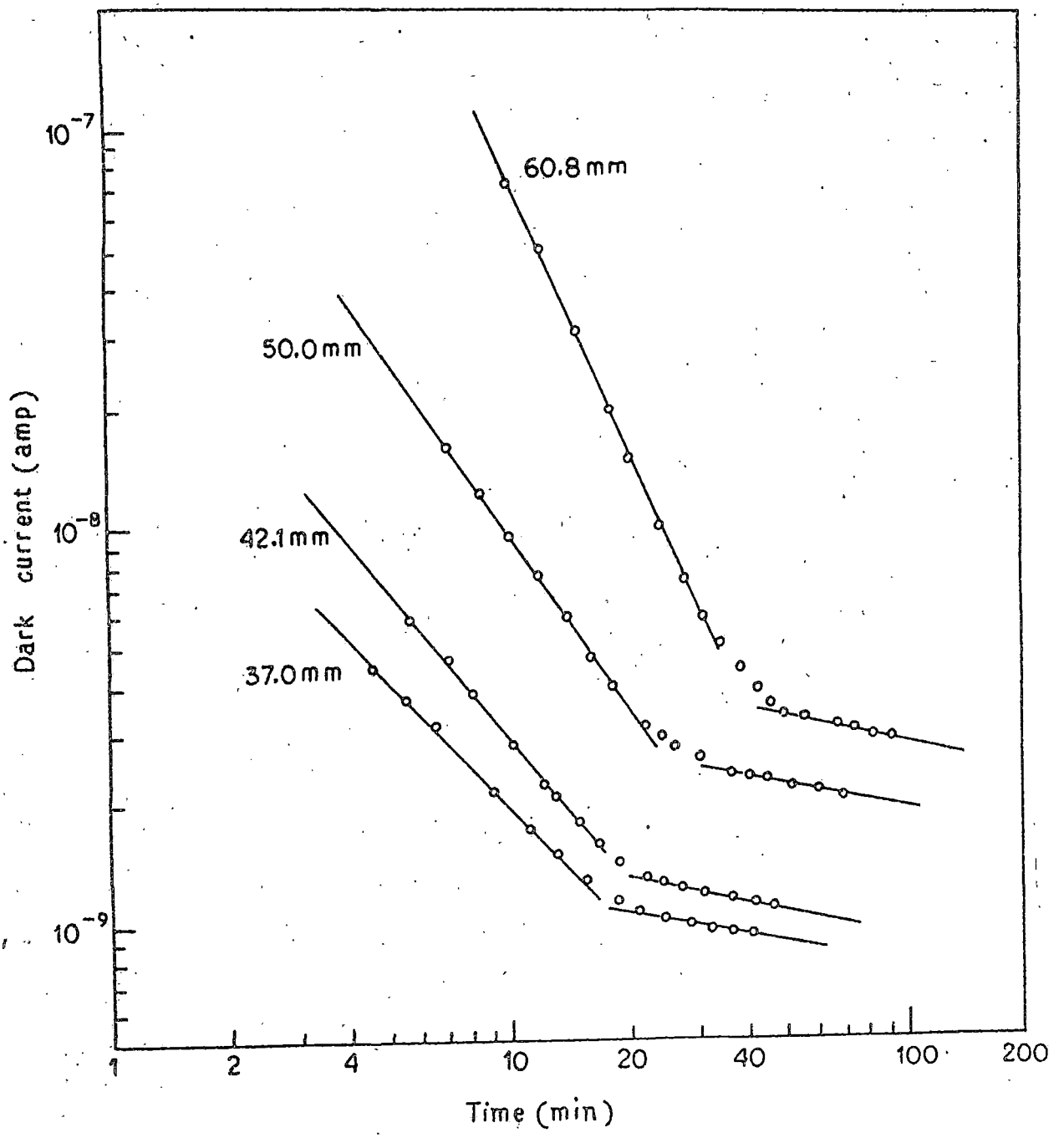

The R - T plot of desorption kinetic data at different vapour pressures for ethyl acetate vapour desorption from 1,4-dinitronaphthalene. (Showing two region linearity before reaching initial conductivity value)

FIGURE - 3.29

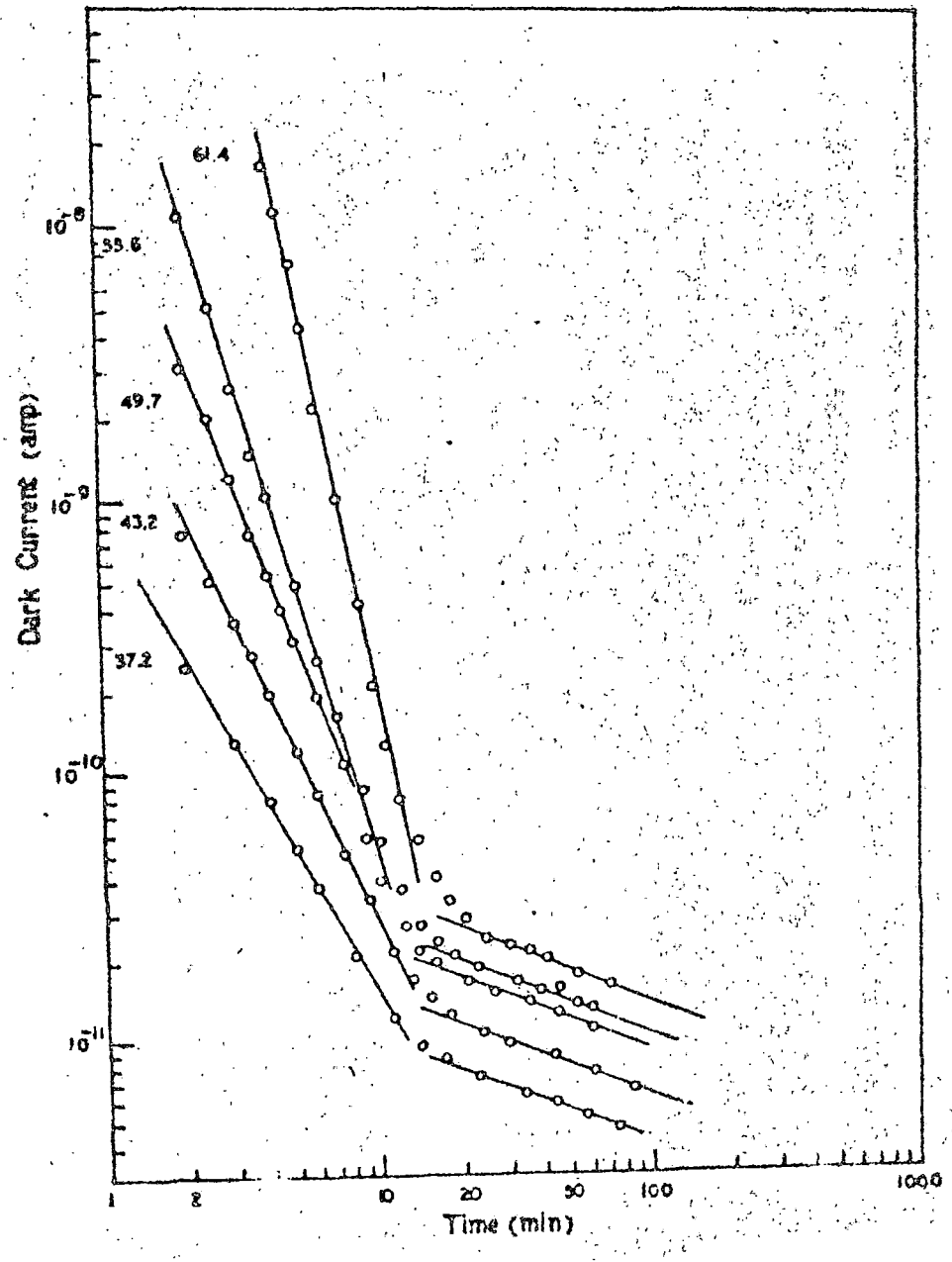

The R ~ t plot of desorption kinetic data at different vapour pressures for ethyl acetate vapour desorption from 1,3,5-trinitrobenzene. (Showing two region linearity before reaching initial conductivity value)

Table 3.3

Vapour pressure dependence of the factors β' and $\beta^{*\prime}$ for different nitroaromatic semiconductors on adsorption and desorption of respective vapours.

Semiconductor	Vapour used	Vapour pressure (mm)	$\beta' \times 10^2$ (ev)	$\beta^{*\prime} \times 10^2$ (ev)
9-nitro-anthracene*	Carbon-tetra-chloride	42.0	2.545	5.385
		51.7	2.037	4.655
		60.8	1.828	3.548
		72.5	1.639	3.244
		84.2	1.504	2.542
1,4-dinitro-naphthalene*	Methanol	42.5	4.342	4.774
		52.3	3.093	3.349
		64.0	1.721	2.249
		71.3	1.220	1.697
1,3,5-trinitro-benzene*	Ethanol	37.1	0.649	1.684
		38.8	0.502	1.247
		45.9	0.384	1.006
		52.1	0.286	0.826
2-nitro-fluorene**	Ethyl-acetate	27	9.19	11.82
		41	5.26	7.72
		45	4.36	5.81
		51	2.43	2.74
		66	1.76	2.08

Contd.

Table 3.3 (Contd.)

Semiconductor	Vapour used	Vapour pressure (mm)	β' x 10^2 (ev)	$\beta^{x'}$ x 10^2 (ev)
O-nitro-benzoic-acid**	Ethyl acetate	18.2	1.26	2.47
		25.3	0.93	2.25
		33.2	0.79	1.65
		47.0	0.56	1.55
m-nitro-benzoic acid**	Ethyl acetate	16.7	2.22	2.32
		25.3	1.18	1.76
		37.3	0.67	1.46
		55.5	0.26	1.30
p-nitro-benzoic-acid**	Ethyl acetate	25.5	1.51	2.59
		44.5	0.86	2.04
		66.0	0.59	1.62
		90.0	0.38	1.24

* Sample cell at 22°C

** Sample cell at 25°C

saturation is reached soon after the short time region linearity is completed. This suggest that R - Z equations :

$$dm/dt = \bar{A} \exp (- \bar{\beta} m / R T) \text{ and}$$

$$dm/dt = -\bar{A}^{*} \exp (- \bar{\beta}^{*} m / k T)$$

with a different activation energy and pre-exponential constant are also applicable in the long time region. Such linearity in the R - Z plots in the long time region have been obtained for adsorption and desorption of ethylacetate, benzene and carbontetrachloride vapour on and from 1,3,5-trinitrobenzene and 1,4 dinitronaphthalene. The activation energies of adsorption (β'') and desorption ($\beta^{*''}$) have been evaluated from the slopes of such lines in the long time region. In table 3.4, the values of β' and $\beta^{*'}$, β'' and $\beta^{*''}$ are presented for ethylacetate vapour adsorption at different vapour pressure. It is noted that for any particular pressure of ambient vapour $\beta^{*'} > \beta'$ and $\beta^{*''} > \beta''$.

3.3 Potential Energy Curves for Vapour Adsorption Process :

There are number of different treatments[140] for the R - Z equation. A simple two stage process after Wiley and Leslie[138] as shown in Fig. 3.30 seems quite satisfactory for vapour-semiconductor pair where the vapour adsorption saturation is quickly

Table 3.4

Vapour pressure dependence of the factors β', β'' and $\beta^{*'}$, $\beta^{*''}$ for adsorption and desorption kinetics respectively in case of ethyl acetate vapour adsorption

Semiconductor	Vapour pressure (mm)	$\beta' \times 10^2$ (ev)	$\beta'' \times 10^2$ (ev)	$\beta^{*'} \times 10^2$ (ev)	$\beta^{*''} \times 10^2$ (ev)
1,4-dinitro-naphthalene	37.0	2.20	6.412	2.385	13.84
	42.1	1.978	6.118	2.089	13.52
	50.0	1.663	5.734	1.736	13.87
	60.8	1.052	5.206	1.111	13.76
1,3,5-trinitro-benzene	37.2	1.777	3.410	1.413	6.451
	43.2	1.071	3.277	1.169	6.508
	49.7	0.965	3.238	0.932	6.469
	58.6	0.612	3.191	0.758	6.468
	61.4	0.465	2.958	0.509	6.312

FIGURE - 3.30

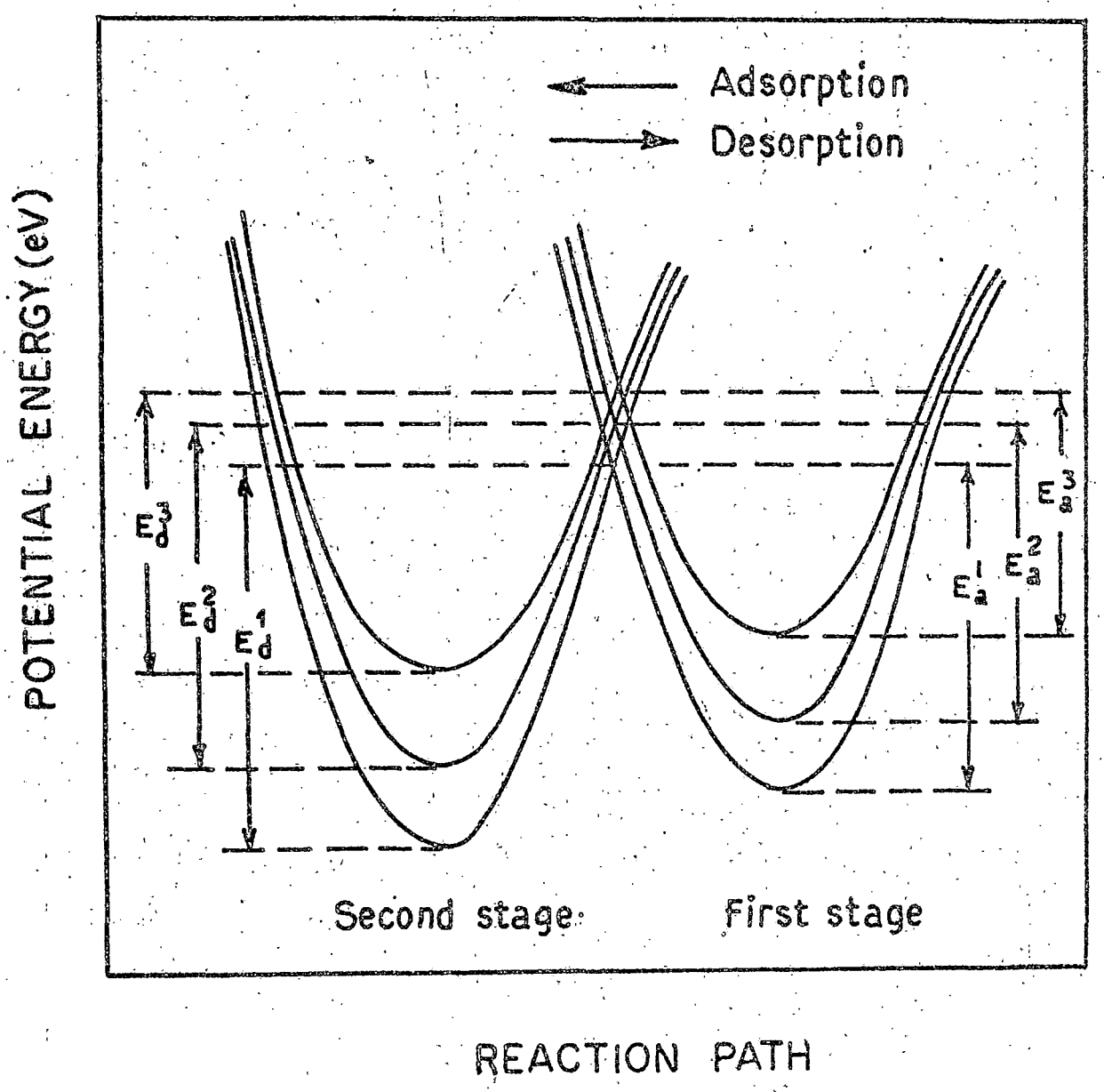

The potential energy curves for "two stage" vapour adsorption explaining the R - t plots (Figs. 3.12 - 3.18 and 3.21 - 3.27). E_d^1, E_d^2 and E_d^3 are activation energies of desorption in order of increasing pressure. Similarly E's are activation energies for adsorption.

reached and the desorption is quick and complete (Figs. 3.1-3.7). R - t plots in such cases do not show any measurable slope in the long time region. In the first stage, a mobile vander Waals' adsorption on the crystal surface gives a Lennard-Jones potential energy curve which is assumed to depend on the fraction of surface coverage. This stage is followed by a Rate determining transition over a potential energy barrier to the final stage of adsorption forming weakly bound complexes between the vapour molecules and the nitroaromatic crystallites. The barrier is formed by the intersection of the two potential energy curves. As more molecules get physically adsorbed (Vander Waals'), a repulsive interaction between the dipoles will raise the potential energy curve for the first stage thereby lowering the barrier height giving decreasing activation energy of adsorption with increasing vapour pressure. As the surface coverage of the second stage rises, this potential energy curve also rises resulting in lowering of desorption activation energy with increasing pressure. The rise of the second stage curve is such that the minimum of this curve is always at lower energy than the minimum of the first stage, the energy difference between these two minima decreases with increase in vapour pressure.

In other cases of vapour adsorption (like Figs. 3.8 and 3.9) an additional stage of adsorption is suggested by the second

linear R = 3 plot in the long time region (Figs. 3.19, 3.20, 3.22 and 3.23). A transition over this second potential barrier occurs and the vapour molecules get strongly bound to the surface molecules of the nitroaromatic crystallites. The measured values of β'' and $\beta^{*\prime\prime}$ are slightly larger than β' and $\beta^{*\prime}$. It is not possible to suggest if this means a higher potential energy barrier in the third stage adsorption than the second stage adsorption as there are no informations about the values of α and α' (α' being the value of α in second stage interaction between vapour and the surface molecules of the semiconductor). The third stage of adsorption potential is possibly smaller as α' is expected to have a smaller value. Even if $\alpha \simeq \alpha'$, Boltzmann factor for crossing the barrier on the left of the second stage potential well will be approximately equal to that on the right as the difference in the barrier heights is insignificant. However, considering the fact that the strongly bound complexes are not easily desorbed as are the weakly bound complexes in the two stage process, it seems that the potential well in the third stage is deep. A model diagram for three stage adsorption process is shown in Fig. 3.31. The desorption activation energy from the third stage, as shown in table 3.4, seems to be independent of vapour pressure. Strongly bound complexes behave more like a chemical species (though the binding energy is very much less) and a certain amount of energy is required to break the bond. $\beta^{*\prime\prime}$ m, the activation energy for

FIGURE - 3.31

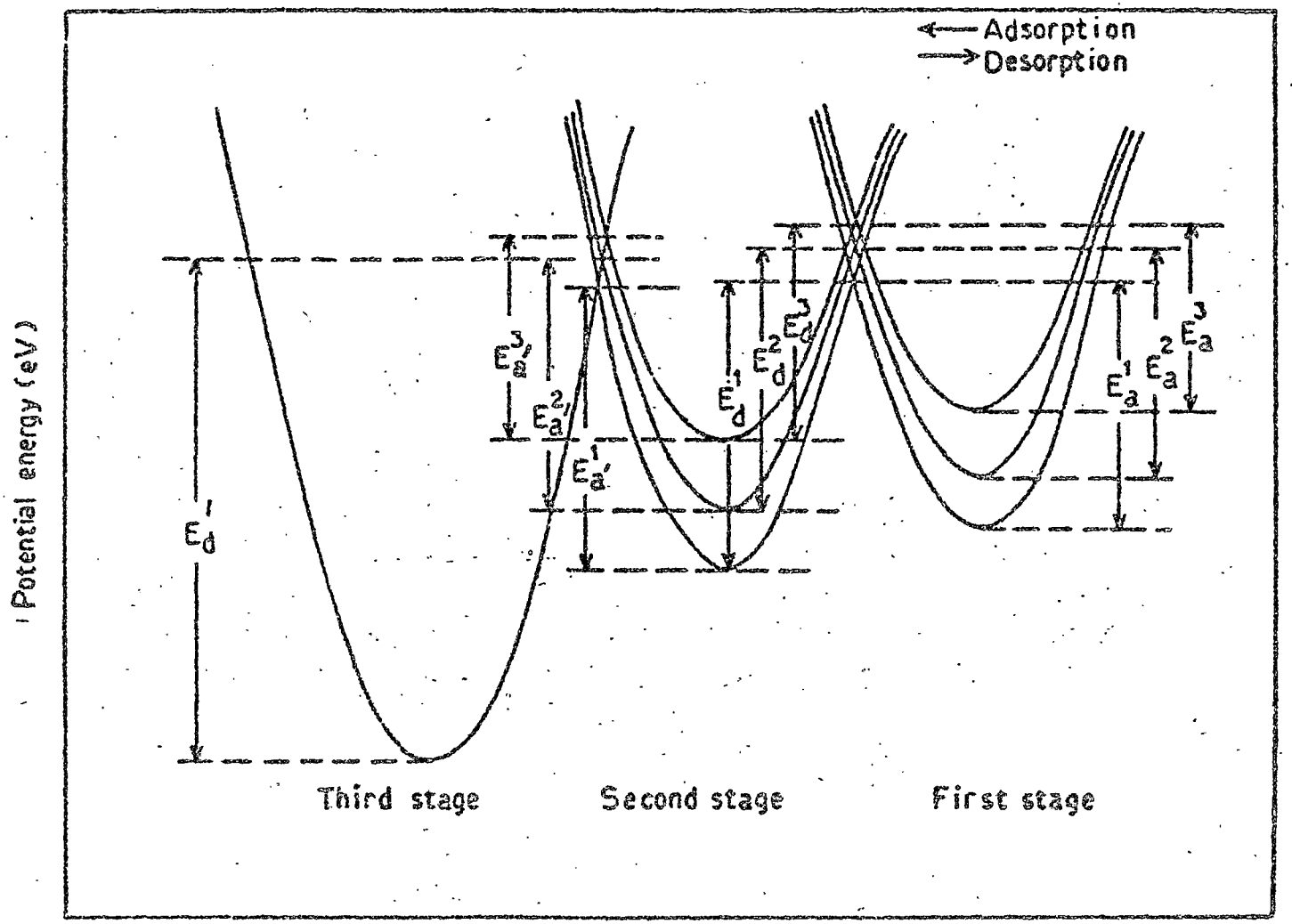

The potential energy curves for "three stage" vapour adsorption explaining the two region linearity in the E-Z plots (Figs. 3.19, 3.20 and 3.28, 3.29). E_a^1, E_a^2, E_a^3 and E_a^1, , E_a^2, , E_a^3, are the activation energies of adsorption in order of increasing pressure in the 2nd and 3rd stage respectively. E_d's are the activation energies of desorption.

desorption from third stage should, apart from a small entropy factor be equal to the binding energy of the vapour surface molecular complex. It has not been possible to estimate the binding energy because the experiments do not provide any numerical value of α and α'.

4. Conclusion

The adsorption of vapours increases the semiconduction current of the nitroaromatic semiconductors. The adsorption and desorption kinetics follow the modified Roginsky - Zeldovich equation. A two stage adsorption process is applicable for such vapour-semiconductor systems where the vapour adsorption saturation is quickly reached and the desorption is quick and complete. In some cases, however, an additional stage of adsorption is suggested by the second linear R - t plot in the long time region. A transition over this second potential barrier occurs and the vapour molecules get strongly bound to the surface molecules of the nitroaromatic crystallites.

CHAPTER - 4

COMPENSATION EFFECT IN SOME NITROAROMATIC SEMICONDUCTORS

1. Introduction

The pre-exponential factor (σ_o) in the operational definition of semiconductors has been a subject of much discussions[40,46,47,50,99,100]. Rosenberg et al[40] have proposed σ_o as an exponential function in their three constant conductivity equation :

$$\sigma_T = \sigma_o' \exp (E/2 K T_o) \exp (-E/2 K T) \quad (1.1)$$

'T_o' is the characteristic temperature often known as 'compensation temperature'. σ_o' and T_o remain invariant for the same compound. The compensation effect is defined by the linear relationship of log σ_o and the activation energy (E). The values of σ_T and E change in such a manner that their effects on σ_o are mutually compensated. Johnston and Lyons[100,101] believe that compensation effect may originate solely from the calculations and it requires no physical interpretation. However, they have suggested that if σ_o and E are physically related, one should get a linear relationship between log σ_T and E yielding the semiconductive parameters in agreement with the values obtained

from other sources. In 'apparent' compensation effect, for each particular E - value, unique values of σ_0 and σ_p does not exist and the system can not be precisely defined. In 'true' compensation effect excellent correlation between log σ_0 and E and also between log σ_p and E are obtained. Thus, both 'true' and 'apparent' compensation effects follow the linear log σ_0 vs. E relationship.

It has been established that when E is changed by chemical vapour or gas adsorption, 'true' compensation effect is indeed observed in some polyene semiconductors and the effect has a physical basis.

In the previous chapter, we have shown that two distinct adsorption processes - one forming weakly bound and the other forming strongly bound complexes characterised by two and three stage adsorption processes respectively are operative in nitro-aromatic semiconductors. In this chapter, we present our results and discussions on the validity of true compensation effect, its physical basis and its relationship with the adsorption and desorption processes in nitroaromatic semiconductor-vapour systems.

2. Experimental and Results

2.1 Effect of vapour adsorption on activation energy :

The semiconduction activation energies of the crystalline powders of the nitroaromatic compounds in a sandwich cell were measured several times in the dry nitrogen atmosphere and also in vacuum. All the measurements gave consistent values. The observed values are 2.00, 1.18, 1.73, 2.25 and 2.51 ev (approx.) for 9-nitroanthracene, 1,4-dinitronaphthalene, 1,3,5-trinitrobenzene, 2-nitrofluorene and O-nitrobenzoic acid respectively. On adsorption of various vapours on the crystallite surfaces, the semiconducting current is enhanced and the activation energy is appreciably increased.

The powdered semiconductors were used in form of a sandwich cell to determine the effect of adsorbed vapours on the semiconduction activation energy. The sample was first allowed to adsorb the vapour at a fixed pressure and come to a steady state at a constant sample cell temperature in the chamber atmosphere containing the vapour in nitrogen. The pressure of the total gas mixture in the chamber was atmospheric and the partial pressure of the vapour was the saturation vapour pressure of the reagent liquid at the temprature at which it was kept. Both inlet and outlet of the chamber were then sealed and the value of the saturation current was noted with time. The saturation current was

found to be almost constant for a long time indicating that the conduction in the system was mainly electronic[141,142]. The cell was then rapidly cooled to about - 30°C. The chamber was then flushed gently with dry nitrogen gas. The out-let of the chamber was kept open and the atmospheric pressure was maintained inside the chamber. The temperature was then slowly increased and the semiconduction current was measured with the increasing temperature of the sample cell. The results of adsorption of a vapour on different nitroaromatic semiconductors are shown in Figs. 4.1-4.5. The straight line portion in the low temperature region shows the semiconductive properties of the nitroaromatics with adsorbed vapour and the slopes of these lines give the activation energies of the respective systems. At considerable higher temperatures, the adsorbed vapour starts desorbing and the rate of desorption increases with increasing temperature and the current begins to diminish. The straight line portions of the curves at the higher temperature region above the point C, give the activation energies of the semiconductors approximately the same as that in dry nitrogen atmosphere. The observed values (1.98, 1.11, 1.75, 2.2 and 2.5 ev) are slightly lower possibly due to incomplete desorption of adsorbed vapours. Similar curves were also obtained with certain other vapours forming very weak revesible complexes with these nitroaromatic semiconductors. For the remaining vapours

FIGURE - 4.1

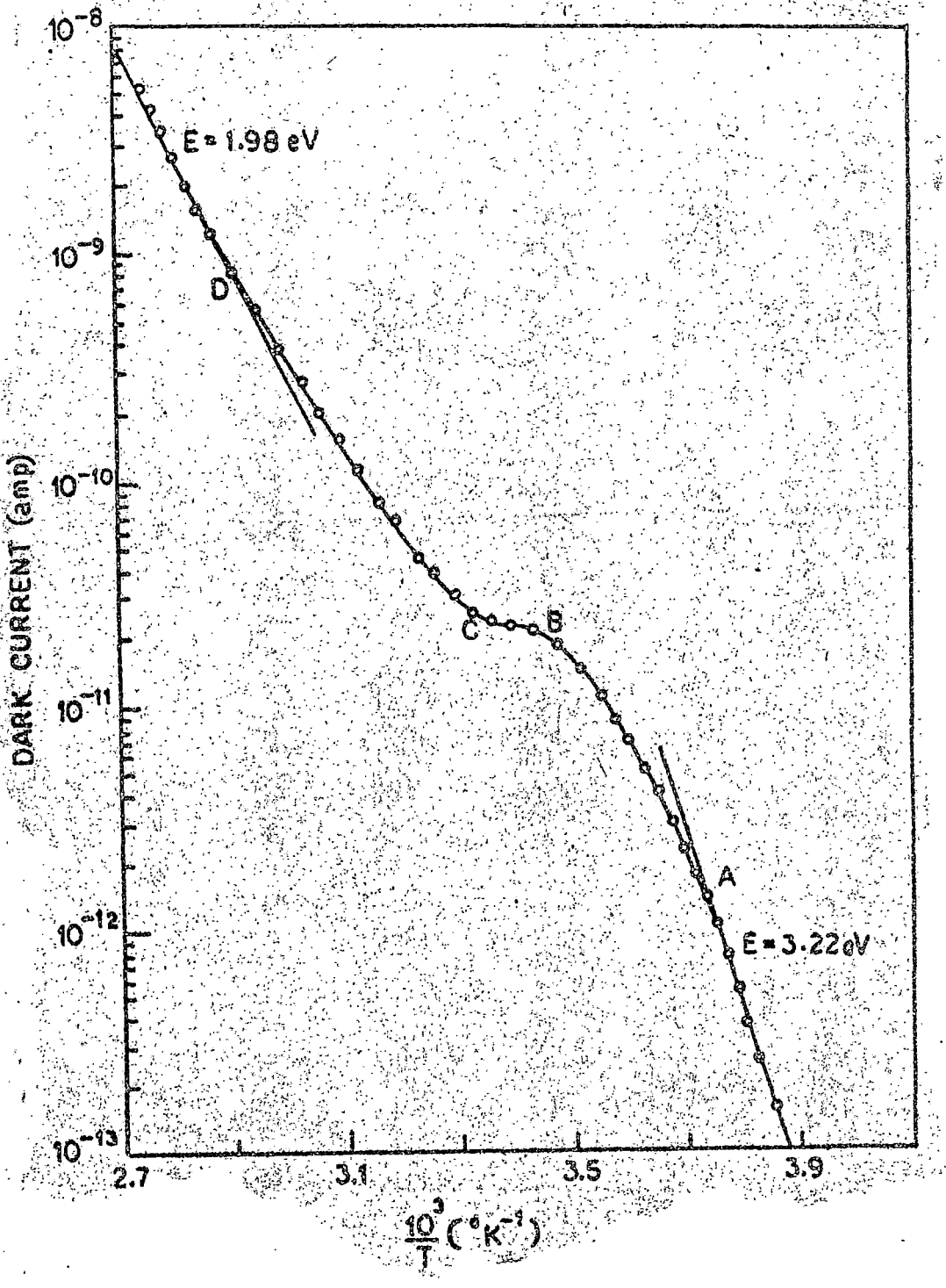

Semiconductivity in a methanol adsorbed 9-nitroanthracene powder cell as a function of temperature. (Ambient vapour pressure 50 mm; adsorbed at sample cell temperature 22°C)

FIGURE - 4.2

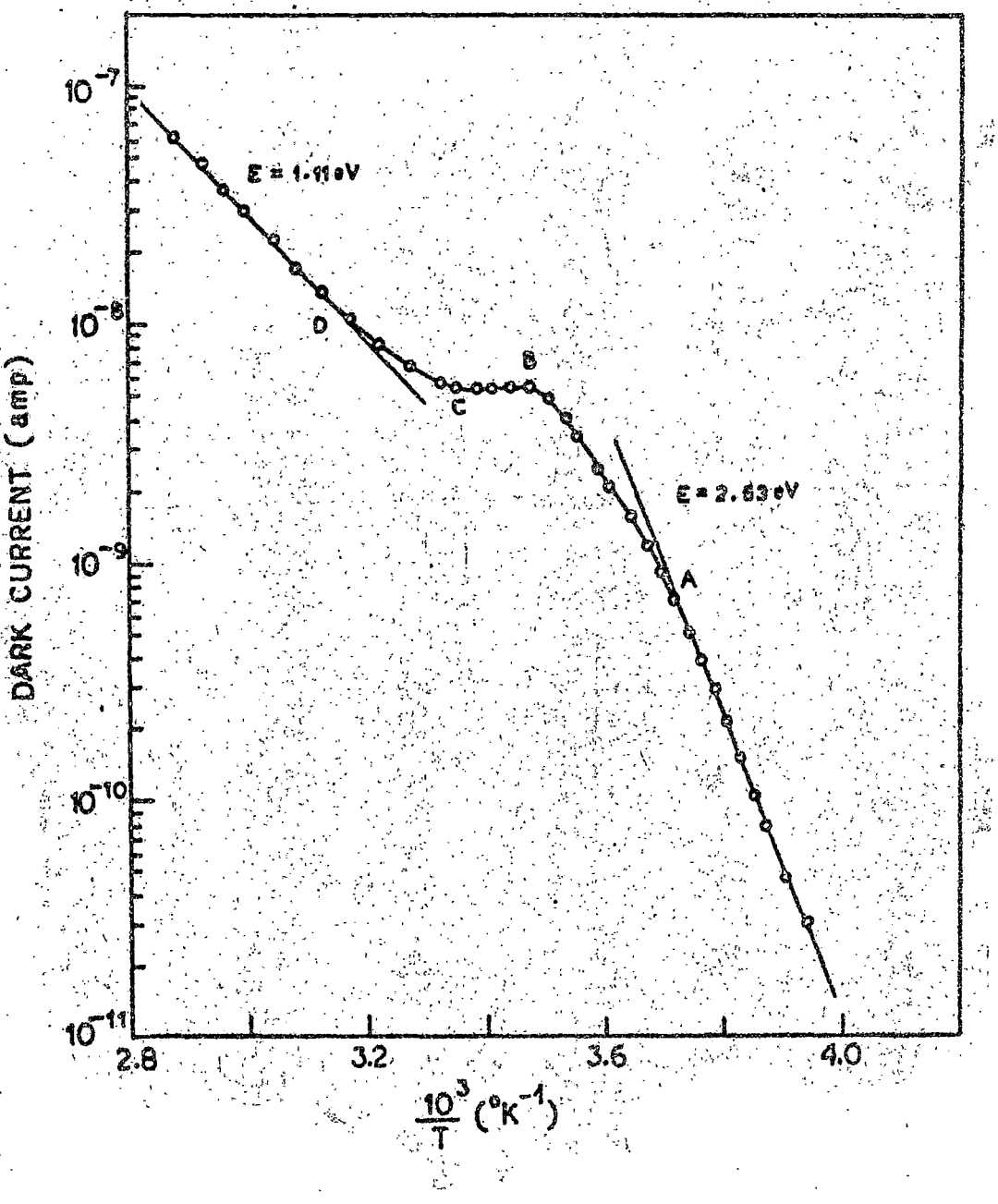

Semiconductivity in a methanol adsorbed 1,4-dinitronaphthalene powder cell as a function of temperature. (Ambient vapour pressure 50 mm, adsorbed at sample cell temperature 22°C)

FIGURE - 4.3

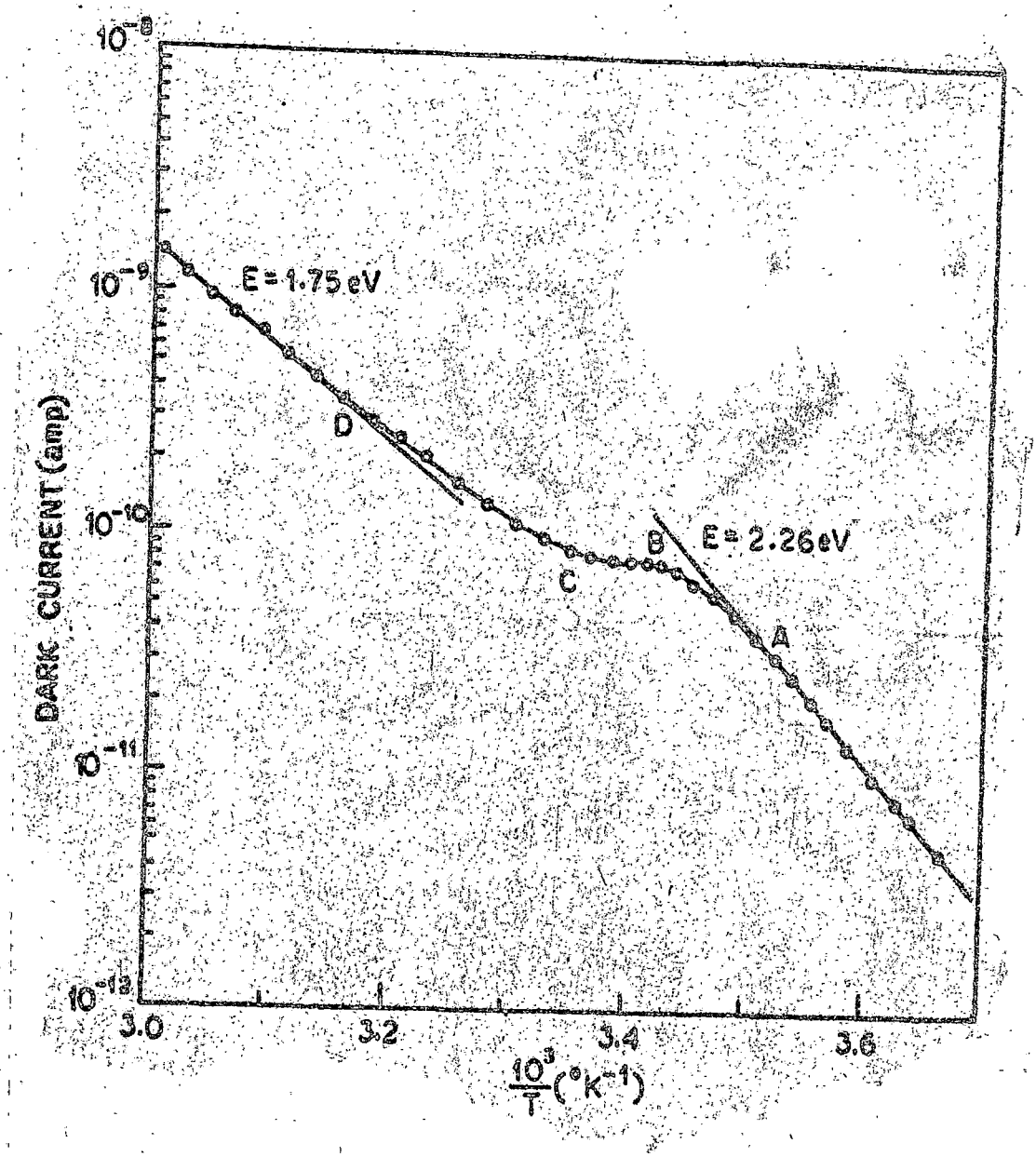

Semiconductivity in a methanol adsorbed 1,3,5-trinitrobenzene powder cell as a function of temperature. (Ambient vapour pressure 60 mm; adsorbed at sample cell temperature 22°C)

FIGURE - 4.4

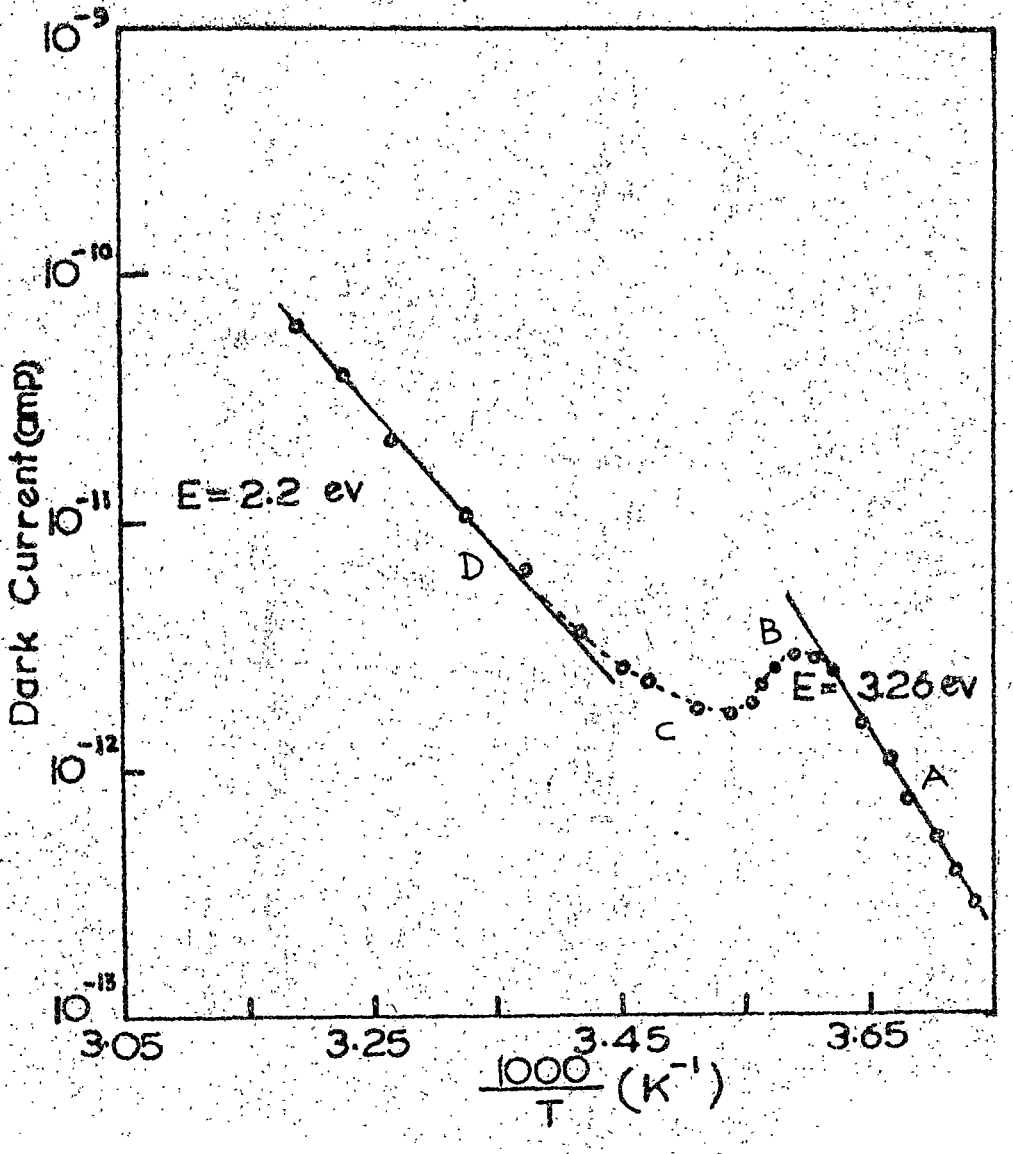

Semiconductivity in a carbontetrachloride adsorbed powder cell as a function of temperature. (Ambient vapour pressure 50 mm; adsorbed at sample cell temperature 25°C)

FIGURE - 4.6

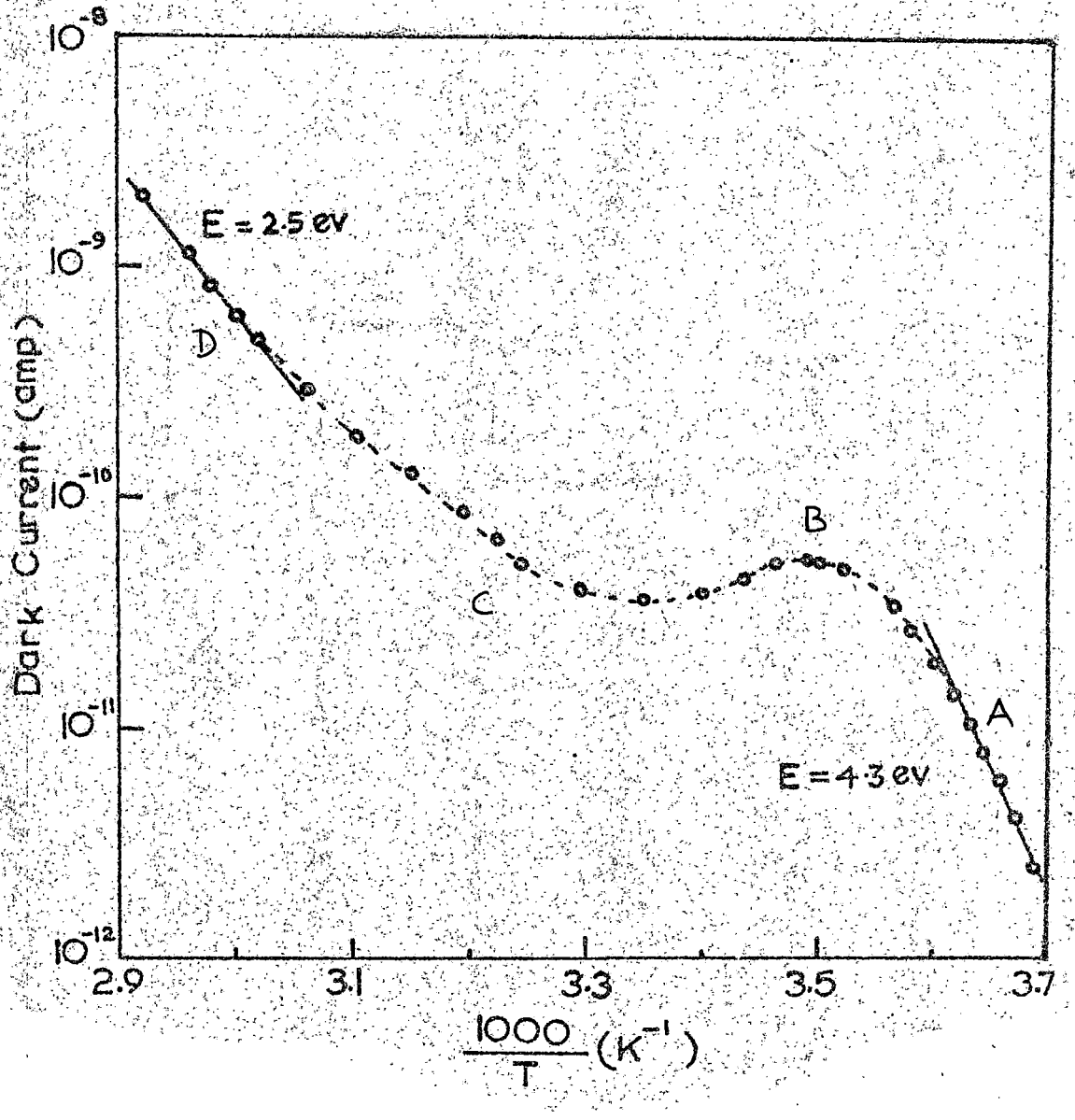

Semiconductivity in a methanol adsorbed O-nitrobenzoic acid powder cell as a function of temperature. (Ambient vapour pressure 50 mm; adsorbed at sample cell temperature 25°C)

that are found to form some sort of strong complexes (as described in the previous chapter), the current does not return to the initial value at the point C and the activation energy in the higher temperature region is not equal to the vacuum / dry nitrogen activation energy value as shown in Figs. 4.6 and 4.7 for ethyl acetate vapour adsorption on 1,4-dinitronaphthalene and 1,3,5-trinitrobenzene. For 9-nitroanthracene, 2 - nitrofluorene and 0-nitrobenzoic acid, vapours of ethanol, methanol, ethylacetate, carbon tetrachloride, benzene and n-hexane; for 1,4-dinitronaphthalene that of ethanol, methanol and cyclohexane and for 1,3,5-trinitrobenzene vapours of ethanol, methanol, cyclohexane and n-hexane were found to form weak reversible complexes and the curves are similar to that in Figs. 4.1 - 4.5.

The effect of adsorption of different vapours on the semiconduction activation energy of these nitroaromatic compounds has been made in the usual manner after adsorbing different vapours at a fixed partial vapour pressure maintaining the sample cell at a constant temperature. In Figs. 4.8 - 4.14, plots of log $\sigma(T)$ vs. 1/T for different nitroaromatic semiconductors are shown in the low temperature region for different vapour adsorption. It is observed that the activation energy values are different for different vapour adsorption. Different vapours forming weak reversible complexes change the activation energies of the nitroaromatics

FIGURE - 4.6

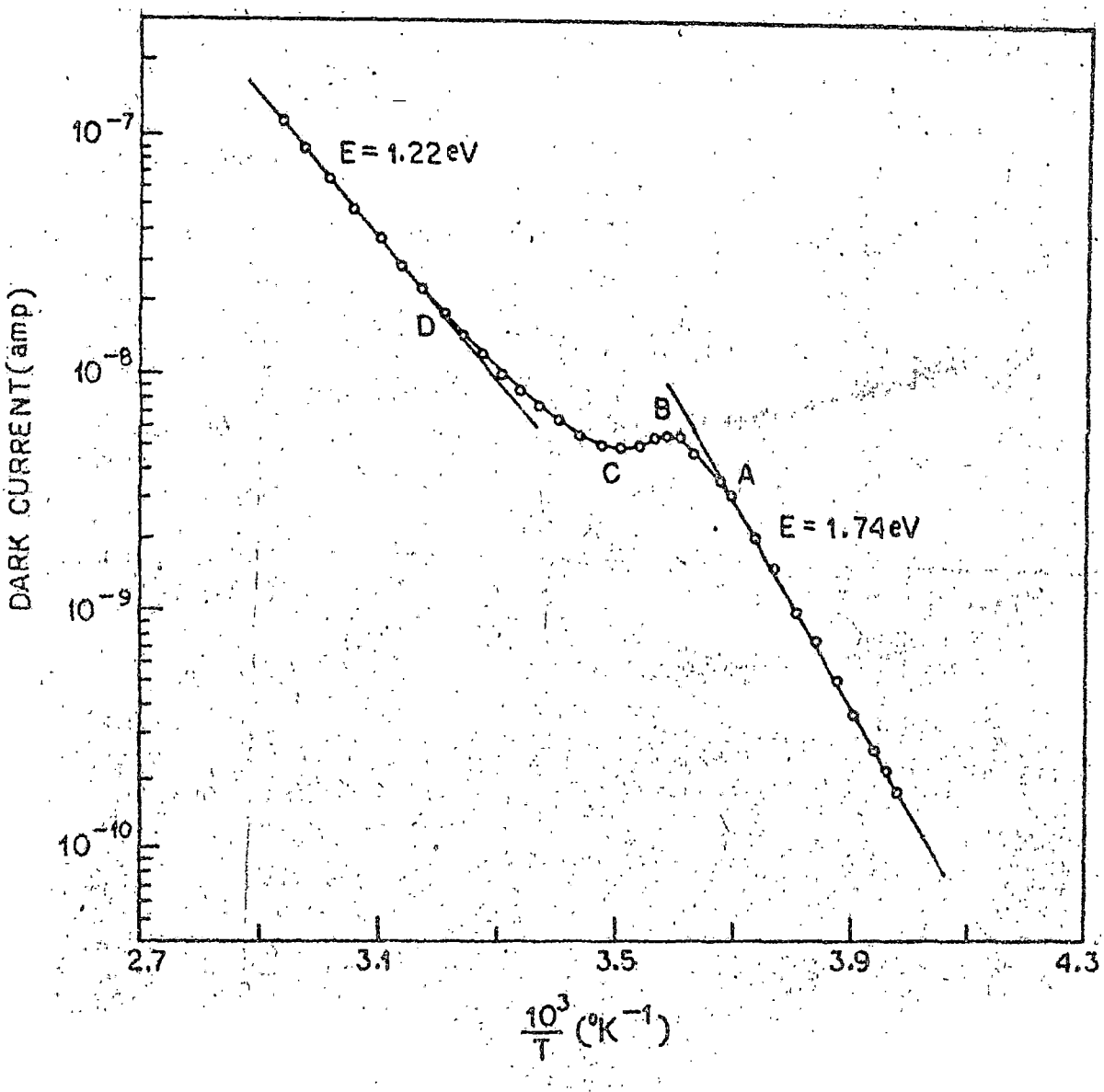

Semiconductivity in an ethyl acetate adsorbed 1,4-dinitro-naphthalene powder cell as a function of temperature. (Ambient vapour pressure 55.5 mm; adsorbed at sample cell temperature 22°C)

FIGURE - 4.7

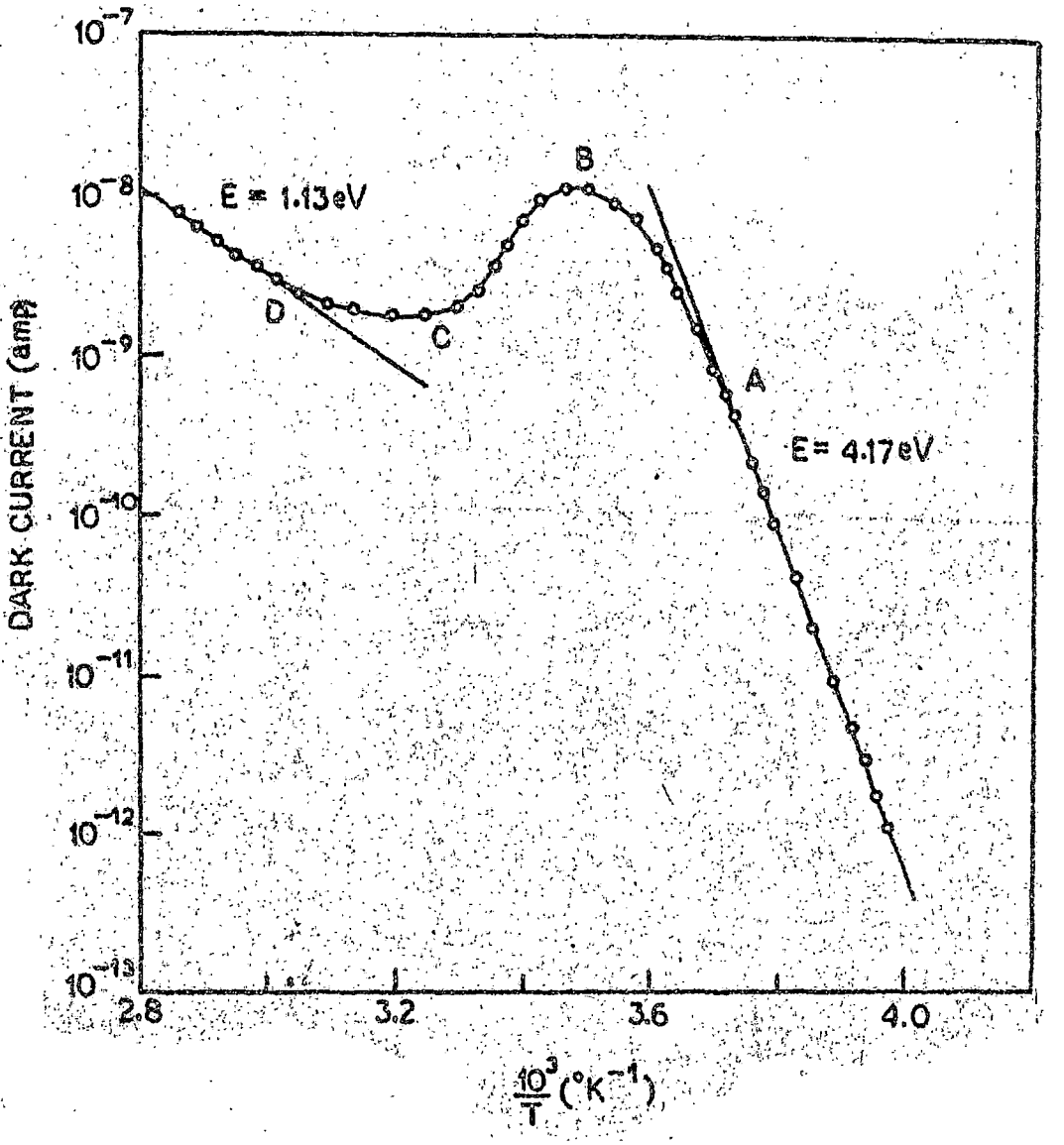

Semiconductivity in an ethyl acetate adsorbed 1,3,5-trinitrobenzene powder cell as a function of temperature. (Ambient vapour pressure 53.5 mm; adsorbed at sample cell temperature 22°C)

FIGURE - 4.8

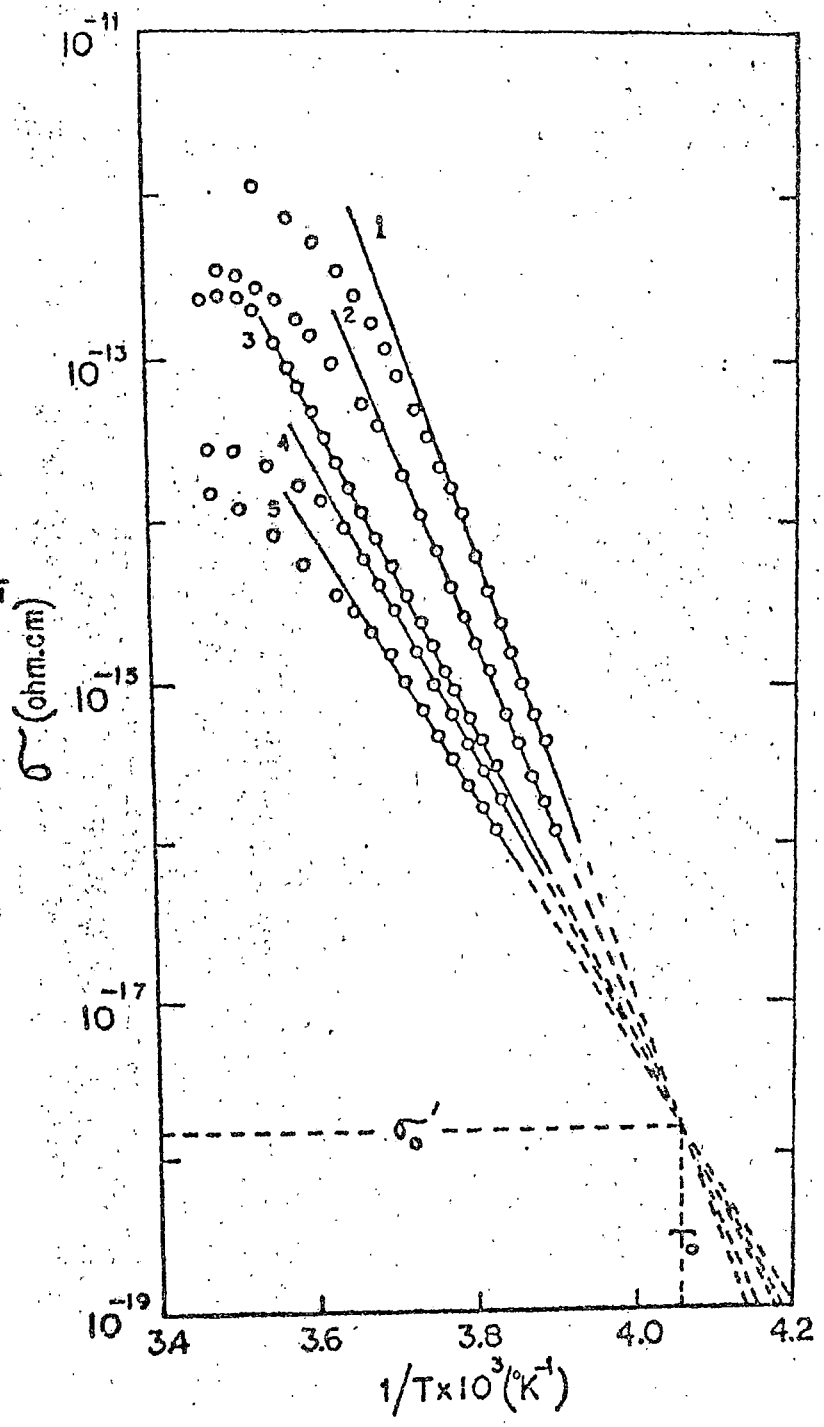

Semiconductivity in a 9-nitroanthracene powder cell (steady state condition) with the adsorption of different vapours at the same vapour pressure (50 mm) and at a sample cell temperature 22°C. Solid lines represent temperature region of measurements, broaken lines are extrapolations. Each line corresponds to a specific vapour adsorbed state : 1. ethanol, 2. ethylacetate, 3. benzene, 4. carbon-tetrachloride and 5. methanol (Refer Table 4.1, 4.3)

FIGURE - 4.9

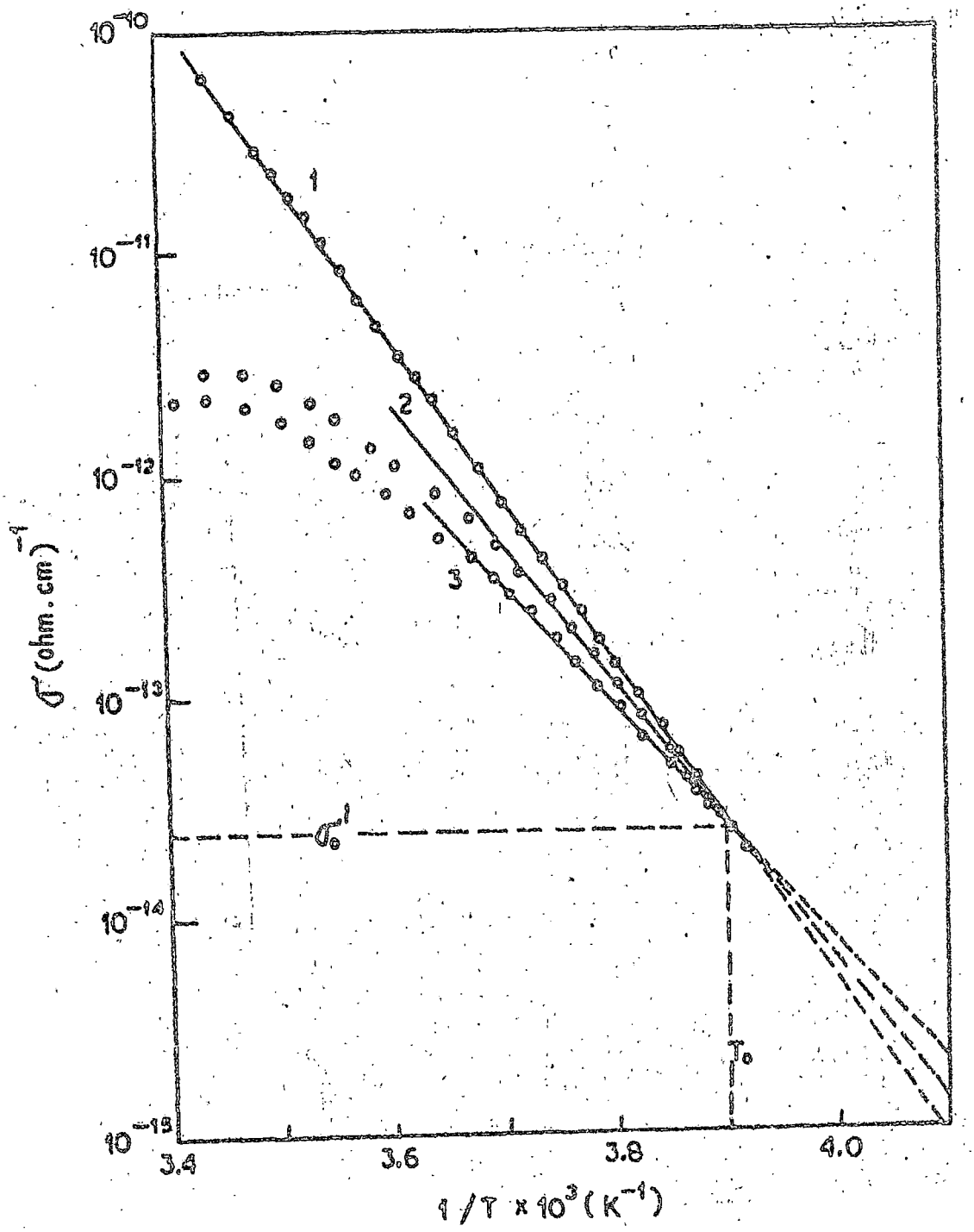

Semiconductivity in a 1,4-dinitronaphthalene powder cell (steady state condition) with the adsorption of different vapours at the same vapour pressure (50 mm) and at a sample cell temperature of 22°C. Solid lines represent temperature region of measurements, broaken lines are extrapolations. Each line corresponds to a specific vapour adsorbed state : 1. ethanol, 2. methanol and 3. cyclohexane. (Refer table 4.1, 4.4)

FIGURE - 4.10

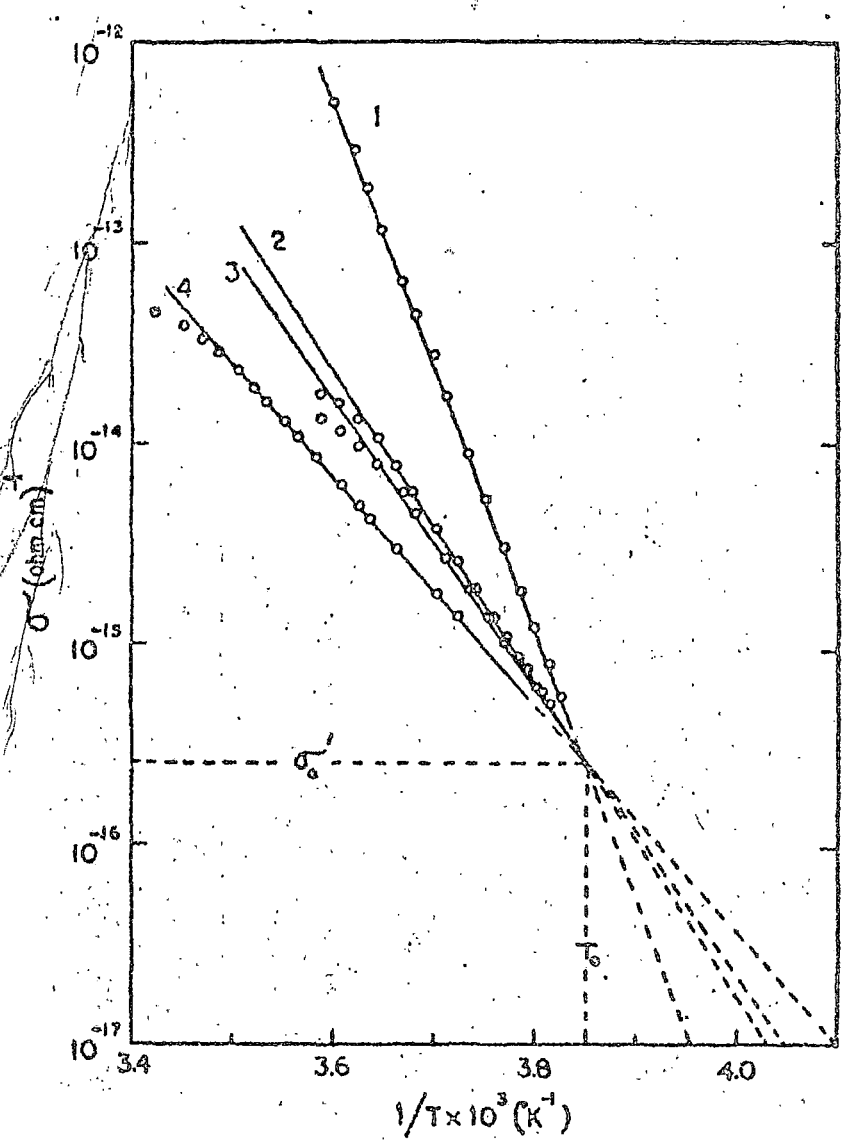

Semiconductivity in a 1,3,5-trinitrobenzene powder cell (steady state condition)with the adsorption of different vapours at the same vapour pressure (60 mm) and at a sample cell temperature of 22°C. Solid lines represent temperature region of measurements, broaken lines are extrapolations. Each line corresponds to a specific vapour adsorbed state : Vapours are 1. ethanol 2. n-hexane 3. cyclohexane and 4. methanol. (Refer Table 4.1, 4.5)

FIGURE - 4.11

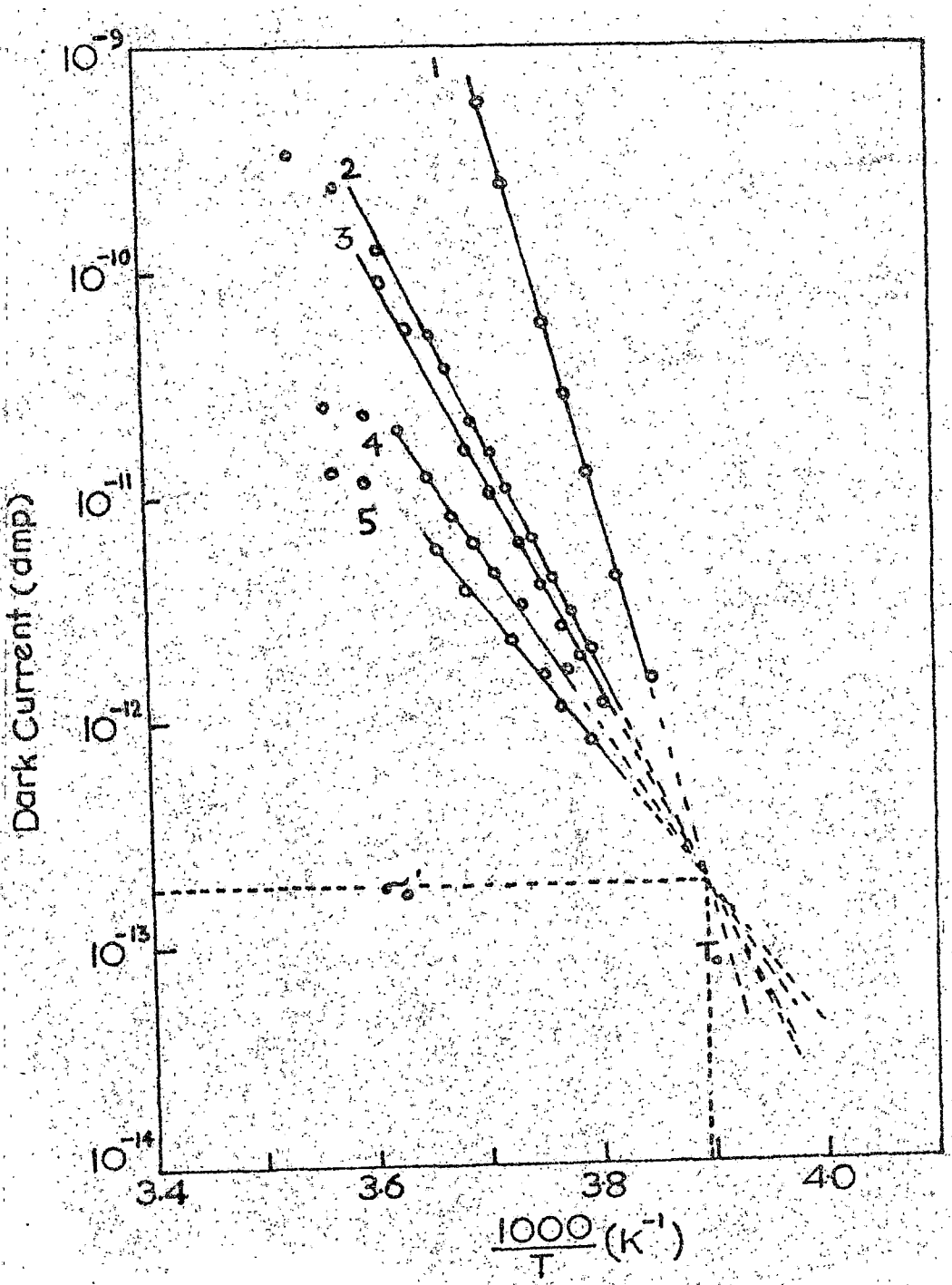

Semiconductivity in a 2-nitrofluorene powder cell (steady state condition) with the adsorption of the same amount of different vapours (solid lines represent temperature region of measurement and broken lines are extrapolations) Each line refers to a specific vapour adsorbed state : Vapours are 1. ethanol, 2. ethylacetate, 3. benzene, 4. carbontetrachloride and 5. n-hexane. (Refer Tables 4.1, 4.6)

FIGURE - 4.12

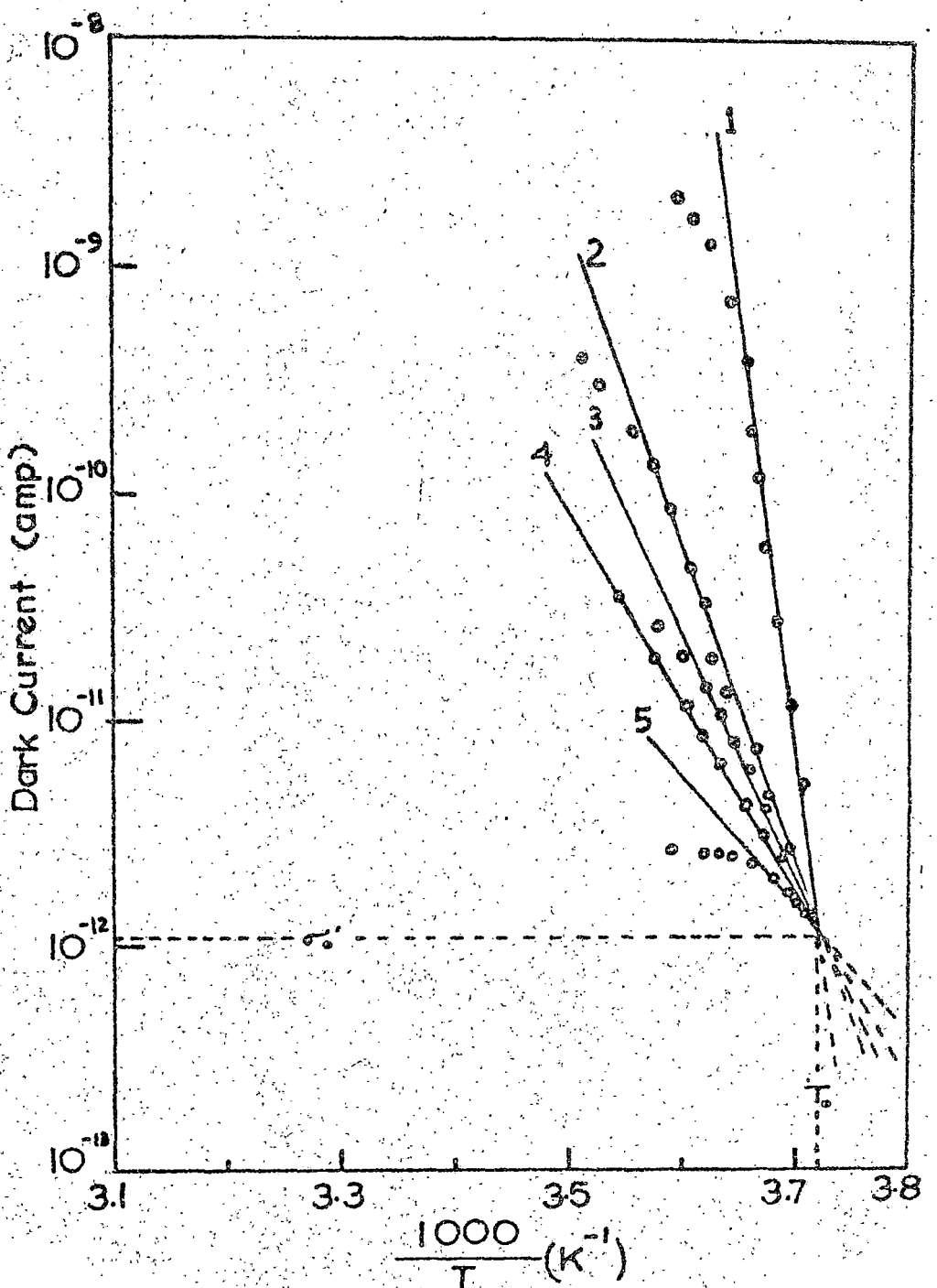

Semiconductivity in a O-nitrobenzoic acid powder cell (steady state condition) with the adsorption of the same amount of different vapours (solid lines represent temperature region of measurement and broaken lines are extra polations) Each line refers to a specific vapour adsorbed state : Vapours are 1. ethyl acetate, 2. ethanol, 3. methanol, 4. carbontetrachloride and 5. n-hexane. (Refer Tables 4.1, 4.7)

FIGURE - 4.13

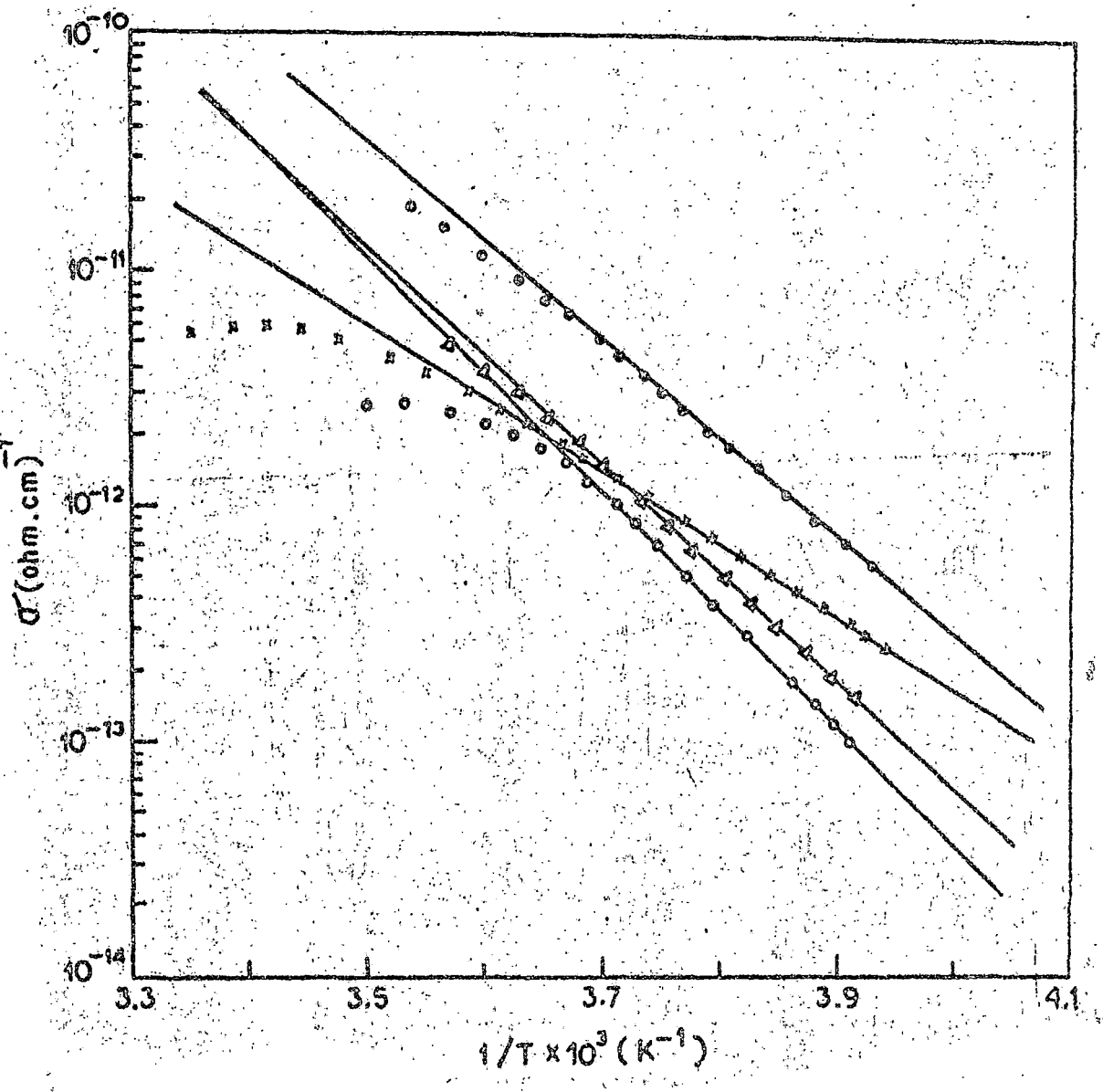

Semiconductivity in a 1,4-dinitronaphthalene powder cell (steady state condition) with the adsorption of different vapours at the same pressure (50 mm) and at sample cell temperature of 22°C. Each line refers to a specific vapour adsorbed state : Ethyl acetate (-•-, E = 1.67 ev);
Carbontetrachloride (-x-, E = 1.25 ev);
n-Hexane (-o-, E = 2.03 ev);
Benzene (-Δ-, E = 1.60 ev)

FIGURE - 4.14

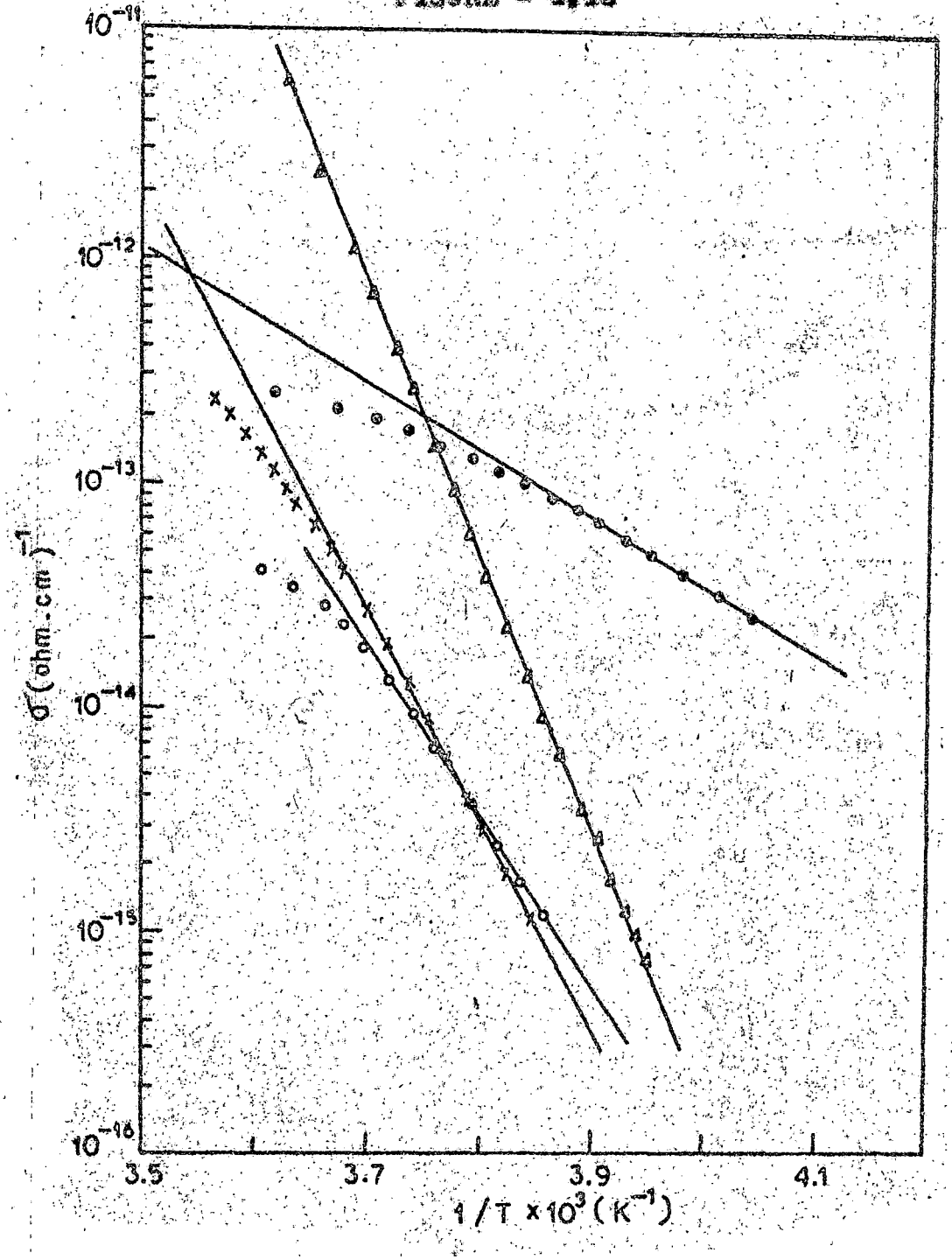

Semiconductivity in a 1,3,5-trinitrobenzene powder cell (steady state condition) with the adsorption of different vapours at the same pressure (60 mm) and at sample cell temperature of 32°C. Each line refers to a specific vapour adsorbed state :

Methylcyclohexane (-●-, E = 1.23 ev);

Ethyl acetate (-△-, E = 4.63 ev) ;

Benzene (-x-, E = 3.76 ev);

Carbontetrachloride (-○-, E = 3.06 ev)

as shown in Figs. 4.8 - 4.12 whereas those giving strong complexes produce the type of activation energy change as shown in Figs 4.13 and 4.14.

2.2 Semiconduction activation energy as a function of the amount of vapour adsorbed :

To study the dependence of the activation energy change on the amount of a particular vapour adsorbed in a sample cell, measurements were done by repeated heating, partially desorbing and cooling cycles. In Figs. 4.15 - 4-19 plots of log σ_T or log I_T vs. 1/T for adsorption of different amounts of a vapour on 9-nitroanthracene, 1,4-dinitronaphthalene, 1,3,5-trinitrobenzene, 2-nitrofluorene and O-nitrobenzoic acid are shown. The slopes of the straight lines decrease with decreasing amounts of the adsorbed vapour. Thus, the value of the activation energy decreases in a regular monotonic fashion as more vapour desorbs from the sample. Also, number of other vapours that are found to form weak complexes with these nitroaromatic semiconductors produce a similar change in activation energy value with the amount of these vapours adsorbed. A set of approximately parallel straight lines is observed in the low temperature region for log σ_T vs. 1/T plots for different amounts of ethylacetate adsorption on 1,4 dinitronaphthalene and 1,3,5-trinitrobenzene as shown in Figs. 4.20 and 4.21

FIGURE - 4.16

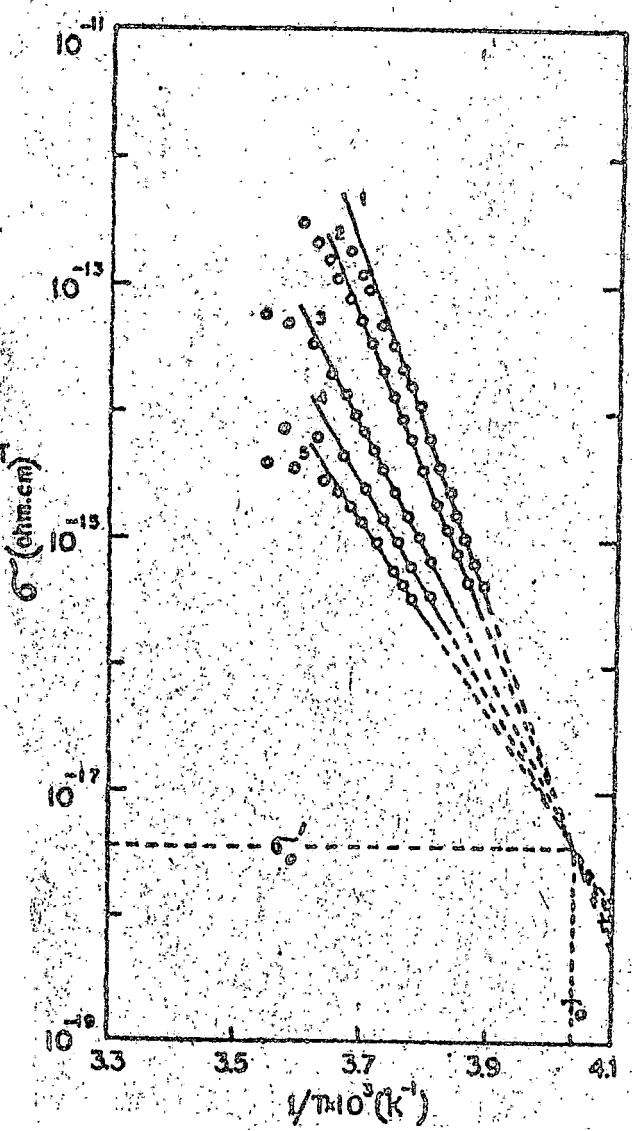

Semiconductivity data for 9-nitroanthracene powder cell (steady state condition) with the adsorption of different amounts of ethanol vapour. Solid lines represent the temperature region of measurements, broaken lines are extrapolations. The lines (1)→(5) refer to the states with the decreasing amount of adsorbed vapour. (Refer Tables 4.1, 4.8)

FIGURE - 4.10

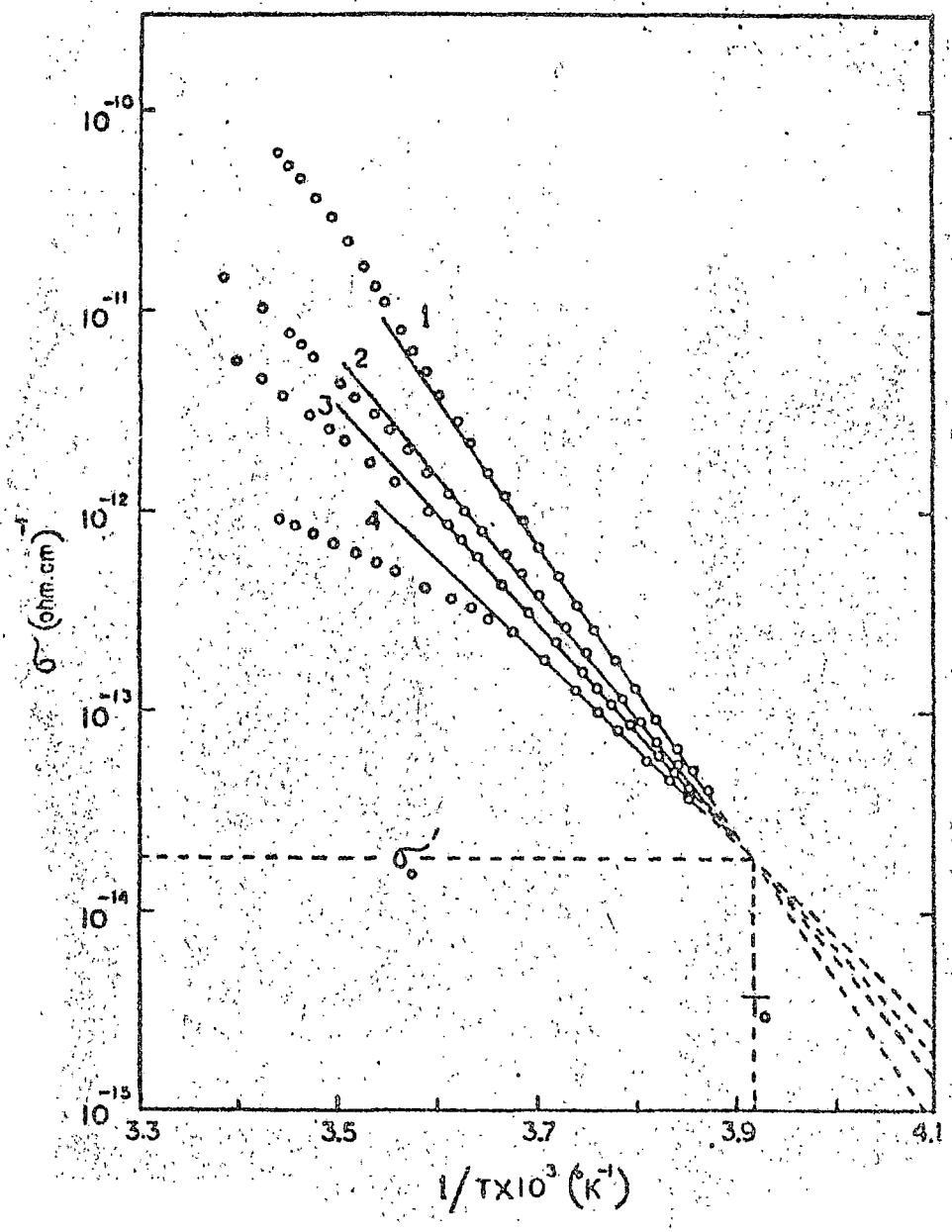

Semiconductivity data for 1,4-dinitronaphthalene powder cell (steady state condition) with the adsorption of different amounts of ethanol vapour. Solid lines represent the temperature region of measurements, broken lines are extrapolations. The lines (1) → (4) refer to the states with the decreasing amount of adsorbed vapour. (Refer Tables 4.1, 4.2)

FIGURE - 4.17

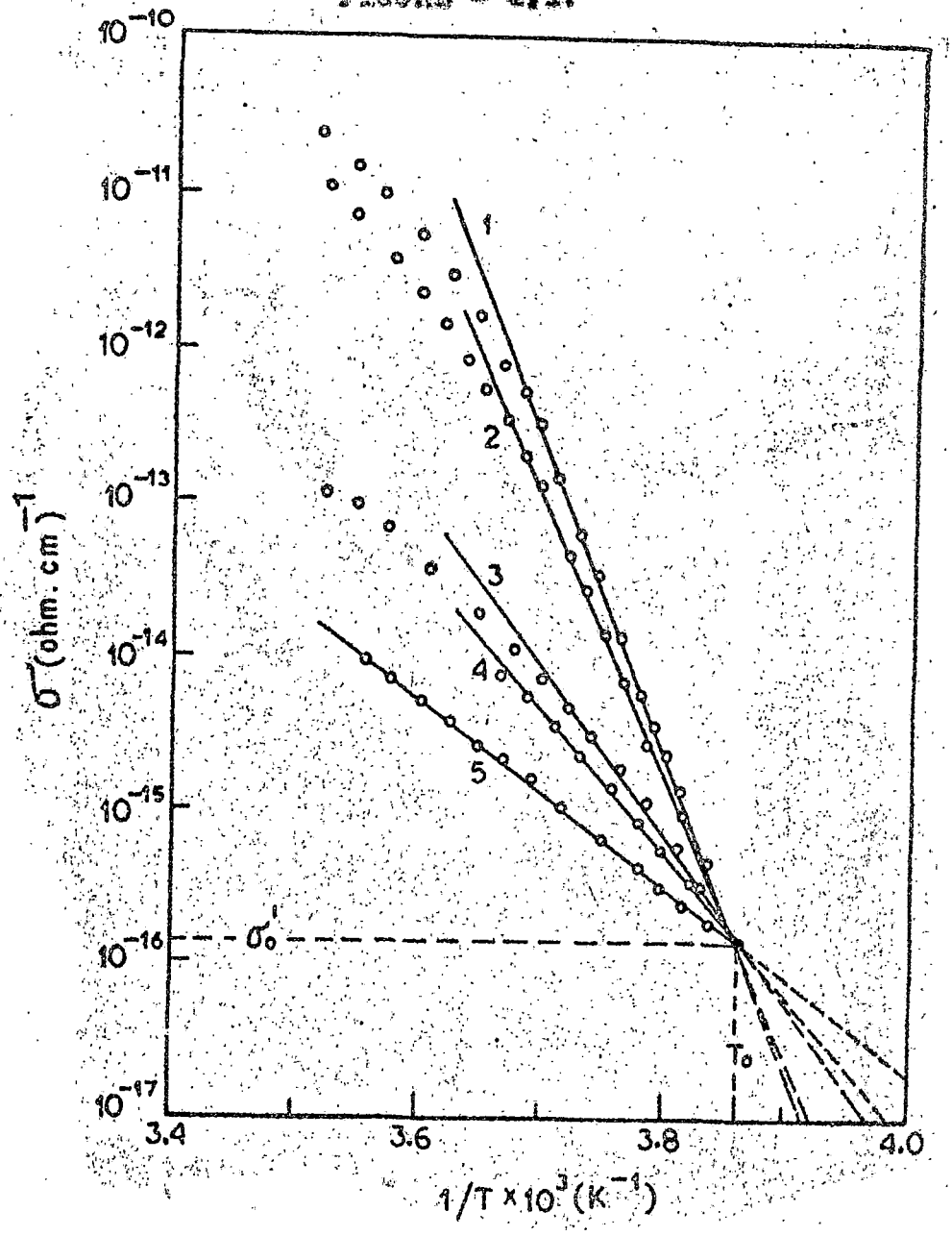

Semiconductivity data for 1,3,6-trinitrobenzene powder cell (steady state condition) with the adsorption of different amounts of ethanol vapour. Solid lines represent the temperature region of measurement, broaken lines are extrapolations. The lines (1) → (5) refer to the states with the decreasing amount of adsorbed vapour. (Refer Tables 4.1 and 4.10)

FIGURE - 4.12

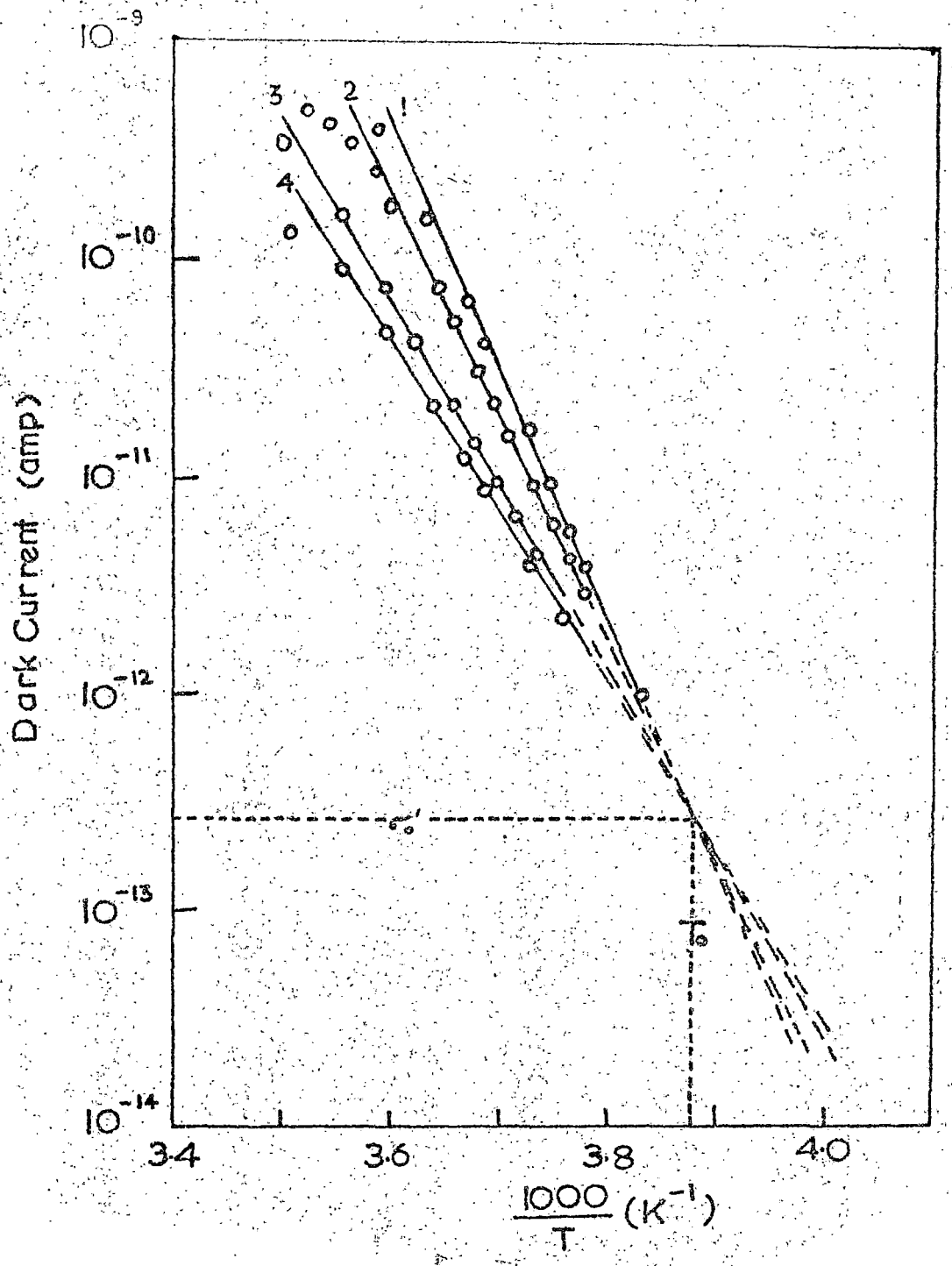

Semiconductivity data for 2-nitrofluorene powder cell (steady state condition) with adsorption of different amount of ethylacetate vapour. Solid lines represent the temperature region of measurement, broaken lines are extrapolations. The lines (1) → (4) refer to the states with decreasing amount of adsorbed vapour. (Refer Tables 4.1, 4.11)

FIGURE - 4.19

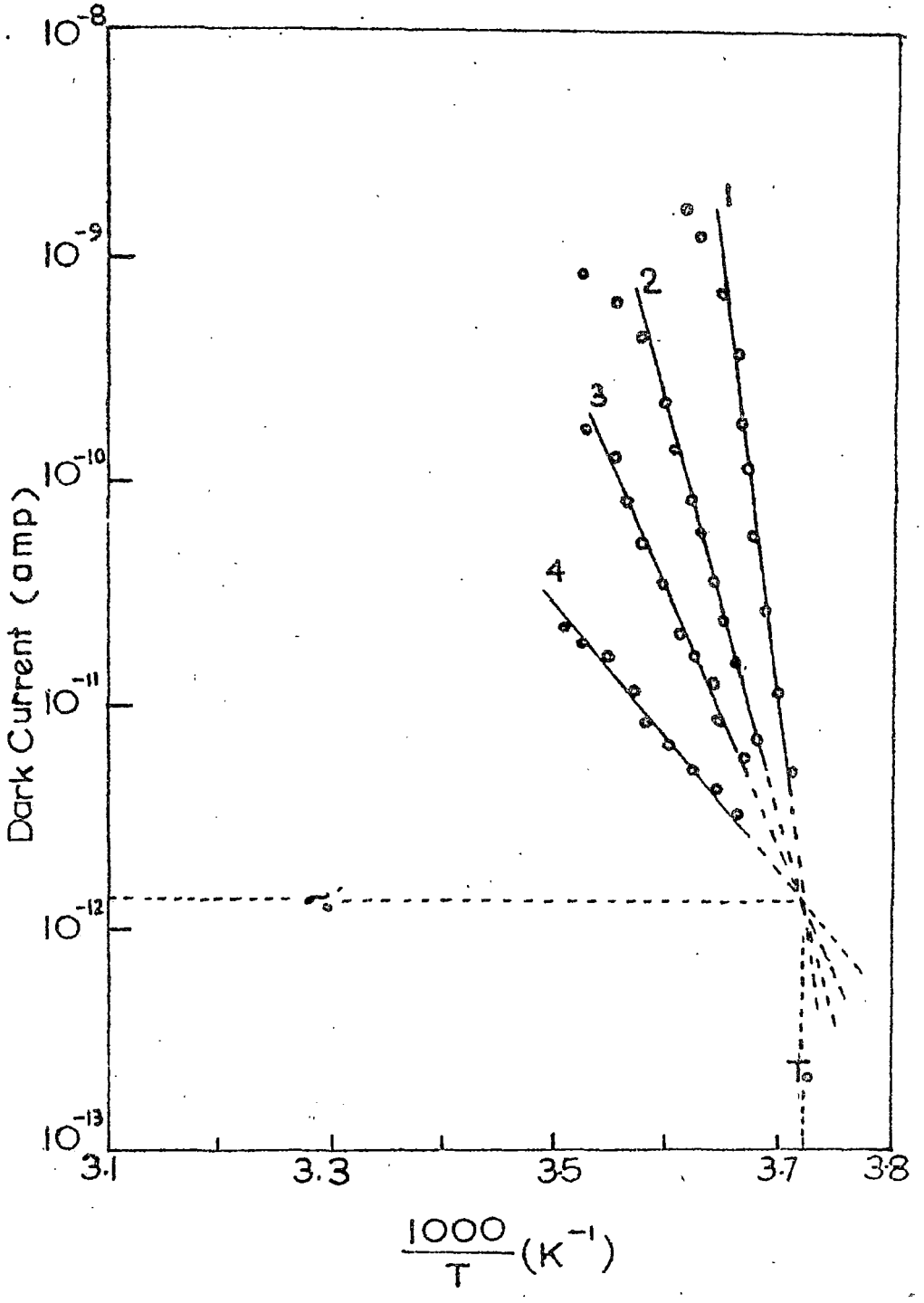

Semiconductivity data for O-nitrobenzoic acid powder cell (steady state condition) with adsorption of different amount of ethylacetate vapour. Solid lines represent the temperature region of measurement, broaken lines are extrapolations. The lines (1)→(4) refer to the states with decreasing amount of adsorbed vapour. (Refer Tables 4.1 and 4.12)

FIGURE - 4.20

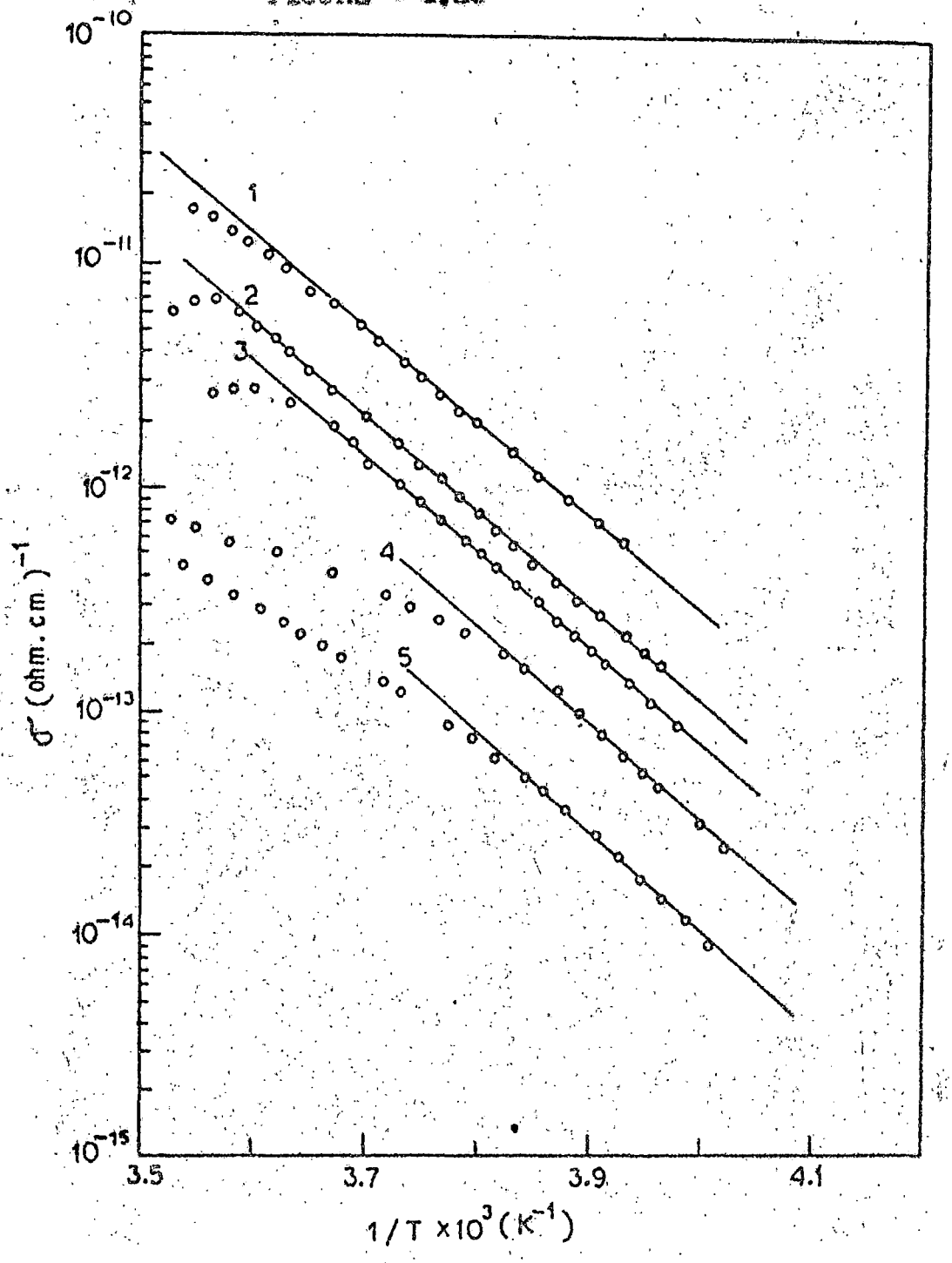

Semiconductivity data for 1,4-dinitronaphthalene powder cell (steady state condition) with the adsorption of different amounts of ethyl acetate vapour. The lines (1)→(5) refer to the states with the decreasing amount of adsorbed vapour. The E - values are (1) 1.67 ev; (2) 1.63 ev; (3) 1.67 ev; (4) 1.70 ev; (5) 1.76 ev.

FIGURE - 4.21

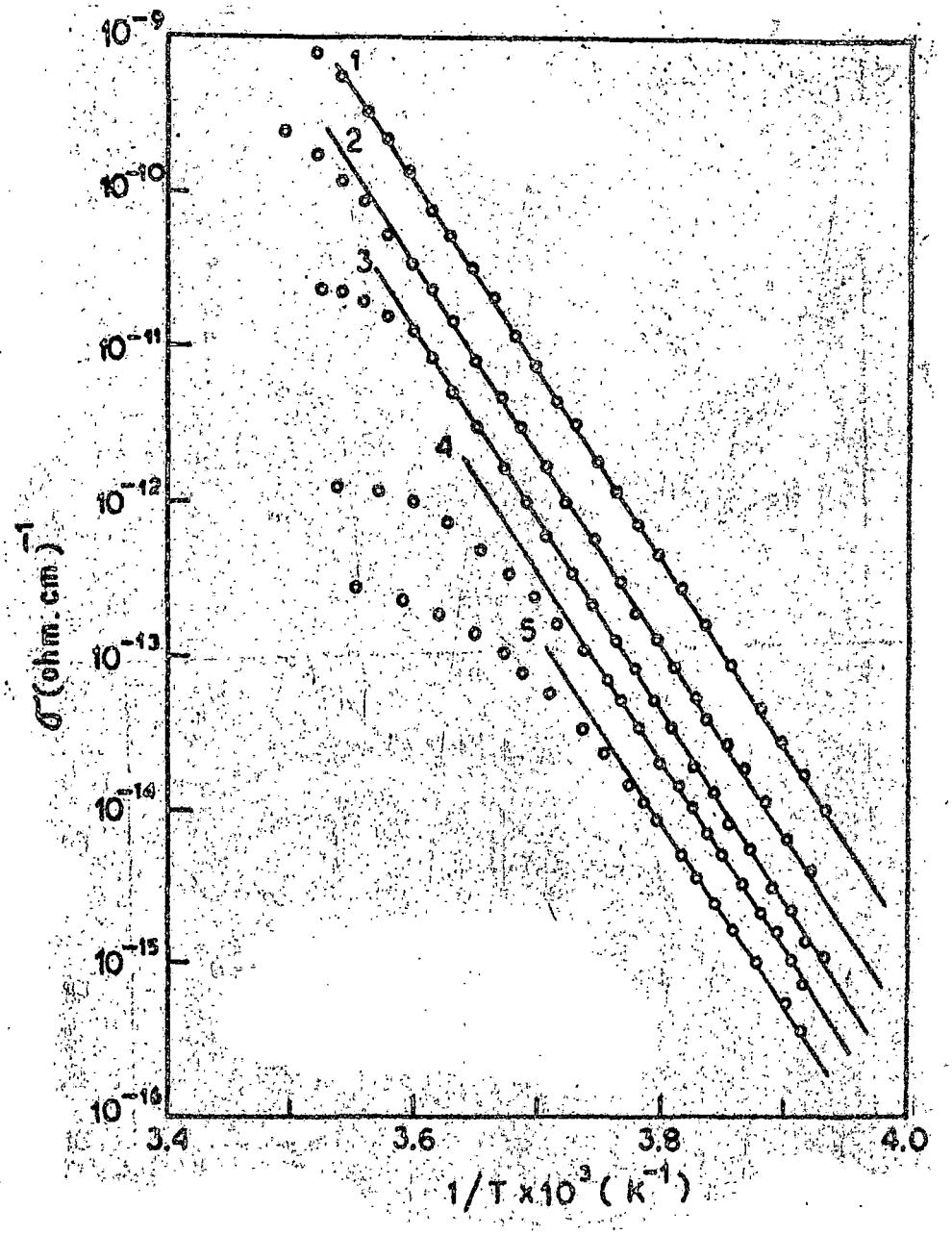

Semiconductivity data for 1,3,5-trinitrobenzene powder cell (steady state condition) with the adsorption of different amounts of ethyl acetate vapour. The lines (1) → (5) refer to the states with the decreasing amount of adsorbed vapour. The E - values are (1) 4.83 ev; (2) 4.85 ev; (3) 4.89 ev; (4) 4.98 ev; (5) 4.79 ev.

respectively. So, in this case of strong complexes approximately the same value of activation energy is obtained with decreasing amount of adsorbed vapour. The other vapours e.g. carbon-tetrachloride, benzene, toluene, methylcyclohexane, n-hexane and n-heptane on 1,4-dinitronaphthalene and carbon-tetrachloride, benzene, toluene, methylcyclohexane and n-heptane on 1,3,5-trinitrobenzene produce the same type of results. The shifting of straight lines in the log σ_T vs. $1/T$ plots i.e. the decrease in the observed conductivity values with less amount of adsorbed vapour may be due to variation in the equivalent thickness of the strongly bound vapour - semiconductor complex.

2.3 Compensation temperature for the nitroaromatic semiconductors

As shown in Figs. 4.8 - 4.12 and 4.15 - 4.19, the extrapolated lines in log σ_T vs. $1/T$ plots of 9-nitroanthracene, 1,4 dinitronaphthalene, 1,3,5-trinitrobenzene, 2-nitrofluorene and O-nitrobenzoic acid intercept the ordinate at a wide varieties of positions and they all pass through a single point of intersection at a temperature 'T_0' as expected from equation (1.1) which can also be written as

$$\log \sigma (T) = \log \sigma_0' + \left[1/T_0 - 1/T\right] E/2.3R \quad (2.31)$$

At this compensation temperature T_0, the value of $\sigma(T_0)$ gives

value. The values of T_0's and σ_0''s obtained from different log σ vs. 1/T plots for the semiconductors studied are shown in Table 4.1. It is observed that the two sets of T_0's and σ_0''s are in good agreement. But in case of Figs. 4.13, 4.14, 4.20 and 4.21, the extrapolated lines in log σ vs. 1/T plots do not intersect at a single point and thus compensation temperature T_0 is not obtained in case of ethylacetate, benzene, carbontetrachloride, n-hexane, toluene and methylcyclohexane vapour adsorption on 1,4-dinitronaphthalene and ethylacetate, benzene, carbontetrachloride, toluene and methylcyclohexane vapour adsorption on 1,3,5-trinitrobenzene.

From functional definition of semiconductor :

$$\sigma(T) = \sigma_0 \exp(-E/2kT) \qquad (2.32)$$

and equation (2.31), it is expected that the plots of log σ_0 vs. E should be linear. In Figs. 4.22 - 4.24, such plots for 9-nitroanthracene, 1,4-dinitronaphthalene, 1,3,5-trinitrobenzene, 2-nitrofluorene and 6-nitrobenzoic acid are shown. The values of T_0's and σ_0''s obtained from the slopes and intercepts respectively of these plots for different nitroaromatics are presented in Table 4.2 for comparison with the values obtained from different log σ vs. 1/T plots. T_0 and σ_0' values obtained from various plots show excellent agreement[143]. Using the values of T_0's and σ_0''s

Table 4.1

The values of T_0's and σ_0''s obtained from different log σ vs. 1/T plots of some nitroaromatic semiconductors.

Semiconductor	Value of T_0 (°K) obtained from the log σ vs 1/T plots for		Value of σ_0' (Ω-cm)$^{-1}$ obtained from the log σ vs. 1/T plots for	
	adsorption of different vapours	adsorption of different amounts of a particular vapour	adsorption of different vapours	adsorption of different amounts of a particular vapour
9-nitro-anthracene[1]	246.4	247.6	1.43×10^{-13}	3.59×10^{-13}
1,4-dinitro-naphthalene[2]	256.4	255.1	2.46×10^{-14}	1.77×10^{-14}
1,3,5-tri-nitrobenzene[3]	259.7	259.1	2.64×10^{-16}	1.51×10^{-16}
2-nitro-fluorene[4]	257.0	257.86	1.20×10^{-16}	2.16×10^{-16}
O-nitro-benzoic-acid[5]	270.27	258.8	8.6×10^{-16}	9.37×10^{-16}

1. From Figures 4.8 and 4.15 2. From Figures 4.9 and 4.16
3. From Figures 4.10 and 4.17 4. From Figures 4.11 and 4.18
5. From Figures 4.12 and 4.19.

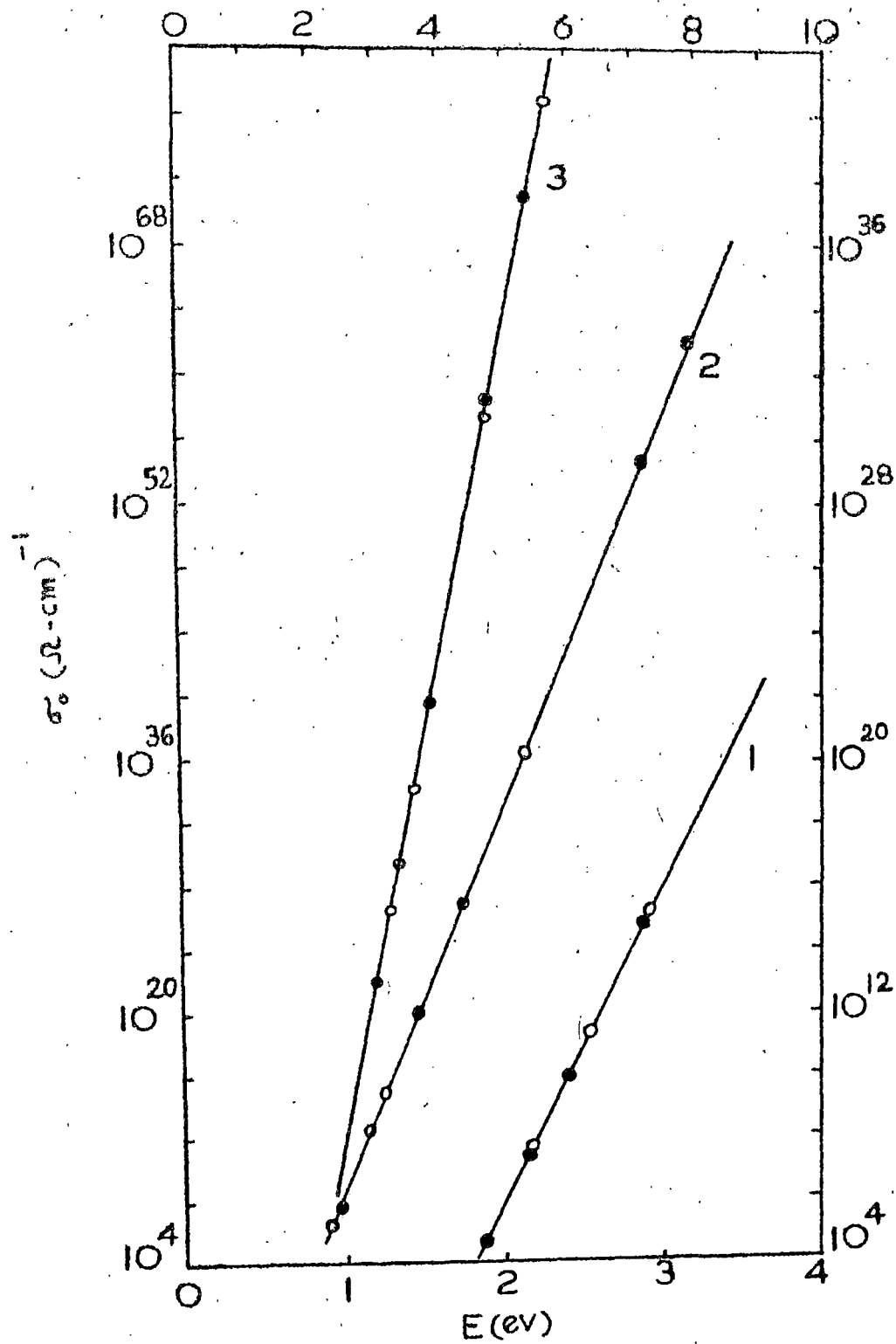

FIGURE - 4.22 : The plots of the log σ_0 at a constant temperature vs. the E - values for (1) 1,4-dinitronaphthalene (right and lower scale), (2) 1,3,5-trinitrobenzene (left and upper scale) and (3) 9-nitroanthracene (right and upper scale). The open circles refer to different vapours and the dark circles to different amounts of a particular vapour (e.g. ethanol). (Refer Table 4.2)

FIGURE - 4.23

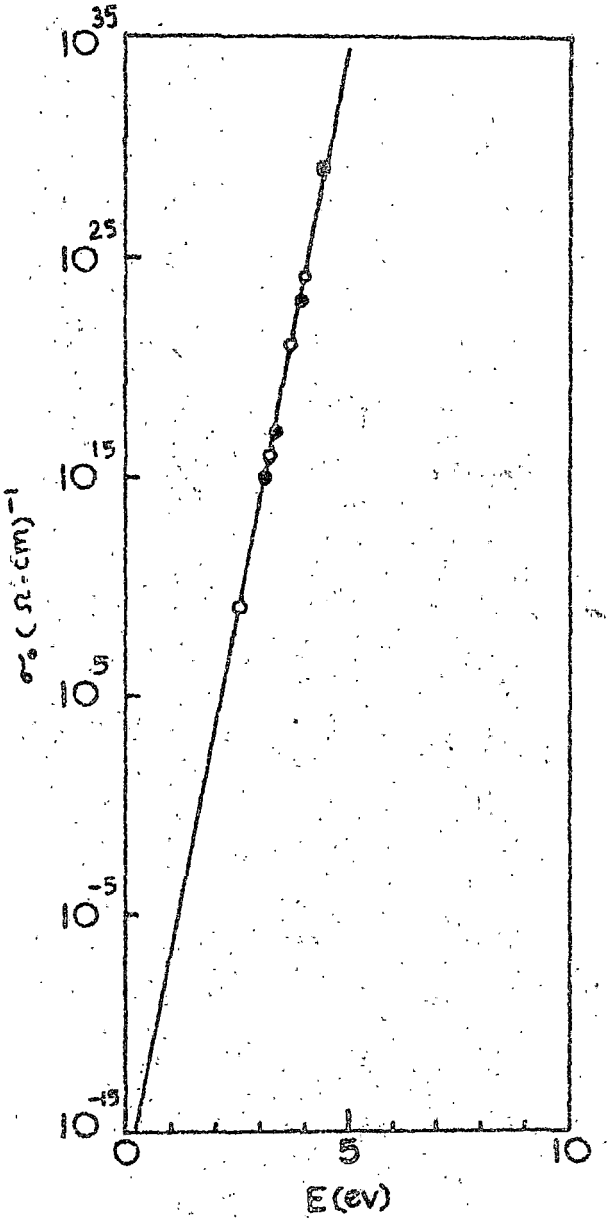

The plot of the log σ_o at a constant temperature vs. the E - values for 2-nitrofluorene. The open circles refer to different vapours and the solid circles to different amount of the same vapour (ethyl acetate) (Refer Table 4.2)

FIGURE - 4.24

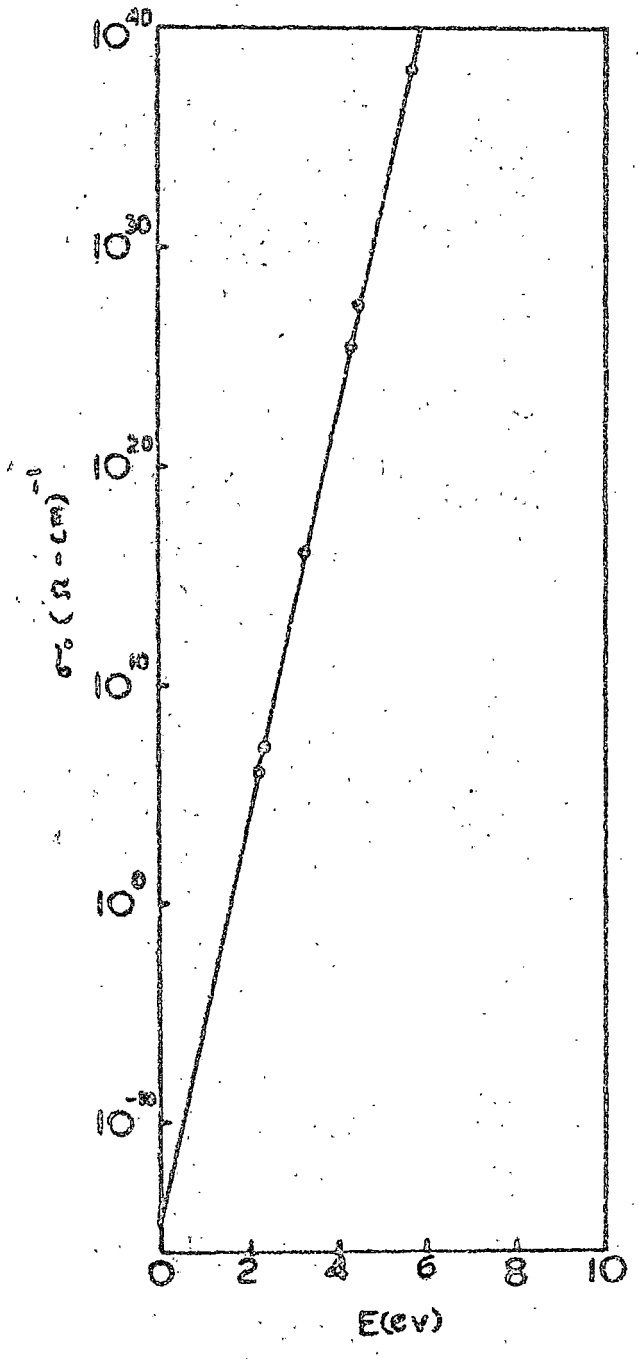

The plot of log σ_o values vs. E at a constant temperature for O-nitrobenzoic acid. The open circles refer to different vapours and the solid circles to different amount of the same vapour (ethyl acetate) (Refer Table 4.2)

Table 4.2

Values of T_0 and σ_0' obtained from various log σ_0 vs. E plots of some nitroaromatic semiconductors.

Semiconductor	Value of T_0 (°K)	Value of σ_0' $(\Omega \cdot cm)^{-1}$
9-nitroanthracene*	249.3	1.41×10^{-18}
1,4-dinitronaphthalene*	256.1	1.51×10^{-14}
1,3,5-trinitrobenzene*	261.8	2.51×10^{-16}
2-nitrofluorene**	257.5	7×10^{-17}
O-nitrobenzoic acid***	269.2	1.2×10^{-15}

* From Figure 4.22

** From Figure 4.23

*** From Figure 4.24

so obtained, we have calculated the expected σ_0 values and compared these values with experimentally measured values. These are shown in the Tables 4.3 - 4.12 for various nitroaromatic semiconductors. These results show that 'true' compensation effect is certainly observed in these semiconductors when E is changed by certain vapour adsorption.

'True' compensation effect is thought to arise from the existence of a linear relationship between the activation energy and the activation entropy of the system. It has been pointed out by Johnston and Lyons[100] that if a true linear free energy relation (LFER) does hold for dark conduction indicating a physical relationship between σ_0 and E, log σ (T_1) vs. E must also be linear, where T_1 is a specific temperature. In Figs. 4.25 - 4.27, such plots for various nitroaromatic semiconductors are shown. The observed slope of the line for each semiconductor is shown in Table 4.13 for comparision with the slope expected from equation (2.31), i.e. with $[1/T_0 - 1/T]\ 1/2K$. The values of σ_0' as obtained from the intercept of each log σ (3) vs. E plot is also shown in this table for comparision with the values obtained from the log σ vs. 1/T and log σ_0 vs. E plots. All these values show excellent consistency. These results show that the σ_0 and E are indeed physically related and thus confirm the validity of the compensation rule in case of adsorption of

Table 4.3

Semiconduction parameters for 9-nitroanthracene on adsorption of various vapours according to equation (2.31)

Vapour adsorbed	9 - nitroanthracene $(2kT_0)^{-1} = 23.43\ ev^{-1}$ $\sigma_0' = 1.41 \times 10^{-18}\ (\Omega\ cm)^{-1}$		
	E (ev)	Calculated $\sigma_0 = \sigma_0' \exp(E/2kT_0)$	measured* σ_0 $(\Omega\text{-}cm)^{-1}$
Ethanol	5.66	5.53×10^{39}	2.05×10^{40}
Ethylacetate	4.72	1.51×10^{30}	5.37×10^{30}
Benzene	3.55	2.11×10^{21}	6.41×10^{21}
Carbontetra-chloride	3.59	4.78×10^{18}	1.39×10^{19}
Methanol	3.22	8.21×10^{14}	2.03×10^{15}

* From Figure 4.8

Table 4.4

Semiconduction parameters for 1,4-dinitronaphthalene on adsorption of various vapours according to equation (2.31)

Vapour adsorbed	1,4-dinitronaphthalene $(2kT_0)^{-1}$ = 22.80 ev^{-1}, σ_0' = 1.51 x 10^{-14} (ohm- cm)$^{-1}$		
	E (ev)	calculated $\sigma_0 = \sigma_0' \exp(E/2kT_0)$ (ohm-cm)$^{-1}$	measured* σ_0 (ohm- cm)$^{-1}$
Ethanol	2.92	1.24 x 10^{15}	1.98 x 10^{15}
Methanol	2.69	1.70 x 10^{11}	2.66 x 10^{11}
Cyclohexane	2.18	3.69 x 10^{7}	5.84 x 10^{7}

* From Figure 4.9

Table 4.6

Semiconduction parameters for 1,3,5-trinitrobenzene on adsorption of various vapours according to equation (2.31)

Vapours adsorbed	1,3,5-trinitrobenzene $(2kT_0)^{-1}$ = 22.30 ev^{-1} σ_0' = 2.61 x 10^{-16} (ohm-cm)$^{-1}$		
	E (ev)	calculated $\sigma_0 = \sigma_0' \exp(E/2kT_0)$ (ohm-cm)$^{-1}$	measured* σ_0 (ohm-cm)$^{-1}$
Ethanol	5.32	8.37 x 10^{35}	2.02 x 10^{36}
n-Hexane	3.12	4.13 x 10^{14}	7.17 x 10^{14}
Cyclohexane	2.88	1.96 x 10^{12}	8.36 x 10^{12}
Methanol	2.26	1.94 x 10^{6}	2.86 x 10^{6}

* From Figure 4.10

Table 4.6

Semiconduction parameters for 2-nitrofluorene on adsorption of various vapours according to equation (2.31)

Vapours adsorbed		2-nitrofluorene $(2kT_o)^{-1}$ = 22.677 ev^{-1} σ_o' = 2 x 10^{-16} (ohm-cm)$^{-1}$	
	E (ev)	calculated $\sigma_o = \sigma_o' \exp(E/2kT_o)$ (ohm-cm)$^{-1}$	measured* σ_o (ohm-cm)$^{-1}$
Ethanol	7.20	1.62 x 10^{65}	2.38 x 10^{65}
Ethylacetate	4.04	5.0 x 10^{23}	1.12 x 10^{24}
Benzene	3.72	8.60 x 10^{20}	8.09 x 10^{20}
Carbontetra-chloride	3.26	2.5 x 10^{16}	1.83 x 10^{16}
n-Hexane	2.84	2.07 x 10^{9}	1.83 x 10^{9}

* From Figure 4.11

Table 4.7

Semiconduction parameters for O-nitrobenzoic acid on adsorption of various vapours according to equation (2.31)

Vapours adsorbed	O-nitrobenzoic acid $(2kT_0)^{-1}$ = 21.664 ev^{-1}, σ_0' = 9 x 10^{-16} (ohm-cm)$^{-1}$		
	E (ev)	calculated $\sigma_0 = \sigma_0' \exp(E/2kT_0)$ (ohm-cm)$^{-1}$	measured* σ_0 (ohm-cm)$^{-1}$
Ethanol	5.66	2.63 x 10^{38}	1.43 x 10^{38}
Methanol	4.31	4.00 x 10^{25}	3.19 x 10^{25}
Carbontetra-chloride	3.3	1.16 x 10^{16}	1.00 x 10^{16}
n-Hexane	2.24	1.138 x 10^{6}	1.06 x 10^{6}

* From Figure 4.12

Table 4.8

Semiconduction parameters for 9-nitroanthracene on adsorption of ethanol vapour of different amounts according to equation 2.31

Curve No. of figure 4.15	9-nitroanthracene $(2kT_0)^{-1}$ = 23.43 ev^{-1} σ_0' = 1.41 x 10^{-18} (ohm-cm)$^{-1}$		
	B (ev)	calculated $\sigma_0 = \sigma_0' \exp(B/2kT_0)$ (ohm-cm)$^{-1}$	measured* σ_0 (ohm-cm)$^{-1}$
1	5.36	4.00 x 10^{36}	2.04 x 10^{37}
2	4.75	3.04 x 10^{30}	1.67 x 10^{31}
3	3.83	1.32 x 10^{21}	5.93 x 10^{21}
4	3.35	1.73 x 10^{16}	6.65 x 10^{16}
5	2.93	2.97 x 10^{12}	1.03 x 10^{13}

Curve No. 1 → 5 corresponds to the decreasing amount of adsorbed ethanol vapour.

* From Figure 4.15

Table 4.9

Semiconduction parameters for 1,4-dinitronaphthalene on adsorption of ethanol vapour of different amounts according to equation (2.31)

Curve No. of Figure 4.16	1,4-dinitronaphthalene $(2kT_0)^{-1}$ = 22.80 ev^{-1} σ_0' = 1.51×10^{-14} (ohm-cm)$^{-1}$		
	E (ev)	calculated $\sigma_0 = \sigma_0' (\exp(E/2kT_0))$ (ohm-cm)$^{-1}$	measured* σ_0 (ohm-cm)$^{-1}$
1	2.87	3.96×10^{14}	6.83×10^{14}
2	2.38	6.57×10^{9}	8.06×10^{9}
3	2.13	1.86×10^{7}	2.67×10^{7}
4	1.86	3.95×10^{4}	6.36×10^{4}

Curve No. 1 $\longrightarrow$ 4 corresponds to the decreasing amount of adsorbed ethanol vapour.

* From Figure 4.16

Table 4.10

Semiconduction parameters for 1,3,5-trinitrobenzene on adsorption of ethanol vapour of different amounts according to equation (2.31)

Curve No. of figure 4.17	1,3,5-trinitrobenzene $(2kT_0)^{-1}$ = 22.90 ev^{-1} σ_0' = 2.61 x 10^{-16} (ohm-cm)$^{-1}$	
	E (ev)	calculated $\sigma_0 = \sigma_0' \exp(E/2kT_0)$ (ohm-cm)$^{-1}$	measured* σ_0 (ohm-cm)$^{-1}$
1	7.93	1.56 x 10^{61}	5.78 x 10^{61}
2	7.18	8.64 x 10^{53}	2.29 x 10^{54}
3	4.36	4.22 x 10^{26}	6.60 x 10^{26}
4	3.65	5.61 x 10^{19}	7.90 x 10^{19}
5	2.41	5.50 x 10^{7}	5.65 x 10^{7}

Curve No. 1 - 5 corresponds to the decreasing amount of adsorbed ethanol vapour.

* From Figure 4.17

Table 4.11

Semiconduction parameters for 2-nitrofluorene on adsorption of ethyl acetate vapour of different amounts according to equation (2.31)

Curve No. of figure 4.18	2-nitrofluorene $(2kT_o)^{-1}$ = 22.677 ev^{-1}, σ_o' = 2×10^{-16} (ohm-cm)$^{-1}$		
	E (ev)	calculated $\sigma_o = \sigma_o' \exp(E/2kT_o)$ (ohm-cm)$^{-1}$	measured* σ_o (ohm-cm)$^{-1}$
1	4.45	1.3×10^{28}	1.44×10^{29}
2	3.96	2.0×10^{23}	2.23×10^{23}
3	3.36	2.46×10^{17}	2.43×10^{17}
4	3.12	1.07×10^{15}	1.06×10^{15}

Curve No. 1 - 4 corresponds to the decreasing amount of adsorbed ethylacetate vapour.

* Figure 4.18

Table 4.12

Semiconduction parameters for O-nitrobenzoic acid on adsorption of ethyl acetate vapour of different amounts according to equation (2.31)

Curve No. of Figure 4.19	O-nitrobenzoic acid $(2kT_0)^{-1} = 21.664\ ev^{-1}$ $\sigma_0' = 8 \times 10^{-16}$ (ohm-cm)$^{-1}$		
	E (ev)	calculated $\sigma_0 = \sigma_0' \exp(E/2kT_0)$ (ohm-cm)$^{-1}$	measured* σ_0 (ohm-cm)$^{-1}$
1	14.7 ev	1.83×10^{123}	3.00×10^{125}
2	8.1	1.46×10^{61}	1.56×10^{61}
3	4.5	1.96×10^{27}	2.74×10^{27}
4	2.33	2.22×10^{7}	2.73×10^{7}

Curve No. 1 $\longrightarrow$ 4 corresponds to the decreasing amount of adsorbed ethylacetate vapour.

* From Figure No. 4.19

FIGURE - 4.25

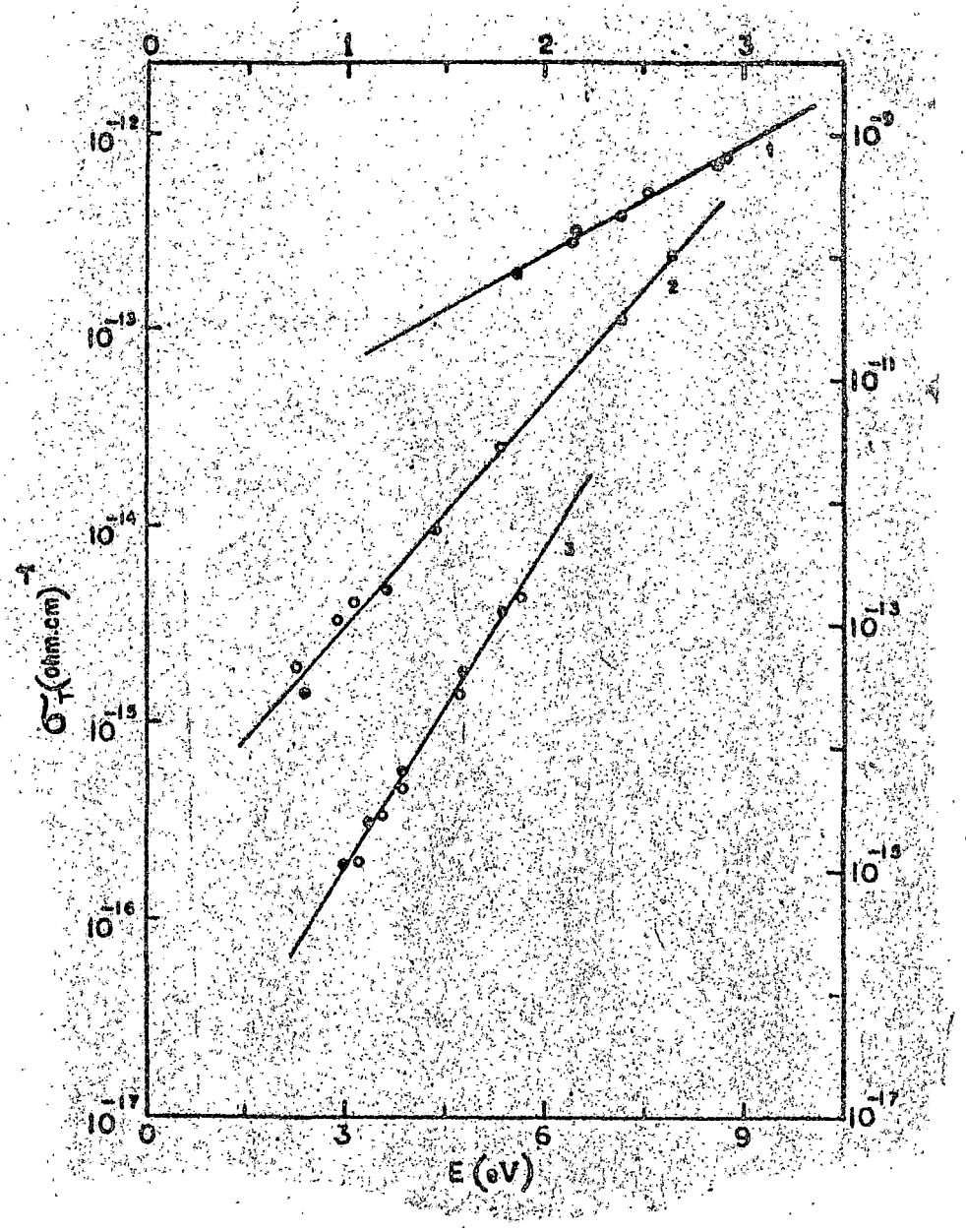

The plots of the log σ_T values at a constant temperature ($1/T_1 = 3.70 \times 10^{-3}\ ^{\circ}K^{-1}$) vs. the E - values for (1) 1,4-dinitronaphthalene (left and upper scale) (2) 1,3,5-trinitrobenzene (left and lower scale) and (3) 9-nitroanthracene (right and lower scale). (Refer Table 4.13)

FIGURE - 4.23

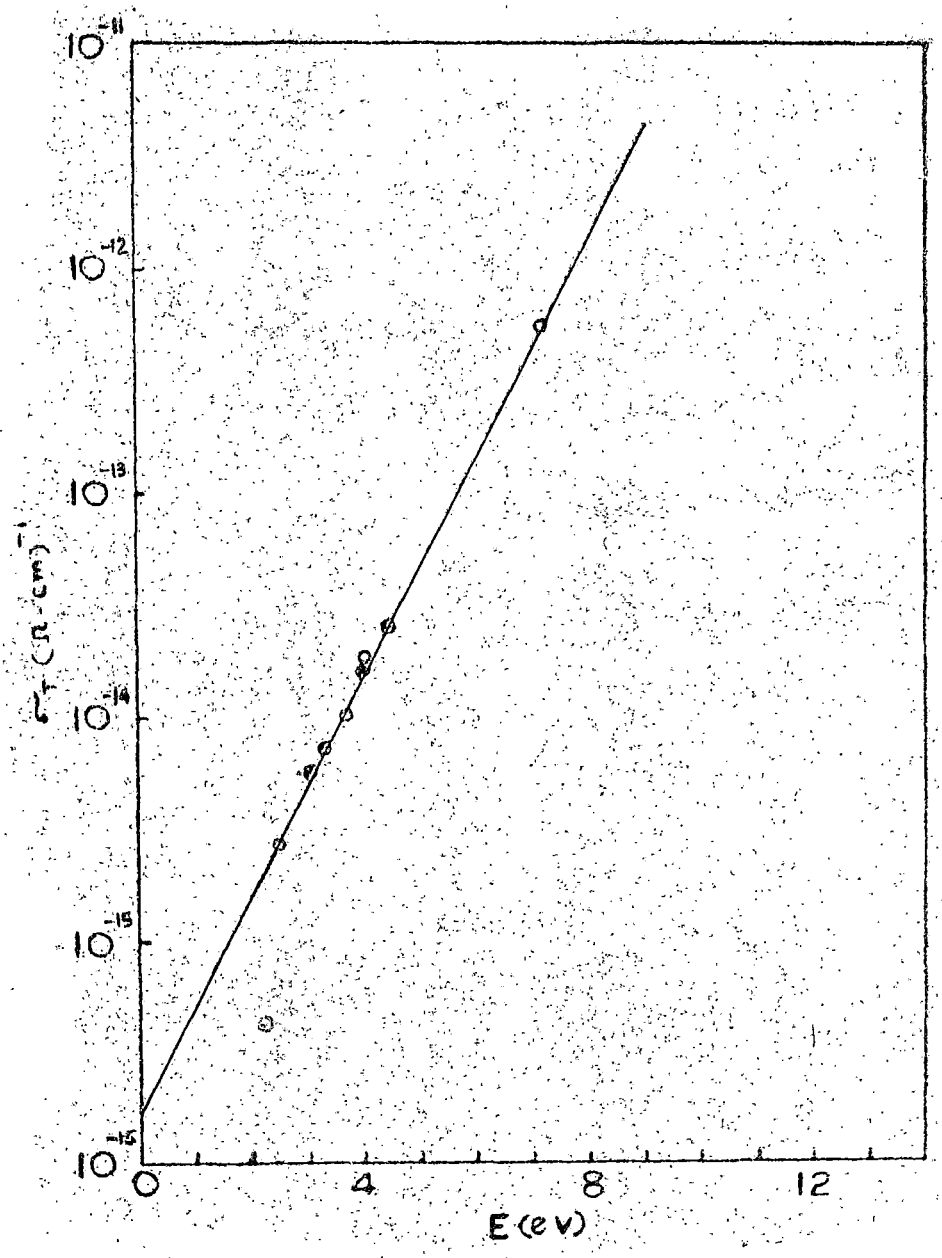

The plot of log σ_m values vs. E for 2-nitrofluorene at a constant temperature (270.25°K). The open circles refer to different vapours and the solid circles to different amount of the same vapour (ethyl acetate) (Refer Table 4.13)

FIGURE - 4.27

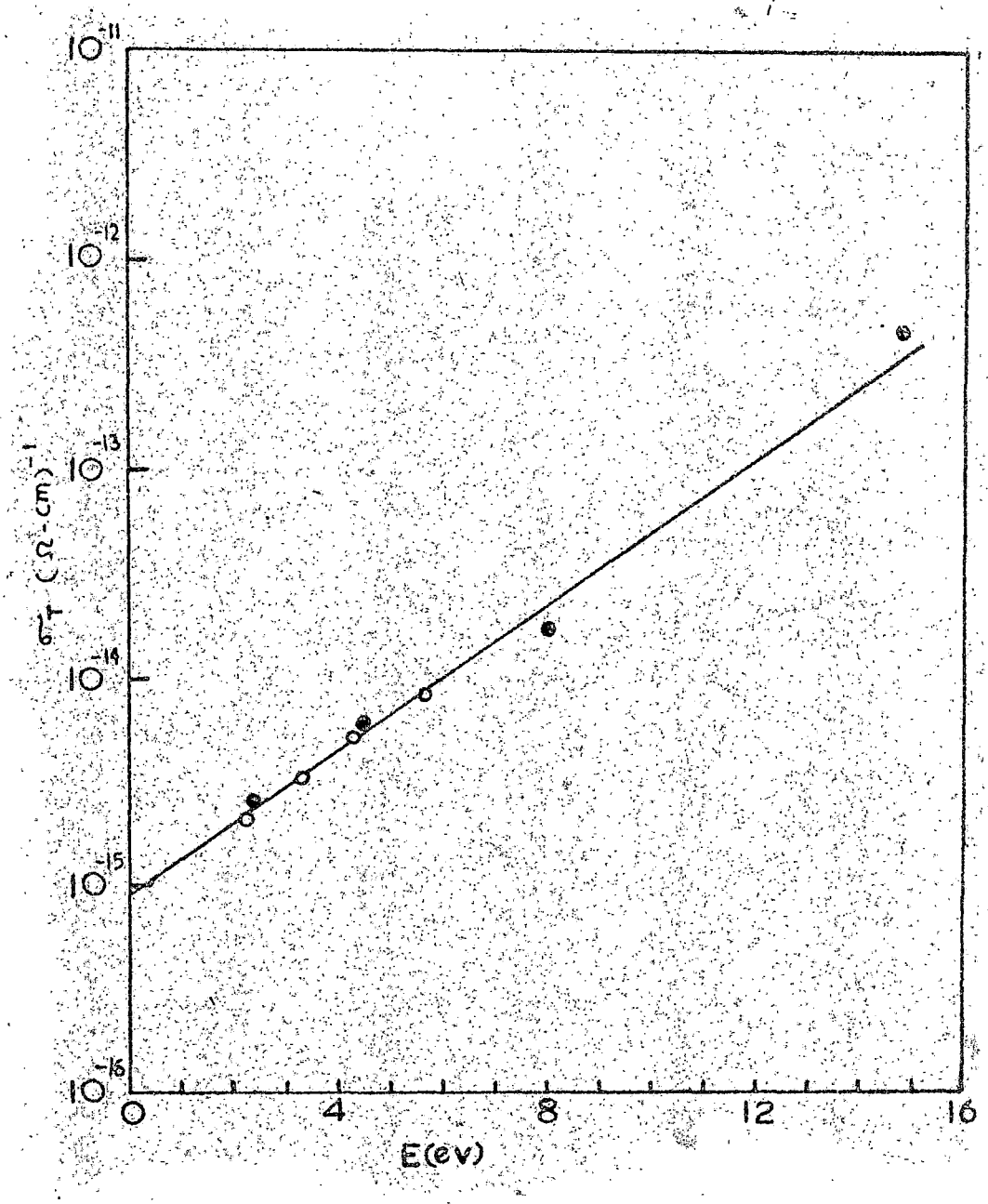

The plot of log σ_F values vs. E for O-nitrobenzoic acid at a constant temperature ($1/T_1 = 3.65\ ^{\circ}K^{-1}$). The open circles refer to different vapours and the solid circles to different amount of the same vapour (ethyl acetate) (Refer Table 4.13)

Table 4.13

Expected (equation 2.31) and observed slopes and observed σ_o' from the log σ vs. E plots for the nitroaromatic semiconductors

Semiconductors	Expected slope $(ev)^{-1}$	Observed slope $(ev)^{-1}$	Observed σ_o' $(ohm\text{-}cm)^{-1}$
9-nitro-anthracene*	0.85	0.83	3.62×10^{-13}
1,4-dinitro-naphthalene*	0.53	0.56	1.76×10^{-14}
1,3,5-trinitro-benzene*	0.36	0.38	2.10×10^{-16}
2-nitro-fluorene**	0.46	0.49	1.65×10^{-16}
O-nitrobenzoic-acid***	0.15	0.178	9.2×10^{-16}

* From Figure 4.25

** From Figure 4.26

*** From Figure 4.27

certain vapours on the nitroaromatic semiconductors.

3. Discussions

There are number of thesis about the mechanism of conduction in organic semiconductors leading to compensation effect. The carrier injection model of Green[105] produces the type of activation energy dependence of the pre-exponential factor as observed experimentally but it does not provide any physical basis for the interpretation of T_o.

Kenony and Rosenberg[41] observed compensation law in tunneling of small polaron through molecular barrier from thermally activated energy levels of molecules. Their model predicts that $T_o = \theta/2$ (where θ is the Debye temperature) and that at $T > T_o$, small polaron tunneling is not possible and compensation effect is not expected to be observed. In the present investigation, the semiconductive behaviour has been studied at $T > T_o$. The experimental results show that the compensation rule is valid in those cases also. Further, Debye - Temperature for these semiconductors are not known precisely. It has been reported[145] that the calculated values of the Debye - temperature for a series of crystals of aromatic compounds lie mainly in the range of 100 - 130°K. Thus, it seems that T_o values measured are far too high to justify the small polaron tunneling model.

Because of the widespread occurrence[103] of the compensation effect (besides semiconduction process, it is observed in chemical reactions, catalytic processes, thermal denaturation of macromolecules, thermal killing of unicellular organisms etc.), Kemony and Mohanti[45] have proposed a theory of electronic charge transport as involved in kinetic processes (also applicable to equilibrium processes) from the absolute rate theory equation[115,116] within two special models. The first one (quadratic polarons) involves the coupling of electrons with a set of oscillators, whereas the second one (magnetic polarons) involves the coupling of electrons with a set of spins. Both the models show that the activation entropy is proportional to the activation energy thus providing a compensation effect. The use of N number of oscillators or of spins to bring about the compensation effect seems to appear reasonable in view of the fact that the variable amount of adsorbed dielectric (vapour) screen off the interaction of a charge with more distant parent molecules; N depending on the number of such molecules with which the charge effectively interacts. But in quadratic polaron model, the characteristic temperature T_0 is always negative in contradiction to the experimental observation. The spin polaron model gives a positive T_0 but predicts no activation energy at very high temperatures. At a temperature around T_0, the process is activated and the activation

energy becomes a function of temperature i.e.

$$E(T) = E(0)\left[1 + \alpha T/T_0\right] \qquad (3.1)$$

Here E (0) is the activation energy at low temperature and α is a function of temperature :

$$\alpha = \left[1/\log 2\right] \log\left[1 + \exp\left\{(-2\log 2)\, T_0/T\right\}\right] \qquad (3.2)$$

Though the experiments were done in a limited temperature range, the excellent linear plots do not suggest such a temperature dependence.

Other theoretical attempts[42,44] to derive the compensation rule were restricted to the temperature dependence of the number of activated carriers in a model consisting of two electronic levels associated with each molecular site, the electronic states being coupled to a set of N oscillators associated with each molecular site. A change in the electronic state (due to vapour adsorption) gives rise to an activation entropy because of a change in vibrational frequencies. If one assumes the semiconduction equation as :

$$\sigma(T) = \sigma_0' \exp(S/K) \exp(-E/2KT) \qquad (3.3)$$

then the variation in both the electronic energy gap (E) and the activation entropy (S) can account for compensation effect if the

changes in these parameters are given by :

$$E = E_0 + nE_1 \quad \text{and} \quad S = S_0 + nS_1 \qquad (3.4)$$

where n is a definite number for each system and E_0, E_1, S_0 and S_1 are same for all the systems. In this case the characteristic temperature is given by $T_0 = [E_1 / 2S_1]$.

Unfortunately due to the fact that the nature of the activated complex (due to vapour adsorption) is not precisely known, the activation entropy S (hence S_1) is a relatively obscure quantity and any quantitative estimate of T_0 is not possible.

The experimental results presented here show that the enhancement in conductivity is associated with a change in activation energy of the semiconductors on vapour adsorption. This change in activation energy depends on the chemical nature and also on the amount of the vapour adsorbed. In all the cases studied the activation energy increases with the increase in conductivity. This behaviour, however, is quite understandable from the conductivity expression (2.31). If $T_0 < T$, where T is any temperature in the working range, then ($1/T_0 - 1/T$) becomes positive and the increase in σ at a temperature T is associated with an increase in activation energy. Thus, a semiconductor having T_0 at a lower side than the working temperature should show an enhancement

in its conductivity with the increase in its activation energy. Such behaviour has been observed in case of nitroaromatic semiconductors. Now, it is clear from the experiments that the characteristic temperature (T_o) of a semiconductor plays an important role in the dark conduction process.

The results of the nitroaromatic semiconductors studied show that when compensation relation is satisfied, the ' T_o' has a low value similar to the polyenes[146] with a conjugated carbonyl group. It is interesting as in these nitroaromatics, the nitrogroup, like that in carbonly group, is also having a nonbonding electron. Thus it seems that the presence of a nonbonding electron, in the molecule of a semiconducting material, is somehow responsible for the low compensation temperature.

4. Conclusion

The validity of the compensation rule in electrical conduction process has been examined in case of some nitroaromatic semiconductors by varying the activation energy by vapour adsorption. The validity or lack of it have been shown to be vapour-semiconductor pair dependent. The vapours for which very weak reversible complexes are formed, true compensation effect is observed. The other vapours which form strong complexes have been found not to satisfy the compensation relationship. Observed T_o value is distinctly

different for different nitroaromatics which supports the view about the dependence of T_0 on the molecular property of the semiconducting material. Our present observation of low value of T_0 is interesting and it seems that the presence of nonbonding electrons play an important role.

REFERENCES (PART - A)

(Semiconductive Investigations)

1. C. G. B. Garrett, "Semiconductors" edited by R. A. Hannay (Reinhold, NY, 1959)

2. H. Inokuchi and H. Akamatu, "Solid State Physics" edited by F. Seitz and D. Turnbull (AP, NY, 1961) p. 93.

3. L. E. Lyons, "Physics and Chemistry of the Organic Solid State" edited by D. Fox, M.M. Labes and A. Weissberger (Interscience NY, 1963) Vol. 1, p. 745.

4. D. R. Kearns, Adv. Chem. Phys., 7, 282 (1964)

5. Y. Okamoto and W. Brenner, "Organic Semiconductors" (Reinhold, NY, 1964)

6. J. Kommandeur, "Physics and Chemistry of the Organic Solid State" edited by D. Fox, M.M. Labes and A. Weissberger (Interscience, NY, 1965) Vol.II p. 1.

7. F. Gutmann and L.E. Lyons, "Organic Semiconductors" (John Wiley & Sons, Inc., NY, 1967)

8. O. H. Le Blanc, "Physics and Chemistry of the Organic Solid State" edited by D. Fox, M.M. Labes and A. Weissberger (Interscience, NY, 1967) Vol.III, p. 175.

9. J. H. Sharp and M. Smith, "Physical Chemistry : An Advance Treatise" edited by W. Jost (A.P., NY, 1970) Vol. X, p. 435.

10. D. H. Hanson,
Crit. Rev. Solid State Sci., 3, 243 (1973)

11. H. Karl,
Adv. Solid State Phys., Festkorperprobleme, 14, 261 (1974)

12. E. P. Goodings,
Chem. Soc. Rev., 5, 95 (1976)

13. H. Inokuchi and Y. Maruyama, "Photoconductivity and Related Phenomenon" edited by J. Mort and D. M. Pai (Elsevier, Amsterdam, 1976) p. 155.

14. J. O. Williams, "Advances in Physical Organic Chemistry" edited by V. Gold and D. Bothell (AP, NY, 1978)p.159.

15. C. B. Duke and L. B. Schein,
Physics Today, 33 (2), 42 (1980)

16. M. Wilk,
Z. Electro Chem., 64, 634 (1960)

17. A. Szent-Gyorgyi, "Introduction to Submolecular Biology" (AP, NY, 1960)

18. R. Mason,
Nature (London), 181, 820 (1958)

19. F. Gutmann and A. Metschey,
J. Chem. Phys., 36, 2356 (1962)

20. B. Rosenberg, R. A. Orlando and J. W. Orlando,
Arch. Biochem. Biophys., 93, 305 (1961)

21. B. W. Abrahamson, J. Marquisee, P. Cavicsi and J. Roubie,
B. Elektrochem., 64, 177 (1960).

22. B. Rosenberg,
J. Chem. Phys., 31, 239 (1959)

23. W. A. Wagins and W. H. Jennige,
Discussions Faraday Soc., No. 27, 190 (1959)

24. G. Wald,
Exptl. Cell Research, Suppl., 5, 338 (1958)

25. H. Fernandez - Moran,
Rev. Mod. Phys., 31, 319 (1959)

26. P. O. Ojostrand,
Rev. Mod. Phys., 31, 301 (1959)

27. B. Rosenberg, "Symposium on Electrical Conductivity in
Organic Solids" edited by H. Kallmann and M. Silver
(Interscience, NY, 1961) p. 291.

28. B. Rosenberg,
J. Chem. Phys., 36, 816 (1962)

29. R. S. Smart,
Trans. Faraday Soc., 58, 754 (1963)

30. D. D. Eley, "Horizons in Biochemistry" edited by M.Kasha
and B. Pullman (AP, NY, 1962)

31. B. Rosenberg,
Faraday disc., Chem. Soc., No. 51, 180 (1971)

32. B. Rosenberg,
Photochem. Photobiol., 1, 117 (1962)

33. B. Rosenberg,
J. Chem. Phys., 31, 238 (1959)

34. B. Rosenberg,
J. Chem. Phys., 34, 63 (1961)

35. B. Rosenberg,
Adv. Radiation Biol., 2, 193 (1966)

36. B. Rosenberg, T. N. Misra and R. Switzer,
Nature, 217, 423 (1968)

37. E. Postow, Ph. D. Thesis, Michigan State University,
See Diss. Abstr. Int. B 30, 77 (1968)

38. B. Rosenberg and E. Postow,
Ann. New York Acad. Sci, 158, 161 (1969)

39. H. T. Tien,
Techniques of Surface and Colloid Chemistry and
Physics, 1, 109 (1972)

40. B. Rosenberg, B. B. Bhowmik, H. C. Harder and E. Postow,
J. Chem. Phys. 49, 4108 (1968)

41. G. Kenney and B. Rosenberg,
J. Chem. Phys. 53, 3649 (1970)

42. G. Kemeny, I. M. Goklany,
J. Theor. Bio., 42, 107 (1973)

43. G. Kemeny and B. Rosenberg,
J. Chem. Phys., 52, 4151 (1970)

44. T. A. Kaplan and S. D. Mahanti,
J. Chem. Phys., 62, 100 (1975)

45. G. Kemeny and S. D. Mahanti,
Proc. Nat. Acad. Sci., U.S.A., 72, 909 (1975)

46. D. D. Eley, A. S. Fawcett and M. R. Willis,
Trans. Faraday Soc., 64, 1613 (1968)

47. E. Ulbert,
Aust. J. Chem., 23, 1347 (1970)

48. G. Sawa, K. Kitagawa and N. Ieda, Jpn. J. Appl. Phys.,
11, 416 (1972)

49. G. Sawa, N. Ieda and K. Kitagawa,
Electronics Letters, 10, 60 (1974)

50. M. Nagai, H. Nagasaka and K. Yahagi,
Jpn. J. Appl. Phys., 16, 177 (1977)

51. J. L. Hats, S. A. Rice, S. I. Choi and J. Jortner,
J. Chem. Phys., 39, 1683 (1963)

52. R. Silbey, J. Jortner, S. A. Rice and M. T. Vala, Jr,
J. Chem. Phys., 42, 733 (1965)

53. R. Silbey, J. Jortner, S. A. Rice and M. T. Vala, Jr.,
J. Chem. Phys., 43, 2925 (1965)

54. R. G. Kepler, "Organic Semiconductors" edited by J. J. Brophy and J. W. Buttrey (Macmillan, NY, 1962) p. 1.

55. F. Seitz, "Modern Theory of Solids" (McGraw Hill Book Company, Inc., NY, 1940)

56. C. Kittel, "Introduction to Solid State Physics" (Wiley Eastern Pvt. Ltd., New Delhi, 1971)

57. W. A. Harrison, "Solid State Theory" (Tata McGraw Hill Publishing Co. Ltd., Bombay and New Delhi, 1970)

58. A. J. Dekker, "Solid State Physics" (Macmillan and Co. Ltd., London, 1970)

59. F. Gutmann and L. E. Lyons, "Organic Semiconductors" (John Wiley and Sons., Inc., NY, 1967) p. 826.

60. O. H. Le Blanc, Jr., J. Chem. Phys., 35, 1275 (1961)

61. D. D. Eley and M. R. Willis, "Symposium on Electrical Conductivity of Organic Solids" edited by H. Kallmann and M. Silver (Interscience Publishers, NY, 1961) p. 257.

62. H. A. Pohl, "Modern Aspects of the Vitreous State" edited by J. D. Mackenzie (Butterworth, London, 1962) p. 105.

63. H. A. Pohl and D. A. Opp, J. Phys. Chem., 66, 2121 (1962)

64. H. Frohlich and G. L. Sewell,
Proc. Phys. Soc. (London) 74, 643 (1959)

65. W. Siebrand, Doctorate Thesis (University of Amsterdam, 1963); Abstracts : Organic Crystal Symposium (N.R.C., Ottawa, 1962) p. 56.

66. E. C. McRae and W. Siebrand J. Chem. Phys. 41, 905 (1964)

67. W. Siebrand,
J. Chem. Phys. 41, 3574 (1964)

68. O. H. LeBlanc, Jr,
J. Chem. Phys. 37, 916 (1962)

69. S. Brunauer, "The adsorption of gases and vapours" (Oxford University Press, London, 1945) Vol. I.

70. D. M. Young and A. D. Crowell, "Physical Adsorption of Gases" (Butterworths, London, 1962)

71. G. C. Bond, "Catalysis by Metals" (AP, NY, 1962)

72. J. H. de Boer,
Adv. Catal. Relat. Subj., 8, 67 (1954)

73. A. D. Crowell, "The Solid-Gas Interface" edited by E. A. Flood (Marcel Dekker, NY, 1967) Vol. I.

74. T. Engel and R. Gomer,
J. Chem. Phys. 52, 5572 (1970)

75. J. Bardeen,
Phys. Rev., 58, 727 (1940)

76. J. E. Lennard-Jones,
Trans. Faraday Soc., 28, 333 (1932)

77. H. Margenau and W. G. Pollard,
Phys. Rev., 60, 128 (1941)

78. E. G. R. Frosen and R. G. Sachs,
Phys. Rev., 61, 65 (1942)

79. I. E. Dzyaloshinskii, E. M. Lifshitz and L. P. Pitaevskii,
Adv. Phys., 10, 165 (1961)

80. C. Mavroyannis,
Mol. Phys., 6, 593 (1963)

81. A. D. Mclachlan,
Mol. Phys., 7, 381 (1964)

82. E. M. Lifshitz,
Zh. Eksp. Theor. Fis., 29, 94 (1955) [Sov. Phys. - J E T P 2, 73 (1956)]

83. W. G. Pollard,
Phys. Rev., 60, 578 (1941)

84. K. F. Wojciechowski,
Acta Phys. Pol., 29, 119 (1966); 33, 363 (1968)

85. G. G. Kleiman and U. Landman,
Phys. Rev. Lett., 31, 707 (1973)

86. G. G. Kleiman and U. Landman,
Phys. Rev. B, 8, 5484 (1973)

87. D. E. Sullivan,
Phys. Rev. B, 20, 3991 (1979)

88. P. C. Hemmer and J. L. Lebowitz, "Phase Transitions and critical Phenomena" edited by C. Domb and M. S. Green (AP, NY, 1976) Vol V B.

89. N. G. Van Kampen, Phys. Rev., 135, A362 (1964)

90. J. K. Percus, Trans. N.Y. Acad. Sci., 26, 1062 (1964)

91. J. L. Lebowitz and J. K. Percus, J. Math. Phys., 4, 116 (1963)

92. C. C. Gimmons and C. Garrod, J. Math. Phys., 14, 1075 (1973)

93. D. Henderson, F. F. Abraham and J. A. Barker, Mol. Phys., 31, 1291 (1976)

94. E. Waisman, D. Henderson and J. L. Lebowitz, Mol. Phys., 32, 1373 (1976)

95. D. E. Sullivan and G. Stell, J. Chem. Phys., 62, Appendix (1975)

96. A. Many, S. Harnik and D. Gerlich, J. Chem. Phys., 23, 1733 (1955)

97. F. Gutmann and L. E. Lyons, "Organic Semiconductors" (John Wiley and Sons., Inc., NY, 1967) p. 423-435

98. N. N. Cardew and D. D. Eley, Discussions Faraday Soc., 27, 115 (1959)

98. D. D. Eley,
J. Polymer Sci, Pt. C, 17, 73 (1967)

100. G. R. Johnston and L. E. Lyons,
Aust. J. Chem., 23, 2137 (1970)

101. G. R. Johnston and L. E. Lyons,
Phys. Status Solidi, 37, K 43 (1973)

102. O. Exner,
Collh. Czech. Chem. Commun., 29, 1094 (1964)

103. G. Kemeny and B. Rosenberg,
Nature, 243, 400 (1973)

104. B. E. C. Banks, V. Damjanovic and C. A. Vernor,
Nature, 240, 147 (1972)

105. M. E. Green,
J. Chem. Phys., 51, 3279 (1969)

106. G. C. Robert,
J. Phys. C, 4, 3167 (1971)

107. M. E. Green,
J. Phys. Chem., 69, 3510 (1965)

108. J. Bardeen,
Phys. Rev., 71, 717 (1947)

109. N.F. Mott and I.N. Sneldon, "Wave Mechanics and its Applications" (Dover Publications, Inc., NY, 1963)

110. S. Yomosa, "Quantum Aspects of Polypeptides and Polynucleotides" edited by M. Weissbluth (Interscience, NY, 1964)

111. M. G. Evans and J. Gergely,
Biochim. Biophys. Acta, 3, 188 (1949)

112. T. Holstein,
Ann. Phys. (NY), 8, 343 (1959)

113. T. Holstein,
Ann. Phys. (NY) 8, 325 (1959)

114. M. V. Volkenstein,
J. Theor. Biol., 24, 193 (1972)

115. S. Glasstone, K. J. Laidler and H. Eyring, " The Theory of Rate Processes" (McGraw-Hill, NY, 1941)

116. E. E. Weston, JR. and H. A. Schwartz, "Chemical Kinetics" (Prentice-Hall, Englewood Cliffs, N.J., 1972)

117. T. N. Misra, B. Rosenberg and R. Switzer,
J. Chem. Phys. 48, 2036 (1968)

118. B. Rosenberg and H. C. Harder,
Photochemistry and Photobiology, 6, 629 (1967)

119. K. M. Jain, A. Ghosh, B. Mallik and T. N. Misra,
Indian J. Phys. 52A, 643 (1978)

120. B. Rosenberg,
J. Chem. Phys. 34, 812 (1961)

121. B. Rosenberg,
J. Chem. Phys. 36, 816 (1962)

122. P. J. Rencroft, O. N. Rudyj and M.N. Labes,
Mol. Cryst., 1, 429 (1966)

123. M. M. Labes and C. N. Rudyj,
J. Am. Chem. Soc., 28, 2055 (1963)

124. P. J. Roucroft, C. N. Rudyj and M. M. Labes,
J. Am. Chem. Soc. 25, 2069 (1963)

125. B. Rosenberg and J. F. Comiscoli,
J. Chem. Phys. 25, 982 (1961)

126. A. G. Chynoweth,
J. Chem. Phys., 22, 1029 (1954)

127. O. Fritsch,
Ann. Physik, 22, 975 (1935)

128. W. Hartmann,
Z. Physik, 102, 709 (1936)

129. H. Mayer and H. Neidel,
Physik. Z. 38, 1014 (1937)

130. T. J. Gray and P. W. Darby,
J. Chem. Phys. 60, 201 (1956)

131. A. D. Martin and K. J. Nolcan,
J. Appl. Phys. 42, 2950 (1977)

132. W. G. Schneider and T. C. Waddington,
J. Chem. Phys., 25, 358 (1956)

133. A. Ghosh, K. N. Jain and T. N. Misra,
Proc. Indian Acad. Sci. (Chem. Sci.)
(in press) 1981

134. B. Mallik, A. Ghosh and T. N. Misra,
Proc. Indian Acad. Sci. (Chem. Sci.)
86A, 25 (1979)

135. A. Ghosh, B. Mallik and T. N. Misra,
Proc. Indian Acad. Sci.(Chem. Sci.)
92, 209 (1980).

136. Ya. Zeldovich,
Acta Physicochim. USSR, 1, 449 (1934)

137(a) S. Roginsky and Ya. Zeldovich,
Acta Physicochim. USSR, 1, 554, 595 (1934)

137(b) S. Elovich and S. Roginsky,
Acta Physicochim. USSR, 7, 235 (1937)

137(c) S. Elovich and O. N. Zhabrova,
Zhur. Fiz. Khim. 13, 1761, 1775 (1939)

138. D. D. Eley and R. B. Leslie, "Advances in Chemical Physics"
(Inter Science Publishers, NY, 1964) Vol 7
p. 238.

139(a) T. L. Hill, Advan. Catalysis 4, 211 (1952)

139(b) T. L. Hill, J. Chem. Phys. 17, 520 (1949); 18, 246 (1950)

139. S. Glasstone, "Text Book of Physical Chemistry" (Macmillan
and Co. Ltd., London, 1951) p. 1200.

140. F. S. Stone, "Chemistry of the Solid State" edited by
W. E. Garner (Butterworths, London, 1955)p. 367.

141. B. Rosenberg,
Nature, 193, 364 (1962)

142. B. Rosenberg, "Physical Processes in Radiation Biology" edited by L. Augenstein, R. Mason and B. Rosenberg (AP, NY, 1964) p. 120.

143. A. Ghosh, K. M. Jain, B. Mallik and T. N. Misra,
Jpn. J. Appl. Physics (in press, 1981)

144. K. M. Jain, A. Ghosh and T. N. Misra,
Proc. Indian Acad. Sci.(Chem. Sci.) (in press, 1981)

145. E. I. Mukhtarov, A. A. Pichurin, A. I. Kitaigorodskii,
Sov. Phys. Solid State (USA), 17, 1371 (1975)

146. B. Mallik, A. Ghosh and T. N. Misra,
Phys. Stat. Sol. (a) 62 (1980)

147. K. M. Jain, A. Ghosh and T. N. Misra,
Jpn. J. Appl. Phys. 19, 1847 (1980)

PART - D

SPECTROSCOPIC INVESTIGATIONS

CHAPTER - 1

GENERAL INTRODUCTION

During the past one and a half decades, interest in both theoretical and experimental studies of the electronic spectral properties of aromatic compounds containing strong mesomeric substituent groups has continued to have a deeper understanding of the electronic structure of and also of the radiative and nonradiative properties of such molecules[1-16]. The presence of strong mesomeric substituents, like nitro (NO_2) group, shows a drastic change in the electronic spectra of parent compounds. The situation some times is so complicated that it becomes difficult to analyse the spectra in terms of the electronic states of the parent compounds. The modification in the spectral characteristics results from the presence of new $n-\pi^*$ and intramolecular charge transfer (CT) states in these substituted molecules. The CT states are suggested to be the primary source of the spectral shift[17] from the parent compounds. The radiative and nonradiative properties of the molecules are severely affected. Some of the nitroaromatics give either fluorescence or phosphorescence only while a few give both emissions. The lack of emission in nitrobenzene is well known[3]. Inspite of a high triplet (t) quantum yield (Φ_t), phospho-

rescence quantum yield (Φ_p) in nitroaromatic molecules is usually small. Nonradiative process from $^1\eta$-π^* is observed to be efficient. These problems brought the electronic spectral studies of nitroaromatic compounds in focus recently[1-16].

The present investigation is an effort to provide informations regarding the electronic spectral properties of some nitroaromatic compounds. The electronic spectral data are collected in UV - Visible region at 298°K and also some times at 77°K. In order to analyse the spectra and to assign the electronic transitions, the standard technique depending upon the solvent effect is used. To have a better understanding of radiative and nonradiative processes, emission polarisation and mixed crystal spectra are also studied in some cases.

Adequate theoretical interpretation of the spectral data rests on modern theories. In the following sections of this chapter, we will discuss briefly the LCAO - MO method, the composite molecule method, the theory of solvent effect on the electronic spectra and the radiative and nonradiative processes.

1.2 <u>LCAO - MO method</u>

In molecular orbital (MO) theory, the molecular orbitals are described in terms of the one electron function in is generally extended over the whole molecule and to which the electrons

are allocated so as to satisfy the Pauli's exclusion principle. There are two principal approximate methods for obtaining molecular orbitals : the free electron method[18] and the LCAO-MO method.

In LCAO - MO approximation MO's (ψ_m) are expressed as a linear combination of atomic orbitals (χ_i) i.e.

$$\psi_m = \sum_i c_{mi} \chi_i \qquad (1.21)$$

where c_{mi} is the coefficient describing the amount of the i th atomic orbital to be found in m th molecular orbital.

This approximation is based on an expectation that when an electron gets close to a nucleus, the influence of the potential field due to that nucleus becomes predominant and as a consequence MO's in that region resemble to the AO's corresponding to those atoms.

These molecular orbitals are assumed to be an effective one electron Hamiltonian (h) for the equilibrium nuclear configuration of the molecule, so that one will have

$$h \psi_m = E_m \psi_m \qquad (1.22)$$

The orbital energies and the coefficients c_{mi} are obtained

using the Variation method if the matrix elements h_{ij} of the Hamiltonian and those S_{ij} of overlap between the atomic orbitals are known. The secular equations are given by :

$$\sum_j C_j (h_{ij} - E S_{ij}) = 0 \qquad (1.23)$$

for each i. If there are n atomic orbitals in the expression for molecular orbitals, there are n secular equations of this type and they will have non trivial solutions only when n th order secular determinant is zero i.e.

$$|h_{ij} - E S_{ij}| = 0 \qquad (1.24)$$

The determination of appropriate numerical values of the matrix elements h_{ij} and S_{ij}'s remains as the only difficult problem. To evaluate those, exact form of h and also the exact form of atomic orbitals are to be known. Let us write few simplifying symbols :

$$\alpha_i = h_{ii}$$

$$\beta_{ij} = h_{ij} = h_{ji} \quad (i \neq j)$$

Here α_i is the coulomb integral of the atomic orbital χ_i . This integral represents the coulomb energy of an electron in the atomic orbital χ_i . β_{ij} is the resonance integral

between the atomic orbitals χ_i and χ_j and it amounts to the energy of interaction of the two atomic orbitals. Both α and β correspond to negative energy. If it is assumed that all the atomic orbitals are normalised, the secular equations (1.23) can be rewritten as

$$\sum_{j \neq i} C_j (\beta_{ij} - E S_{ij}) + C_i (\alpha_i - E) = 0 \qquad (1.25)$$

for each i.

It is known that the absorption spectra of aromatic hydrocarbons in the near UV - Visible region are due to transitions of the π - electrons. The approximations to these secular equations for these π - orbitals, called the Huckel approximations, are the following [19-22]

1) α_i are taken to be same for each atomic orbital and this is expressed by α .

2) S_{ij} are assumed to be zero for $i \neq j$.

3) β_{ij} are considered to be nonzero only between neighbouring atoms. So $\beta_{ij} \neq 0$ if atom i is bonded to j i.e. ($i \leftrightarrow j$).

4) All the resonance integrals for neighbouring carbon atoms are assumed to be equal and are denoted by β .

Using these approximations, equation (1.25) becomes :

$$\sum_{j \to i} C_j \beta + C_i (\alpha - E) = 0 \qquad (1.26)$$

for each i.

By dividing equation (1.26) by β and writing

$$(\alpha - E)/\beta = W \qquad (1.27)$$

following simple form is obtained :

$$\sum_{j \to i} C_j + W C_i = 0 \qquad (1.28)$$

for each i.

The secular determinant now has W everywhere on the diagonal, and 1 in the off-diagonal elements of row i and column j if atoms i and j are neighbours, but zero otherwise. Thus we can easily set up the secular determinant for any π - electronic system consisting entirely of the carbon π -centres. The n th order secular determinantal equation can be solved to give n solutions for W. The energy of the n th molecular orbital is given by :

$$E_n = \alpha + W_n (-\beta)$$

That is, W is the orbital energy as expressed in units of $(-\beta)$ with reference to α .

$$W_m = (E_m - \alpha) / (-\beta)$$

Since $(-\beta)$ is a positive quantity, a negative or positive value of W means a lower or higher energy of the α .

If the molecular orbitals are normalised, use of Huckel approximations leads to

$$E_m = \alpha + 2 \sum_{i \to j} C_{mi} C_{mj} \beta$$

and $W_m = -2 \sum C_{mi} C_{mj}$

When applying the simple LCAO - MO method to a π - system containing a heteroatom, the difference of the coulomb integrals for the atomic orbitals can be allowed for by expressing the coulomb integrals α_i as $(\alpha + h_i \beta)$ where α and β are standard coulomb integral and resonance integral respectively. An appropriate value is assigned to the parameter h_i.

In simple LCAO - MO method distinction between singlet and triplet states can not be made. It is because in this method electronic repulsive interactions have been ignored. When it is considered in advanced MO method[23] (ASMO) antisymmetrised configuration functions are no longer eigenfunctions of the

Hamiltonian. True eigen functions are then made by the method of configuration interaction[24] (ASMO CI). In the self consistent - field molecular orbital method (SCF MO)[25], the required integrals are estimated by the use of assumed forms of the atomic orbitals and no empirical parameters are used. Pariser and Parr[26,27] have developed a method which incorporates empirical elements with the ASMOCI method and is applicable to more complex molecules. In the Pariser - Parr method zero - differencial - overlap approximation is used and some required integral values are determined by empirical and semiempirical method. A set of simplifying approximations have been introduced into the SCF MO method by Pople. Some times, the Pariser-Parr method and the Pople method are combined together commonly known as PPP method.

1.3 Composite - Molecule Method

Method of Simple Composite Molecule[29-31] in the one electron approximation is described which may be used to interpret the electronic absorption spectra of systems where strong mesomeric groups are substituted on the ring. Let us consider a composite conjugate system R - S where, say, for substituted benzene, the ring is taken as R and substituent as S linked to each other by a formally single bond between the atoms 'r' and 's' which belong to R and S resp.

In the LCAO approximation, the π -MO's of the composite system R - S can be obtained as linear combinations of π - orbitals of fragments R and S and their energies can be obtained by solving the proper secular equations based on the π - orbitals of the seperated fragments.

Now let $\Phi_{m(R)}$'s $\Phi_{n(S)}$'s and $\Psi_{k(RS)}$'s are the π -orbitals of R, S and R - S resp. which are the solutions of the equations :

$$h^R \Phi_{m(R)} = \eta_{m(R)} \Phi_{m(R)}$$

$$h^S \Phi_{n(S)} = \eta_{n(S)} \Phi_{n(S)} \qquad (1.31)$$

$$h^{RS} \Psi_{k(RS)} = \mathcal{E}_{k(RS)} \Psi_{K(RS)}$$

where $h^R = T + V^R$, $h^S = T + V^S$ and $h^{RS} = T + V^R + V^S$ are the effective one electron Hamiltonian operators for R, S and R - S resp. Here, V^R and V^S are the effective potentials acting on the electron in R and S resp. and T is the kinetic energy operator for the electron.

The effective one electron Hamiltonian for the composite system may also be expressed as :

$$h^{RS} = h^0 + h' \qquad (1.32)$$

where h^{o} is the Hamiltonian for the system of the two seperated fragments and h is the perturbation operator representing, interaction between R and S. Since, $\Phi_{n(R)}$'s and $\Phi_{n(S)}$'s are localised in R and S regions respectively and V^{R} and V^{S} are important in the R and S regions only, the required matrix elements of the operator h^{RS} can be approximately given by :

$$h^{RS}_{n(R),\,u(R)} = b^{R}_{n\,(R),\,u\,(R)} = \delta_{nu}\,\eta_{n(R)} \qquad (1.33)$$

$$h^{RS}_{n(S),\,v(S)} = h^{S}_{n(S),\,v(S)} = \delta_{nv}\,\eta_{n(S)} \qquad (1.34)$$

and

$$h^{RS}_{n(R),\;n(S)} = h_{n(R),\;R(S)} = b_{n(R),\,r}\,b_{n(S),\,s} \cdot \beta_{rs} \qquad (1.35)$$

where δ is the Kronecker symbol; $b_{n(R),r}$ and $b_{n(S),s}$ are the coefficients of the atomic orbitals χ_r and χ_s in $\Phi_{n(R)}$ and $\Phi_{n(S)}$ respectively and β_{rs} is the resonance integral between χ_r and χ_s i.e.

$$\beta_{rs} = \int \chi_r\, h^{RS}\, \chi_s\, d\tau = \int \chi_r\, h'\, \chi_s\, d\tau \qquad (1.36)$$

In the LCAO approximation, the form and energies of the molecular orbitals of R + S can be obtained by using perturbs-

tion theory, instead of solving the secular equations. Thus, if the relation :

$$|h'_{m(R),n(S)}| << |\eta_{m(R)} - \eta_{n(S)}| \qquad (1.37)$$

holds good for any pair of $\Phi_{m(R)}$ with one of the $\Phi_{n(S)}$'s, one of the molecular orbitals of R - S and its energy can be approximately expressed as follows :

$$\Psi_{K(RS)} = N_K\left[\Phi_{m(R)} + \sum_{n(S)}\left\{\frac{h'_{m(R),n(S)}}{(\eta_{m(R)} - \eta_{n(S)})}\right\}\Phi_{n(S)}\right] \qquad (1.38)$$

$$= \Phi^{P}_{m(R)}$$

$$\varepsilon_{K(RS)} = \eta_{m(R)} + \sum_{n(S)}\frac{(h'_{m(R),n(S)})^2}{(\eta_{m(R)} - \eta_{n(S)})} = \eta^{P}_{m(R)} \qquad (1.39)$$

Thus, if S is regarded as a mesomeric substituent, by the use of perturbation theory, we can express in an analytical form the changes in energies and forms of the molecular orbitals of a molecule R produced by the introduction of the substituent S.

This theory of composite molecule predicts the absorption intensity of a CT band as a function of angle of twist (θ_{rs}) of the bond between r and s. Suzuki[32] has shown that the oscillator strength (f) of a CT band is proportional to $\cos^2\theta_{rs}$. If the molar extinction coefficient at the absorption maxima can be taken to be proportional to f, its proportiona-

lity to the cosine square of the angle of twist, i.e. the relation originally assumed by Braude[33] is reached.

Simple composite molecule method essencially has the same limitations in interpreting electronic spectra as simple LCAO-MO has. In advanced composite molecule method, the electronic interactions have been included and the π- electronic states of a conjugated system are described as arising from mixing of electronic configurations expressed in terms of π- orbitals located on its fragments under the correct total π- electronic Hamiltonian for the system[34,35].

1.4 Nitroaromatics as Composite Molecules

A nitroaromatic molecule can be considered as a composite system with two fragments. The first fragment being the aromatic ring (R) while the other one is the nitro group (G). The fragments are linked to each other in R - G by a single bond between atom r (carbon atom) belonging to R and atom g (nitrogen atom) belonging to G. A method of simple composite molecule in the one electron approximation can be used to interpret the electronic absorption spectra of such a system. In this method, the π-MO's of the composite conjugated system (R - G) are regarded as arising from mixing of the π- MO's of the two fragments under the influence of the effective one electron Hamiltonian for the composite system. This method has been developed mainly by Dewar

and is known as Simple Composite Molecule method or LCMO method.

1.41 Nitro group

In the planar nitro group, there are four π- electrons ; two from the nitrogen atom and one each from the oxygen atoms. The 2 $p\pi$- AO (χ_N) of nitrogen and 2 $p\pi$- AO's of oxygen atoms (χ_{O1} and χ_{O2}) combine to give three π- MO's Φ_{-1}, Φ_0 and Φ_{+1} of the nitro group.

There exists a symmetry plane which is perpendicular to the nitro group plane. It bisects the angle between the two N - O bonds. Thus, the two oxygen atoms O_1 and O_2 are equivalent and the following group orbitals can conveniently be formed from the two oxygen 2 $p\pi$ - AO's :

$$\chi_{O(s)} = (2)^{-1/2} (\chi_{O1} + \chi_{O2}) \qquad 1.411$$

$$\chi_{O(a)} = (2)^{-1/2} (\chi_{O1} - \chi_{O2}) \qquad 1.412$$

The symmetrical group orbitals $\chi_{O(s)}$ interacts with the nitrogen 2 $p\pi$ - AO χ_N and the antisymmetrical group orbital $\chi_{O(a)}$ does not. Therefore, the three π- MO's of the nitro group in the zero-overlap approximation can be expressed as :

$$\Phi_{-1} = b_{-1,1}\,\chi_N - b_{+1,1}\,\chi_{O(S)} \qquad 1.413$$

$$\Phi_0 = \chi_{O(a)} \qquad 1.414$$

$$\Phi_{+1} = b_{+1,1}\,\chi_N + b_{-1,1}\,\chi_{O(S)} \qquad 1.415$$

J. Tanaka has evaluated the values of the coefficients $b_{-1,1}$ and $b_{+1,1}$ to be equal to 0.7003 and 0.7133 respectively. Φ_{-1}, Φ_0 and Φ_{+1} are the antibonding, nonbonding and bonding π - orbitals respectively. The antibonding orbital (Φ_{-1}) remains vacant while the other two lower orbitals Φ_{+1} and Φ_0 are occupied in the ground state.

The highest bonding orbital is designated by + 1 and the lower orbitals in order of decreasing energies are designated by + 2, + 3, ··· and so on in a mesomeric system. Similarly - 1 represents the lowest antibonding orbital and higher orbitals in order of increasing energies are designated as - 2, - 3, ··· and so on.

1.43 Energies and Wave functions of Nitroaromatics

S. Nagakura and Nagakura *et al*[13] calculated the energies and wave functions of π - electronic states of nitrobenzene. They have taken into account eight singlet electron configurations : the ground configuration (V_0 or G), five locally

excited (L E) and two CT configurations for nitrobenzene. Of the five LE configurations, four are the configurations corresponding to the α , p , β and β' states of benzene and one is the configuration arising from the $(\pi-\pi^*)$ S - S transition within the nitrogroup i.e. from Φ_0, to $\Phi_{-1'}$. The energies of these LE configurations E_α, E_p, E_β, $E_{\beta'}$ and E_{NO_2} were determined as 4.89, 6.17, 6.08, 6.98 and 6.26 ev respectively from the observed positions of the corresponding absorption bands of benzene and nitromethane. The CT configurations arising from the one electron transition from Φ_{+1} to $\Phi_{-1'}$ and the another one arising from Φ_{+2} to $\Phi_{-1'}$. The energies of these CT configurations were evaluated as 4.03 and 5.06 ev respectively by the use of the equation

$$E(CT) = I_B - A_{NO_2} - C \qquad (1.421)$$

where I_B and A_{NO_2} are the ionisation potential of benzene (9.24 ev) and the electron affinity of nitro group (0.4 ev) respectively and C is the coulomb interaction between the negative charge distributed in the nitrogroup and the positive charge distribution in the benzene ring in the CT configuration. The off-diagonal matrix elements of the total π- electronic Hamiltonian (H) necessary for the calculation of configuration interaction can be evaluated in terms of β^c_{CH}, the core

resonance integral between the adjecent carbon and nitrogen 2 $p\pi$- AO's. The nonzero interaction matrix elements are $\langle LE_p | H | CT_s \rangle$, $\langle G | H | CT_s \rangle$, $\langle LE_\alpha | H | CT_a \rangle$, $\langle LE_\beta | H | CT_a \rangle$ and $\langle LE_\beta | H | CT_a \rangle$. The other off diagonal elements are zero.

It has been shown that in nitrobenzene, the ground state has 93.3% G and 6.6 % CT_s and very little of LE_p and LE_β. The first excited state has 48.5% of both LE_α and CT_a. The second excited state contains 70.3 % of CT_s.

1.5 Solvent Effect on the Electronic Spectra

The electronic spectral changes in the presence of solvent molecules arise due to the introduction of a local field around the solute molecule, which is different than that in a free space and also due to alteration in the charge density of the molecule. In general, changes in both the intensity and the energy of a band are observed[36,37]. In addition, some times, weak or forbidden transitions may also gain intensity. Following are the predominant effects :

1) Dielectric effects : These are the dipolar effects between the solute and the solvent molecules;

2) Dispersive effects: These are due to Vander Waals forces;

3) Short range specific effects: These are developed due to a field introduced by the weak bond formation like hydrogen bond between the solute and solvent molecules;

4) Concentration effect: If the concentration of the solute molecules in solvent is not very small, then the solute - solute interaction may not be avoided. These may cause dimer formation between the two monomer solute molecules; and

5) The long range intermolecular resonance effects: These are very important in the emission studies.

All these effects are to be considered while calculating the spectral energy shift or spectral intensity change.

1.51 Solvent Effect on Transition Energy of an Allowed Transition

Upon absorption the electro-magnetic radiations, the permanant dipole of the molecule in the ground state (μ_g) changes to the dipole moment in the excited state (μ_e). In presence of solvent molecules, owing to the solute solvent interaction, ground and excited states stabilise differently. The change in the stabilisation energy ΔW is given by :

$$\langle \Delta W \rangle = h \Delta \nu^a \qquad (1.511)$$

where $\Delta\nu^a$ is the change in the absorption maxim frequency and h is the Planck's constant.

Thus, we see that the study of the solvent shift may reveal various features of the ground and excited states of the molecules. In general $n-\pi^*$ states show blue shift while $\pi-\pi^*$ and CT states show red shifts.

Using quantum mechanical perturbation theories, Ooshika[38] has calculated first time the stabilisation energy of an electronic state due to solute solvent interaction in 1954. The same method was used later by Longuet - Higgins and Pople[39] and by McRae[40].

Here, we will discuss the quantum mechanical theory on the solvent effect on electronic spectra. The proposed theory is the stationary theory where the translational motion of the molecules is neglected completely. The theory will hold only for slow perturbations. The time dependence of Hamiltonian for the absorbing system has also been considered but the complications and difficulties associated with such a theory in evaluating the interaction is obvious.

Let us consider a dilute solution so as to avoid solute - solute interaction. The problem is now to find the appropriate stationary energy states of a system consisting of a single

solute surrounded by a set of solvent molecules in a given configuration and then average over all possible configurations. Let Φ_m, $\mathcal{E}_n$ and Ψ_n, E_n are the eigenfunctions and eigenvalues of solute and solvent molecule respectively. Then a set of basis functions $\Psi_{mn} = \Phi_n \Psi_n$ can be used for the interacting pair. The next step is to introduce the perturbation Hamiltonian H, and the interaction energy to second order in H, using perturbation theory which may be written as :

$$W_{mn} = \langle \Phi_m \Psi_n | H' | \Phi_m \Psi_n \rangle + \sum_{n' \neq n} \frac{|\langle \Phi_m \Psi_n | H' | \Phi_m \Psi_n \rangle|^2}{E_n - E_{n'}}$$

$$+ \sum_{m' \neq m} \frac{|\langle \Phi_m \Psi_n | H' | \Phi_m \Psi_n \rangle|^2}{\mathcal{E}_m - \mathcal{E}_{m'}} + \sum_{m' \neq m, n' \neq n} \sum \frac{|\langle \Phi_m \Psi_n | H' | \Phi_m \Psi_n \rangle|^2}{\mathcal{E}_m - \mathcal{E}_{m'} + E_n - E_{n'}} \qquad (1.512)$$

If we assume that H' represents the electrostatic interaction between the solute and the solvent molecules, then the perturbation operator may be written as :

$$H' = \sum_i \frac{\mu_0 \mu_i}{r_i^3} \Phi_i \qquad (1.513)$$

where μ_0 and μ_i represent the dipole moment of the solute and i th solvent molecule respectively; r_i and Φ_i are the distance and the mutual orientation between the solute and the i th solvent molecule. The above simple dipolar representation of the molecular interaction is not operative in cases where the

specific short range forces like hydrogen bonding, charge transfer etc. are present.

Using equations (1.513), equation (1.512) becomes :

$$W_{mn} = (\langle \Phi_m | M_0 | \Phi_m \rangle) \sum_i \frac{\langle \Psi_n | M_i | \Psi_n \rangle}{r_i^3} \oplus_i + \langle \Phi_m | M_0 | \Phi_m \rangle^2 \sum_{i,j}^{i} \sum_{n' \neq n} \frac{\langle \Psi_n | M_i | \Psi_{n'} \rangle \langle \Psi_n | M_j | \Psi_{n'} \rangle}{(E_n - E_{n'}) r_i^3 r_j^3} \oplus_i \oplus_j + \sum_{m' \neq m} \sum_{i,j} \frac{M_i M_j}{r_i^3 r_j^3} \oplus_i \oplus_j \frac{\langle \Phi_m | M_0 | \Phi_{m'} \rangle}{\mathcal{E}_m - \mathcal{E}_{m'}} + \sum_{m' \neq m} \sum_{i,j} \sum_{n' \neq n} \frac{\langle \Phi_m | M_0 | \Phi_{m'} \rangle^2 \langle \Psi_n | M_i | \Psi_{n'} \rangle \langle \Psi_n | M_j | \Psi_{n'} \rangle}{(\mathcal{E}_m - \mathcal{E}_{m'} + E_n - E_{n'}) r_i^3 r_j^3} \oplus_i \oplus_j \qquad (1.514)$$

The first term arising from the first order perturbation theory. It represents the interaction between two permanent dipoles. The second term corresponds to the permanent dipole of the solute with dipole induced in solvent. The third term represents the interaction of the permanent dipole of solvent with the dipole induced in the solute. The last term represents the second order interaction with states in which both the molecules are excited, corresponds to the dispersive interactions.

In order to make above expression available for any practical use, we will have to assume a specific model for solvent solute system. Direct evaluation of the integrations is not possible due to our lack of knowledge of molecular eigen

functions.

The relatively simple Onsager model[41] having broad physical meaning for liquid dielectric is most suitable to simplify expression (1.514) in terms of refractive index (n) and the dielectric constant (D) of the solvent and the polarisability of the solute molecule. In Onsager model, the solute molecule is considered as a point dipole at the centre of a homogeneous spherical solvent dielectric cavity.

In Onsager's theory, the dipolemoment of a solute in solution μ_m' is related to the dipole moment of the isolated solute molecule μ_m , its static polarizability α_m and a suitable reaction field R_i (this field arises from the orientation induction polarisation of the dielectric by the solute dipole), as

$$\mu_m' = \mu_m + \alpha_m R_i \qquad (1.515)$$

where the reaction field due to induction $[R_i\ (\text{ind})]$: $R_i\ (\text{ind}) = 2\mu_m/a^3\ [(n^2-1)/(n^2+2)]$ and reaction field due to orientation $[R_i\ (OR)]$: $R_i\ (OR) = 2\mu_m/a^3\left[(D-1)/(D+2) - (n^2-1)/(n^2+2)\right]$. Here, 'a' is the Onsager's cavity radious.

In order to apply this theory, let us imagine a solute molecule surrounded by N solvent molecules. Fixing the solute

molecule, let N molecular distribution function be

$$f(1, 2, \quad N) = f_0 + f_1 \qquad (1.516)$$

where f_0 is the hypothetical distribution function when the dipolemoment of the solute molecule is assumed to be zero and f_1 represents the orientation of the solvent molecules by the dipole of the solute molecule in solution. The orientation relaxation time of solvent molecules should be much larger than the time required for light absorption (10^{-16} second) by the solute. Using the statistical concepts, averaging of the various interaction terms in (1.514) over the molecular distribution function can be performed to get the energy change of the solute molecule in the state n due to solvent solute interaction as $\langle V_{nn} \rangle$. The frequency shift of the absorption maximum is the difference between $\langle W \rangle$ for the ground (g) and excited (e) states of the solute molecule, the solvent molecules being in the g - state. The general expression for the solvent shift of a solute molecule in nonpolar solvent is given by :

$$h\Delta\nu^a = \langle W_{eg} \rangle - \langle W_{gg} \rangle$$
$$= \frac{1}{a^3}\left(\frac{2n^2+1}{n^2+2}\right)\left\{2\mu_g(\mu_g-\mu_e)\left(\frac{D-1}{D+2}-\frac{n^2-1}{n^2+2}\right)+\left(\frac{n^2-1}{n^2+2}\right)\right.$$
$$\left.(\mu_g^2-\mu_e^2)+\frac{2}{a^3}\left(\frac{n^2-1}{n^2+2}\right)\frac{E}{E+\varepsilon}\left\{|P_{eg}|^2+\varepsilon(\alpha_g-\alpha_e)\right\}\right. \qquad (1.517)$$

where P_{eg} is the transition moment of solute for the electronic transition between the states 'g' and 'e'. The first term represents the polarisation effects while the second term is the term representing the dispersive effects which exists in all the systems irrespective of the polar character of the solute and the solvent.

In case of polar solvents, one extra interaction term will also be arising. This comes from the orientation - induction effect of solvent dipole on the solute molecule. The shift due to this interaction term is given by :

$$h\Delta\nu^{a}(OR-IN) = \frac{3}{(2D+1)} \cdot \frac{(2D+1)^2(D-n)^2}{(2D+n^2)\ D} \cdot \frac{kT}{3a^3}(\alpha_e-\alpha_g) + \frac{1}{a^3}\left(\frac{2D-2}{D+2}\right)^2(\mu_e^2\alpha_e - \mu_g^2\alpha_g)$$

(1.518)

From (1.517) and (1.518), it can be noted that this is only the temperature dependent term in the solvent shift expression. Therefore, the informations about this interaction can be obtained by the temperature effect studies on the electronic spectral shift.

1.43 Solvent Effect on the Intensity of Allowed Electronic Transitions

The oscillator strength (f) is related to the transition

moment (M_{ij}) corresponding to the absorption band of the molecule and is given by :

$$f \propto \{ |M_{ij}|^2 = |\langle i| M |j\rangle|^2 \} \qquad (1.431)$$

It is obvious that M_{ij} is sensitive to the exact form of the states 'i' and 'j' which are subject to modifications due to solute - solvent interactions.

According to classical dispersion theory f is given by :

$$f = 4.315 \times 10^{-5} \int \varepsilon(\nu)\, d\nu \qquad (1.432)$$

where $\varepsilon(\nu)$ is the extinction coefficient at wave-number ν. The integration is over the band considered.

The effect of solvent on the unperturbed oscillator strength f_i of solute i has traditionally been accounted for by the Onko's factor $\{(n^2+2)^2/9n\}$ in the expression :

$$f_i \{(n^2+2)^2/9n\} = K \cdot S = f_s \qquad (1.433)$$

where f_s is the oscillator strength in a very dilute solution.

The solvent correction factor in the brackets of (1.433) arises from the use of the Lorentz local field for the electric

field acting on the solute molecule in solution and was first introduced by Onsko in 1934[42]. He, however, did not take into account the polarizability changes due to the presence of solvent molecules. The inadequacy of his correction is further accentuated by the fact that the Lorentz field does not take account of the translational fluctuations in the fluid. Onsko's factor is always greater than unity and is same for all the solutes in a given solvent. Contrary to this, various authors[43,44] have pointed out that the experimental solvent correction was in cases less than or equal to one and thus the factor has shown its dependence on the properties of both solute and solvent.

Theoretical investigations[45-50] of the problem have generally focused on either the changes in polarizability, often without clearly distinguishing between them. Recently the problem has been thoroughly investigated by S. Abdulnur and B. Linder[51] to show that the Onsko's factor is of minor importance as compared to an additional intermolecular forces (IMF) factor.

Let us consider a system of N non overlaping nonpolar spherical molecules with centres located at $\bar{R}_1$, $\bar{R}_2 \cdots \bar{R}_N \equiv \bar{R}^N$, where R^N is the vector in three dimensional vector space. In presence of field $E(t) = E_0 e^{i\omega t}$, the Hamiltonian of the system can be written as :

$$H = H_0 + H^{in} + K + H^{ex} \qquad (1.434)$$

where H_0 : Hamiltonian for the electronic motion of free molecules

H^{in} : Interaction between the molecules

K : Kinetic energy operator taking care of the translational fluctuations

H^{ex} : Interactions of the system with the radiation field

The problem is treated by double perturbation theory : time - dependent in the interaction with the field and time independent in the intermolecular interaction. The Hamiltonian may also be written as :

$$H = H^0 - M.E_0 \exp (i\omega t + \xi t) \qquad (1.435)$$

where $H^0 = H_0 + H^{in} + K$ and $M = \sum_j \bar{m}_j = \sum e_n \bar{r}_n$, where n numbers the charges in the molecule and $\bar{r}_n$ is the radious vector of the n th charge with respect to an arbitrary origin. The factor $e^{\xi t}$ insures the adiabatic switching-on of the field. The average induced moment, linear in E_0 is given by[61]

$$\langle \bar{M} \rangle = -\frac{i}{\hbar} \int_0^\infty dJ \; Tr\Big[\bar{M}\Big\{\exp\Big(-\frac{iH^\circ J}{\hbar}\Big)\Big\}(-\bar{M}\cdot\bar{E}_o)$$
$$\exp\Big(\frac{iH^\circ J}{\hbar}\Big) - \Big\{\exp\Big(-\frac{iH^\circ J}{\hbar}\Big)\Big\}(-\bar{M}\cdot\bar{E}_o)$$
$$\Big\{\exp\Big(\frac{iH^\circ J}{\hbar}\Big)\Big\}\bar{M}\Big]\rho$$
$$\exp\{(i\omega + \xi)(t-J)\} \qquad (1.436)$$

where ρ is the statistical operator of the system of interacting molecules in the absence of the applied field i.e.

$$\rho = \exp(-\beta H^\circ) \Big/ Tr[\exp(-\beta H^\circ)]$$

and $\beta = 1/kT$

At ordinary temperatures, only the ground electronic state is populated in most of the molecules while the partitioning of the molecules among the translational energy levels is classical i.e. within an energy interval kT, the energy levels are densely spaced. Now, in addition, using the fact that the electronic motion is rapid than the nuclear motion, one can obtain an expression for $\langle M \rangle$ which would be independent of kinetic parameters and will be in terms of transition moment between the states considered.

Using the statistical concepts and by developing the virial expansion for the extinction coefficient, integrated over an allowed band, the following expression is obtained :

$$\left[\frac{(n^2+2)^2}{9n}\right] f_i \left[1+\left(\frac{N_j}{f_i V}\right) \times \int g^{(2)}(\bar{R}_{ij})\, f_{ij}(\bar{R}_{ij})\, d\bar{R}_{ij}\right] = K \cdot \int \quad (1.437)$$

where (N_j/V) is the number of solvent molecules 'j' per C.C. of the solution; $g^{(2)}(R_{ij})$ is the ordinary two body distribution function; f_i is the oscillator strength of the isolated unperturbed solute molecule i ; $f_{ij}(R_{ij})$ is an oscillator strength function of particals 'i' and 'j' and is parametrically dependent upon R_{ij} . The integration of LHS extends strictly over the volume of the solution sample. However, since the fuction f_{ij} drops off very quickly with internuclear distance (R_{ij}^{-6} dependence) the integration can be extended to infinity without introducing much error.

Comparision of (1.433) and (1.437) shows that the former can be reduced to the latter if one neglects the integration. This is only possible in the case of an absorber in a very rarified gas when $(N_i/V) \longrightarrow 0$.

The main difficulties arise involving the configurational integration of the LHS of (1.437) in trying to numerical estimates for the solvent correction from that equation. The first

stems from a lack of knowledge of accurate wave-functions of the isolated molecules needed to estimate the various matrix elements in the expression for f_{ij}. The second difficulty is to estimate the summation over all the discrete states and the implied integration over the continuum states in each of the various terms of f_{ij}.

1.5 Radiative and Nonradiative Decay Processes

The ground state of most of the stable organic molecules is a singlet and the lowest excited state is a triplet[37]. Although one can observe the spectra due to triplet $\longleftrightarrow$ singlet transitions, the very severe multiplicity restriction on the transition is apparent when the observations show that the radiative life time of the t-states of the organic molecules are in the range of 10^{-2} - 1 seconds while those of the lowest singlets are of the order of 10^{-9} - 10^{-6} seconds. The light emission transition between the states with the same spin multiplicity is called fluorescence while that between the states with different multiplicities is called phosphorescence transition. In addition to light emission, there are always various radiationless transitions in polyatomic molecules. A nonradiative transition between the states with same multiplicities is known as 'internal conversion' while that between the states with different multiplicities is known as 'inter system crossing' (ISC). The observed decay time of an excited state

depends upon the radiative and nonradiative transition probabilities (K_r and K_{nr} respectively) and is given by

$$\tau = \frac{1}{K_r + K_{nr}} \qquad (1.51)$$

1.51 Radiative processes

The interaction of an electronic system with quantised radiationfield causes emission and absorption of photons. Let H is the Hamiltonian of the total system given by :

$$H = H_{el} + H_{rad} + H_{int} \qquad (1.511)$$

$$= H_0 + H_{int}$$

where, H_{el} and H_{rad} are the Hamiltonians corresponding to the electronic system and the radiation field.

The eigen functions Ψ_M of H_0 are the unperturbed stationary states given by :

$$\Psi_M = \Psi_M^{el}(\bar{r}) \cdot \Phi^{ph}_{n_1, n_2, \ldots n_\lambda} \qquad (1.512)$$

where $\Psi_M^{el}(\bar{r})$ is the m th state of the electronic system with eigen values E_m^{el}, and $\Phi^{ph}_{n_1,n_2\ldots} = \varphi_{n_1} \cdot \varphi_{n_2} \cdots \varphi_{n_\lambda}$ means that there are n_1 photons of energy E_1^{ph}, n_2 photons of

E_2^{ph} and soon.

The perturbation caused by H_{int} causes the transition to the state

$$\Psi_N = \Psi_n^{el}(\bar{r}) \quad \Phi_{n_1' n_2' \ldots}^{ph} \qquad (1.513)$$

The transition probability is proportional to the square of the matrix element $\langle \Psi_M | H_{int} | \Psi_N \rangle$. Let $E_m^{el} > E_n^{el}$; then assuming radiation field to be in vacuo with respect to matter, the one photon emission probability ω_{MN} for isolated molecules, where the interaction between the molecules is neglected, can be given by :

$$\omega_{MN} = \frac{64\pi^4\nu^3}{3hc^3} |M_{nm}|^2 + \frac{8\pi^3}{3h^2} |M_{nm}|^2 \rho(\nu) \qquad (1.514)$$

where $\rho(\nu)$ is the energy density of emitted photons. The first and second terms in equation (1.514) are the spontaneous and the induced emission probabilities respectively.

When molecules are embedded in a fluid or solid solvents and there are no specific interactions between the molecules and the medium, then following formula can be derived :

$$\omega_{MN} = \frac{64\pi^4\nu^3}{3hc^3 n} |M_{nm}|^2 + \frac{8\pi^3}{3h^2 n} |M_{nm}|^2 \rho(\nu) \qquad (1.515)$$

where n is the refractive index of the medium.

Oscillator strength is an important quantity concerning the practical aspects of transition probability. The oscillator strength is related to the spontaneous emission probability as :

$$f_{nm} = \frac{8\pi^2 m\nu}{3\,h\,e^2} \left| M_{nm} \right|^2 \qquad (1.516)$$

The electronic spectra with vibrational structures can be well understood on the basis of Born - Oppenheimer approximation[54] and the Franck - Condon principle. According to Born - Oppenheimer approximation, molecular wave functions can be written in terms of the product of electronic and nuclear parts i.e.

$$\left.\begin{aligned} \Psi_n^{el} &= \Psi_{n\nu''} \simeq \Psi_n \cdot \Phi_{n\nu''} \\ \Psi_m^{el} &= \Psi_{m\nu'} \simeq \Psi_m \cdot \Phi_{m\nu'} \end{aligned}\right\} \qquad (1.517)$$

Using equations (1.517), the expression for oscillator strength can be obtained as :

$$f_{nm} \simeq f_{no,m} = \frac{4\pi mc}{3\hbar}\,\bar{\nu} \left| Q_{nm}(\bar{R}_e) \right|^2 \cdot \sum_{\nu'} \left| S_{no,m\nu'} \right|^2 \qquad (1.518)$$

where $e \cdot Q_{n\nu'',m\nu'}$ represents the relative contribution of the

$n\,v'' \leftrightarrow m\,v'$ transition to M_{nm}, which is a sum of many vibronic contributions of this type and $S_{nv'',mv'} = \int \phi^{*}_{nv''}(\bar{R})\,\phi_{mv'}(\bar{R})\,d\bar{R}$ is the vibrational overlap integral.

Equation (1.518) clearly indicates that the Franck - Condon principle, which states that during the electronic transition the nuclear configuration of a molecule remains approximately at the equilibrium configuration $\bar{R}_e$ of the initial state, plays an important role.

1.511 Forbidden Transitions

Usually the transitions between the states with different multiplicities are forbidden. Let the electronic wave function may be written as a product of space $\Psi_m(r)$ and spin $\Theta_m(s)$ parts i.e.

$$\Psi_m \simeq \Psi_m(r) \cdot \Theta_m(s) \qquad (1.5111)$$

The transition moment M_{mn} is thus,

$$M_{mn} = \langle \Psi_m(r)\,\Theta_m(s) | M | \Psi_n(r)\,\Theta_n(s) \rangle$$
$$= \langle \Psi_m(r) | M | \Psi_n(r) \rangle \cdot \langle \Theta_m(s) | \Theta_n(s) \rangle \qquad (1.5112)$$

$\Theta_m(s), \Theta_n(s)$ are orthogonal, if the two states have

different multiplicities and then H_{mn} becomes zero. Thus the transition will be multiplicity forbidden. The transition, however, is weakly allowed as the Spin - Orbit (S - O) coupling increases. The S - O interaction can be enhanced not only by the heavy atom in the molecule (internal heavy atom effect) but also by the interaction with other molecules containing heavy atoms (external heavy atom effect)[55]

1.52 Non-radiative Processes

The interaction between the electronic and nuclear motions causes the radiationless transitions. As mentioned earlier the molecular electronic states (Φ) in the Born-Oppenheimer approximation are given by

$$\Phi = \Phi_{mv'}(\bar{R}_i, \bar{r}_j) \simeq \Psi_m(\bar{R}_i, \bar{r}_j) \cdot \bar{\Phi}_{mv'}(\bar{R}_i) \quad (1.521)$$

where $\Psi_m(\bar{R}_i, \bar{r}_j)$ is the stationary states of the electronic system in presence of fixed nuclei. Equation (1.521) represents the wave function of the unperturbed Hamiltonian H^0. The transition occurs between the states Φ_i and Φ_f due to the kinetic energy operator of the nuclear motion $H' = T_N$ with the transition probability per unit time as :

$$\omega_{if} = \frac{2\pi}{\hbar} \left| \langle \Phi_f | H' | \Phi_i \rangle \right|^2 \delta(E_f - E_i) \quad (1.522)$$

where E_i and E_f are the energies of initial and final states Φ_i and Φ_f respectively. $\delta (E_f - E_i)$ is the delta function which represents the conservation of energy in the transition. The transition probability can be obtained by integrating over the final state i.e.

$$\omega = \frac{2\pi}{\hbar} \left| \langle \Phi_f | H' | \Phi_i \rangle \right|^2 \rho(E_f) \qquad (1.523)$$

where $\rho (E_f)$ is the level density of the final state. Equation (1.523) is valid only when H is time independent and the final state is continuous. This indeed is the situation in solutions and solids where intermolecular interactions make the level density larger :

The matrix elements of equations (1.522) and (1.523) may be written as

$$\langle \Phi_f | H' | \Phi_i \rangle = -\hbar^2 \sum_i \langle \Psi_n | \frac{\partial}{\partial \bar{R}_i} | \Psi_m \rangle \langle \Phi_{nv''} | \frac{\partial}{\partial \bar{R}_i} | \Phi_{mv''} \rangle \qquad (1.524)$$

The integral in (1.524) may be written using perturbation theory as

$$\langle \Psi_n | \frac{\partial}{\partial \bar{R}_i} | \Psi_m \rangle \simeq \frac{\langle \Psi_n^e(\bar{R}_i) | \left(\frac{\partial H^0}{\partial \bar{R}_i}\right)_e | \Psi_m^e(\bar{R}_i) \rangle}{(E_m^e - E_n^e)} \qquad (1.525)$$

Here, the superscript and subscript 'e' represents the quantities

in equilibrium nuclear configuration.

The first term in (1.524) corresponds to the electronic transition moment integral of radiative transition and second one is the vibrational overlap, the square of which is the Franck Condon factor. This second term plays an important role in the radiation-less process. The value of this factor depends upon ($E_m^0 - E_n^0$). The transition probabilities of the nonradiative processes $S_3 \rightsquigarrow S_2$, $S_2 \rightsquigarrow S_1$ etc. may be much larger than that of the $S_1 \rightsquigarrow 0$ process. The second term in (1.524) will affect the transition probabilities in a similar way because this factor may be larger for the smaller energy gap in general.

When the molecules are dissolved in solvents, the interaction of the solute molecule with the solvent molecules generally enhances the radiationless transition probability. For i th normal mode :

$$\tau_i(m\,n) = \langle \Psi_n | \frac{\partial}{\partial \bar{R}_i} | \Psi_m \rangle$$

where $\Psi_\eta(\bar{R}_1)$ are the electronic states corresponding to the Hamiltonian : $H = H_0 + H_{SO}$

where H_0 represents the K. E. and P. E. for electrons, H_{SO} is the spin-orbit interaction operator and both H_0 and H_{SO} contains

nuclear coordinates as parameters and so can be expanded in the Taylor series. The wave function is given by

$$\Psi_n(\bar{R}_i) \simeq \Psi_n^e + \sum_{l\neq n}\left[\frac{\langle\Psi_l^e|H_{so}^e+\sum_i\left(\frac{\partial H_0}{\partial\bar{R}_i}\right)_e\bar{R}_i+\sum_i\left(\frac{\partial H_0}{\partial\bar{R}_i}\right)_e\bar{R}_i|\Psi_n^e\rangle}{(E_n^e-E_l^e)}\right.$$
$$+\sum_{k\neq n}\left\{\frac{\langle\Psi_l^e|H_{so}^e|\Psi_k^e\rangle\langle\Psi_k^e|\sum_i\left(\frac{\partial H_0}{\partial\bar{R}_i}\right)_e\bar{R}_i|\Psi_n^e\rangle}{(E_n^e-E_l^e)(E_n^e-E_k^e)}\right.$$
$$\left.\left.+\frac{\langle\Psi_l^e|\sum_i\left(\frac{\partial H_0}{\partial\bar{R}_i}\right)_e\bar{R}_i|\Psi_k^e\rangle\langle\Psi_k^e|H_{so}^e|\Psi_n^e\rangle}{(E_n^e-E_l^e)(E_n^e-E_k^e)}\right\}\right]\Psi_l^e \qquad (1\cdot526)$$

Using (1·526), $\tau_i(mn)$ is given by:

$$\tau_i(mn) \simeq \frac{\langle\Psi_n^e|\left(\frac{\partial H_{so}}{\partial\bar{R}_i}\right)_e|\Psi_m^e\rangle}{(E_m^e-E_n^e)}$$
$$+\sum_{l\neq m}\left[\frac{\langle\Psi_n^e|H_{so}^e|\Psi_l^e\rangle\langle\Psi_l^e|\left(\frac{\partial H_0}{\partial\bar{R}_i}\right)_e|\Psi_m^e\rangle}{(E_n^e-E_l^e)(E_m^e-E_n^e)}\right.$$
$$\left.+\frac{\langle\Psi_n^e|\left(\frac{\partial H_0}{\partial\bar{R}_i}\right)_e|\Psi_l^e\rangle\langle\Psi_l^e|H_{so}^e|\Psi_m^e\rangle}{(E_m^e-E_l^e)(E_m^e-E_n^e)}\right] \qquad (1\cdot527)$$

Here the 1st term is the direct compling between the initial and the final state by the spin vibronic interaction. In the 2nd term, the initial state couples with the intermediate state Ψ_1^e through the vibronic interaction and the intermediate state interacts with the final state by the S - O coupling. In the 3rd term, the initial state interacts with the intermediate state through the S - O coupling and the intermediate state couples with the final state through the vibronic interaction.

CHAPTER 8

ELECTRONIC SPECTRA OF 9-NITROANTHRACENE : SOLVENT EFFECT ON $^1A \longrightarrow {}^1L_a$ AND $^1A \longrightarrow {}^1L_b$ TRANSITIONS.

1. Introduction

In aromatic hydrocarbons, four $\pi - \pi^*$ bands are usually observed. In benzene, the lowest singlet state is ^1L_b with the next higher as ^1L_a.

In cata-condensed hydrocarbons as one moves from benzene to higher polyacenes, both ^1L_a and ^1L_b energy levels of benzene move to lower energy. The lowering in energy of ^1L_a is steeper than the ^1L_b. The correlation diagram of Klevens and Platt[56] for the spectra of polyacene series predicts that ^1L_b band should be hidden under the stronger ^1L_a transition in anthracene. Moffitt[57], Pariser[58] and Ham et al[59] also support this prediction from theoretical view point. In an effort to provide direct experimental evidence, Chay[60] and Sidman[61] failed to observe ^1L_b band in anthracene molecule. However, the situation is quite different in substituted anthracenes. Strong mesomeric substituents like nitro group in anthracene molecule are expected to show strong effect on the $\pi - \pi^*$ electronic states of anthracene owing to their substitutional perturbations. We have chosen 9-nitroanthracene (NA) molecule to see if ^1L_b band appears on

nitro group substitution. Intramolecular CT band is expected to be the lowest and should be of very low intensity as this molecule is found to have nonplanar structure. The interplanar angle[62] between the nitro group plane and the anthracene ring plane is as large as 85°. The situation in NA is quite different than that of anthracene and it is quite possible that the ^1L_b band of anthracene may shift to an accessible spectral region in this molecule.

In this chapter, we present the results of our studies on the electronic absorption and emission spectra of NA and show that indeed in this molecule the lowest energy state is having the predominantly π - character and is different from ^1L_a. The effects of various polar and non-polar solvents have also been investigated.

2. Experimental

The compound, a gift from Prof. R. S. Becker, was further purified by repeated recrystallization using purified benzene. Needle shaped yellow crystals having melting point at 146°C were obtained. The spectrograde solvents (BDH and E - merck) were used.

The absorption spectra in various solvents were recorded at 303°K on a Perkin Elmer 202 recording spectrophotometer and also on Spectromom 202 spectrophotometer of Hungarian Optical

Works. Aminco Bowman spectrofluorimeter was used to measure the emission spectrum.

3. Results and Discussions :

The absorption spectra of NA in various nonpolar and polar solvents with the same concentration at room temperature (298 K) are reproduced in Figs. 2.1 and 2.2 respectively. The results of the analysis of the bands are summarised in Tables 2.1, 2.2 and 2.3. In all the solvents, a well defined intense band system at about 26100 cm^{-1} is observed with vibrational structure. In non-polar solvents, however, few more weak bands appear towards the lower energy side of this band system. In polar solvents, these weak bands lose their structure and a general broad weak absorption band is observed in this spectral region.

A close examination of the absorption spectra of NA in various solvents reveals that the strong band system at about 26100 cm^{-1} resembles the lowest energy absorption band of anthracene as shown in Fig. 2.3. The bands on the lower energy side are structurally different from the bands in the intense system and possibly belong to different electronic transition. This deduction has been further substantiated by the vibrational analysis of the spectra in various solvents.

It has been pointed out by Coggeshall and Pomefsky[63] that

Figure - 2.1

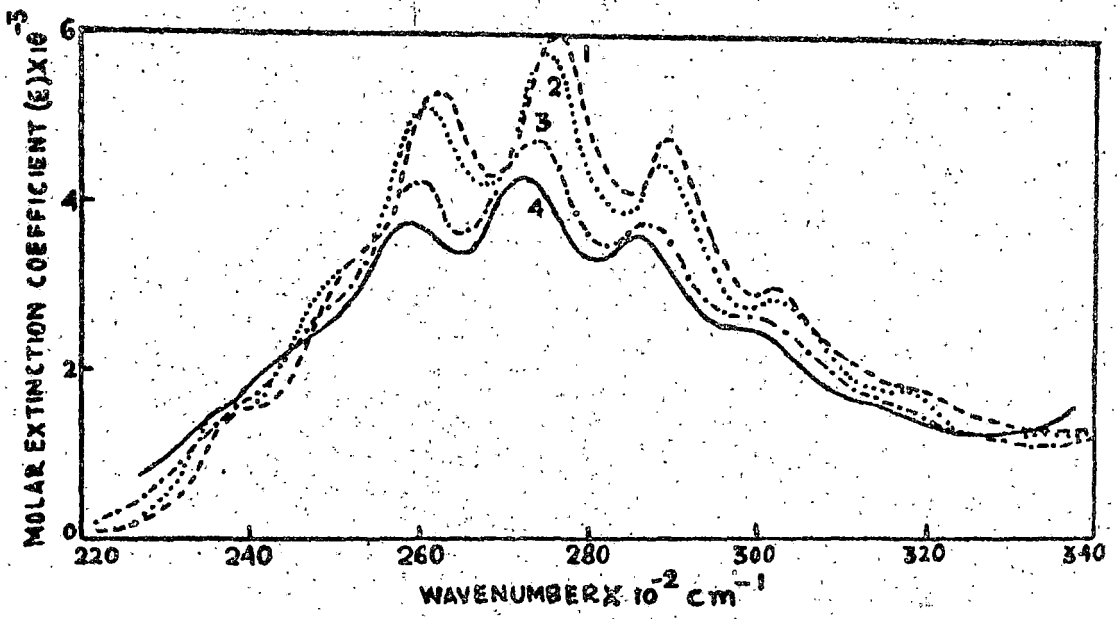

Electronic spectra of 9-nitroanthracene in various nonpolar solvents.

1. n - Hexane;
2. Cyclohexane;
3. Carbontetrachloride;
4. Benzene.

Figure - 2.2

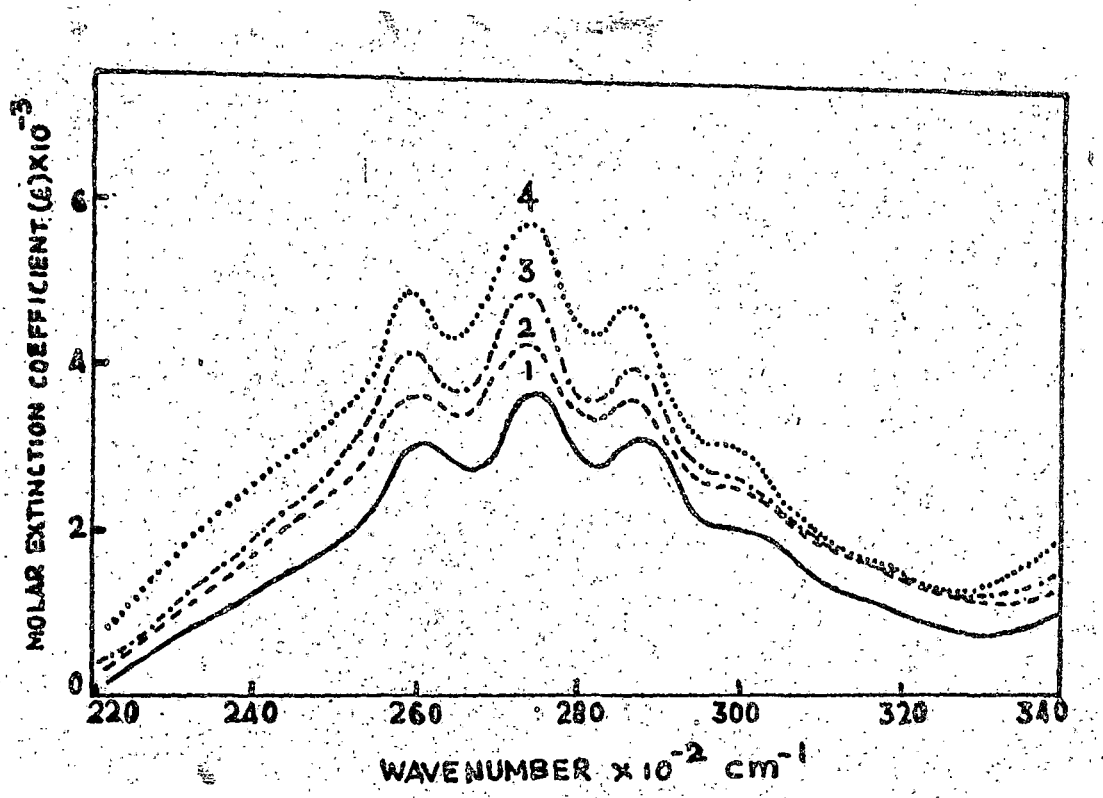

Electronic spectra of 9-nitroanthracene in various polar solvents.

1. Methanol;
2. Tetrahydrofuran;
3. 1, 4 - Dioxane
4. Chloroform.

Figure - 2.3

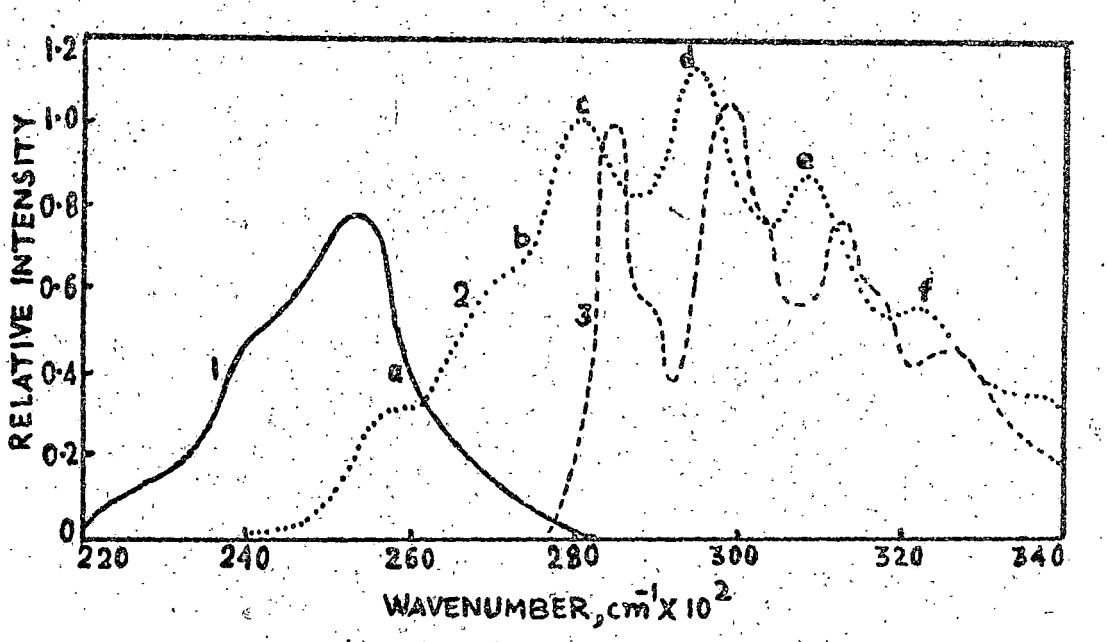

Emission and absorption spectra in Cyclohexane at room-temperature.

1. Emission spectrum of 9-nitroanthracene;
2. Absorption spectrum of 9-nitroanthracene;
3. Absorption spectrum of anthracene.

Table 2.1 Absorption Bands of 9-Nitroanthracene in Various Non-polar Solvents at Room Temperature.

n - Hexane			Cyclohexane		
Wave number cm^{-1}	Intensity	Tentative assignment	Wave-number cm^{-1}	Intensity	Tentative assignment
24150	w	0_1	24000	w	0_1
25200	vw	0_1 + 1050	25000	vw	0_1 + 1050
26250	s	0_2	26075	s	0_2
27625	vs	0_2+1400±25	27475	vs	0_2 + 1400
28000	s	0_2+2x1400 ±25	28000	s	0_2 + 2 x 1400 ± 25
30350	w	0_2+3x1400 ±25	30275	w	0_2 + 3 x 1400 ± 25

Contd. .. 2.

Table - 2.1 (contd.)

Carbon tetrachloride			Benzene		
Wave number cm^{-1}	Intensity	Tentative assignment	Wave-number cm^{-1}	Intensity	Tentative assignment
23900	vw	0_1	23700	vw	0_1
24050	vvw	$0_1 + 1050$	24750	vvw	$0_1 + 1050$
25975	s	0_2	25850	s	0_2
27375	vs	$0_2 + 1400$	27250	vs	$0_2 + 1400$
28750	s	$0_2+2\times1400 \pm 25$	28650	s	$0_2 + 2 \times 1400$
30100	vw	$0_2+3\times1400 \pm 50$	30000	vw	$0_2 + 3 \times 1400 \pm 50$

w, weak; v, very; s, strong

Table - 2.2 Absorption Bands of 9-Nitroanthracene in Various Polar Solvents at Room Temperature.

Methanol			Tetrahydrofuran		
Wave-number cm^{-1}	Intensity	Tentative assign-ment	Wave-number cm^{-1}	Intensity	Tentative assign-ment
Broad and weak absorption in the range 25500cm^{-1} to 22000cm^{-1}			Broad and weak absorption in the range 25300cm^{-1} to 22000cm^{-1}		
25100	s	0_2	25250	s	0_2
27550	vs	0_2 + 1400	27350	vs	0_2 + 1400
28925	s	0_2 + 2 x 1400 $\pm$ 25	28725	s	0_2 + 2 x 1400 $\pm$ 25

Contd.

Table - 2.2 (contd.)

1, 4 - Dioxane			Chloroform		
Wave-number cm^{-1}	Intensity	Tentative assignment	Wave-assign-ment	Intensity	Tentative assignment
Broad and weak absorption in the range 25500 cm^{-1} to 22500 cm^{-1}			Broad and weak absorption in the range 25000 cm^{-1} to 23000 cm^{-1}		
23900	s	O_2	23875	s	O_2
27300	vs	O_2 + 1400	27275	vs	O_2 + 1400
23700	s	O_2 + 2 x 1400	23675	s	O_2 + 2 x 1400

v, very and s, strong.

Table - 2.3 Experimental Oscillator Strength Values and the X - Factors

Solvent	Oscillator strength	(1 + X)	Solvent	Oscillator strength	(1 + X)
Non-polar			Polar		
n - Hexane	0.1231	0.1044	Methyl alcohol	0.0801	0.0674
Cyclohexane	0.1221	0.0981	Tetrahydrofuran	0.1075	0.0866
Carbon-tetrachloride	0.1130	0.0869	1, 4 Dioxane	0.1141	0.0902
Benzene	0.1070	0.0799	Chloroform	0.1341	0.1048

in benzene and naphthalene spectra, the vibrational spacing involving transitions to a ^1L_a state is of the order of 1400 cm^{-1} and in transition to a ^1L_b state it is of the order of 1000 cm^{-1}. The 1400 cm^{-1} vibration is associated with the C - H in-plane bending whereas the 1000 cm^{-1} vibration is the breathing vibration of the ring.

The spectral analysis of NA shows that the separation between the bands in the intense system is about 1400 cm^{-1} which possibly is C - H in-plane bending vibration which forms a progression in the absorption spectra of anthracene solution at room temperature. But the separation between the bands 'b' and 'c' is about 900 cm^{-1} as shown in Fig. 2.3. This observation suggests that 'b' and 'c' belong to two different electronic transitions. The separation between the bands 'a' and 'b' of the lower energy band system is much less than 1400 cm^{-1} and is about 1050 cm^{-1}. It seems that possibly the breathing vibration of the ring forms the progression in the weak low energy band system. We assign this band system to $^1A \longrightarrow {}^1L_b$ transition.

The emission spectrum of NA in cyclohexane is reproduced in Fig. 2.3. A good overlapping between the observed emission and weak low energy absorption spectrum is observed. Contrary to a previous statement[3], thus, 9-nitroanthracene actually is a weakly fluorescent molecule. This observation is interesting

in view of the fact that the luminescence of nitroaromatics is not yet clearly understood. The lowest excited singlet and triplet states of nitroaromatic compounds are usually nearly degenerate and both π-π^* and n - π^* states are present in each molecule. A good overlapping between the lowest energy weak absorption and the emission shows that both initiates from the same states which has a π-π^* character. It has been suggested by Plotnikov[64] that as the size of the aromatic system increases, π-π^* state moves to a level lower than the n-π^* state energy level. Intramolecular CT character of the low energy state is also expected to increase with the size of the polynuclear nitroaromatics. All these considerations may causes an increase in the $^1B_1 \longrightarrow {}^1A_g$ radiative transition probability.

Thus, we conclude that the lowest excited singlet state in H_A is a π-π^* state and that the system having origin at about 23200 cm^{-1} belongs to $^1A \longrightarrow {}^1L_b$ and the other having origin at about 26100 cm^{-1} belongs to $^1A \longrightarrow {}^1L_a$ transition.

3.2 Solvent Effect

3.21 Solvation energy

In polar solvents like methanol, tetrahydrofuran (THF), 1,4 dioxane and chloroform as shown in Fig. 3.3 though $^1A \longrightarrow {}^1L_a$ transition shows a vibrational structure, in $^1A \longrightarrow {}^1L_b$ transition

the vibrational structure is not generally observed. In non-polar solvents like n - hexane, cyclohexane, carbontetrachloride and benzene as shown in Fig. 2.1, the vibrational structure of both $^1A \longrightarrow {}^1L_a$ and $^1A \longrightarrow {}^1L_b$ transitions are observed. However the vibrational structure observed in saturated hydrocarbons is appreciably blurred in the solvents like carbontetrachloride and benzene, possibly due to stronger interaction between the solute and solvent molecules.

The solvent effect on the absorption spectra is known to be due to dispersive interaction, dipolar interaction and in case of polar solvents also due to orientation induction effects[12,38] of the solvent dipole on the solute molecule. In addition, local interaction like bond formation etc. may also affect the transition energy. Quantitative estimation of the absorption energy could be made for $^1A \longrightarrow {}^1L_a$ transition only. For both nonpolar and polar solvents, plots of transition energy against the factor $\left[\frac{(n^2 - 1)}{(n^2 + 2)}\right]$ give good straight lines. The linear plot for the polar solvents is, however, on the lower energy range and has a different slope than that for non-polar solvents as shown in Fig. 4. The linear plot in non-polar solvents indicates that the dispersive interactions predominates over the dipolar interactions. For the $^1A \longrightarrow {}^1L_a$ transition of medium intensity, this possibly further suggests that the change

Figure - 2.4

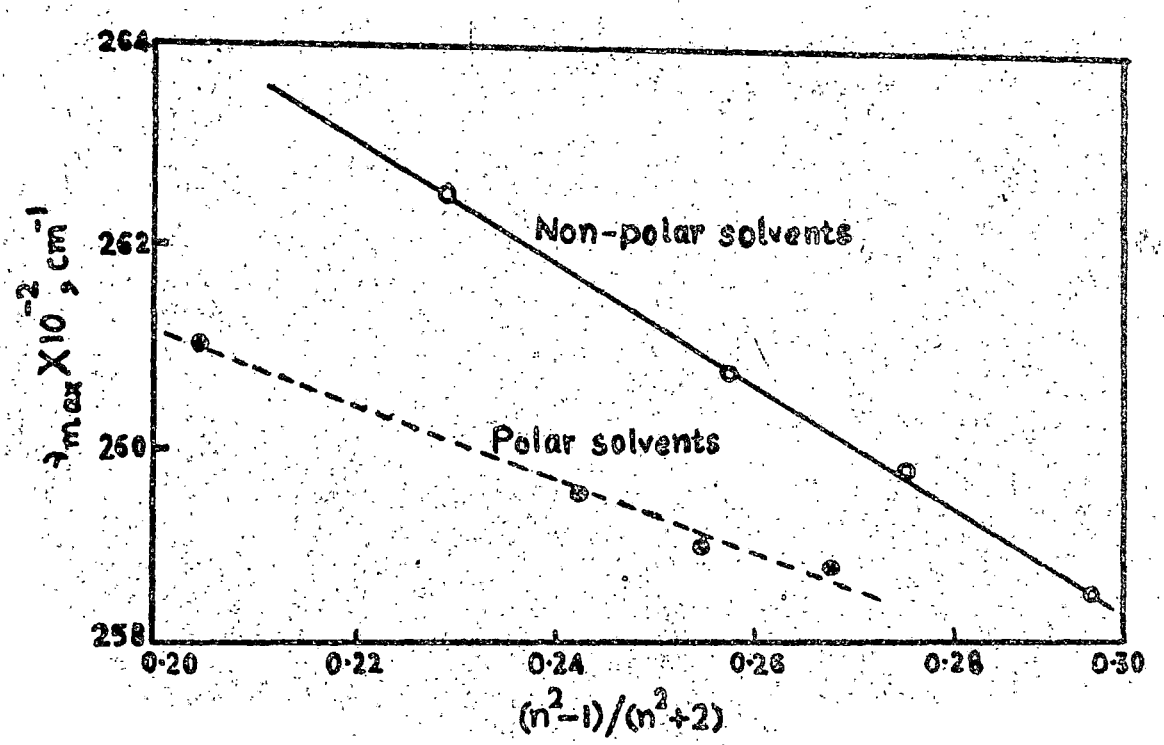

The plot of transition energy of $^1A \longrightarrow {}^1L_a$ band of 9-nitroanthracene against the factor $(n^2 - 1)/ (n^2 + 2)$.

in the dipole moment on excitations is small in this molecule. The linear plot in polar solvents is not easy to rationalise. It possibly indicates that the difference in dipole moment in the excited and ground state is small and also the sum total of orientation - induction effect and local interaction is not much dependent on the solvent refractive index. Small refractive index dependence is, however, present giving a different slope of the linear plot. Indeed, 9-nitroanthracene is expected to have strong local interaction with some polar solvents[63-69].

3.22 Oscillator - Strength (f) :

Theoretical studies on the solvent effect on the f - value of an electronic transition in the solute molecule have been mostly concerned with the local field effect[42,43]. The results are always analysed in terms of local field distributions and distortions of electronic charge distribution by the surroundings. 'Chako's Correction Factor' for the spectral intensity change is not sufficient to explain the observed results. Recently, considering long range dispersive forces to be operative, Abdulnur[51,52] has shown that for the conversion of f - value in solution from the corresponding isolated molecular value, Chako's factor is of minor importance compared to an additional 'DF factor' originating from the intermolecular forces between the solute and the solvent molecules and from the translational

fluctuations between the induced moments.

Our results for the f - values in various solvents can not be explained by Chako's factor ($\frac{1}{\gamma}$) alone. Expanding the KKP factor to include local interactions as well, the experimental oscillator strength in solution f_s can be expressed by an empirical relation :

$$\frac{1}{\gamma}(1 + x)\ f_i = f_s$$

where f_i is the free molecular oscillator strength. We have estimated the values of (1 + X) f_i from the experimentally observed oscillator strengths in solution which are presented in Table 2.3. With the increase of n_2 while in polar solvents the f - value increases, f - value decreases in nonpolar solvents. In case of nonpolar solvents, the dispersive interaction plays a very important role. In going from n - hexane to benzene, the solute solvent dispersive interaction increases. The X - factor increases with the increase of refractive index. Thus, the observed decrease in X - factor indicates a negative value for this factor in nonpolar solvents. In polar solvents the contribution to the X - factor is not only due to dispersive interaction or dipolar interactions but also due to local interactions. Thus, the X - factor in polar solvents will be in the order:

$$X_{\text{benzene}} > X_{\text{THF}} > X_{\text{dioxane}} > X_{\text{chloroform}}$$

The experimentally observed f - values increase in the same order indicating a positive value for the K - factor.

4. Conclusions

The ^1L_b band, which is hidden under the intense ^1L_a band in anthracene, seperates out in 9-nitroanthracene owing to the nitrogroup substitutional perturbation. The molecule (NA) is observed to fluoresce very weakly. The solvent effect on the electronic spectra has been explained interms of the predominant dispersive and other local interactions. Intermolecular forces between the solute and solvent molecules are found to be important.

CHAPTER - 3

ELECTRONIC SPECTRA OF 2 - NITROFLUORENE ; SOLVENT EFFECT ON $^1A \longrightarrow {}^1L_a$ TRANSITION.

1. Introduction

In the near UV region, fluorene shows two electronic band systems: one of low intensity at 300 nm is due to the $^1A \longrightarrow {}^1L_b$ transition and the other which is intense appearing at 260 nm is due to the $^1A \longrightarrow {}^1L_a$ transition. According to Platt[70], ^1L_b band is short axis polarised and ^1L_a is long axis polarised. On the other hand, Zvarich[71] concluded, from his polarisation studies of the electronic absorption and the fluorescence spectrum of oriented single crystal that the 300 nm band is long axis polarised.

Substitution of various groups are known to influence the electronic spectra of the parent molecule. The perturbation caused by strong mesomeric substituents is very strong. The complications may arise due to the presence of nonbonding electrons. Appearance of n -π^* and intramolecular CT bands, some times, make the assignment of the observed bands difficult. Thus, the substitution of nitro group at position 2 on fluorene molecule is expected to show a strong perturbation on the long axis polarised transition. The luminescence properties of 2 - nitrofluorene has

been investigated by Roy and Becker[10] Khalil et. al[3] and Nagakura et. al.[9]

In this chapter, we present our results on the investigations of the electronic spectra of 2 - nitrofluorene under various conditions and confirm that the ^1L_a band of fluorene is a long axis polarised band. Further, the assignment of the bands and the solvent effect on the electronic absorption spectra of this molecule have also been presented.

2. Experimental

The compound 2-nitrofluorene (NF) from 'Eastman Organic Chemicals' was recrystallised several times from purified ethanol. Solvents of spectrograde quality were used.

Zone-refined biphenyl was used as a host for the mixed crystal spectra. Crystals were grown from the melt with guest concentrations of about 10^{-2}M by slowly lowering the temperature.

The spectra were recorded at room temperature (25°C) on a Spectromom - 202 spectrophotometer.

3. Results and Discussions

3.1 Spectra and Assignment

In Fig. 3.1, the absorption spectra of fluorene and NF in

methanol solution are reproduced. A close examination of the figure reveals that the $^1A \longrightarrow {}^1L_a$ band (33400 cm^{-1}) of fluorene very much resembles the intense band system of NF. But the other band system corresponding to $^1A \longrightarrow {}^1L_b$ band of fluorene is not observed in NF. It seems that as a result of strong nitro group perturbation, the ^1L_a band experiences a larger red shift than ^1L_b band, which appears to be hidden under the intense ^1L_a band. At this point, it may be noted that NO_2 - substitution at second position of the fluorene ring system imparts a strong dipole moment along the C - N bond direction which interacts with the long axis transition dipole moment more strongly than with the short axis transition dipole and thereby perturbs the long axis transition much more. This confirms that 260 nm band of fluorene is a long - axis one but does not confirm that the 300 nm band is a short-axis transition because the oscillator strength value for this transition is one order of magnitude lower than that for the 260 nm band.

Due to the presence of nitro group, as one observes in nitrobenzene[15], in addition to ^1L_a, ^1L_b bands, intramolecular CT and also $^1n\,\pi^*$ transitions may appear in NF.

The electronic absorption spectra of the compound in n-hexane are reproduced in Fig. 3.2. The ν_{max} position of the intense band

FIGURE 3.1

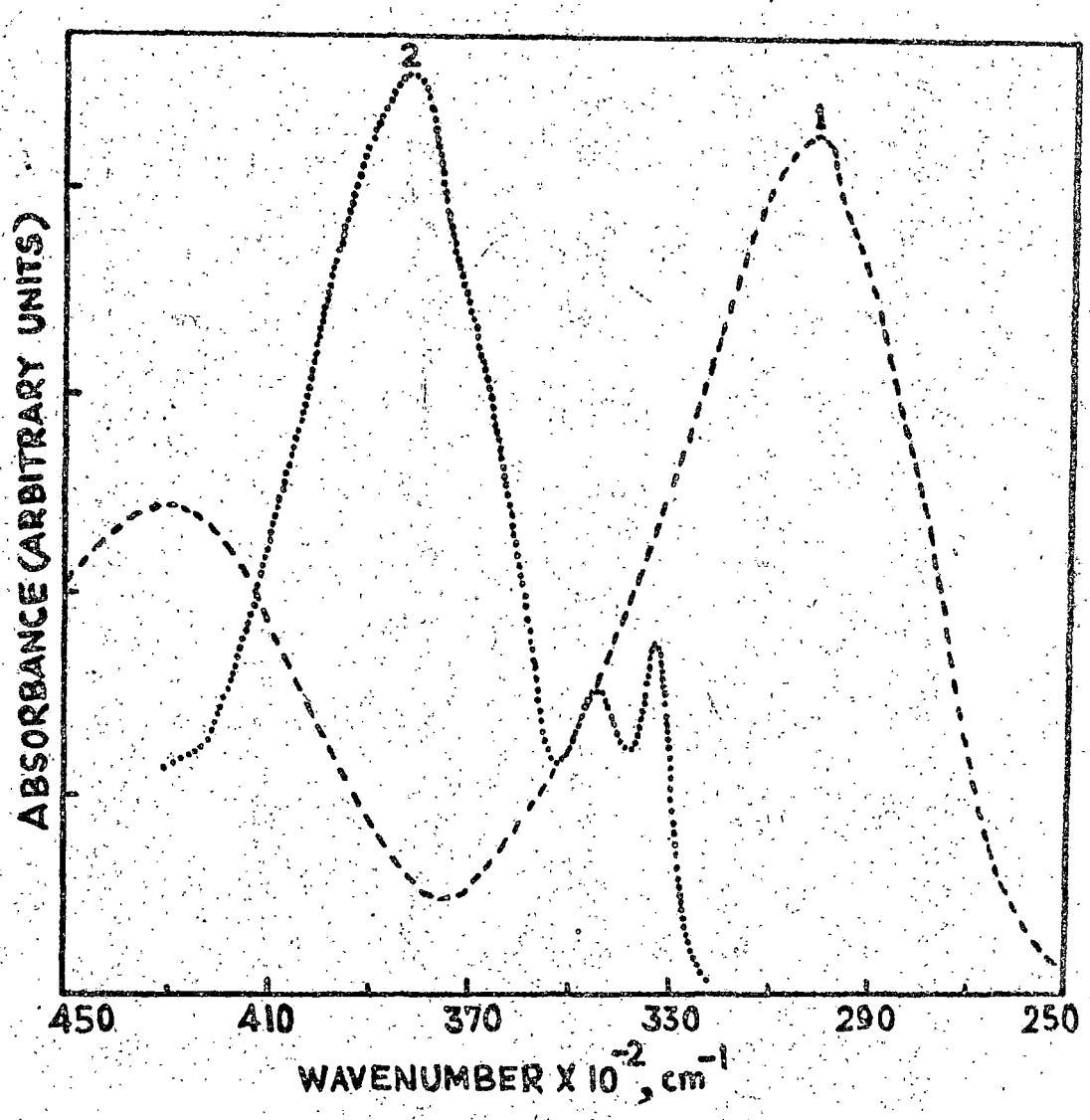

Electronic absorption spectra of 2-nitrofluorene (1) and fluorene (2).

FIGURE 3.2

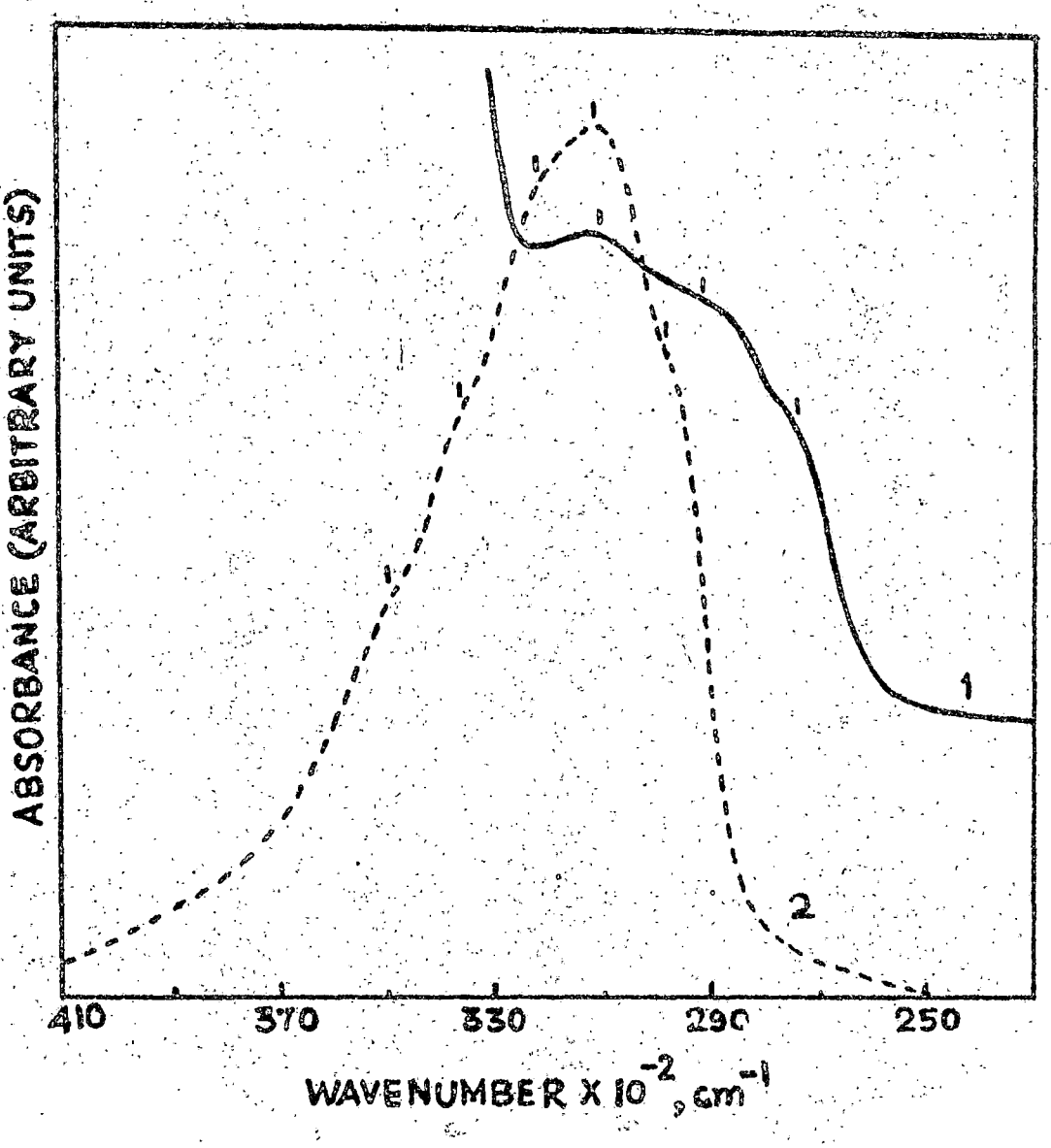

Electronic absorption spectra of 2-nitrofluorene :

(1) : 2-nitrofluorene guest-biphenyl host mixed crystal

(2) : solution spectrum in n- hexane.

in different solvents and the results of the spectral analysis (in n - hexane and mixed crystal) are summarised in Table 3.1. An intense band is observed at about 31175 cm^{-1} with a very blurred fine structure. The spectral analysis shows that the spacing between the bands in n - hexane is approximately 1275 cm^{-1} which is possibly the vibrational structure of the $^1A \longrightarrow {}^1L_a$ band. No indication as to the presence of $^1A \longrightarrow {}^1L_b$, CT and $^1n\pi^*$ bands could be observed. Investigations with other polar and non polar solvents failed to reveal these bands. We have, therefore, studied the spectra of HP in solid state using biphenyl as matrix. The mixed crystal spectrum is also included in Fig. 3.2. The spacing between the bands is of the order of 1800 cm^{-1} which is much larger than 1275 cm^{-1}, the progression - forming vibrational frequency of the molecule. This suggests that these three bands observed in the mixed crystal are three different electronic band systems.

It seems that the weak ^1L_b band appears in the mixed crystal spectra as a result of guest host interaction. It is expected that this interaction is larger for intense $^1A \longrightarrow {}^1L_a$ transition causing more red shift than weak $^1A \longrightarrow {}^1L_b$ transition. The third longest wave length band in the mixed crystal might be either ^1CT or $^1n\pi^*$ transition. But usually the $^1n\ \pi^*$ transitions appear[15] at much longer wavelengths, it is more probable for the longest wave length

TABLE 3.1

Table - 3.1 Spectral Analysis Of The Electronic Spectrum Of 2 - Nitrofluorene.

n - Hexane		Mixed Crystal	
Wavenumber cm^{-1}	Assignment	Wavenumber cm^{-1}	Assignment
29850 (h)	0_2	27397 (msb)	0_1
31175 (ve)	0_2 + 1275 ± 25		
32253 (h)	0_2+ 2 x 1275± 50	29154 (msb)	0_2
33670 (h)	0_2+ 3 x 1275± 50		
34965 (h)	0_2+ 4 x 1275± 50	31055 (msb)	0_3

V, very; m, medium; s, strong; h, hump and b, band

mixed crystal band to be the intramolecular CT band.

The fluorescence from this nitro-aromatic could not be detected in any of the solvents used. This possibly suggests that the n π^* transition is the lowest energy singlet-singlet transition in this molecule and is forbidden. The nonradiative decay route from this state to the ground state must be very efficient.

3.2 Solvent Effect

The effect of various solvents has been investigated in the $^1A \longrightarrow {}^1L_a$ band of 2 - nitrofluorene. The non-polar solvents n - hexane, cyclohexane, benzene and carbontetrachloride and polar solvents methanol, ethanol, iso-propanol, tert-butanol, 1, 4 dioxane, tetrahydrofuran (THF), acetone, chloroform and water have been used.

The weak vibrational structure could not be observed in other solvents. In none of the solvents, ^1L_b band system could be seperated out from the intense band and the band maxima gives the ν_{max} for $^1A \longrightarrow {}^1L_a$ transition.

The solvent effect on the absorption spectra is known to be due to dipolar, dispersive and orientation-induction effects[12,36]. In addition, a weak bond formation between the solute and solvent also contribute to the spectral shift. Evidently, μ_g and μ_e are

important as they determine the stabilisation of ground and excited states as a result of dipolar interaction.

For non-polar solvents, the plot of transition energy against the factor f (n) i.e. ($n^2 - 1$)/ ($n^2 + 2$) gives a straight line as shown in Fig. 3.3. Assuming that the solute dipole solvent induced dipole interaction is weak and any significant local interaction is absent, the predominant interaction in these non-polar solvents is the dispersive interaction. This is in confirmity with our experimental observation of bathocromic shift with the increase in n - value and the linear plot of Fig. 3.3.

The electronic absorption spectra of NF in n - hexane solution is increasingly red shifted as the polarity of the solvents is increased. This red shift can be explained by the increase in μ_e which is responsible for the lowering of the excited state energy from the Franck Condon state to the equilibrium state of the solute molecule. The reorientation of the solvent dipoles is also taking place in the solvation shell during the excited state life time. Thus, the extent to which the spectrum is red shifted depends upon the polarity of the solvent used. However, the examination of Table 3.2 shows that the polar solvents can be classified into two groups according to the magnitude of the shift. In 1, 4 - dioxane, THF, $CHCl_3$ and acetone, the red shift is more than in

FIGURE 3.3

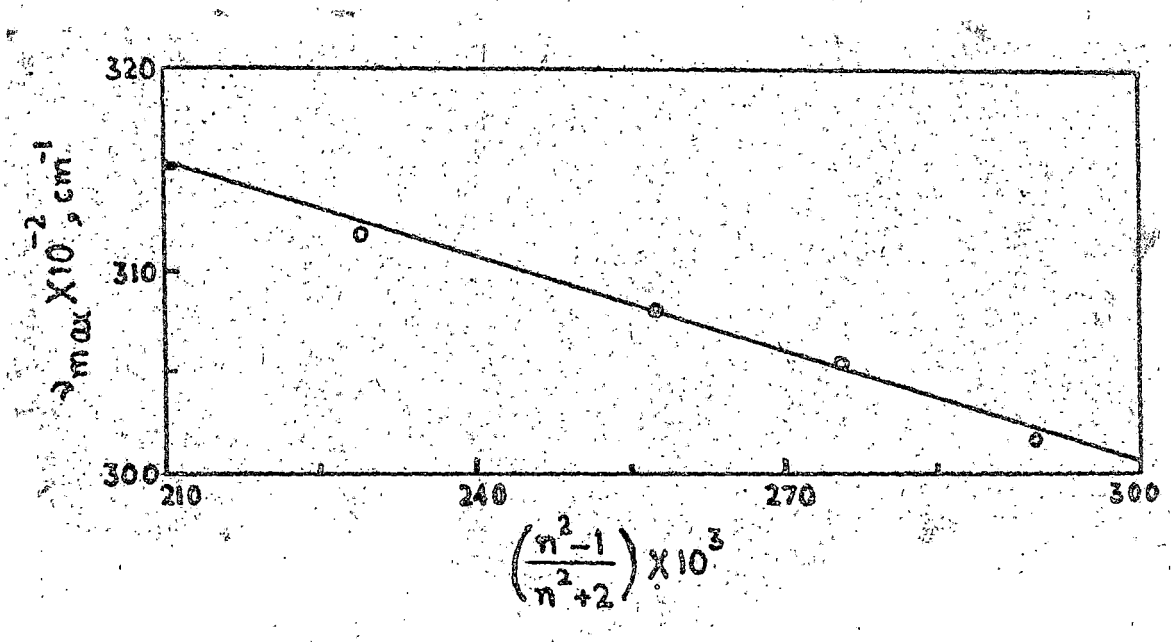

The plot of transition energy of $^1A \rightarrow {}^1L_a$ band of 2-nitrofluorene against the factor $(n^2 - 1) / (n^2 + 2)$.

TABLE 3.2

Table - 3.2 Solvent Effect on $^1A \longrightarrow {}^1L_a$ Transition of 2 - Nitrofluorene.

Solvent	$\nu_{max}(cm^{-1})$
n - Hexane	31176
Cyclohexane	30800
Carbontetrachloride	30525
Benzene	30150
Methanol	30225
Ethanol	30303
Iso-Propanol	30395
tert-Butanol	30441
1, 4 dioxane	30300
THF	30050
$CH\ Cl_3$	29950
Acetone	29850
Water*	23650

* Very sparingly soluble - hot solution

alcohols for equivalent molecular dipole moment values. This is expected in view of the fact that in the above mentioned nonalcoholic polar solvents the solvent absorption band is close to NF band. The results in alcohols and water are different are attributable to the hydrogen bonding and to the resultant erroneous values of the local fields in the solute solvent systems.

Oscillator strength and K - factor[72] calculations for $^1A \rightarrow {}^1L_a$ transition in various solvents could not be made because of the superimposition of other transitions on this intense band.

4. Conclusions

The nitro-group perturbation on position 2 of fluorene molecule confirms that the ^1L_a is long axis polarised. In a mixed crystal spectra three band systems have been observed whereas in solution only the intense ^1L_a band could be observed. The solvent effect on $^1A \longrightarrow {}^1L_a$ transition energy has also been investigated in various polar and nonpolar solvents.

CHAPTER - 4

ELECTRONIC ABSORPTION AND EMISSION SPECTRA OF 1, 4-DINITRONAPHTHALENE

1. Introduction

The electronic absorption and emission spectra of nitroaromatic compounds are of considerable interest and indeed significant amount of work has already been reported[1-16] on some nitroaromatic compounds though clear understanding is still to be achieved. The interest mainly lies in intramolecular charge transfer (CT) band characteristic of the electron donor - acceptor interaction involving the aryl moiety and the nitro group. In addition, the nonbonding electron of the nitro group giving a set of the $n-\pi^*$ states and their interaction with the close lying $\pi-\pi^*$ states affect the radiative and nonradiative processes of the lowest excited states in the nitroaromatic molecules. In Chapter - 2 we have investigated the electronic spectra of 9-nitroanthracene with the aromatic residue comparatively large thus giving the lowest excited states of both singlet and triplet manifold a dominantly $\pi-\pi^*$ character contrary to that observed in nitrobenzene with small aryl moiety[8]. Investigations on the spectroscopic properties of nitronaphthalenes are interesting in view of the fact that the size of the aromatic residue in these molecules is intermediate between that in nitrobenzenes and nitroanthracenes. The electronic spectral properties of 1,4-dinitro-

naphthalene is not well understood. The assignment of lowest triplet state as $^3n\text{-}\pi^*$ by Becker et al[10] is quite doubtful[3]. So, we have investigated the electronic absorption and emission spectra of 1,4-dinitronaphthalene in order to assign low-lying electronic states and to study luminescence characteristics of this molecule. In this chapter, we present our results.

2. Experimental

The compound 1,4-dinitronaphthalene from Eastman Organic Chemicals was recrystallised several times from purified methanol. Solvents used were of spectrograde quality. The absorption spectra in various solvents were recorded at room temperature 298° K on a Shimadzu 210 A spectrophotometer. Emission spectra were recorded on a Perkin Elmer MPF 44A spectrofluorimeter at 77°K. Phosphorescence was isolated by a rotating can phosphorescope. Phosphorescence life time was measured using a HCIL CS 769 oscilloscope display. The emission of the protonated species was studied in a mixture of sulfuric acid with ethanol/methanol (1:1 by volume). Precaution was taken to ensure that no chemical reaction occured in the acid media. The criterion in this regard was that the spectra of the acid solution obtained immediately upon mixing did not there after change in time.

3. Results and Discussions

3.1 Absorption Spectra

The absorption spectrum of 1,4-dinitronaphthalene in methanol at room temperature is shown in Fig. 4.1. In the UV - Vis region, three broad bands with λ_{max} at about 213 nm, 240 nm and 337 nm in decreasing order of intensity are observed. This absorption spectrum is similar to that of 1,5-dinitronaphthalene[1] except that the bands are red shifted in this polar 1,4-dinitronaphthalene molecule. Absorption spectrum of naphthalene in methanol is also shown in Fig. 4.1 for comparison. The absorption spectrum of 1,4-dinitronaphthalene differs considerably from that of naphthalene. Here, we confine our discussion to the low lying states i.e. the broad band in the spectral region 320 nm - 380 nm only. In H_2SO_4 mixture in methanol the broad band is seen to consist of two distinct bands with λ_{max} at 337 nm (Band II) and at 380 nm (Band I) respectively. λ_{max} for the two bands could be easily located for the polar solvents though in nonpolar solvents the significant overlap of the two bands impaired λ_{max} location for the low energy band I. In Table 4.1, solvent effect on the λ_{max} of the two bands is shown. It is observed that the λ_{max} of the low energy band shows a large red shift with solvent polarity and in acidic media this band is almost completely seperated from the high energy band II. This means that the upper state responsible for this band is extremely polar.

FIGURE 4.1.

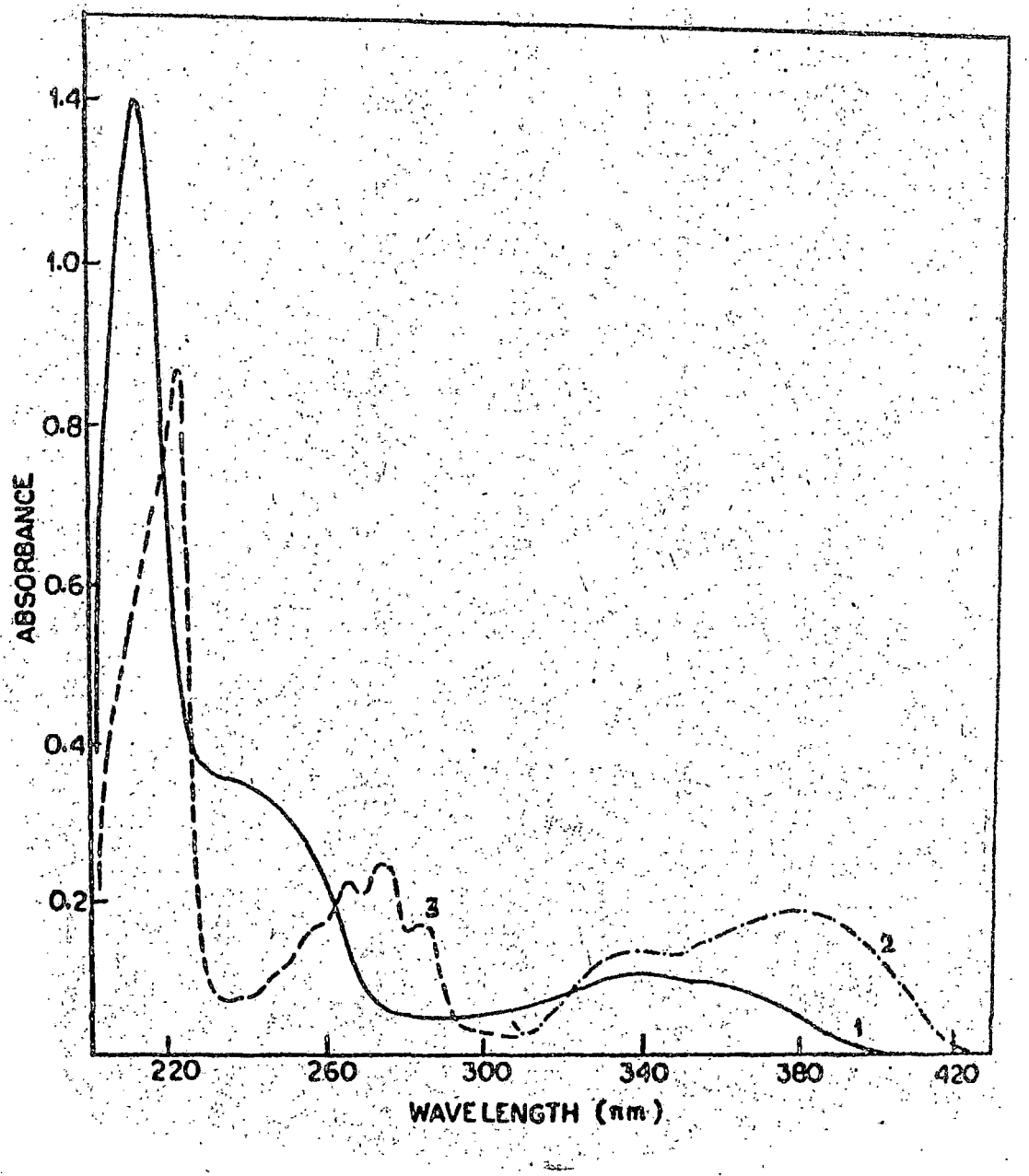

Fig. 4.1 : Electronic absorption spectra of 1,4-dinitronaphthalene at 298°K.

1. Methanol; 2. Acidic ethanol. (Naphthalene in methanol (3) is also shown for comparision)

Table 4.1

Solvent effect on band I and II of 1,4-Dinitronaphthalene.

Solvent	Band I.	Band II
n - Hexane	28409	29705
n - Heptane	28392	29690
Cyclohexane	28328	29650
Methylcyclohexane	28328	29650
Benzene	28089	29240
1,4 Dioxane	28050	29450
Tetrahydrofuran	27920	29660
Ethanol	27855	29720
Methanol	27894	29736
Ethyl acetate	27548	29710
Methanol + 100% H_2SO_4	26315	29720

Band II, on the other hand, shows a little red shift with solvent refractive index (n). These results suggest that Band I is a predominantly CT band where as Band II corresponds mostly to the localised naphthalene ^1L_b band. We, thus, assign band I and band II as ($S_o \rightarrow {}^1CT$) and ($S_o \rightarrow {}^1\pi\text{-}\pi^*$) respectively. Kojima, Tanaka and Nagakura[1] attributed the broad low energy band (corresponding to our band I and band II) of 1,5-dinitronaphthalene to two overlapping bands, the low energy one corresponding mainly to the ^1L_a of naphthalene mixed to some extent with naphthalene ^1L_b and the ^1CT transition. The high energy band includes the above mentioned three transitions in almost equal proportion. This is appreciably different from what our results of 1,4-dinitronaphthalene as discussed above suggest.

The effect of various solvents on band I and II has been investigated. The nonpolar solvents n - hexane, n - heptane, cyclohexane, methylcyclohexane carbontetrachloride, benzene and polar solvents 1,4-dioxane, tetrahydrofuran, chloroform, ethanol, methanol and ethylacetate have been used.

The solvent effect on the absorption spectrum of a solute molecule is known to be due to dipolar interaction, dispersive interaction and also due to orientation induction effect of the solvent dipoles on the solute molecules[36,12]. Evidently the dipole-moment in the ground (μ_g) and in the excited state (μ_e) are important as they determine the stabilisation of the ground and the excited states as a result of dipolar interaction. In addition

a field developed by the local interaction like weak bond formation between the solute and the solvent molecules also attribute to the spectral shift. It is interesting to note that both for polar and non polar solvents plot of transition energy ν_{max} against a factor f (n) i.e. ($n^2 - 1$)/($n^2 + 2$) for band II give good straight line (Fig. 4.2). This indicates that here the dispersive interaction predominates over the dipolar interaction. For the polar molecule 1,4-dinitronaphthalene, this further suggests that the change in the dipolemoment on excitation to the state responsible for this band is small. In some solvents like dioxane, chloroform, carbontetrachloride and benzene, the plot ν_{max} against f (n) for band II though show linearity, form a different straight line and with larger slope than that for other solvents. This possibly is due to these solvents having electronic absorption band close to band II of 1,4-dinitronaphthalene. For band I, such linearity for ν_{max} vs. f (n) plot could not be obtained and this indeed is what one can expect for a highly polar excited state for a CT band where dipolar interactions predominates.

3.2 Emission and Excitation Spectra

The emission spectra of 1,4-dinitronaphthalene in nonprotic and protic solvents at 77°K are shown in Fig. 4.3. The spectral range 360 nm to 475 nm has been recorded without and rest upto 750 nm with a phosphorescence chopper. The phosphorescence spectrum consists of

FIGURE 4.2

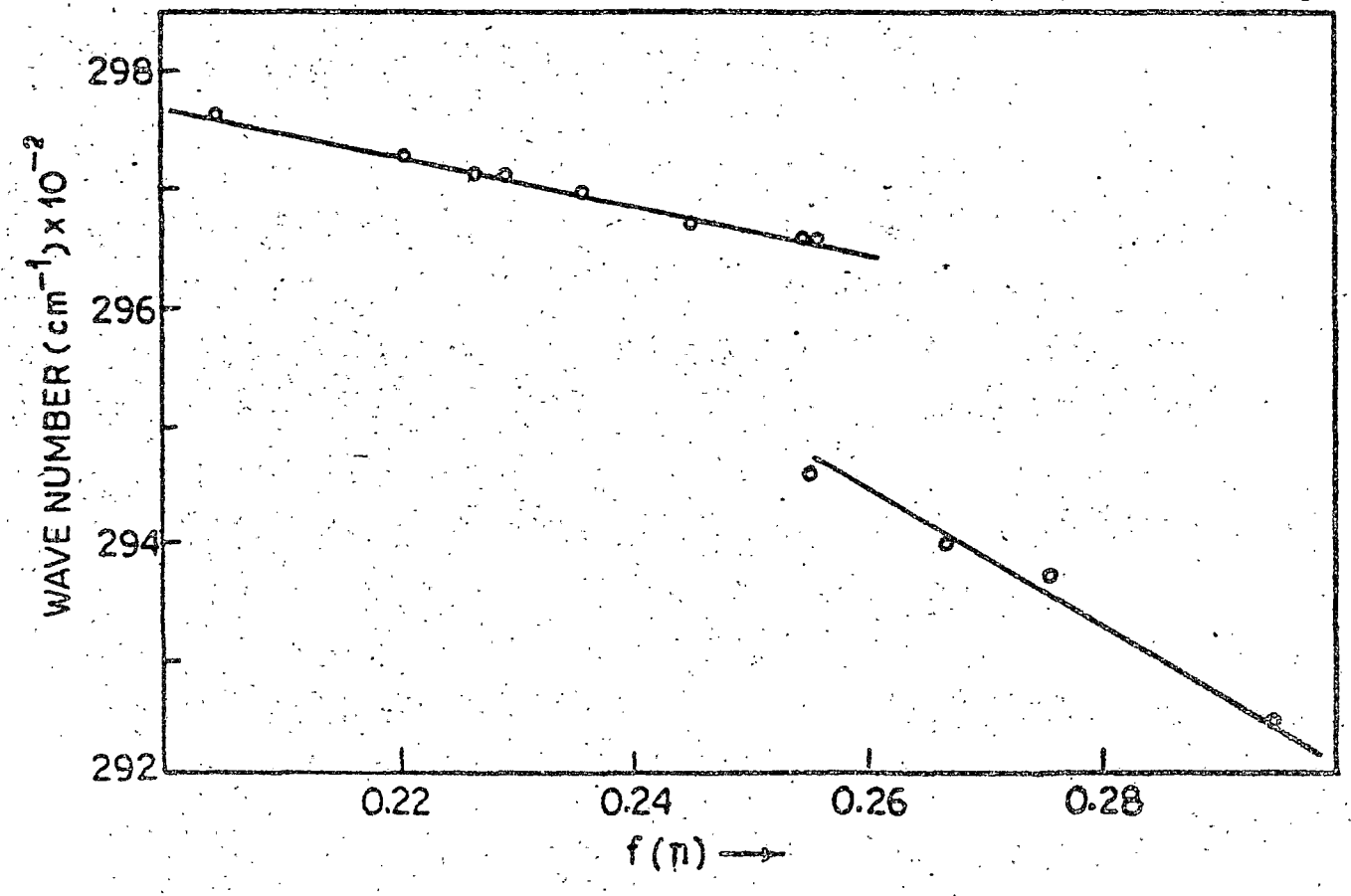

Fig. 4.2 : The plot of transition energy of band II of 1,4-dinitronaphthalene against the function f (n) = ($n^2 - 1$)/ ($n^2 + 2$).

FIGURE 4.3

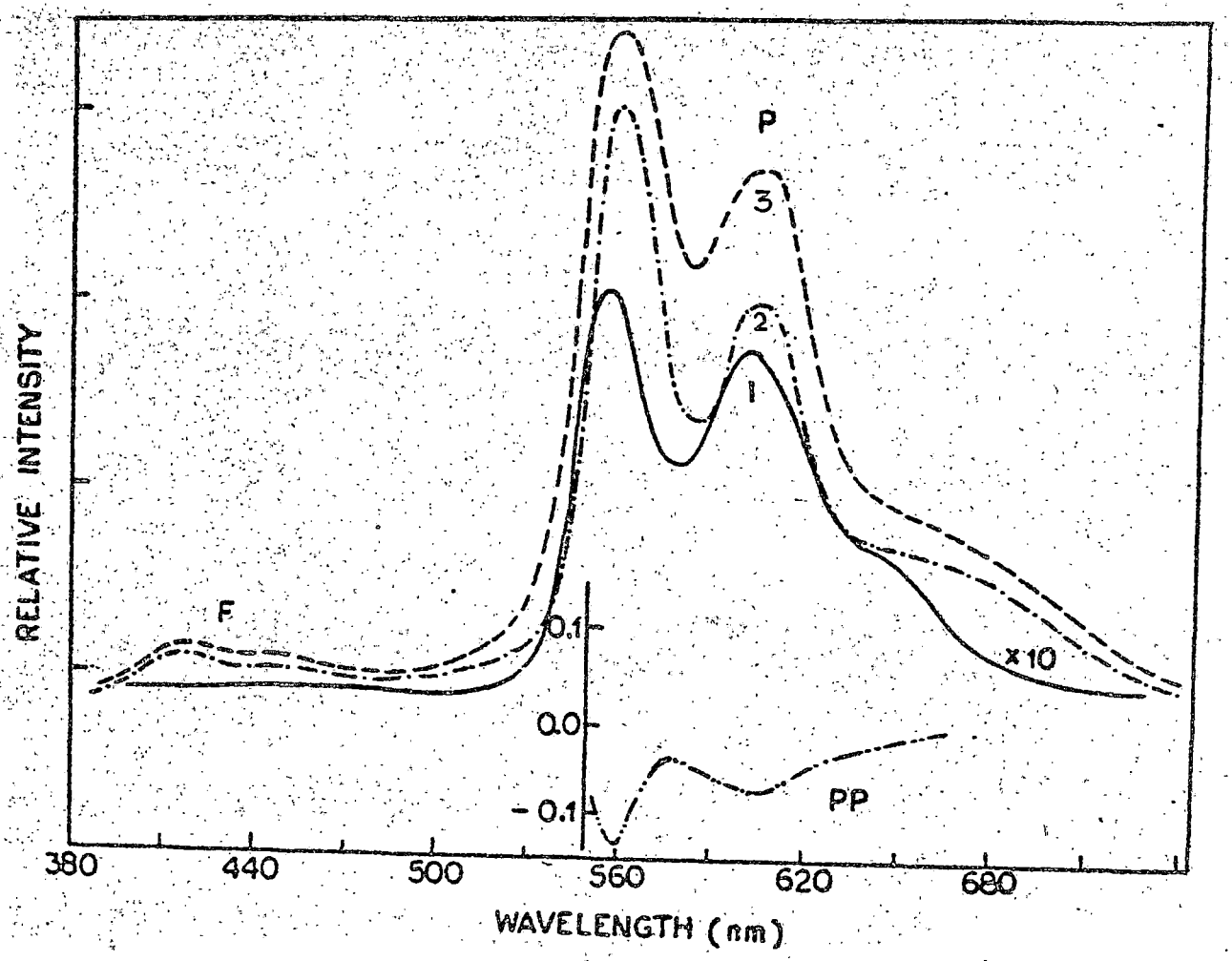

Fig. 4.3 : Emission spectra of 1,4-dinitronaphthalene at 77°K (F - Fluorescence, P - Phosphorescence, PP - Phosphorescence polarisation curve; spectra, 475 nm onwards, are recorded using a phosphorescence chopper) 1. Methylcyclohexane; 2. Ethanol; 3. Acidic ethanol.

three broad bands with the 0 - 0 band at 19050 cm^{-1}, 17955 cm^{-1} and at 17950 cm^{-1} in methylcyclohexane (MCH), ethanol and in acidic ethanol i.e. in H_2SO_4 in ethanol mixture respectively thus showing a red shift in protic solvents. The band positions and a tentative vibrational assignment of the phosphorescence spectrum is shown in Table 4.2. In methylcyclohexane glass at 77°K, the phosphorescence is very weak and no fluorescence is observed even with maximum sensitivity of the fluorimeter indicating a quantum yield $\Phi_F < 10^{-5}$. We estimate the phosphorescence quantum yield in methylcyclohexane $\Phi_P \simeq 10^{-2}$. In protic solvents the phosphorescence intensity is enhanced and in addition weak fluorescence appears in the 400 nm-475 nm region. This behaviour of 1,4-dinitronaphthalene (DNN) molecule is similar to that observed in many polycyclic monoazines such as quinoline, isoquinoline and acridine. However, in monoazines, the triplet quantum yield is small (0.2 for quinoline, 0.3 for isoquinoline[73]) whereas in nitronaphthalenes large triplet quantum yield has generally been observed (0.63 for 1-nitronaphthalene and 0.83 for 2-nitronaphthalene[6,2]). Unfortunately we have not been able to measure the triplet yield for 1,4-dinitronaphthalene molecule and to see if it is really large.

The phosphorescence polarisation has been measured in ethanol glass at 77°K with 337 nm excitation. This is also shown in Fig. 4.3. On $^1\pi-\pi^*$ excitation, the polarisation degree is negative throughout the whole spectral range and the phosphorescence origin has a negative

Table 4.2

Phosphorescence bands of 1,4-dinitronaphthalene in various glasses at 77K.

Solvent	Band Position (cm^{-1})	Tentative Assignment
Methylcyclohexane	18050	(0, 0)
	16695	0 + 1355
	15380	0 + 2 x 1355 ± 40
Ethanol	17955	(0, 0)
	16610	0 + 1355 ± 10
	15265	0 + 2 x 1355 ± 20
Ethanol + 100% H_2SO_4	17950	(0, 0)
	16610	0 + 1355 ± 15
	15270	0 + 2 x 1355 ± 30

value 0.13. From the solvent behaviour and from the negative polarisation on $^1\pi$-π^* excitation we assign the lowest triplet state as a $^3\pi$-π^* state. This conclusion differs from that of Roy and Becker[10] who assigned the lowest triplet state as ^3n-π^* state. As has been pointed out by Khalil, Beck and McGlynn[3], their result is quite ambiguous possibly because of the low probability associated with the excitation into the very weak, poorly resolved ^1n-π^* region. The phosphorescence polarisation of 1 - nitro 4 - methyl naphthalene has been investigated by Krishna et.al.[75], and $^3\pi$-π^* has been shown to be the lowest triplet state. Indeed the structure of the phosphorescence spectrum of the 1,4-dinitronaphthalene molecule is naphthalonic.

Now, it is quite likely that the next higher triplet state might be the ^3n-π^* state. If it is so, then owing to the "proximity effect"[74], vibronic interaction between the close-lying triplet states would be important and the radiative and nonradiative decay processes must be affected. A low value of phosphorescence quantum yield can reasonably be attributed as an immediate consequence of it. We have also measured the phosphorescence life time monitoring the decay of both the 557 nm and 602 nm peaks. The mean phosphorescence life time in ethanol glass is 10 ms. This value is significantly less than that of naphthalene which is 2 sec. It has been shown by Lim[74] that a close-lying ^3n-π^* state can shorten the $^3\pi$-$\pi^* \rightarrow S_0$ phosphorescence life times significantly due to the vibronic interaction between ^3n-π^* and $^3\pi$-π^* states.

The position of the CT state, among others, determine the rate of intersystem crossing (ISC) in nitroaromatics[9]. ^{1}CT state in 1-nitronaphthalene has been shown to be at higher energy than the lowest singlet state which is $^1\eta$-π^* state and the initial state of ISC is $^1\eta$-π^* where as the final state is $^3\pi$-π^*. From our absorption spectra, we have observed the state with predominantly CT character at 360 nm range and we have not observed any $^1\eta$-π^* state though in nitroaromatic molecules $^1\eta$-π^* is accepted as the lowest singlet state[3,8]. The weak fluorescence emission we have observed in protic solvents originates at about 395 nm where no absorption band is observed and which quite on the red side of the lowest absorption band I (^{1}CT $\longleftarrow$ S_o) observed. It is quite likely that the $^1\eta$-π^* state is located in this spectral region and the observed fluorescence is due to $^1\eta\pi^* \rightarrow S_o$ transition.

To determine the initial state of ISC, we have studied the Phosphorescence excitation spectra in protic and nonprotic solvents. This is shown in Fig. 4.4. It is interesting to note that in methylcyclohexane, the excitation spectrum is a broad band with λ_{max} at about 354 nm i.e. the CT band we have observed in absorption. In protic solvents, however the excitation spectrum looks complex and in addition to the broad band some overlapping relatively sharp bands with the origin at 395 nm are observed. These results show that in nonprotic solvents, the initial state of ISC is ^{1}CT state whereas in protic solvents another state with the origin at 395 nm, which we

FIGURE 4.4

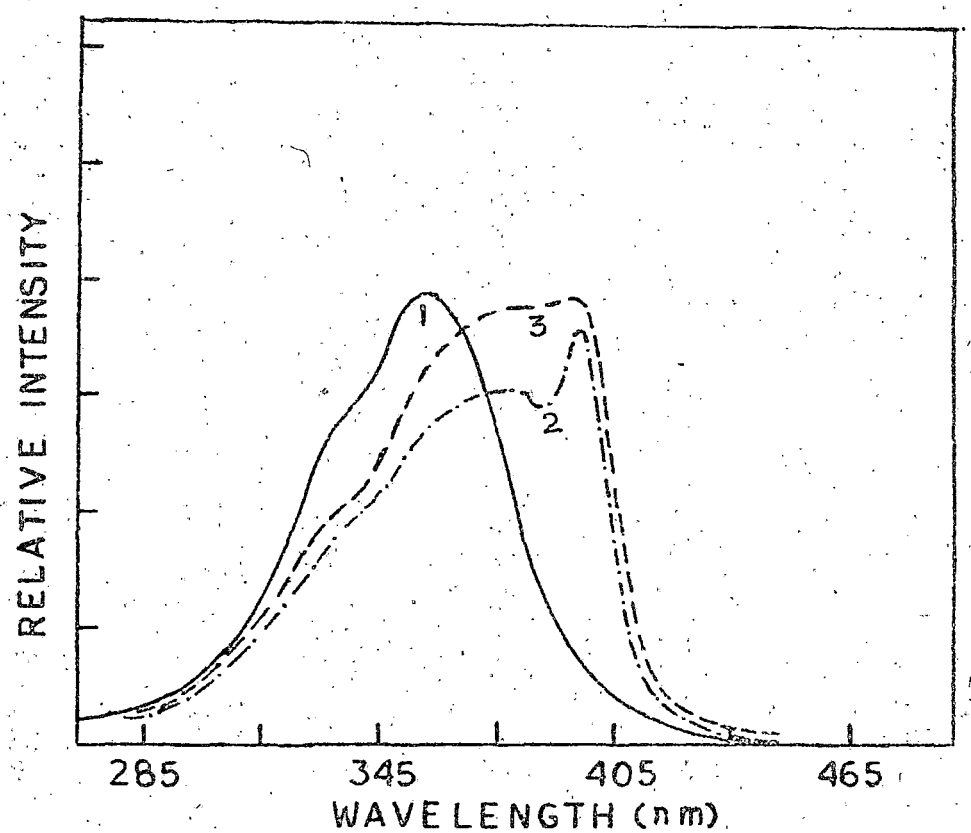

Phosphorescence excitation spectra of 1,4-dinitronaphthalene at 77°K.

1. Methylcyclohexane;
2. Ethanol;
3. Acidic ethanol.

think is the $^1n-\pi^*$ state, is principally the initial state for ISC though some amount of energy is also transferred from the ^1CT state. Thus, we conclude that the leveling scheme for the low lying states in 1,4-dinitronaphthalene molecule is

$$S(S_0) < E(^3\pi-\pi^*) < E(^3n-\pi^*) < E(^1n-\pi^*) < E(^1CT) < E(^1\pi-\pi^*)$$

Now the questions naturally arise why firstly in MCH the initial state of ISC is ^1CT and not the $^1n-\pi^*$ state and secondly no fluorescence from there. Seperation between the ^1CT and $^1n-\pi^*$ is more in nonprotic solvents than in protic solvents and as such the nonradiative decay route $^1n-\pi^* \rightsquigarrow S_0$ due to 'proximity effect' in hydrocarbon solvents is expected to be less efficient. This suggests that there is some other decay route from the $^1n-\pi^*$ state.

We have recorded the total luminescence spectra in various solvents without the phosphoroscope. The luminescence spectra in ethanol and in MCH glass (77^0K) are shown in Fig. 4.6. In ethanol, usual phosphorescence bands as shown in Fig. 4.3 are observed. In MCH, however, an intense broad band with λ_{max} at about 540 nm is obsorved along with the phosphorescence bands appearing very weak in the tail of the spectrum. As the concentration of DNN decreases, the intensity of the broad band decreases and at 10^{-7} M this band does not appear. We have looked into the temperature dependence of this broad

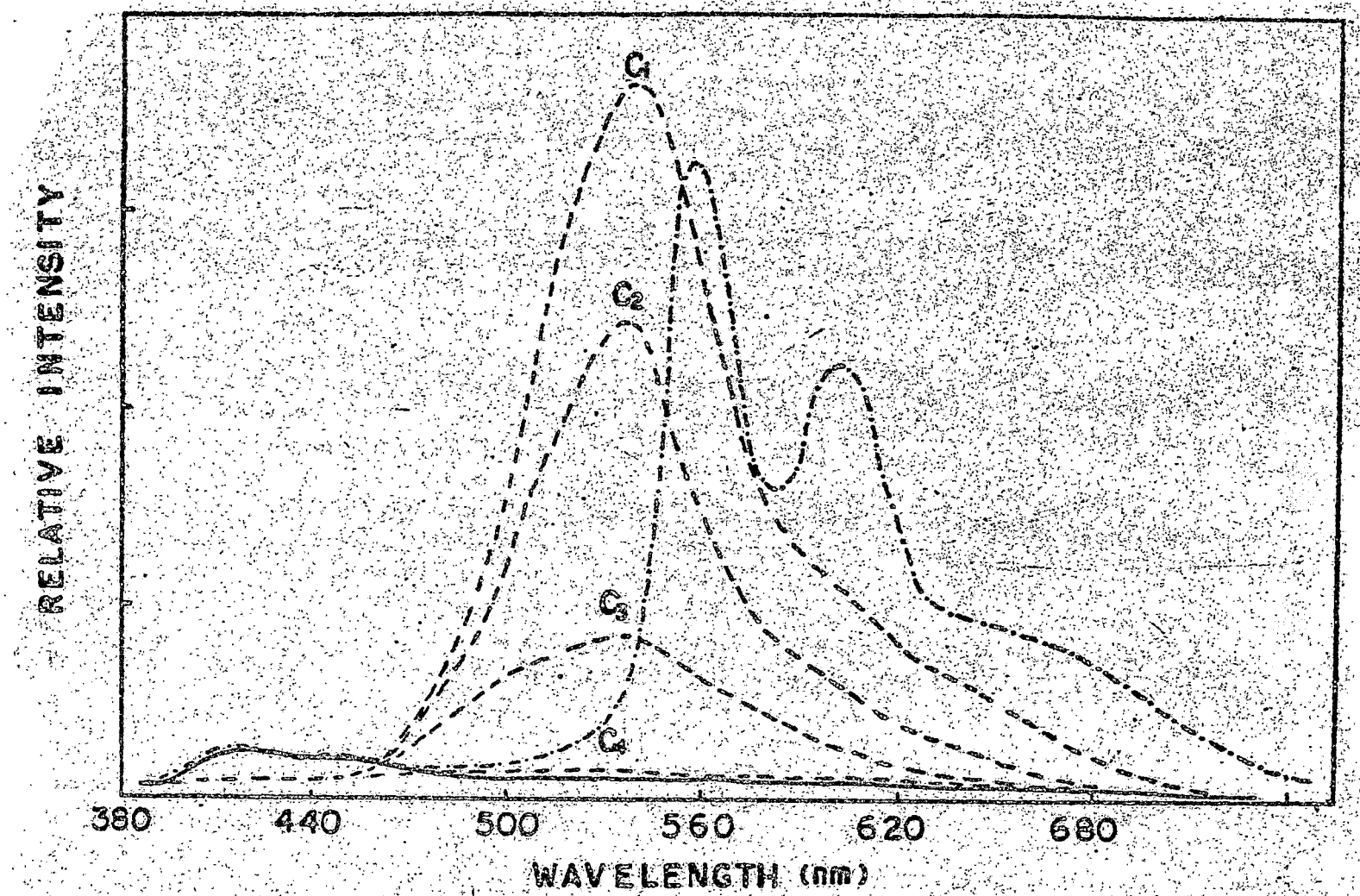

Fig. 4.5 : Total luminescence spectra of 1,4-dinitronaphthalene without chopper(The intensities of the spectra in different solvents are not normalised; concentrations $C_1 = 0.65 \times 10^{-4}$ M; $C_2 = 0.65 \times 10^{-5}$ M; $C_3 = 0.65 \times 10^{-6}$ M and $C_4 = 0.65 \times 10^{-7}$ M) in ethanol at 77°K (-.-.-.-); in methylcyclohexane at 303°K (————); in methylcyclohexane at 77°K (- - - - -).

band. Intensity of this broad band decreases with the temperature and at room temperature this emission disappears and a weak fluorescence of DMN is observed. The broad emission band in MCH does not seem to be a solvent associated impurity emission as similar spectra are observed at 77K in other hydrocarbon solvents we have examined like n-pentane, n-hexane, iso-pentane and iso-octane. Absence of this emission in protic solvents excludes its being due to solute associated impurity emission. We have examined the absorption spectrum of concentrated solution of DMN in hydrocarbon solvents at 77K. No absorption band in the spectral region 410 nm - 550 nm is observed. This suggests that the broad emission band is not due to dimer emission. All these observations clearly indicate about the involvement of some new state, which in all probability is the excimer state (D^*) in hydrocarbon condensed media at low temperature. With decrease in concentration, the intensity of the broad excimer emission decreases while that of phosphorescence increases.

The phosphorescence and the excimer excitation spectra are different (Fig. 4.6). From the solvent effect on absorption spectra, the band at about 354 nm is found to have predominantly CT character. The phosphorescence in MCH is mainly due to ^1CT excitation, the initial state of ICC is ^1CT and the final state may be either $^3\pi\text{-}\pi^*$ or $^3n\text{-}\pi^*$. The excitation spectra corresponding to the excimer emission looks complex where, in addition to the broad ^1CT absorption band, some sharp bands with origin at about 23900 cm^{-1} are observed.

FIGURE 4.6

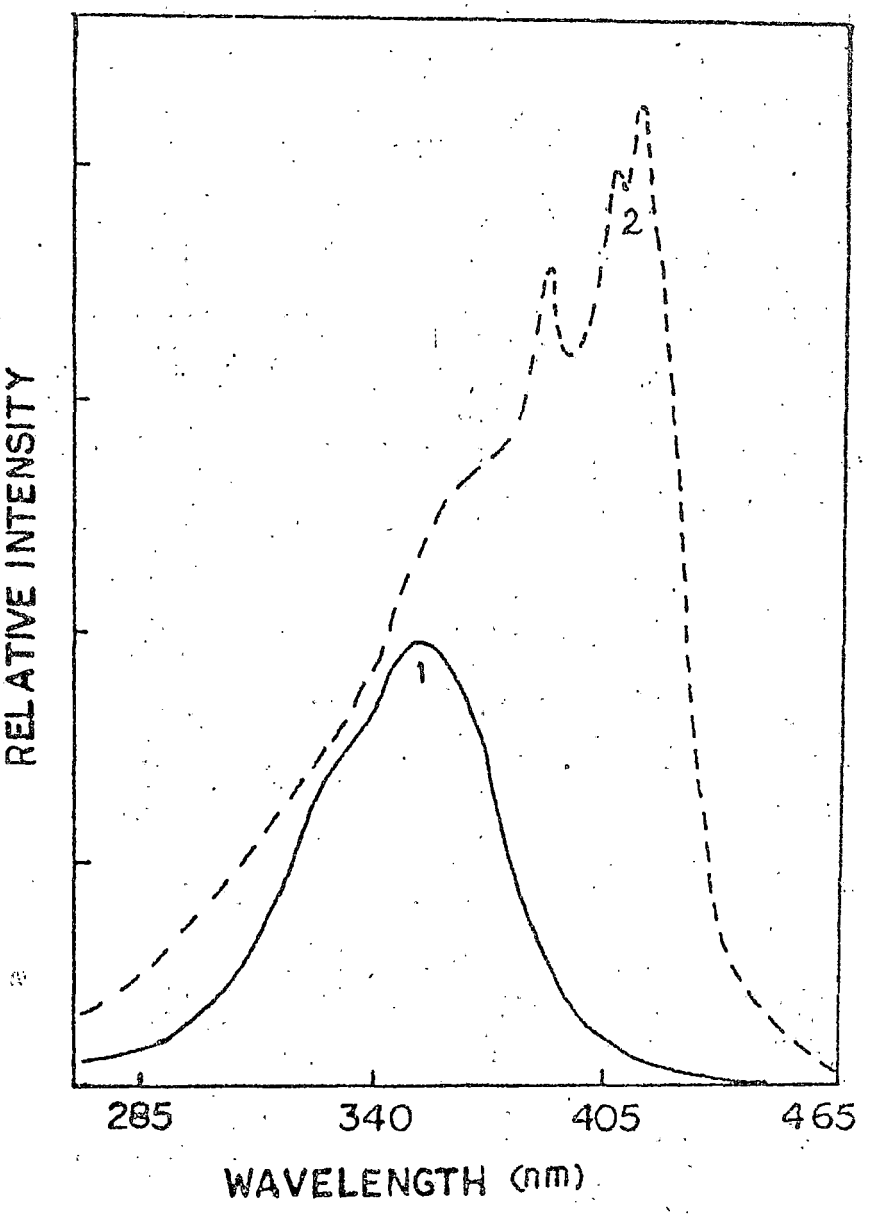

Excitation spectra of 1,4-dinitronaphthalene in methyl cyclohexane at 77°K.

1. Phosphorescence excitation spectra;

2. Excimer excitation spectra.

Those sharp bands, in our opinion, are due to $^1n-\pi^*$ excitation. Indeed, the weak fluorescence observed from DNN originates from this $^1n-\pi^*$ state.

The absence of fluorescence and the presence of a weak phosphorescence in hydrocarbon solvents at low temperature is evidently due to the efficient $^1n\text{-}\pi^* \rightsquigarrow D^*$ energy transfer which makes the $^1n\pi^* \rightsquigarrow {}^3n\pi^*$ ISC less probable.

Such an exciner emission is not observed in protic solvents. Nitroaromatic molecules in protic solvents are known to form a hydrogen bonding in which oxygens of the nitro group are proton acceptors while the solvent is proton donor[67-69]. This type of local solute-solvent interaction may result in a low probability of D^* formation. Thus, in protic solvents $^1n\text{-}\pi^* \rightsquigarrow D^*$ route is absent and $^1n \longrightarrow S_o$ fluorescence is observed with low intensity because of the efficient $^1n\text{-}\pi^* \rightsquigarrow S_o$ nonradiative process.

4. Conclusions

The low-lying singlet and the triplet states have been assigned from solvent effect on the absorption and the emission spectra and also from polarisation, decay and excitation spectra studies of the phosphorescence emission.

Strong 'proximity effect' between the close lying $^3\pi-\pi^*$ and $^3n\text{-}\pi^*$ states has been observed. The quenching of the radiative $^1n\text{-}\pi^* \longrightarrow S_o$

transition in hydrocarbon glasses, however, has been attributed not to the proximity effect but to the efficient $^1n\text{-}\pi^* \rightsquigarrow D^*$ route resulting in the excimer fluorescence emission. In protic solvents, excimer(D^*) formation could not be observed because of the local solute-solvent interactions.

REFERENCES (PART - B)

(Spectroscopic Investigations)

1. M. Kojima, J. Tanaka and S. Nagakura;
Theoret. Chim. Acta. 3, 432 (1965)

2. R. Hurley and A. C. Testa;
J. Am. Chem. Soc. 90, 1949 (1968)

3. O. S. Khalil, H. C. Beck and S. P. McGlynn;
J. Mol. Spectrosc. 35, 455 (1970)

4. E. C. Lim and J. Stanislaus;
Chem. Phys. Lett. 6 (3), 195 (1970)

5. R. Rusakovics and A. C. Testa;
Spectrochimica Acta 27A, 787 (1971)

6. J. J. Mikula, R. W. Anderson, L. E. Harris and E.W. Stuebing;
J. Mol. Spectrosc. 42, 360 (1972)

7. R. W. Anderson, R. M. Hochstrasser, H. Lutz and C. W. Scott;
Chem. Phys. Lett. 28, 153 (1974)

8. C. J. Seliskar, O. S. Khalil and S. P. McGlynn; in "Excited States" Vol. 1, edited by E.C. Lim, (Academic Press, NY, 1974) p. 231.

9. H. Ohtani, T. Kobayashi, K. Suzuki and S. Nagakura;
Bull. Chem. Soc. Jpn 53(1), 43 (1980)

10. J. K. Roy and R. S. Becker;
Proc. Int. Conf. on Spectrosc. Bombay, India, Jan 1967;
Chem. Abs. 144937 69, 1969

11. S.P. McGlynn, T. Azumi and M. Kinoshita; "Molecular Spectroscopy of the Triplet State". (Prentice-Hall, Englewood Cliffs, N. J., 1969)

12. H. Suzuki;"Electronic Absorption Spectra and Geometry of Organic Molecules" (AP, NY, 1967)

13. S. Nagakura, M. Kojima and Y. Maruyama;
J. Mol. Spectrosc. 13, 174 (1964)

14. J. M. Morkill and I. J. Graham - Bryce;
J. Chem. Soc. 3803 (1961)

15. H. Labhart;
Tetrahedron Suppl. (2) 19, 223 (1963)

16. G. Millefiori, G. Favini, A. Millefiori and D. Grasso;
Spectrochimica Acta 33A, 21 (1977)

17. T. Fujii, S. Suzuki and M. Fujishima;
Bull. Chem. Soc. Jpn. 50(4), 847 (1977)

18. J. R. Platt;
J. Chem. Phys. 17, 484 (1949)

19. E. Huckel;
Z. Physik 70, 204 (1931)

20. E. Huckel;
Z. Physik 72, 310 (1931)

21. E. Huckel;
Z. Physik 76, 628 (1932)

22. E. Huckel;
Z. Physik 83, 632 (1933)

23. M. Goeppert-Mayer and A. L. Sklar;
J. Chem. Phys. 6, 645 (1938)

24. D. P. Craig;

Proc. Roy. Soc. (London) A200, 474 (1950)

25. C. C. J. Roothaan;

Rev. Modern Phys. 23, 69 (1951)

26. R. Pariser and R. G. Parr;

J. Chem. Phys. 21, 466 (1953)

27. R. Pariser and R. G. Parr;

J. Chem. Phys. 21, 767 (1953)

28. J. A. Pople;

Faraday Soc. 42, 1375 (1953)

29. M. J. S. Dewar;

Proc. Cambridge Phil. Soc. 45, 639 (1949)

30. M. J. S. Dewar;

J. Chem. Soc. 2329 (1950)

31. M. J. S. Dewar;

J. Am. Chem. Soc. 74, 3341, 3345, 3350, 3353, 3355, 3357 (1952)

32. H. Suzuki;

Bull. Chem. Soc. Jpn. 25, 1253 (1952)

33. E. A. Braude and F. Sondheimer;

J. Chem. Soc. 3754 (1955)

34. H. C. Longuet-Higgins and J. N. Murrell;

Proc. Phys. Soc. (London) A68, 601 (1955)

35. J. N. Murrell;

Ibid A68, 969 (1955)

36. S. Basu; in"Advances in Quantum Chemistry"; edited by P.O. Lowdin (AP, NY, 1964) p. 157.

37. H. Hatage and T. Kubota; "Molecular Interactions and Electronic Spectra". (Marcel Dekker, INC. NY, 1970)

38. Y. Ooshika;
J. Phys. Soc. Jpn. 9, 594 (1954)

39. H. C. Longuet-Higgins and J. A. Pople;
J. Chem. Phys. 27, 192 (1957)

40. E. G. McRae;
J. Chem. Phys. 31, 562 (1957)

41. L. Onsager;
J. Am. Chem. Soc. 58, 1486 (1936)

42. N. Q. Chako;
J. Chem. Phys. 2, 644 (1934)

43. R. S. Mulliken and C. A. Ricke;
Rep. Prog. Phys. 8, 231 (1941)

44. L. E. Jacobs and J. R. Platt;
J. Chem. Phys. 16, 1137 (1948)

45. J. Schuyer;
Recl. Trav. Chim. Phys-Bas 72, 933 (1953)

46. A. A. Chifford and B. Crawford Jr;
J. Phys. Chem. 70, 1536 (1966)

47. O. E. Weigang Jr;
J. Chem. Phys. 41, 1435 (1964)

48. G. W. Robinson;

J. Chem. Phys. 46, 572 (1967)

49. N. S. Bayliss and G. W. Johnson;

Spectrochim. Acta. A24, 551 (1968)

50. N. S. Bayliss and G. W. Johnson;

Spectrochim Acta A24, 563 (1968)

51. S. Linder and G. Abdulnur;

J. Chem. Phys. 54A, 1807 (1971)

52. G. Abdulnur;

J. Chem. Phys. 58(10), 4175 (1973)

53. Th. Forster; Fluoreszenz Organischer Verbindungen; (Vandenhoeck and Ruprecht Gottingen, 1951)

54. M. Born and J. R. Oppenheimer;

Ann. Physik. 84, 457 (1927)

55. M. Kasha;

J. Chem. Phys. 20, 71 (1952)

56. H. B. Klevenes and J. R. Platt;

J. Chem. Phys. 17, 470 (1949)

57. W. Moffitt;

J. Chem. Phys. 22, 320 (1954)

58. R. Pariser;

J. Chem. Phys. 24, 250 (1956)

59. N. S. Ham and K. Ruedenberg;

J. Chem. Phys. 25, 13 (1956)

60. E. Char;

Spectrochim. Acta 4, 116 (1950)

61. J. W. Sidman;

J. Chem. Phys. 25, 115 (1956)

62. J. Trotter;

Acta. Cryst. 11, 564 (1958)

63. H. D. Coggeshall and A. Pozefsky;

J. Chem. Phys. 19, 980 (1951)

64. V. G. Plotnikov;

Optics Spectrosc 20, 332 (1966)

65. P. Groth and O. Hassel;

Acta. Chem. Scand. 19, 120 (1965)

66. P. Groth and O. Hassel;

Proc. Chem. Soc., 379 (1962)

67. G. S. Hammond and F. J. Modic;

J. Am. Chem. Soc. 75, 1385 (1953)

68. K. B. Wiberg;

Physical Organic Chemistry (Wiley, NY, 1964) p. 139.

69. H. J. Kamlet, E. O. Kaysor, J. W. Kastes and W.H. Gilligan;

J. Am. Chem. Soc. 95, 5210 (1973)

70. J. R. Platt;

J. Chem. Phys. 19, 101 (1951)

71. H. J. Suarich; Ph.D.Thesis, University of British Columbia, 1968.

72. K.M. Jain, B. Mallik and T.N. Misra;

Ind. J. Pure and Appl. Phys. 14, 53 (1976)

73. S. L. Najed, S. Okajima and E. C. Lim;
J. Chem. Phys. 65, 1219 (1976)

74. E. C. Lim; Excited States Vol. 3 edited by E. C. Lim
(AP, NY, 1977) p. 305.

75. Quoted by Khalil et. al (Ref. 3).

APPENDIX

List of Publications

1)* K. N. Jain, D. Mallik, K. C. Mandal and T. N. Misra
"Electronic spectra of polyenes : evidence of a low-lying forbidden transition in some linear conjugated polyenes"
Indian J. Pure and Appl. Phys. 13, 699 (1975)

2) K. N. Jain, D. Mallik and T. N. Misra
"Electronic spectra of 9-nitroanthracene : solvent effect on $^1A \rightarrow {}^1L_a$ and $^1A \rightarrow {}^1L_b$ transitions"
Indian J. Pure and Appl. Phys., 14, 59, (1976)

3)* K. N. Jain, D. Mallik and T. N. Misra
"Evidence of a low-lying forbidden transition in methyl bixin"
Indian J. Pure and Appl. Phys., 15, 289 (1977)

4) K. N. Jain, D. Mallik and T. N. Misra
"Electronic spectra of 2-nitrofluorene : solvent effect on $^1A \rightarrow {}^1L_a$ transition"
Indian J. Pure and Appl. Phys., 15, 267 (1977)

5)* K. N. Jain, D. Mallik and T. N. Misra
"Charge-transfer spectrum of all trans - β carotene"
Indian J. Biochem. Biophys., 15, 233, (1978)

6)* K. N. Jain, D. Mallik and T. N. Misra,
"Charge transfer complexes of some linear conjugated Polyenes"
Biochem. J., 189, 547 (1980)

7) K. N. Jain and T. N. Misra
"On the luminescence of 1,4-dinitronaphthalene"(communicated to Chem. Phys. Lett.)

8) K. N. Jain and T. N. Misra
"Low-lying energy states in 1,4-dinitronaphthalene"
(communicated to Chem. Phys.)

9) K. N. Jain, A. Ghosh, D. Mallik and T. N. Misra
"Semiconductive properties of organic compounds : gas-adsorption effect on 9-nitroanthracene"
Indian J. Phys., 52A, 643 (1978)

10) K. N. Jain, A. Ghosh and T. N. Misra
"Gas-adsorption effect on the semiconductive properties of nitrobenzoic acids"
Jpn. J. Appl. Phys., 19, 1947 (1980)

11) K. N. Jain, A. Ghosh, R. Mallik and T. N. Misra
"Compensation effect in the electrical conduction process in some nitroaromatic semiconductors"
Jpn. J. Appl. Phys. (in press, 1981)

12) K. N. Jain, A. Ghosh and T. N. Misra
"Effect of adsorption of vapours on the electrical conductivity of some nitroaromatic semiconductors : adsorption and desorption kinetics"
Proc. Indian Acad. Sci.(in press, 1981)

13) K. N. Jain, A. Ghosh and T. N. Misra
"Two stage adsorption and desorption processes in some nitroaromatic semiconductor - vapour systems : implication in compensation effect in dark conduction process"
Proc. Indian Acad. Sci. (in press, 1981)

14) K. N. Jain, A. Ghosh and T. N. Misra
"On the validity of the compensation effect in some nitroaromatic semiconductors" (communicated to Chem. Phys. Lett.)

15) K. M. Jain and T. N. Misra
"Lowest triplet state in 1,4- Dinitronaphthalene
Spectrosc. Lett. vol. 14 (3), 00, 1981

* Not included in the Thesis.

VITA

KAPUR MAL JAIN

DATE OF BIRTH	July 1, 1950
PLACE OF BIRTH	Nagda, Dhar, Madhya Pradesh (INDIA)
EDUCATION	
B.Sc.	Vikram University, Ujjain (M.P.) (1970)
M.Sc. (Physics)	Birla Institute of Science and Technology, Pilani (Rajasthan) (1973)
RESEARCH AND TEACHING ASSIGNMENTS	
Lecturer in Physics	Govt. P.G. College, Khargone (M.P.) (1973 - 74)
C.S.I.R. Junior Fellow	Physics Department, North Bengal University, Darjeeling (India) (1974 - 76)
C.S.I.R. Senior Fellow	Physics Department, North Bengal University, Darjeeling (1976 - 77)
Lecturer in Physics	Govt. Arts and Science College, Durg (M. P) (Since November' 1977)
UGC Teacher Fellow (From Govt. Arts & Sc. College Durg M.P.)	Optics Dept., I.A.C.S., Calcutta-32 (Since May' 1980)

Indian Journal of Pure & Applied Physics
Vol. 14, January 1976, pp. 53-57

Electronic Spectra of 9-Nitroanthracene : Solvent Effect on $^1A \rightarrow {}^1L_a$ and $^1A \rightarrow {}^1L_b$ Transitions

KAPUR MAL JAIN, BISWANATH MALLIK & T N MISRA
Department of Physics, University of North Bengal, Darjeeling

Received 17 *March* 1975

Two band systems have been observed in the electronic absorption spectra of 9-nitroanthracene in the near ultraviolet region having origins at 26100 and 23800 cm^{-1}. These have been assigned as $^1A \rightarrow {}^1L_a$ and $^1A \rightarrow {}^1L_b$ transitions respectively. The emission spectrum of this nitro aromatic compound has also been reported. A good overlapping between the emission spectrum and the $^1A \rightarrow {}^1L_b$ absorption band has been observed. It has been suggested that the low energy excited singlet state is a $\pi\pi^*$ and not a $n\pi^*$ state as in some nitro aromatic compounds. $^1A \rightarrow {}^1L_b$ band which is hidden under the intense $^1A \rightarrow {}^1L_a$ band in anthracene, thus, appears in this molecule due to the substitutional perturbation of nitro group. The solvent effect on the $^1A \rightarrow {}^1L_a$ transition energy has been explained in terms of predominent dispersive interaction and weak dipolar interaction in non-polar solvents and in terms of orientation-induction effect and local interaction in polar solvents. The observed change in oscillator strength of $^1A \rightarrow {}^1L_a$ has been explained in terms of intermolecular forces between the solute and the solvent molecules, the translational fluctuations between the induced moments and local interactions. 'Intermolecular force factors' for various solvents have been estimated.

1. Introduction

In catacondensed hydrocarbons, as one moves from benzene to higher polyacenes, both ^1L_a and ^1L_b energy levels of benzene move to lower energy. The lowering in energy of ^1L_a is steeper than that of ^1L_b and in anthracene the longest wavelength band is due to $^1A \rightarrow {}^1L_a$ transition and $^1A \rightarrow {}^1L_b$ band appears to be hidden under the stronger $^1A \rightarrow {}^1L_a$ transition[1] at 3700 Å.

The nitro group is an important chromophore. In the ground state, each of the two lower bonding and non-bonding orbitals of nitro group is occupied by two electrons and the anti-bonding orbital is vacant. Substitution of nitro group in the anthracene ring is expected to show a strong effect on the π-electronic states of anthracene molecule. It was, therefore, thought worthwhile to study the electronic spectra of 9-nitroanthracene. The effect of various polar and non-polar solvents on the electronic absorption spectra of this molecule has also been investigated.

2. Experimental Procedure

The sample of 9-nitroanthracene, a gift from Prof. R. S. Becker, was further purified by repeated recrystallization using purified benzene. Needle-shaped yellow coloured crystals having melting point at 146°C were obtained. Solvents of spectrograde quality were used.

The absorption spectra in various solvents were recorded at room temperature (25°C) on a Perkin-Elmer 202 recording spectrophotometer and also on a Spectromom 202 spectrophotometer of Hungarian Optical Co. The emission spectrum was recorded on Aminco Bowman spectrofluorometer.

3. Results and Discussion

3.1 Spectra

The absorption spectra of 9-nitroanthracene in various non-polar and polar solvents with the same concentration at room temperature are reproduced in Figs. 1 and 2 respectively. The results of the analysis of the bands are summarized in Tables 1, 2 and 3. In all the solvents, a well defined intense band system at about 26100 cm^{-1} is observed with vibrational structure. In non-polar solvents, however, few more weak bands appear towards the lower energy side of this band system. In polar solvents, these weak bands lose their structure and a general broad weak absorption band is observed in this spectral region.

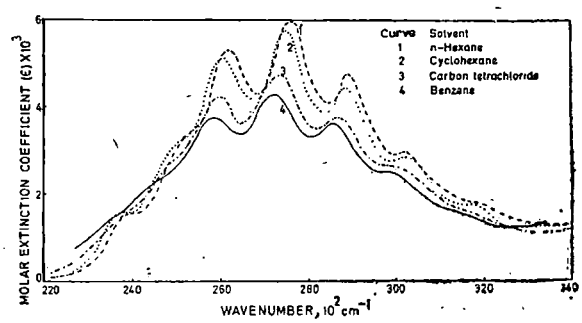

Fig. 1—Electronic spectra of 9-nitroanthracene in various non-polar solvents

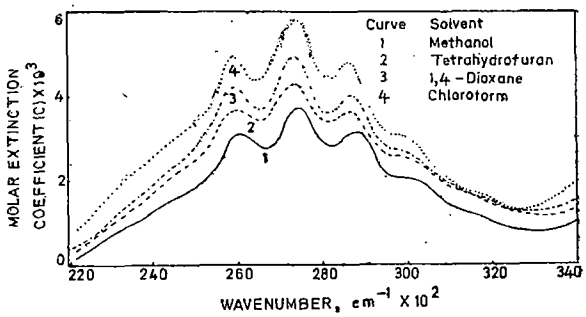

Fig. 2—Electronic spectra of 9-nitroanthracene in various polar solvents

A close examination of the absorption spectra of 9-nitroanthracene in various solvents reveals that the strong band system at about 26100 cm^{-1} resembles the lowest energy absorption band of anthracene (Fig. 3). The bands on the lower energy side are structurally different from the bands in the intense system and possibly belong to different electronic transitions. This deduction has been further substantiated by the vibrational analysis of the spectra in various solvents.

It has been pointed out by Coggeshell and Pozefsky[2] that in benzene and naphthalene spectra the vibrational spacing involving transitions to a ^1L_a state is of the order of 1400 cm^{-1} and in transitions to a ^1L_b state it is of the order of 1000 cm^{-1}. The 1400 cm^{-1} vibration is associated with the C—H in-plane bending whereas the 1000 cm^{-1} vibration is the breathing vibration of the ring.

The analysis of the spectra of 9-nitroanthracene shows that the separation between the bands in the intense system is about 1400 cm^{-1} which possibly is C—H in-plane bending vibration. This vibration forms a progression in the absorption spectra of anthracene solution at room temperature (Fig. 3). But the separation between the bands *b* and *c* is about 900 cm^{-1}. This suggests that *b* and *c* belong to two different electronic transitions. The separation between the bands *a* and *b* of the lower energy band system is much less than 1400 cm^{-1} and is about 1050 cm^{-1}. It seems that possibly the breathing vibration of the ring forms the progression in the weak low energy band system. We assign this band system to $^1A \rightarrow {}^1L_b$ transition, which has been shifted to red more than the intense $^1A \rightarrow {}^1L_a$ transition and the two band systems have been resolved in this 9-nitroanthracene molecule.

The emission spectrum of 9-nitroanthracene has been investigated. In cyclohexane, emission has been observed. The emission spectrum is reproduced in Fig. 3. A good overlapping between the observed emission and weak low energy absorption spectrum is observed. This observation is interesting in view of the fact that the luminescence of nitroaromatics is not yet clearly understood. Many nitroaromatic compounds exhibit either fluorescence or phosphorescence and few exhibit both types of emission. The lowest excited singlet and triplet states of nitroaromatic compounds are usually nearly degenerate and both $\pi\pi^*$ and $n\pi^*$ states are present in each molecule. A good overlapping between the lowest energy weak absorption and the emission shows that both initiates from the same states which has a $\pi\pi^*$ character. It has been suggested by Plotnikov[3] that as the size of the aromatic system increases, $\pi\pi^*$ state moves to a level lower energy than the $n\pi^*$ state energy level. Intramolecular charge transfer character of the low energy state is also expected to increase with the size of the polynuclear nitroaromatics. This should increase the $^1\pi\pi^* \rightarrow {}^1\pi\pi^\circ$ transition probability.

Thus, we conclude that the lowest excited singlet state in 9-nitroanthracene molecule is a $\pi\pi^*$ state and that the system having origin at about 23800 cm^{-1} belongs to $^1A \rightarrow {}^1L_b$ and the other having origin at about 26100 cm^{-1} belongs to $^1A \rightarrow {}^1L_a$ transition.

3·2. Solvent Effect

Solvation energy—The solvent effects on the electronic absorption spectra of 9-nitroanthracene have been studied. The non-polar solvents *n*-hexane, cyclohexane, carbon tetrachloride and benzene and polar solvents methanol(MeOH), tetrahydrofuran (THF), 1, 4-dioxane and chloroform have been used.

In polar solvents, though $^1A \rightarrow {}^1L_a$ transition shows a vibrational structure, in $^1A \rightarrow {}^1L_b$ the vibrational structure is not generally observed. In non-polar solvents the vibrational structure of both $^1A \rightarrow {}^1L_a$ and $^1A \rightarrow {}^1L_b$ transitions are observed. However, the vibrational structure observed in saturated hydrocarbons is appreciably blurred in the solvents like carbon tetrachloride and benzene, possibly due to stronger interaction between the solute and solvent molecules.

The solvent effect on the absorption spectra of a solute is known to be due to dispersive interaction, dipolar interaction and in case of polar solvents also due to the orientation-induction effects of the solvent dipole on the solute molecule.[4,5] In addition, local interaction like bond formation, etc. may also affect the transition energy. Quantitative estimation of the absorption energy could be made for $^1A \rightarrow {}^1L_a$ transition only. For both non-polar and polar solvents, plots of transition energy against the factor $(n^2 - 1)/(n^2 + 2)$ give good straight lines, where n is the refractive index of the solvent used. The linear plot for the polar solvent is, however, on the lower

Table 1—Absorption Bands of 9-Nitroanthracene in Various Non-polar Solvents at Room Temperature

n-Hexane			Cyclohexane			Carbon tetrachloride			Benzene		
Wave-number cm^{-1}	Intensity	Tentative assign-ment	Wave-number cm^{-1}	Intensity	Tentative assign-ment	Wave-number cm^{-1}	Intensity	Tentative assign-ment	Wave-number cm^{-1}	Intensity	Tentative assign-ment
24150	w	0_1	24000	w	0_1	23900	vw	0_1	23700	vw	0_1
25200	vw	0_1+1050	25000	vw	0_1+1050	24950	vvw	0_1+1050	24750	vvw	0_1+1050
26250	s	0_2	26075	s	0_2	25975	s	0_2	25850	s	0_2
27625	vs	$0_2+1400\pm25$	27475	vs	0_2+1400	27375	vs	0_2+1400	27250	vs	0_2+1400
29000	s	$0_2+2\times1400\pm25$	28900	s	$0_2+2\times1400\pm25$	28750	s	$0_2+2\times1400\pm25$	28650	s	$0_2+2\times1400$
30350	w	$0_2+3\times1400\pm25$	30275	w	$0_2+3\times1400\pm25$	30100	vw	$0_2+3\times1400\pm50$	30000	vw	$0_2+3\times1400\pm50$

w, weak; v, very; and s, strong

Table 2—Absorption Bands of 9-Nitroanthracene in Various Polar Solvents at Room Temperature

Methanol			Tetrahydrofuran			1, 4-Dioxane			Chloroform		
Wave-number cm^{-1}	Intensity	Tentative assign-ment	Wave-number cm^{-1}	Intensity	Tentative assign-ment	Wave-number cm^{-1}	Intensity	Tentative assign-ment	Wave-number cm^{-1}	Intensity	Tentative assign-ment
Broad and weak absorption in the range 25500 cm^{-1} to 22000 cm^{-1}			Broad and weak absorption in the range 25300 cm^{-1} to 22000 cm^{-1}			Broad and weak absorption in the range 25500 cm^{-1} to 22500 cm^{-1}			Broad and weak absorption in the range 25000 cm^{-1} to 22000 cm^{-1}		
26100	s	0_2	25950	s	0_2	25900	s	0_2	25875	s	0_2
27550	vs	0_2+1400	27350	vs	0_2+1400	27300	vs	0_2+1400	27275	vs	0_2+1400
28925	s	$0_2+2\times1400\pm25$	28725	s	$0_2+2\times1400\pm25$	28700	s	$0_2+2\times1400$	28675	s	$0_2+2\times1400$

v, very; and s, strong.

Table 3—Experimental Oscillator Strength Values and the *X*-Factors

Solvent	Oscillator strength	$(1+X)f_i$	Solvent	Oscillator strength	$(1\times X)f_i$
Non-polar			Polar		
n-Hexane	0·1281	0·1044	Methyl alcohol	0·0801	0·0674
Cyclohexane	0·1221	0·0961	Tetrahydrofuran	0·1078	0·0866
Carbon tetrachloride	0·1130	0·0869	1, 4 Dioxane	0·1141	0·0902
Benzene	0·1070	0·0799	Chloroform	0·1341	0·1042

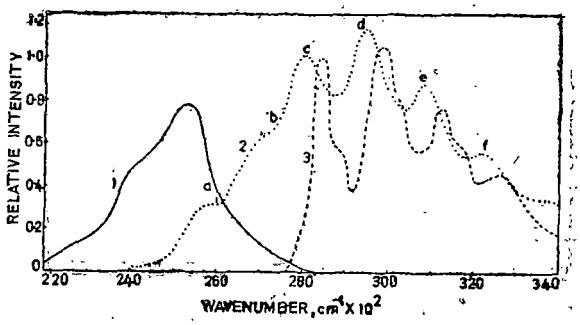

Fig. 3—Emission and absorption spectra in cyclohexane [1, Emission spectrum of 9-nitroanthracene; 2, absorption spectrum of 9-nitroanthracene; and 3, absorption spectrum of anthracene]

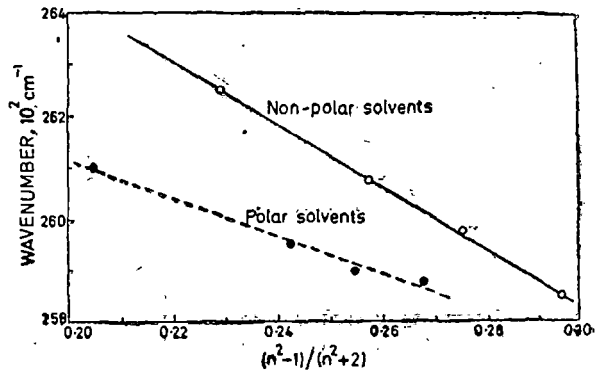

Fig. 4—The plot of transition energy of $^1A \rightarrow {}^1L_a$ band of 9-nitroanthracene against $(n^2-1)/(n^2+2)$ where n is the refractive index of the solvent

energy range and has a different slope than that for non-polar solvents (Fig. 4). A close examination of the expression for solvent shift in the absorption spectra of a solute as discussed by Basu[5] leads to some interesting conclusions. The linear plot in non-polar solvents indicates that the dispersive interaction predominates over the dipolar interaction. For the $^1A \rightarrow {}^1L_a$ transition of medium intensity, this possibly further suggests that the change in the dipole moment on excitation is small in 9-nitroanthracene molecule. The linear plot in polar solvents is not easy to rationalize. It possibly indicates that the difference in dipole moment in the excited and in the ground state is small and also the sum total of orientation induction effect and local interaction is not much dependent on the solvent refractive index. Small refractive index dependence is, however, present giving a different slope of the linear plot. Indeed, 9-nitroanthracene is expected to have strong local interaction with some polar solvents used. It is known[6,7] that 1, 4 dioxane forms a weak N·····O bond in the same way as alcohol forms hydrogen bond. The hydrogen bond is much more stronger than N·····O bond. Tetrahydrofuran is more polar than dioxane and is similar in structure and may form a stronger N·····O bond than dioxane.

Oscillator strength—Theoretical studies on the solvent effect on the f-value of an electronic transition in the solute molecule have been mostly concerned with the local field effect, e. g. Lorentz-Lorenz field by Chako[8] or Bottcher-Onsager field by Schuyer and Bakhsier *et al.*[9] The results are always analyzed in terms of local field contributions and distortions of electronic charge distribution by the surroundings. Chako's correction factor for the spectral intensity change is not sufficient to explain the observed results. Recently, considering long range dispersive forces to be operative, Abdulnur[10] has shown that for the conversion of the oscillator strength value in solution from the corresponding isolated molecular value, Chako's correction factor (n being the refractive index of the solvent) is of minor importance compared to an additional 'IMF' factor originating from the intermolecular forces between the solute and the solvent molecules and from the translational fluctuations between the induced moments.

Our results for the f-values in various solvents cannot be explained by Chako's correction factor alone. Expanding the 'IMF' factor to include local interactions between the solute and the solvent molecules as well, the experimental oscillator strength in solution f_s can be expressed by the empirical relation

$$\frac{1}{\gamma}(1 + X)f_i = f_s$$

where $1/\gamma$ is the Chako's factor, f_i is the free molecular oscillator strength and X is the expanded IMF factor. We have estimated the values of $(1 + X)f_i$ from the experimentally observed oscillator strengths in solution which are presented in Table 3. With the increase of n, while in polar solvents the f-value increases, f-value decreases in non-polar solvents. In case of non-polar solvents, the dispersive interaction plays a very important role. In going from n-hexane to benzene the solute-solvent interaction increases. The X factor increases with the increase of refractive index. Thus, the observed decrease in f-value followed by increase in X factor indicates a negative value for this interaction factor in non-polar solvents. In polar solvents the contribution to the X factor is not only due to dispersive interaction or dipole interactions but also due to local interactions. As has been pointed out before, local bond formation with 9-nitroanthracene and solvent molecule is possible. Thus, the X factor in polar solvents will be in the order :

$$X_{\text{MeOH}} > X_{\text{THF}} > X_{\text{Dioxane}} > X_{\text{Chloroform}}$$

The experimentally observed f-values increase in the same order indicating a positive value for the X-factor in polar solvents.

Acknowledgement

The authors express their thanks to Prof. R. K. Mishra of the All India Institute of Medical Sciences, New Delhi, for providing them with the laboratory emission work. One of them (K.M.J.) expresses his facilities for thanks to CSIR, New Delhi, for the award of a research fellowship.

References

1. Klevenes H B & Platt J R, *J. chem. Phys.*, **17** (1949), 4770.
2. Coggeshell & Pozefsky, *J. chem. Phys.*, **19** (1951), 980.
3. Plotnikov V G, *Optics Spectrosc.*, **20** (1966), 332.
4. Suzuki H, *Electronic absorption spectra and geometry of organic molecules* (Academic Press Inc., New York), 1967, 93.
5. Basu S, *The theory of solvent effects on molecular electronic spectra,* in *Advances in quantum chemistry*, edited by P. O. Lowdin (Academic Press Inc., New York), 1964, 157.
6. Groth P & Hassel O, *Acta chem. scand.*, **19** (1965), 120.
7. Groth P & Hassel O, *Proc. chem. Soc.*, (1962), 379.
8. Chako N Q, *J. chem. Phys.*, **2** (1934), 644.
9. Schuyer J, *Rec. Trav. Chim.*, **72** (1953), 933.
10. Abdulnur S F, *J. chem. Phys.*, **58** (1973), 4175.

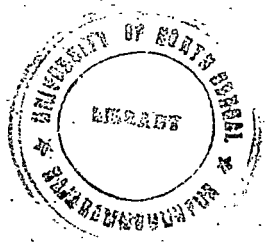

Indian J. Phys., **52A**, 543–551 (1978)

Semiconductive properties of organic compounds : gas adsorption effect on 9-nitroanthracene

KAPUR MAL JAIN*, ALPANA GHOSH, BISWANATH MALLIK AND T. N. MISRA

Optics Department, Indian Association for the Cultivation of Science, Jadavpur, Calcutta-700032

(*Received* 14 *October* 1977)

The conductivity of powdered 9-nitroanthracene in a sandwich cell has been studied. Conductivity of this organic compound follows the operational semiconductivity relation

$$\sigma(T) = \sigma_0 \exp.(-E/2kT).$$

The intrinsic value of the activation energy (E) is found to be 2 ev both in vacuum and in dry nitrogen atmosphere. The specific conductivity σ (27°C) and the pre-exponential factor (σ_0) are $0{\cdot}9031 \times 10^{-15}$ $\Omega^{-1}\text{cm}^{-1}$ and 75·11 $\Omega^{-1}\text{cm}^{-1}$ respectively. Effect of the adsorption of various vapours e.g., carbontetrachloride, benzene, ethyl acetate, methanol, ethanol and iso-propanol has been studied at a constant vapour pressure. The change in conduction current shows a distinct inverse relationship with the ionization energies of the adsorbed gases. This suggests that charge-transfer interaction may be responsible for such change. The rise in conductivity is exponential with increasing vapour pressure. The adsorption kinetics observed is fast and efficiently reversible which follows the modified Roginsky-Zeldovich equation.

$$\frac{dm}{dt} = A \exp.(-\beta m/kT)$$

where A is a constant and βm is the activation energy associated with the rate of adsorption (dm/dt). The factor β has been found to have inverse dependence upon vapour pressure.

1. INTRODUCTION

Semiconductive properties of organic crystals on adsorption of gases on the crystallite surfaces in a sandwich cell depend on the nature and strength of interaction between the adsorbed gas molecules and the semiconductor. This results in change in semiconduction current and the activation energy of the semiconductor. Both organic and inorganic semiconductors are very much sensitive to the ambient atmosphere (Gutmann & Lyons 1967). It has been speculated by Rosenberg *et al.* that a weak charge-transfer complex formation between vapour molecule and the semiconductor is responsible for the enhancement in the conductivity and lowering in the activation energy in case of polyenes and other compounds (Misra *et al* 1968, Rosenberg *et al* 1968). Attempts have also been made

* Present Address : Nagda, Dist. Dhar., (M.P.)-454001.

to explain such change of conduction current on gas adsorption in terms of physical mixing of original unperturbed semiconductor and the perturbed (due to gas adsorption) compound at the surface, resulting in so called compensation effect (Ulbert 1970). A three constant conductivity equation involving change in the pre-exponential factor (σ_0) has also been proposed (Rosenberg *et al* 1968).

We have undertaken a programme on the systematic investigations of the conductive properties of various organic compounds in a sandwich cell on gas adsorption at different vapour pressures using nitrogen as carrier gas. In this paper we present our results on the conductive properties of 9-nitroanthracene, adsorption and desorption kinetics and vapour pressure dependence of the semiconduction current in various ambient atmospheres.

2. Experimental Procedure

Commercial 9-nitroanthracene was further purified by repeated recrystallization using purified benzene. Needle-shaped yellow coloured crystals having melting point at 146°C were obtained. Solvents of high purity were used to study gas adsorption phenomenon. The compound in the form of fine powder was pressed in a sandwich cell between a conducting glass and a stainless steel electrode. Separation between the electrodes was maintained by 3 mil thick teflon spacers. A d.c. voltage of 22·5 volts was applied across the cell which was placed on a thermal bar platform in a suitably designed conductivity chamber made of brass and fashioned with teflon. The temperature of the sandwich cell could be controlled from outside. Gas inlet and outlet were also provided for gas adsorption study. Temperature measurements were made using a copper-constantan thermocouple, attached at the top of the metal electrode and a millivolt potentiometer. All the conductivity measurements were made in dry nitrogen atmosphere/vacuum with an electrometer amplifier EA 814 of Electronics Corporation of India Limited. To pass various vapours inside the chamber, nitrogen was used as a carrier gas which was passed through the bubbler kept at constant temperature. Repeated heating and cooling of the sample in nitrogen atmosphere ensured desorption of adsorbed water, oxygen or any other gas molecules prior to the experimental run. Tempertature of the sample was maintained constant at 27°C during adsorption studies at different vapour pressures.

3. Results

3.1 *Conductivity of 9-nitroanthracene powder*

The conductivity of powdered 9-nitroanthracene studied in a sandwich cell in the temperature range of 30°C to 103°C in dry nitrogen atmosphere follows the operational conductivity relation for semiconductors :

$$\sigma = \sigma_0 \exp(-E/2kT) \qquad \ldots (1)$$

as shown in Fig. 1. In high temperature region, a higher value of activation energy (about 2 eV.) is observed than that of low temperature region which is about 1·4 ev. Thus, the high temperature region might be attributed to the

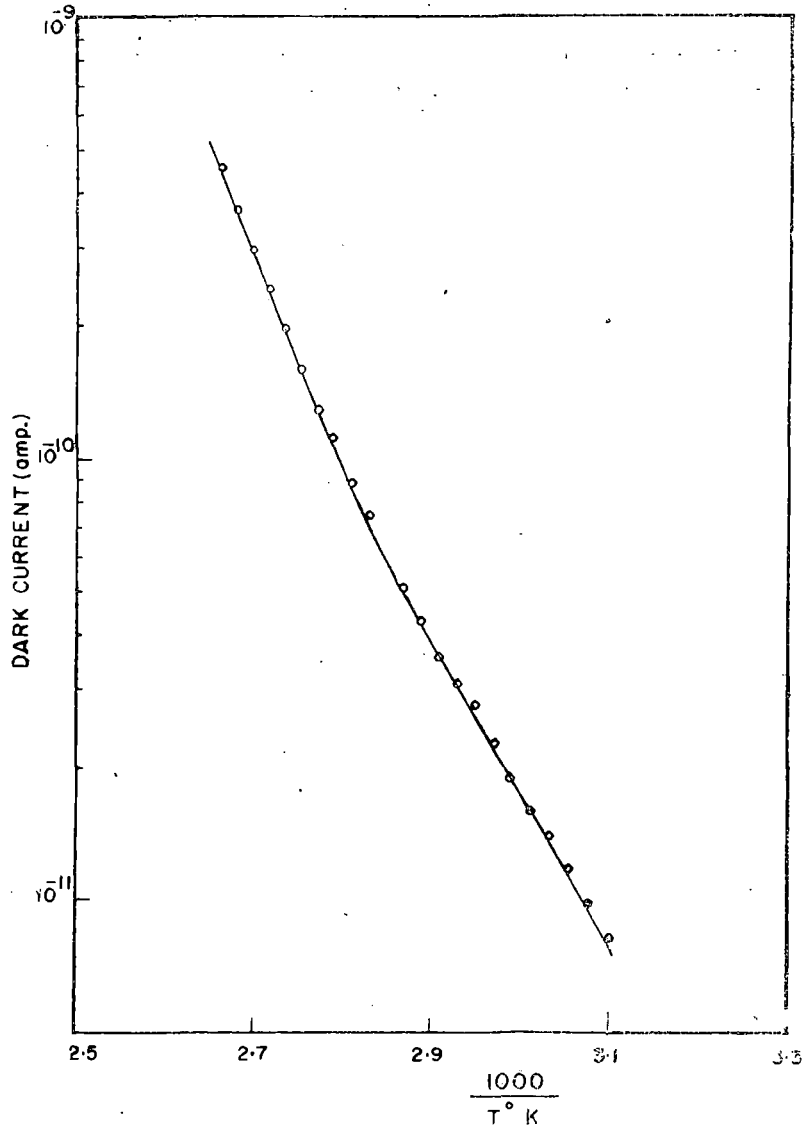

Fig. 1. Conductivity in a 9-nitroanthracene powder cell.

intrinsic region for this semiconductor. The specific conductivity (σ) at 27°C and the pre-exponential factor (σ_0) were found to be of the order of $0{\cdot}9031 \times 10^{-15}$ $\Omega^{-1}cm^{-1}$ and 75·11 $\Omega^{-1}cm^{-1}$ respectively.

3.2 *Gas Adsorption Effect*

The adsorption of various vapours, e.g., carbon-tetrachloride, benzene, ethyl acetate, methanol, ethanol and iso-propanol have been observed to have a pronounced effect on the enhancement in the conductivity as shown in table 1. The adsorption process is fast and efficiently reversible. The initial value of dark current is reached quickly simply by flushing the chamber with dry nitrogen. This is shown in Fig. 2.

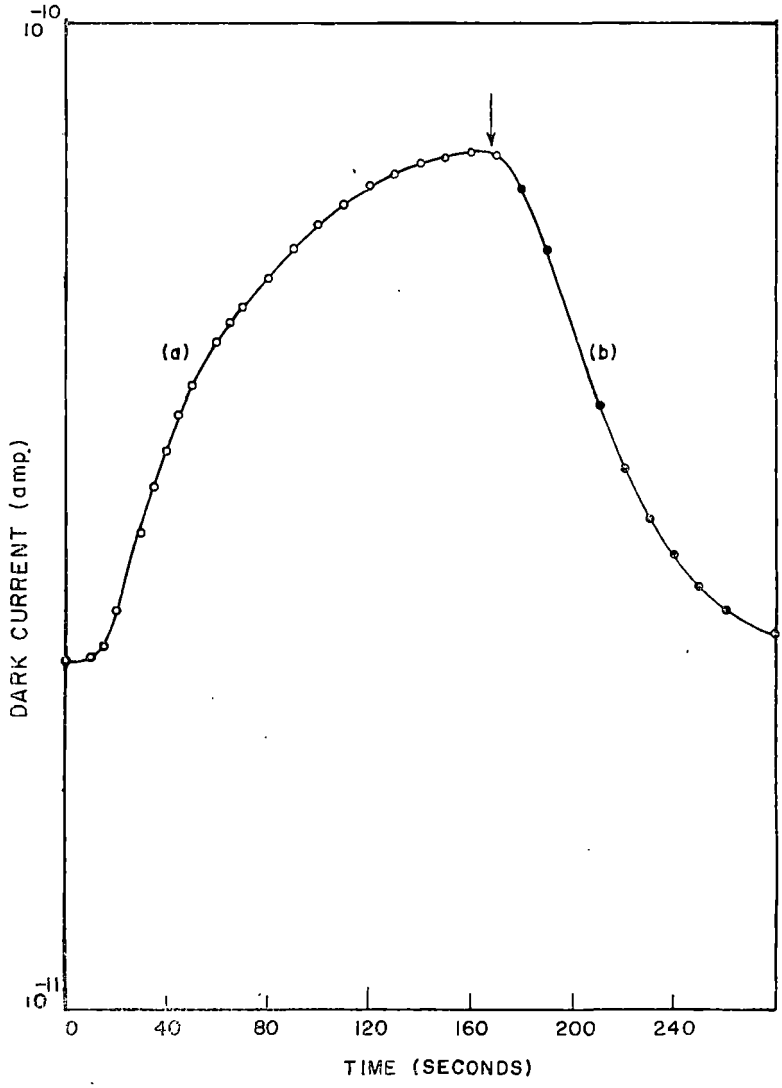

Fig. 2. The change in dark current in a 9-nitroanthracene powder cell with (*a*) adsorption and (*b*) desorption of carbon-tetrachloride vapour at 32·4 mm. vapour poressure (sample kept at 27°C).

3.3 *Vapour Pressure Dependence*

Measurements were made on the conductivity rise at constant temperature as a function of partial vapour pressure of carbon-tetrachloride inside the chamber. The total gas mixture inside the chamber was at atmospheric pressure and the partial vapour pressure was the vapour pressure of the chemical used. At constant flow and constant vapour pressure the conductivity after adsorption $\sigma_A(m)$ follows the relation (Misra *et al* 1968)

$$\sigma_A(m) = \sigma_V \exp(\alpha m) \quad \ldots (2)$$

where α is a constant and m is the amount of the vapour adsorbed. m depends on the partial vapour pressure of the chemical and in the initial period, also on the time of exposure. After sometime, however, an equilibrium is established. Thus we assume that in the initial region

$$m(t) = Q(b).\ p \quad \ldots (3)$$

$Q(t)$ is a function of time. At equilibrinm

$$m_0 = Q_0.\ p \quad \ldots (3)$$

where Q_0 is another constant. So, at equilibrium

$$\sigma_A(m_0) = \sigma_V \exp(\alpha.Q.p). \quad \ldots (4)$$

A plot of $\log \sigma_A(m_0)$ versus vapour pressure (p) is expected to be linear. Our experimental result in Fig. 3 shows a good agreement with this. When small

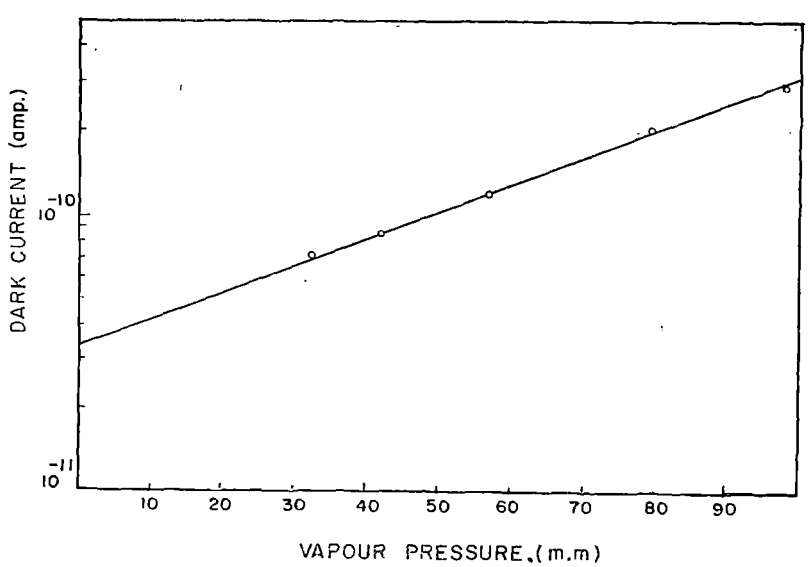

Fig. 3. Change in the dark current of 9-nitroanthracene powder cell as a function of the vapour pressure of carbon-tetrachloride.

fraction of the surface is covered by gas molecules equation (3) is expanded from Langmuir's adsorpition isotherm.

4. Discussion

4.1 *Change in Semiconduction current*

When the powdered semiconductor is exposed to some vapour, then the molecules at the surface will be influenced much causing change in the conductivity. If the resulting conductivity change is due to physical mixing of the original semiconductor and the perturbed semiconductor due to gas adsorption then, a relationship between the conductivity enhancement and the dielectric constant of the chemical used is expected. But our experimental results for conductivity rise at the same vapour pressure as shown in table 1 do not suggest this. The static dielectric constants are in the order carbon-tetrachloride < benzene < ethyl acetate < iso-propanol < ethanol < methanol which is not in agreement with the semiconduction current enhancement. 9-nitroanthracene is an electron acceptor because of the presence of nitro-group chromophore. The adsorbed molecule having electron donating nature may form a weak (D^+A^-) charge-transfer complex causing change in the conductivity. Carbon-tetrachloride and benzene both have approximately the same value of static dielectric constant, but the conductivity enhancement in benzene is about ten times than that of carbon-tetrachloride, possibly due to the more electron donating nature of benzene than carbon-tetrachloride. Indeed the enhancement of conductivity shows a distinct inverse relationship with the ionisation energies of the adsorbed gases.

Table 1. Rise in the dark current in a 9-nitroanthracene powder cell due to adsorption of various vapours at the same vapour pressure of 50 mm.

Vapour	Measured factor for current rise $[\sigma(\text{steady state})/\sigma(\text{initial})$
Carbon-tetrachloride	3
Methanol	6
Ethyl Acetate	3×10
Benzene	3×10
Ethanol	$1{\cdot}2\times10^2$
Iso-Propanol	$9{\cdot}2\times10^2$

4.2 *Kinetics*

The change in dark current in a 9-nitroanthracene powder cell with adsorption and desorption of carbon-tetrachloride vapour at 32·4 mm. vapour pressure is shown in Fig 2. Adsorption kinetics follows Roginsky-Zeldovich equation in a modified form (Misra *et al* 1968, Eley *et al* 1964). It was assumed that there is an activation energy associated with the adsorption rate, which increases

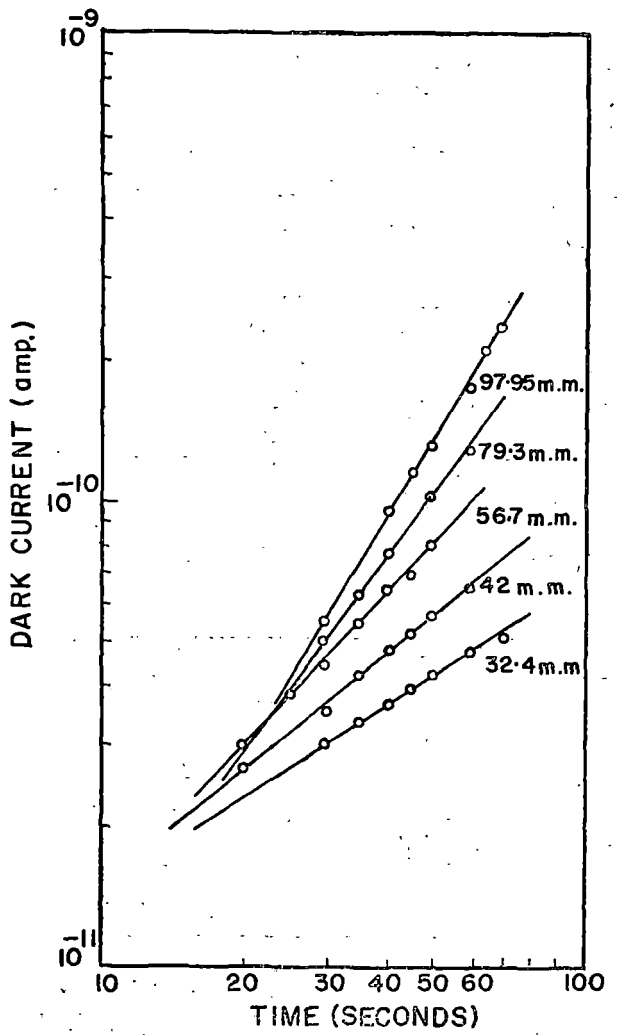

Fig. 4. Adsorption kinetics data plotted according to Roginsky-Zeldovich equation.

linearly with the amount of adsorbed gas. Thus, the rate of adsorption (dm/dt) will be

$$\frac{dm}{dt} = A \exp(-\beta m/kT) \quad \ldots (5)$$

where β is a constant.

Integrating (5), we get

$$m(t) = \frac{kT}{\beta} \log(t+t_0) + \text{constant} \quad \ldots (6)$$

combining (3a) and (6),

$$p = \frac{kT}{\beta Q(t)} \log(t+t_0) + \text{constant.} \quad \ldots (7)$$

Now, expression (2) can be re-written as

$$\log \sigma_A = \alpha Q(t)\, p + \text{constant.} \quad \ldots (8)$$

Substitution for p from (7) in (8) results in

$$\log \sigma_A = \frac{\alpha kT}{\beta} \log(t+t_0) + \text{constant.} \quad \ldots (9)$$

A linear plot of $\log \sigma_A$ versus $\log (t+t_0)$ is suggested and our experimental results in Fig 4 are in good agreement. Different slopes observed at different vapour pressures for the same value of α shows the vapour pressure dependence of β. (Table 2).

Table 2. Vapour pressure dependence of the factor β' for carbon-tetrachloride vapour adsorption kinetics.

Vapour Pressure (mm)	(β/α) (ev.)
32·4	$4{\cdot}074 \times 10^{-2}$
42·0	$3{\cdot}218 \times 10^{-2}$
56·7	$2{\cdot}458 \times 10^{-2}$
79·3	$1{\cdot}907 \times 10^{-2}$
97·95	$1{\cdot}577 \times 10^{-2}$

Our experimental results indicate that the activation energy associated with the rate of adsorption is not linearly increasing with the amount of the adsorbed vapour.

ACKNOWLEDGMENT

Thanks are due to the Council of Scientific & Industrial Research, New Delhi for financial support for the project. Thanks are also due to Prof. G. S. Kastha for his kind interest.

REFERENCES

Eley D. D. & Leslie R. B. 1964 *Advances in Chemical Physics* (Interscience Publishers, Inc., New York), **7**, 238.

Gutmann F. & Lyons L. E. 1967 *Organic Semiconductors* (John Wiley), 197.

Misra T. N., Rosenberg B. & Switzer R. 1968 *J. Chem. Phys.* **48**, 2096.

Rosenburg B., Bhowmik B. B., Harder H. C. & Postow E. 1968 *J. Chem. Phys.* **49**, 4108.

Rosenberg B., Misra T. N. & Switzer R. 1968 *Nature* **217**, 5127.

Ulbert K. 1970 *Aust. J. Chem.* **23**, 1347.